

INFORMATION TO USERS

This material was produced from a microfilm copy of the original document. While the most advanced technological means to photograph and reproduce this document have been used, the quality is heavily dependent upon the quality of the original submitted.

The following explanation of techniques is provided to help you understand markings or patterns which may appear on this reproduction.

1. The sign or "target" for pages apparently lacking from the document photographed is "Missing Page(s)". If it was possible to obtain the missing page(s) or section, they are spliced into the film along with adjacent pages. This may have necessitated cutting thru an image and duplicating adjacent pages to insure you complete continuity.
2. When an image on the film is obliterated with a large round black mark, it is an indication that the photographer suspected that the copy may have moved during exposure and thus cause a blurred image. You will find a good image of the page in the adjacent frame.
3. When a map, drawing or chart, etc., was part of the material being photographed the photographer followed a definite method in "sectioning" the material. It is customary to begin photoing at the upper left hand corner of a large sheet and to continue photoing from left to right in equal sections with a small overlap. If necessary, sectioning is continued again — beginning below the first row and continuing on until complete.
4. The majority of users indicate that the textual content is of greatest value, however, a somewhat higher quality reproduction could be made from "photographs" if essential to the understanding of the dissertation. Silver prints of "photographs" may be ordered at additional charge by writing the Order Department, giving the catalog number, title, author and specific pages you wish reproduced.
5. PLEASE NOTE: Some pages may have indistinct print. Filmed as received.

Xerox University Microfilms

300 North Zeeb Road
Ann Arbor, Michigan 48106

76-8342

WILSON, John Michael, 1947-

I. THE STEREOCHEMICAL COURSE OF PENTADIENYL
RADICAL ELECTROCYCLIZATION. II. THERMOLYSIS
OF BIS($\Delta^{1,1}$ -DICYCLOHEXYLMETHYL) OXALATE.
III. THERMOLYSIS OF BIS(4-METHYLBENZHYDRYL)
OXALATE: COMPETING FRAGMENTATION TO RADICALS
AND CARBENES.

The University of Oklahoma, Ph.D., 1975
Chemistry, organic

Xerox University Microfilms, Ann Arbor, Michigan 48106

THE UNIVERSITY OF OKLAHOMA

GRADUATE COLLEGE

- I. THE STEREOCHEMICAL COURSE OF PENTADIENYL RADICAL ELECTRO-
CYCLIZATION
- II. THERMOLYSIS OF BIS($\Delta^{1,1'}$ -DICYCLOHEXENYLMETHYL) OXALATE
- III. THERMOLYSIS OF BIS(4-METHYLBENZHYDRYL) OXALATE: COMPETING
FRAGMENTATION TO RADICALS AND CARBENES

A DISSERTATION

SUBMITTED TO THE GRADUATE FACULTY

in partial fulfillment of the requirements for the

degree of

DOCTOR OF PHILOSOPHY

By

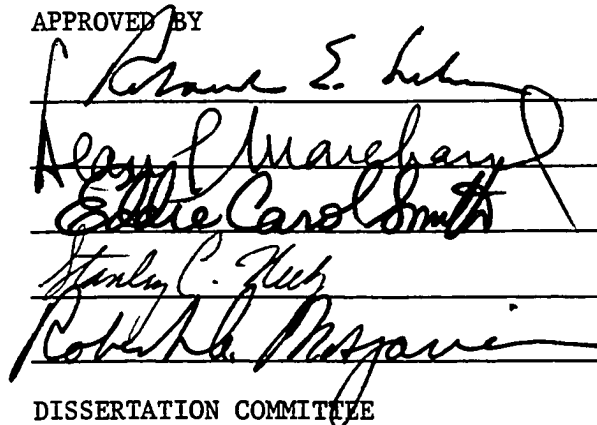
J. MICHAEL WILSON

Norman, Oklahoma

1975

- I. The Stereochemical Course of Pentadienyl Radical Electrocyclization
- II. Thermolysis of Bis($\Delta^{1,1'}$ -dicyclohexenylmethyl) Oxalate
- III. Thermolysis of Bis(4-methylbenzhydryl) Oxalate: Competing Fragmentation to Radicals and Carbenes

APPROVED BY


The signatures are written on a set of five horizontal lines. From top to bottom, the signatures appear to be: 1. A signature that looks like 'R. E. L.' 2. A signature that looks like 'Margaret' 3. A signature that looks like 'E. C. Smith' 4. A signature that looks like 'Stanley C. Kee' 5. A signature that looks like 'Robert H. Mesrobian'

DISSERTATION COMMITTEE

DEDICATION

**Dedicated to Glennis and Melissa, whose love
and devotion have made my life a pleasure**

ACKNOWLEDGMENTS

The author wishes to express his gratitude to Dr. Roland E. Lehr for his guidance and patience during this project and for his willingness to teach. The author thanks Dr. Eddie Smith, Dr. Tom Karns, Dr. Ray Gross, and Dr. William Youngblood for their advice and conversation. Sincerest thanks go to friends and associates, Dr. Robert Allen, Dr. David Vanderah, Bob Hayes, Michael Conway, Michael Griffin, and Ron Stermer, for their stimulating and educational exchanges. The author expresses his deepest love and gratitude to his parents, Wesley and Norma Wilson, for his rearing and for their continuing support of his endeavors.

TABLE OF CONTENTS

	Page
LIST OF FIGURES	vi
LIST OF TABLES	x
 Part I. THE STEREOCHEMICAL COURSE OF PENTADIENYL RADICAL	
ELECTROCYCLIZATION	1
INTRODUCTION	1
RESULTS AND DISCUSSION	15
EXPERIMENTAL	109
BIBLIOGRAPHY	129
 Part II. THERMOLYSIS OF BIS($\Delta^{1,1'}$ -DICYCLOHEXENYLMETHYL)	
OXALATE	133
INTRODUCTION	133
RESULTS AND DISCUSSION	135
EXPERIMENTAL	151
BIBLIOGRAPHY	157
 Part III. THERMOLYSIS OF BIS(4-METHYLBENZHYDRYL) OXALATE:	
COMPETING FRAGMENTATION TO RADICALS AND CARBENES . .	158
INTRODUCTION	158
RESULTS AND DISCUSSION	159
EXPERIMENTAL	173
BIBLIOGRAPHY	179

LIST OF FIGURES

Figure	Page
 Part I	
1. Generalized Representation of Electrocyclic Reactions.	2
2. Orbital Correlation Diagrams for the Electro- cyclization of Pentadienyl Radical	5
3. 60 MHz PMR Spectrum (CDCl ₃) of XXXVI	20
4. 70 eV Mass Spectrum of XXXVI	21
5. 60 MHz PMR Spectrum (CCl ₄) of XXXVII	22
6. 70 eV Mass Spectrum of XXXVII.	23
7. 60 MHz PMR Spectrum (CDCl ₃) of XXXVIII, Upper Trace Offset +2σ	25
8. 70 eV Mass Spectrum of XXXVIII	26
9. 100 MHz PMR Spectrum (C ₆ D ₆ , 5°C) of XXXIV	28
10. IR Spectrum (CCl ₄) of XXXIV	29
11. 70 eV Mass Spectrum of XXXIV	30
12. Schematic of Vacuum Decomposition Apparatus	35
13. GLC Trace of Products Produced by Ambient Temperature Vacuum Decomposition of XXXIV	37
14. 60 MHz PMR Spectrum (CDCl ₃) of XLVIII-a	40
15. 70 eV Mass Spectrum of XLVIII-a	41
16. IR Spectrum (film) of XLVIII-a)	42

LIST OF FIGURES (continued)

Figure	Page
17. 60 MHz PMR Spectrum (CDCl ₃) of XLVIII-b	43
18. 70 eV Mass Spectrum of XLVIII-b	44
19. IR Spectrum (film) of XLVIII-b	45
20. 100 MHz PMR Fourier-Transform Spectrum (CDCl ₃) of XLIX-a	46
21. 70 eV Mass Spectrum of XLIX-a	47
22. IR Spectrum (film) of XLIX-a	48
23. 100 MHz Fourier-Transform Spectrum (CDCl ₃) of XLIX-b	49
24. 70 eV Mass Spectrum of XLIX-b	50
25. IR Spectrum (film) of XLIX-b	51
26. 100 MHz PMR Fourier-Transform Spectrum (CDCl ₃) of XLIX-c	52
27. 70 eV Mass Spectrum of XLIX-c	53
28. IR Spectrum (film) of XLIX-c	54
29. GLC Trace of Products Produced by Decomposition of XXXIV in GLC Injection Port	57
30. Schematic of Vacuum Hot Tube	59
31. 100 MHz PMR Fourier-Transform Spectrum (CDCl ₃) of L-a .	62
32. 70 eV Mass Spectrum of L-a	63
33. IR Spectrum (film) of L-a	64
34. 100 MHz PMR Fourier-Transform Spectrum (CDCl ₃) of L-b .	65
35. 70 eV Mass Spectrum of L-b	66
36. IR Spectrum (film) of L-b	67

LIST OF FIGURES (continued)

Figure	Page
37. 100 MHz PMR Fourier-Transform Spectrum (CDCl ₃) of L-c	68
38. 70 eV Mass Spectrum of L-c	69
39. IR Spectrum (film) of L-c	70
40. 60 MHz PMR Spectrum (CDCl ₃) of LIII	74
41. 70 eV Mass Spectrum of LIII	75
42. 60 MHz PMR Spectrum (CCl ₄) of LIV	76
43. 70 eV Mass Spectrum of LIV	77
44. 60 MHz PMR Spectrum (CCl ₄) of LI	78
45. 70 eV Mass Spectrum of LI	79
46. IR Spectrum (film) of LI	80
47. 60 MHz PMR Spectrum (CCl ₄) of LVIII	84
48. 70 eV Mass Spectrum of LVIII	85
49. 60 MHz PMR Spectrum (CCl ₄) of LIX	86
50. 70 eV Mass Spectrum of LIX	87
51. 60 MHz PMR Spectrum (CCl ₄) of LVI	88
52. 70 eV Mass Spectrum of LVI	89
53. IR Spectrum (film) of LVI	90
54. 60 MHz PMR Spectrum (C ₆ D ₆) of LV	91
55. 70 eV Mass Spectrum of LV	92
56. IR Spectrum (film) of LV	93
57. GLC Traces of Products Produced by Vacuum Hot Tube Decomposition of XXXIV at a) 250°, b) 300°, and c) 350°	96
58. Solid Addition Bulb for Hot Tube Thermolyses	119

LIST OF FIGURES (continued)

Figure	Page
Part II	
1. 60 MHz PMR Spectrum (THF) of LXVIII; Offset +36	138
2. 70 eV Mass Spectrum of LXVIII	139
3. IR Spectrum (CHCl ₃) of LXVIII	140
4. 60 MHz PMR Spectrum (CCl ₄) of LXIX	141
5. 70 eV Mass Spectrum of LXIX	142
6. IR Spectrum (CCl ₄) of LXIX	143
7. 60 MHz PMR Spectrum (C ₆ D ₆) of LXVII	144
8. IR Spectrum (KBr) of LXVII	145
9. 70 eV Mass Spectrum of LXVII	146
Part III	
1. 60 MHz PMR Spectrum (CDCl ₃) of LXXI	161
2. 70 eV Mass Spectrum of LXXI	162
3. IR Spectrum of LXXI	163
4. 60 MHz PMR Spectrum (CDCl ₃) of LXXXI	164
5. 70 eV Mass Spectrum of LXXXI	165
6. IR Spectrum (CHCl ₃) of LXXXI	166

LIST OF TABLES

Table	Page
Part I	
1. Product Distribution; Ambient Temperature Vacuum Decomposition of XXXIV	36
2. Product Distribution <u>versus</u> Time; Decomposition of Hexane Solution of XXXIV	55
3. Product Distribution; Decomposition of XXXIV in GLC Injection Port	56
4. "N" Values for Compounds Analyzed by GLC	100
5. Product Distribution; Vacuum Hot Tube Decompositions of XXXIV	101
Part III	
1. Product Distribution; Thermal Decomposition of LXXI . . .	167
2. Deuterium Content of Products Produced in the Thermolysis of LXXI-d ₂ at 650°	169

I. THE STEREOCHEMICAL COURSE OF PENTADIENYL

RADICAL ELECTROCYCLIZATION

CHAPTER 1

INTRODUCTION

In recent years, the state of organic chemistry has been greatly enhanced through the application of the molecular orbital (MO) theory of bonding to organic molecules.¹⁻³ MO theory has played an important role in expanding our understanding of the mechanisms of organic reactions in general, and has had a profound impact in the particular area of concerted organic reactions.

In 1965, a theoretical treatment of concerted reactions was first set forth in a series of communications by Woodward and Hoffmann.^{4a-c} In this series of preliminary communications and later in a more fully developed treatise form,⁵ they laid the foundation for a new principle governing all concerted reactions: the conservation of orbital symmetry. Other methods for treating concerted reactions have since evolved,^{6a-c} each differing in conceptual approach and rigor. But, all have contained a consideration of the symmetries of the molecular orbitals involved in the reaction.

The application of MO methods and orbital symmetry considerations to systems containing an even number of conjugated electrons have achieved

much success in predicting and rationalizing the stereochemical course and outcome of concerted reactions. While these theoretical methods have proven highly suitable in their application to closed shell molecules, they are less definitive in regard to the concerted reactions of odd electron, open shell molecules. Because of the importance of this area of study, it seemed highly desirable to determine the relative merits of the various theoretical approaches which have been developed and to determine, if possible, the limits to which they may be applied. In this regard, we have directed our attention and endeavors toward an area of concerted reactions where theoretical conflict occurs: the electrocyclization of odd electron, open shell systems. The following discussion of the difficulties encountered in dealing with such systems will be limited to thermal reactions, that is, electrocyclization occurring from the ground electronic states of conjugated radicals, since our experimental work is also limited to that area.

Electrocyclic reactions, which comprise a large class of concerted reactions, are represented schematically in the general form shown in Figure 1. They are defined as the cyclization of an $n\pi$ -electron system

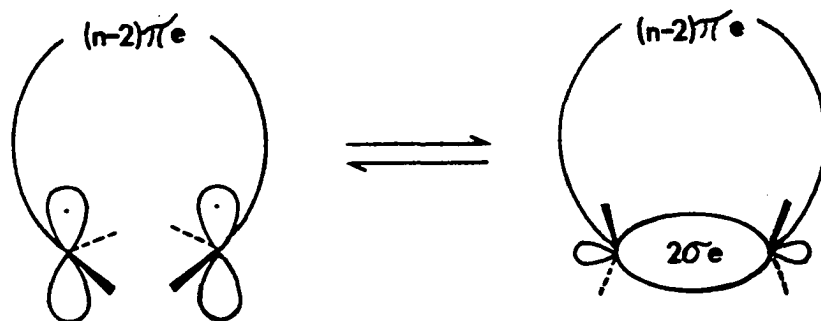
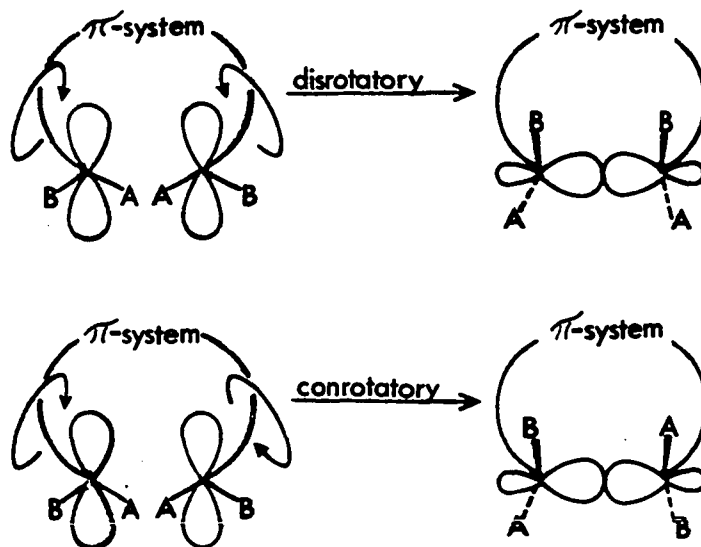


Figure 1 Generalized Representation of Electrocyclic Reactions

to an $(n-2)\pi + 2\sigma$ -electron system or the reverse process (electrocyclic ring opening).⁵ The transition state of electrocyclic reactions is such that all first order bonding changes take place on a closed curve of continuous orbital overlap. For this reason, Woodward and Hoffmann have termed reactions such as these "pericyclic".⁵

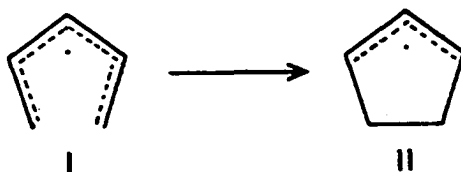


Scheme 1

Scheme 1 shows the two distinct cyclization modes (or the reverse ring opening modes) which are possible for electrocyclic reactions. These modes are termed "disrotatory" and "conrotatory". In systems where the substituents on the terminal π -lobes are suitably labelled (i.e., $A \neq B$ in Scheme 1), the two alternative modes for electrocyclization lead to distinctly different products. Thus, these stereochemical labels provide direct evidence for the processes under consideration. In general, electrocyclic reactions show a high degree of stereospecificity in regard to the two alternative modes of cyclization.

Orbital correlation diagrams have served well to illustrate the role of orbital symmetry in electrocyclic reactions.^{6a} For example,

Consider the cyclization of pentadienyl radical (I) to cyclopentenyl radical (II). The orbital correlation diagrams for the two possible modes



of electrocyclization are shown in Figure 2. The MO's used here are simple Hückel molecular orbitals (HMO's). The symmetry elements for electrocyclization are a two-fold rotation axis (C_2) for the conrotatory mode and a mirror plane (m) for the disrotatory mode.^{6a} The proper construction of correlation diagrams are described in the literature.^{5,6a,7}

The principle of conservation of orbital symmetry⁵ requires that the symmetry characteristics of the reactant and product orbitals remain unchanged throughout a concerted reaction and, further, levels of like symmetry may not cross (non-crossing exclusion rule). In the Woodward and Hoffmann treatment, a reaction is said to be "symmetry allowed" when the electronic states of the reactant and product correlate and "symmetry forbidden" when the electronic states of the reactant and product do not correlate.⁵

The orbital correlation diagrams in Figure 2 reveal precisely the difficulty of dealing with odd electron systems: neither mode of cyclization correlates the ground state of I with the ground state of II via a "symmetry allowed" pathway! This situation is not isolated to the particular case at hand, but pertains to the electrocyclization of virtually*

*In certain cases, the odd electron may occupy a degenerate orbital which does enable the correlation of reactant and product states.

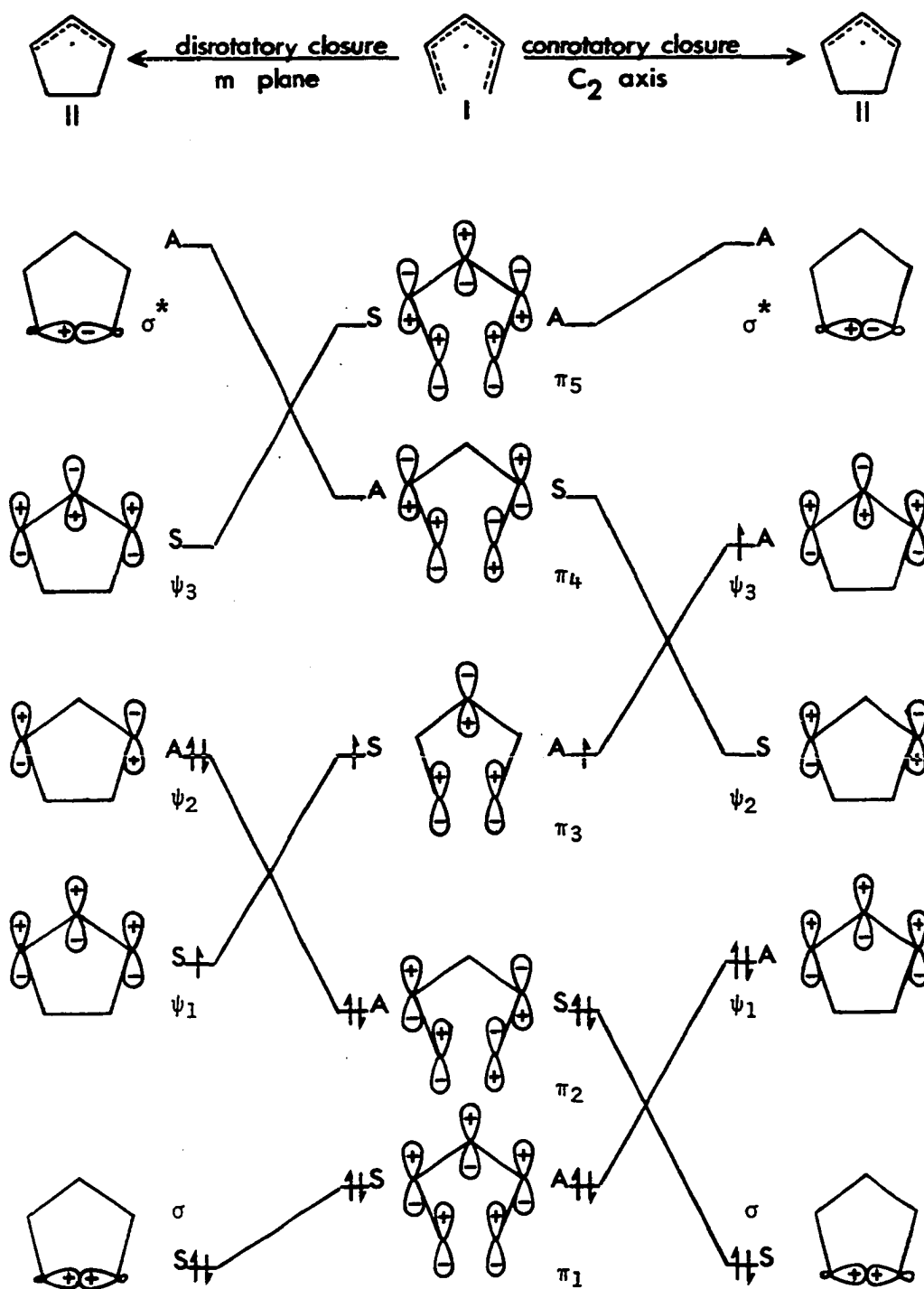


Figure 2 Orbital Correlation Diagrams for the Electrocyclization of Pentadienyl Radical

all odd electron systems as well, whether neutral free radical, anion radical, or cation radical.

In dealing with electrocyclic reactions in general, Woodward and Hoffmann^{4a} placed a special emphasis on the highest occupied molecular orbital (HOMO). They suggested that the course of electrocyclization should occur in a manner such that a maximum bonding interaction occur between the terminal lobes of the HOMO of the acyclic polyene system. For odd electron systems, they suggested that electrocyclization should follow the same stereochemical course as the even electron system containing one electron further. In other words, electrocyclization for pentadienyl radical should be the same as that for the anion: disrotatory. Likewise, they predicted that the ring-opening of cyclopropyl radical to allyl radical should occur by the conrotatory mode.^{4a} These arguments were supported by extended Hückel (EH) calculations.^{4a,8}

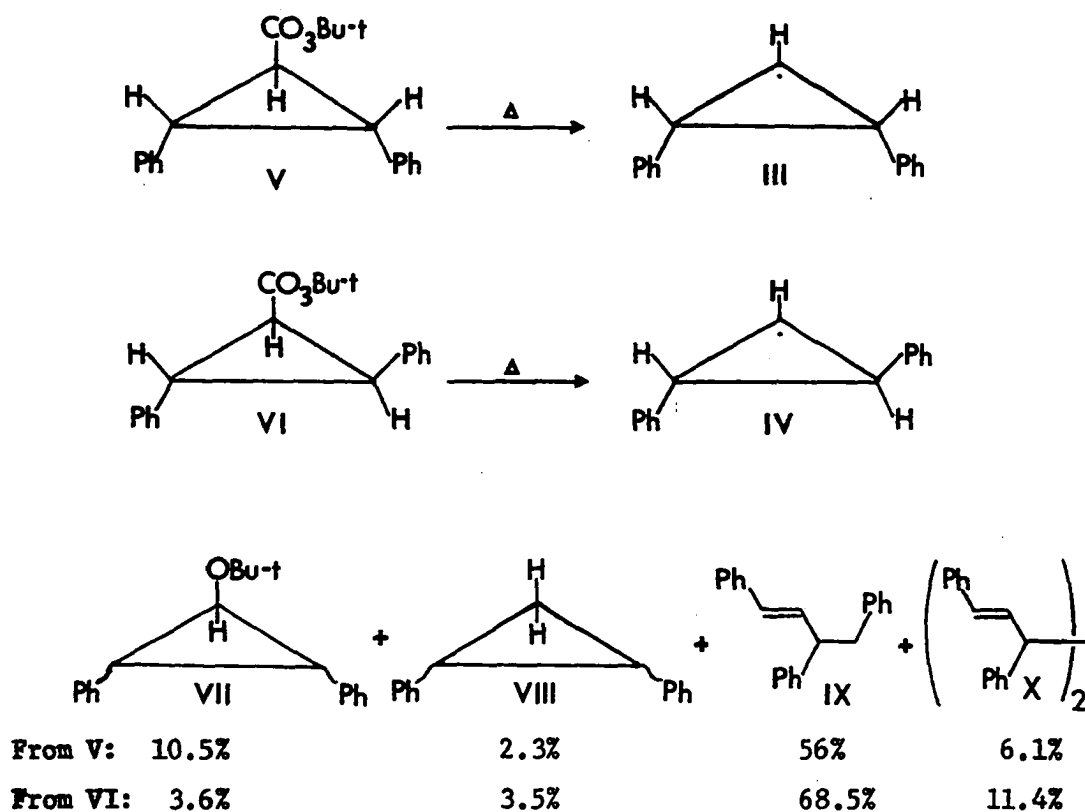
Consideration of the orbital correlation diagrams in the case of cyclopropyl ring opening led Longuet-Higgins and Abrahamson^{6a} to suggest that either mode of ring opening should show a much larger activation energy than the corresponding thermal transformation of the cyclopropyl anion or cation. State correlation diagrams indicated that the conrotatory ring opening in cyclopropyl radical was only slightly favored over the disrotatory pathway. From this, these authors concluded that electrocyclic reactions of radicals might be non-stereospecific.^{6a}

The perturbational molecular orbital (PMO) method of Dewar^{3,6e} has been instrumental in clearly defining aromaticity, non-aromaticity, and anti-aromaticity in cyclic conjugated systems. The PMO method has also given definition to the nature of transition states in pericyclic reactions.⁹ In the PMO treatment of closed shell systems, thermally

induced pericyclic reactions proceed preferentially via aromatic transition states whereas the corresponding photochemically induced reactions proceed via excited forms of anti-aromatic transition states. The PMO treatment of electrocyclization in radicals leads to a prediction of non-stereospecificity, since all cyclic conjugated radicals are non-aromatic within the limits of the PMO method.³

Dewar and co-workers¹⁰ have investigated the electrocyclic ring opening of cyclopropyl radical using the method of modified intermediate neglect of differential overlap (MINDO/2).¹¹ The calculated activation energy for the disrotatory ring opening of 25 kcal/mol clearly favored this process over the conrotatory pathway whose calculated energy of activation was 52.6 kcal/mol. The results here indicate the preferred ring opening mode for cyclopropyl radical to be disrotatory, in direct contradiction to HOMO considerations and E_H^{4a} calculations. The activation energy for cyclopropyl radical ring opening in the vapor phase has been experimentally estimated at 20-22 kcal/mol¹² which is in fair agreement with that calculated for the disrotatory pathway by the MINDO/2 method.

Rüchardt and co-workers^{13a,b} have studied the ring opening of cis- and trans-2,3-diphenylcyclopropyl radicals (III) and (IV), which were generated by thermolysis of the corresponding t-butyl peroxyesters (V) and (VI).



Scheme 2

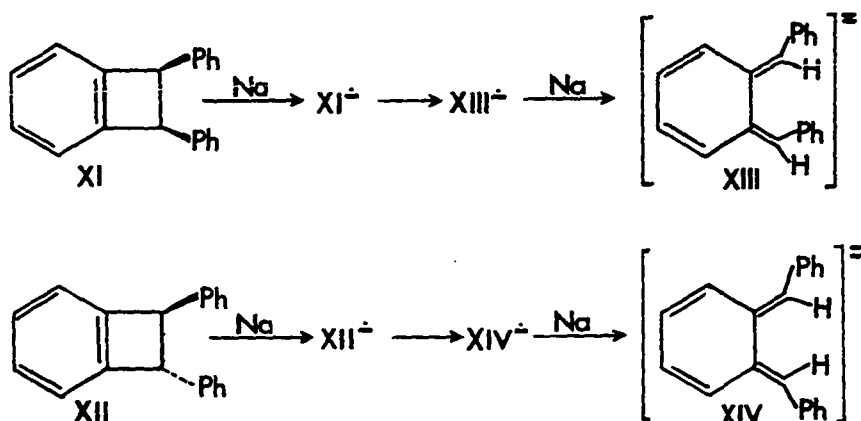
Decomposition of V and VI in ethylbenzene gave rise to mixtures containing products in which the cyclopropyl ring had remained intact (represented by the structures VII and VIII in Scheme 2) and products which were derived from allyl radicals (represented by the structures IX and X in Scheme 2).

Direct evidence for the mode of ring opening was not attainable through examination of product stereochemistry. The higher incidence of ring opened products (IX) and (X) obtained from VI indicated that the trans-2,3-diphenylcyclopropyl radical (IV) ring opened more easily than did cis-2,3-diphenylcyclopropyl radical (III). This observation was interpreted^{13b} as evidence for a stereoselective ring opening process in these radicals. That disrotatory ring opening could occur was established

by examination of a series of cyclopropyl radicals which were structurally constrained to ring open only by the disrotatory mode.^{13c}

These workers concluded that both disrotatory and conrotatory processes may be operative in the ring opening of cyclopropyl radicals. Based upon the differences in yields of ring opened products from III and IV and theoretically supported assumptions^{13d} of the activation energies involved, they interpreted their experimental data as evidence which favored the disrotatory ring opening mode.^{13b} These arguments, however, were clearly not unequivocal and may be subject to further interpretation.

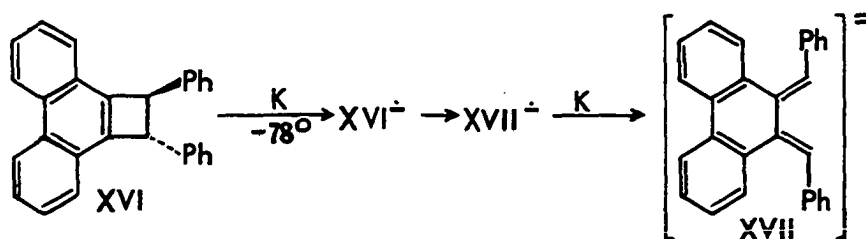
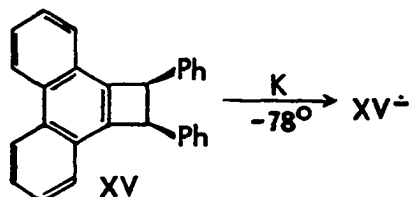
Bauld and co-workers^{14a} have observed a large preference for conrotatory ring opening in the anion radicals of cis- and trans-3,4-diphenylbenzocyclobutenes (XI) and (XII).



Their results, based upon quenching studies and NMR studies of the dianions (XIII²⁻) and (XIV²⁻) established the sequences: XI → XI^{•-} → XIII^{•-} → XIII²⁻ and XII → XII^{•-} → XIV^{•-} → XIV²⁻. In both of these cases, the initially formed anion radicals (XI^{•-}) and (XII^{•-}) underwent facile conrotatory ring opening at -78° to (XIII^{•-}) and (XIV^{•-}), respectively, followed by fast reduction to their respective dianions (XIII²⁻) and (XIV²⁻). Attempts to observe any paramagnetic species by ESR were unsuccessful due

to the rapidity of the processes involved in their conversions to the diamagnetic dianions.

In related work, Bauld *et al*^{14b} have studied the reduction of cis- and trans-1,2-diphenylphenanthro[1]cyclobutenes (XV) and (XVI) with potassium, sodium, and lithium biphenyl anion radical.



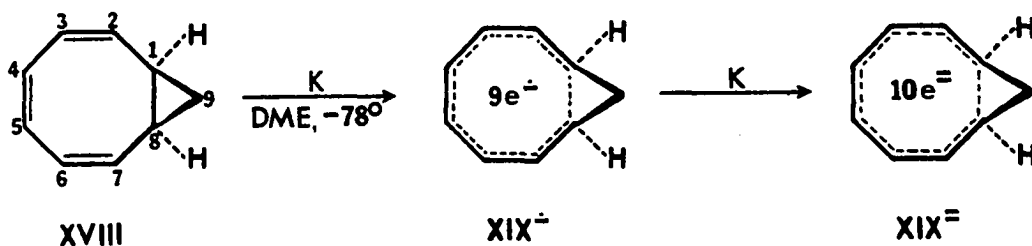
The reduction of the cis compound (XV) at -78° led to the formation of the anion radical (XV^{•-}) which was indefinitely stable at -78° and resisted decomposition up to 0°. The identity of XV^{•-} was established by ESR. In striking contrast, the reduction of the trans compound (XVI) led to the rapid formation of the dianion (XVII²⁻) presumably via the sequence: XVI → XVI^{•-} → XVII^{•-} → XVII²⁻. No paramagnetic species could be detected (ESR) during this latter process. The stereochemistry of the dianion (XVII²⁻) could not be directly established due to a rapid E,E ⇌ Z,E equilibration which occurred even at -78°.

The observed failure for the cis anion radical (XV^{•-}) to undergo ring cleavage and the extreme ease of ring cleavage in the trans anion radical (XVI^{•-}) are easily understood on the basis of steric repulsion

which would develop in the conrotatory opening of cis $XV^{\dot{-}}$ but not in trans $XVI^{\dot{-}}$. This behavior is similar to that observed in the thermal conrotatory ring openings of neutral 3,4-diphenylcyclobutene derivatives.¹⁵ On this basis, these workers^{14b} inferred that the stereochemistry of $XVII^{\dot{-}}$ initially formed by reduction of XVI was E,E and concluded that the observed rate order for ring cleavage in the anion radicals ($XVI^{\dot{-}} > XV^{\dot{-}}$) was diagnostic for conrotation in such systems. These studies have clearly demonstrated that in the interconversion of the cyclobutene-butadiene anion radicals, the preferred mode is the same as for the neutral cyclobutene-butadiene systems: conrotatory.

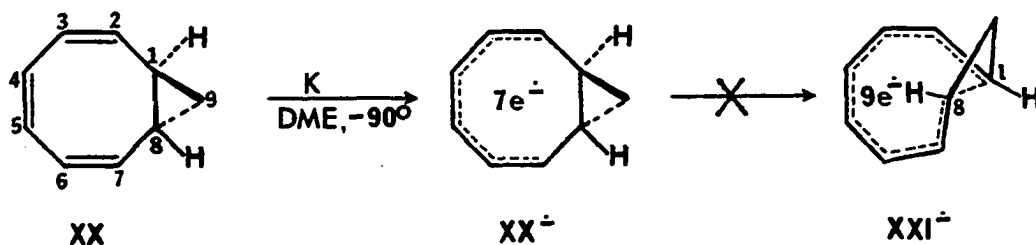
Further support for conrotatory ring opening in the cyclobutene anion radicals was presented by way of INDO/MO calculations.^{14b} These calculations, performed on the unsubstituted cyclobutene and benzocyclobutene anion radical parent systems, clearly favored the conrotatory ring opening pathway. The results of these experimental and theoretical studies not only question the predominance of the singly occupied HOMO interaction but even its qualitative importance.

Winstein and co-workers^{16a-c} have reported that addition of an electron to cis-bicyclo-(6.1.0.)nona-2,4,6-triene (XVIII) gives rise to the homoconjugated, 9-electron anion radical ($XIX^{\dot{-}}$) in which the cyclopropyl C_1-C_8 bond has been ruptured in a manner which is clearly disrotatory. Katz, et al^{16d} reported that electrolysis of XVIII produced essentially



identical results. Further reduction of this system leads to the formation of the homoaromatic dianion ($\text{XIX}^{\bar{2}}$). The structures of these electronated species were firmly established by ESR for $\text{XIX}^{\dot{-}}$ and NMR for $\text{XIX}^{\bar{2}}$.

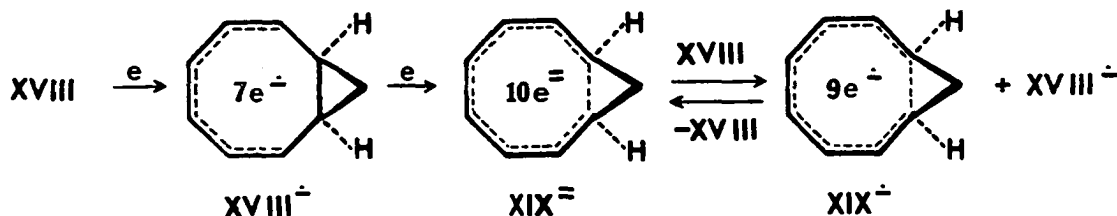
The disrotatory rupture (or partial rupture) of the $\text{C}_1\text{-C}_8$ bond in XVIII may be explained on the basis of the symmetry of the singly occupied HOMO in $\text{XIX}^{\dot{-}}$.^{16a,b; 5} In order to test this possibility, Winstein, *et al.*^{16b} also examined the reduction of trans-bicyclo-(6.1.0)nona-2,4,6-triene (XX) by potassium metal in glyme (DME). In this case, reduction of XX led



to the formation of the anion radical ($\text{XX}^{\dot{-}}$) in which the cyclopropyl $\text{C}_1\text{-C}_8$ bond remained intact and uninvolved in delocalization of the unpaired electron. The structure of $\text{XX}^{\dot{-}}$ was established by ESR. The radical ($\text{XX}^{\dot{-}}$) showed no tendency to rearrange to any other paramagnetic species (i.e., $\text{XXI}^{\dot{-}}$) nor to undergo further reduction to a dianionic species.

The disrotatory rupture of the $\text{C}_1\text{-C}_8$ bond in $\text{XX}^{\dot{-}}$ would lead to a very unfavorable $\text{C}_1\text{-C}_8$ interaction in the trans, cis, cis, cis-cyclonona-tetraene anion radical ($\text{XXI}^{\dot{-}}$). It is clearly more advantageous for $\text{XX}^{\dot{-}}$ to remain a hexatriene type anion radical in which the odd electron is delocalized only over the relatively planar $\text{C}_2\text{-C}_7$ portion than to rupture partially or fully the $\text{C}_1\text{-C}_8$ bond in this fashion. It is also clear from the experimental data that a conrotatory $\text{C}_1\text{-C}_8$ bond rupture did not occur in $\text{XX}^{\dot{-}}$.

These results have been cited⁵ as an example of HOMO symmetry control in open shell systems. Recently, however, Winstein, *et al.*^{16c} have raised the question of the possible involvement of the dianion (XIX⁼) in the ring opening process. The sequence of events below show how this might reasonably provide an alternative explanation.



The initially formed 7-electron anion radical (XVIII^{•-}) may undergo further reduction concurrently with disrotatory rupture of the C₁-C₈ bond which would lead to the dianion (XIX⁼). In this case, the HOMO of XIX⁼ is doubly occupied and the disrotatory C₁-C₈ rupture is "allowed" by symmetry considerations⁵ and also by orbital correlation diagrams.^{6a} The disproportionation between the dianion (XIX⁼) and a neutral molecule of XVIII would then provide an equilibrium concentration of the homoconjugated species (XIX^{•-}). Similar disproportionation phenomena are known to occur between the anion radicals and dianions of cyclooctatetraene^{17,18} and its derivatives.¹⁹

Summary

In this chapter, we have discussed the various theoretical treatments which have been generated to deal with concerted reactions in general and electrocyclic reactions in particular. We have also discussed the available experimental studies which pertain to an area where theoretical conflict occurs, namely, in the treatment of electrocyclization of odd electron, open shell systems.

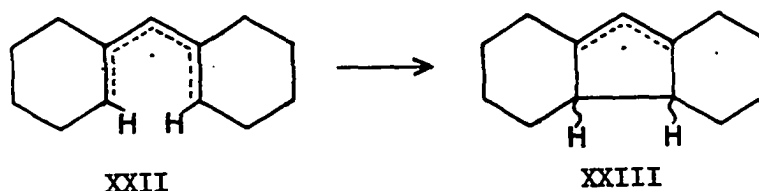
When we began this work (Fall 1969), only the experimental studies of Winstein, et al.^{16a-c} and Katz, et al.^{16d} were available. Since then, the body of experimental data in this area has not been greatly increased and theoretical justifications have just begun to appear. In the following chapter, we add our experimental contribution, the stereochemical course of electrocyclization of a pentadienyl radical, to this area of endeavor.

CHAPTER 2

RESULTS AND DISCUSSION

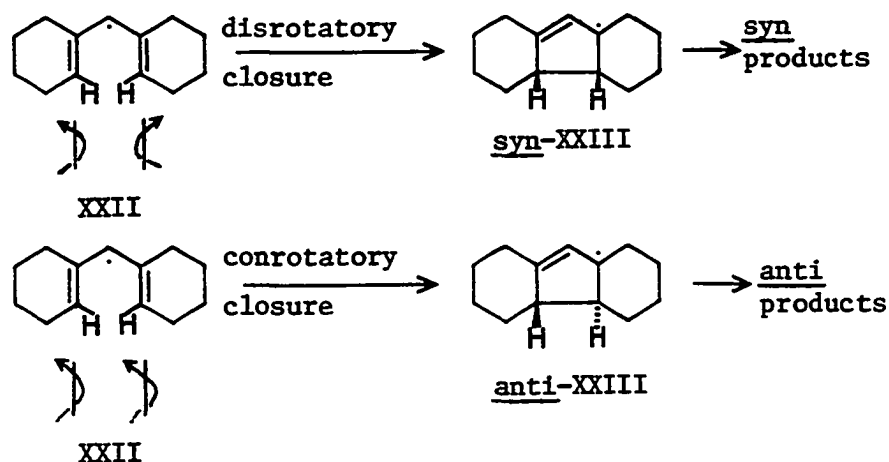
There are no reports in the literature on the stereochemical course of cyclization in pentadienyl radicals. The cyclization of unsubstituted pentadienyl radical to cyclopentenyl radical (I→II) in the gas phase has been studied by Egger and Benson.²⁰ Although very little cyclization occurred under their reaction conditions, they were able to estimate an activation energy of 24 kcal/mol for the cyclization, which is an energetically accessible region for the studies proposed herein.

We chose to study the electrocyclization of $\Delta^{1,1'}$ -dicyclohexenylmethyl radical (XXII). Our proposed plan of study was to generate XXII from a suitable precursor under conditions whereby the electrocyclization (XXII→XXIII) would be effected.



Our aim was to isolate and identify the neutral products arising from XXII and XXIII. By examining these products, we hoped to determine the stereochemical course of the electrocyclization (XXII→XXIII). Specifically, we sought products derived from the cyclized radical (XXIII) which

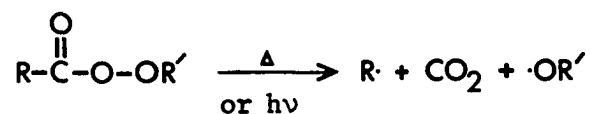
retained intact the stereochemistry at the points of cyclic fusion. Those products which contained the syn backbone stereochemistry would indicate disrotatory closure (XXII → syn-XXIII) and those which contained the anti backbone stereochemistry would indicate conrotatory closure (XXII → anti-XXIII) (see Scheme 3). The exact nature of the aforementioned products would depend upon the method used for generation of XXII.



Scheme 3

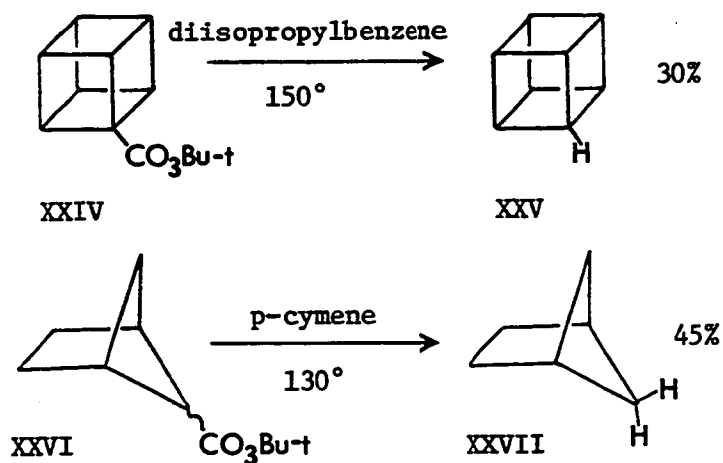
Choice of Radical Precursor

Peroxyesters are known^{21,22} to decompose upon thermolysis or photolysis according to Scheme 4 giving rise to large yields of alkyl and alkoxy radicals. Due to the large yields of radicals produced, peroxyesters

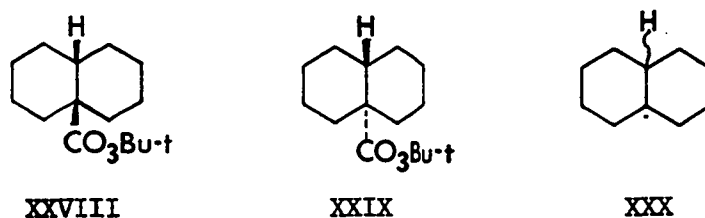


Scheme 4

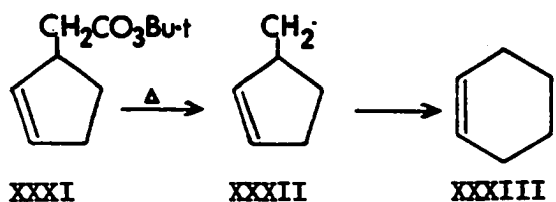
have been successfully employed in synthesis. For example, the final step in the synthesis of cubane (XXV) was thermolysis of the peroxyester (XXIV) in diisopropylbenzene.²³ Similarly, the peroxyester (XXVI) was thermolyzed in p-cymene in the synthesis of bicyclo-(2.1.1.)hexane (XXVII).²⁴



The cis- and trans-9-carbo-t-butylperoxydecalins (XXVIII) and (XXIX) were used to generate and study the stereochemistry of the 9-decalyl free radical (XXX).²⁵



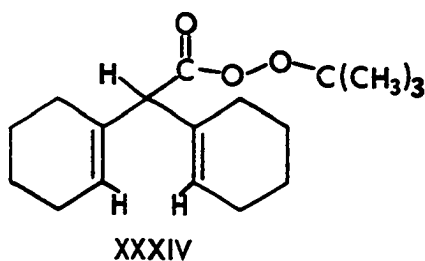
Peroxyesters have also shown their utility as radical precursors for studies of free radical rearrangements. Thus, the thermal decomposition of XXXI generated the Δ^2 -cyclopentenylmethyl radical (XXXII) which subsequently rearranged to the 4-cyclohexenyl radical (XXXIII) via a 1,2-vinyl



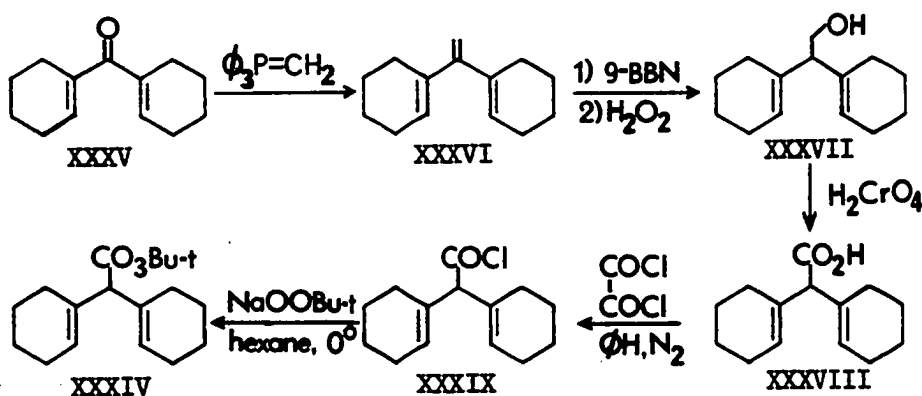
group shift.²⁶ This observation was made through isolation and identification of products derived from both XXXII and XXXIII.

As previously discussed, the electrocyclic ring openings of several substituted cyclopropyl radicals have been studied by thermolysis of their corresponding *t*-butyl peroxyesters.^{13a-c} Other recent uses of peroxyesters as radical precursors have been described by Singer.²⁷

Based on the utility demonstrated by peroxyesters as radical precursors, we chose to prepare and study the thermal decomposition of *t*-butyl $\Delta^{1,1}$ -dicyclohexenylperoxyacetate (XXXIV). The synthesis of XXXIV



was accomplished according to the sequence outlined in Scheme 5.



Scheme 5

Synthesis of Peroxyacetate (XXXIV)

The treatment of $\Delta^{1,1'}$ -dicyclohexenyl ketone (XXX)²⁸ with pre-generated triphenylphosphonium methyllide in ether gave the triene (XXXVI). The product was usually isolated by chromatography on silica gel in yields of 75-84%. Further purification by short-path distillation at ca. 50°/0.05 torr gave XXXVI as a clear colorless oil. The 60 MHz PMR spectrum in CDCl_3 (Figure 3) showed: δ 5.65 (2H multiplet, ring olefinic protons), 4.8 (2H singlet, methylene protons), 1.4-2.3 (16H multiplet, ring protons). The 70 eV mass spectrum (Figure 4) showed: m/e 188 (M^+ , parent ion), 146 (base peak, $\text{M}^+ - \text{C}_3\text{H}_6$). The IR spectrum (film) showed: cm^{-1} 1630 and 1590 (C=C), 880 (C=CH₂), 850 (C=CH).

The triene (XXXVI) was subjected to hydroboration using 9-borabicyclo-(3.3.1)nonane (9-BBN) in tetrahydrofuran followed by oxidation in basic hydrogen peroxide, according to the procedure of Knights and Brown,²⁹ to give the unsaturated alcohol (XXXVII). The alcohol (XXXVII) was isolated by chromatography on silica gel. Recrystallization gave pure white XXXVII, mp 38-39.5°, in 78% yield. The 60 MHz PMR spectrum on CCl_4 (Figure 5) showed: δ 5.45 (2H multiplet, olefinic protons), 3.55 (2H doublet, J=7 Hz, protons on carbon bearing oxygen), 2.5 (1H broad triplet, J=7 Hz, di-allylic proton), 1.4-2.2 (17H multiplet, ring protons and hydroxylic proton). The 70 eV mass spectrum (Figure 6) showed: m/e 206 (M^+ , parent ion), 188 ($\text{M}^+ - \text{H}_2\text{O}$), 175 (base peak, $\text{M}^+ - \text{CH}_2\text{OH}$). The IR spectrum (KBr) showed: cm^{-1} 3280 (O-H), 1050 (C-O).

The alcohol (XXXVII) was subjected to further oxidation using a Jones reagent which was prepared according to the method of Djerassi, et al.³⁰ Slow, dropwise addition of the Jones reagent to a stirred solution of XXXVII in acetone resulted in reaction mixtures which contained

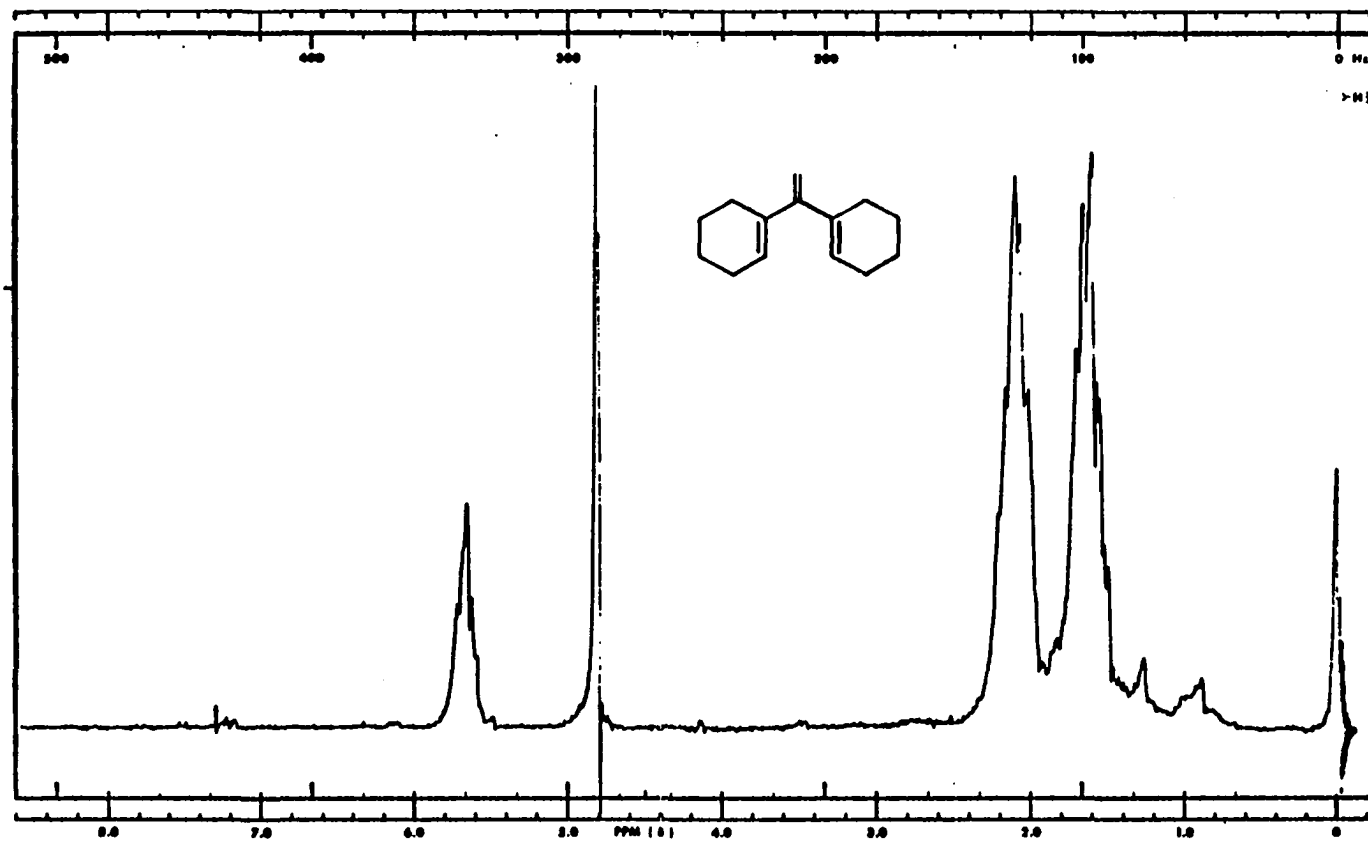


Figure 3 60 MHz PMR Spectrum (CDCl_3) of XXXVI

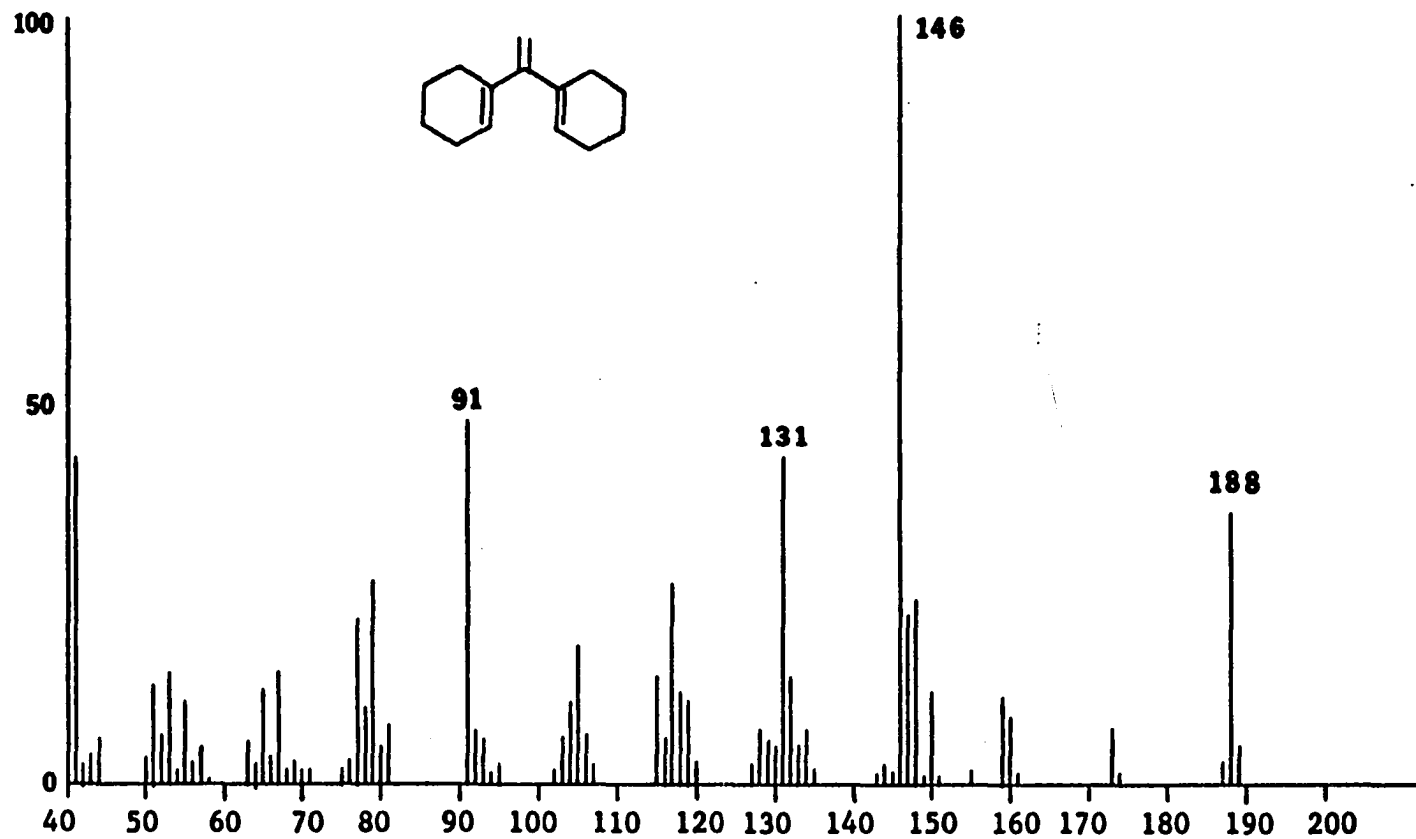


Figure 4 70 eV Mass Spectrum of XXXVI

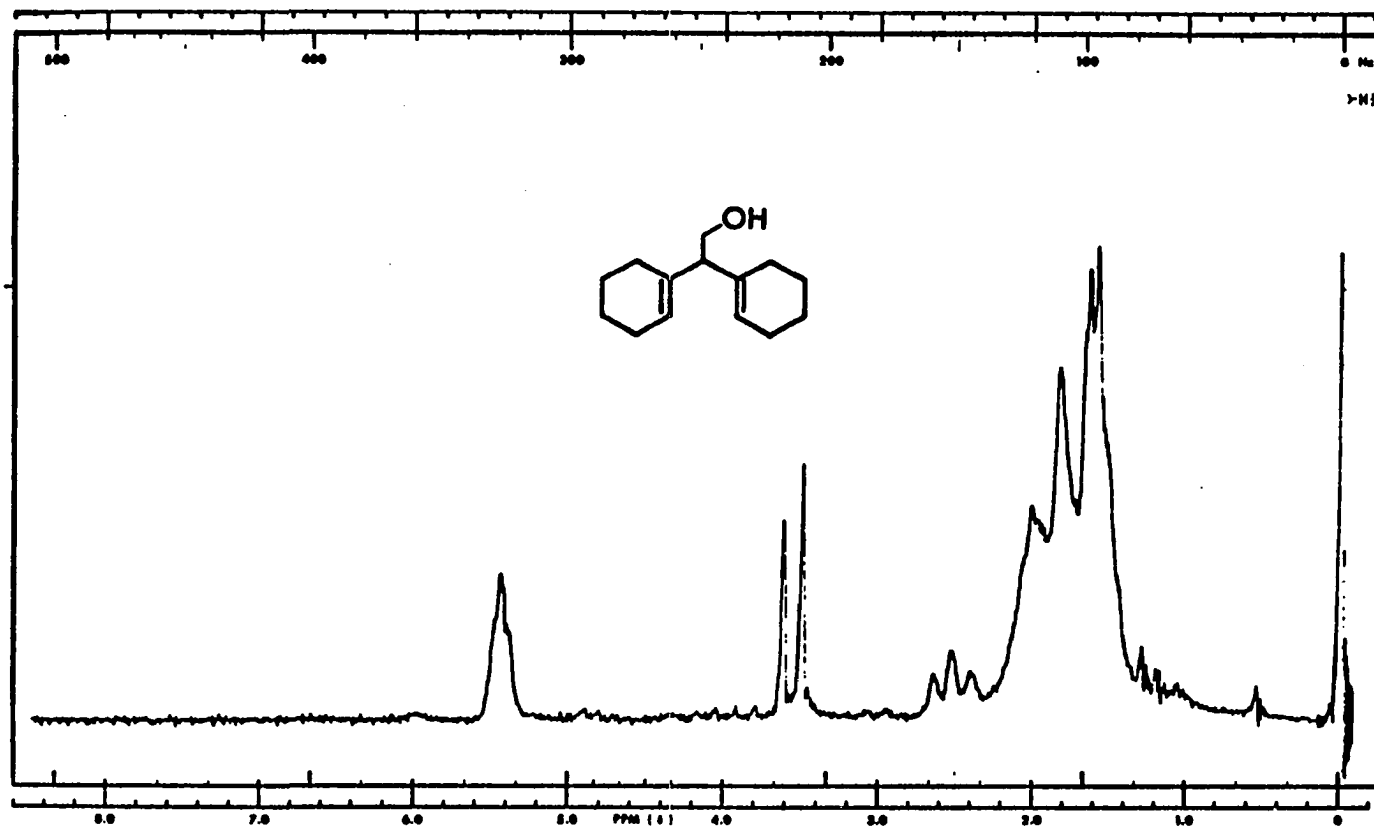


Figure 5 60 MHz PMR Spectrum (CCl_4) of XXXVII

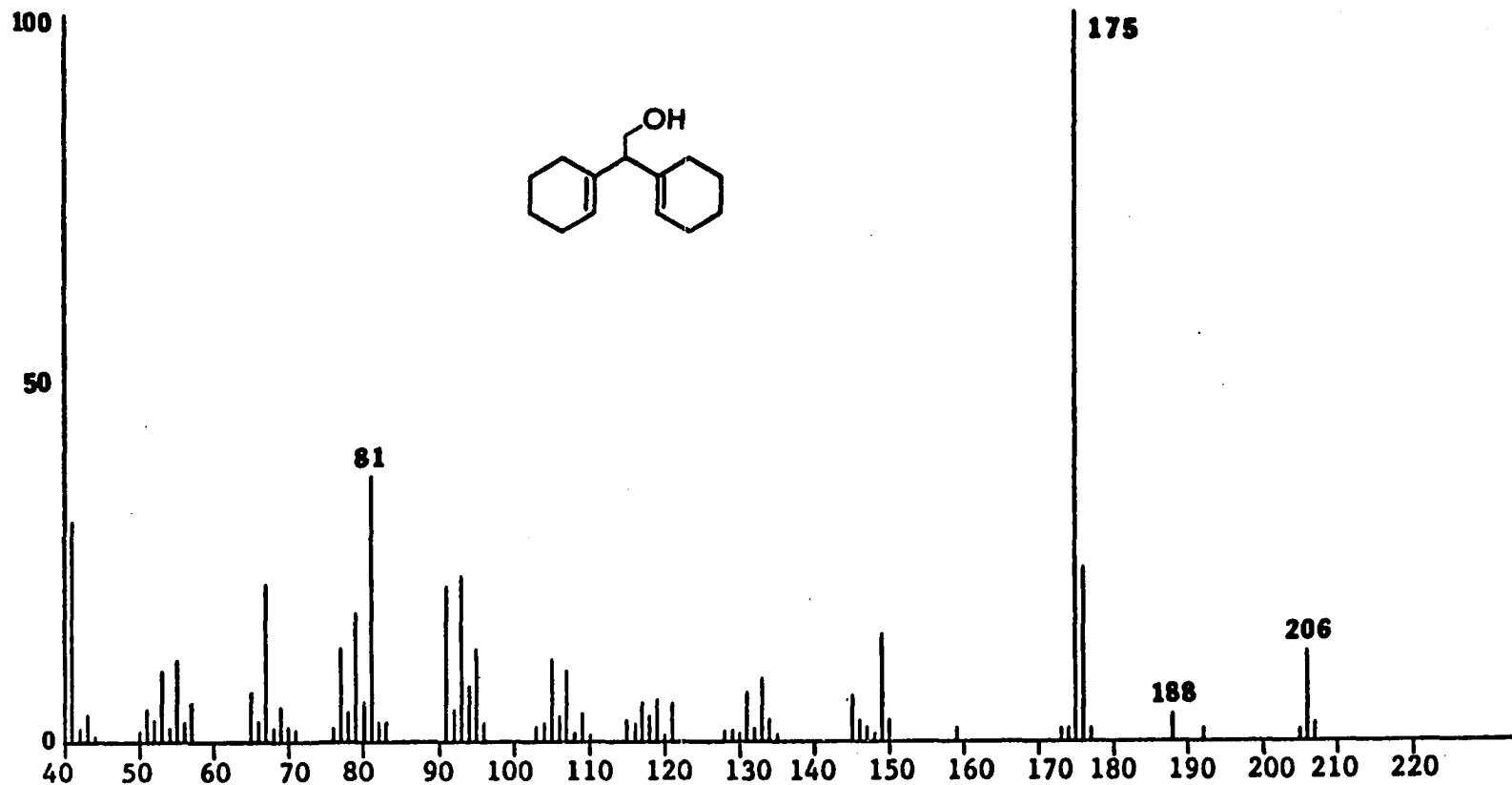
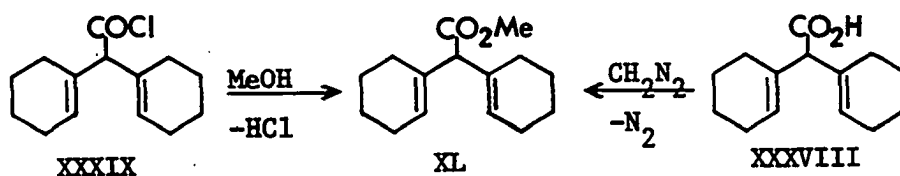


Figure 6 70 eV Mass Spectrum of XXXVII

the desired acid (XXXVIII) in rather low and irreproducible yields. The isolation of XXXVIII from such a procedure was difficult due to the darkened thick, syrupy nature of the reaction mixture. This procedure also produced the ketone XXXV as a major by-product. In this work, the best yields of XXXVIII were obtained when the alcohol (XXXVII) in acetone was treated with excess Jones reagent added at once, followed by quenching with isopropyl alcohol after a five minute reaction time. When the reaction was run in this manner, the thick, syrupy reaction mixture was avoided and XXXVIII was more easily obtained in yields of 45-49%. Recrystallization from hexane afforded XXXVIII as pure white crystals, mp 114-115.5°. The 60 MHz PMR spectrum in CDCl_3 (Figure 7) showed: δ 10.1 (1H broad singlet, acidic proton), 5.65 (2H multiplet, olefinic protons), 3.55 (1H broad singlet, proton α to carboxyl carbon), 1.4-2.3 (16H multiplet, ring protons). The 70 eV mass spectrum (Figure 8) showed: m/e 220 (M^+ , parent ion), 175 ($\text{M}^+ - \text{CO}_2\text{H}$), 81 (base peak). The IR spectrum (KBr) showed: cm^{-1} 3450 (O-H), 1700 (C=O), 1125 and 1080 (C-O).

The acid (XXXVIII) was smoothly converted into the acid chloride (XXXIX) by treatment in anhydrous benzene (under dry N_2) with oxalyl chloride. The course of the reaction was easily followed by quenching small amounts of the reaction medium in excess methanol. This served to convert the acid chloride (XXXIX) in the sample into the methyl ester (XL) as shown in Scheme 6. Thin layer chromatography (TLC) of this resulting



Scheme 6

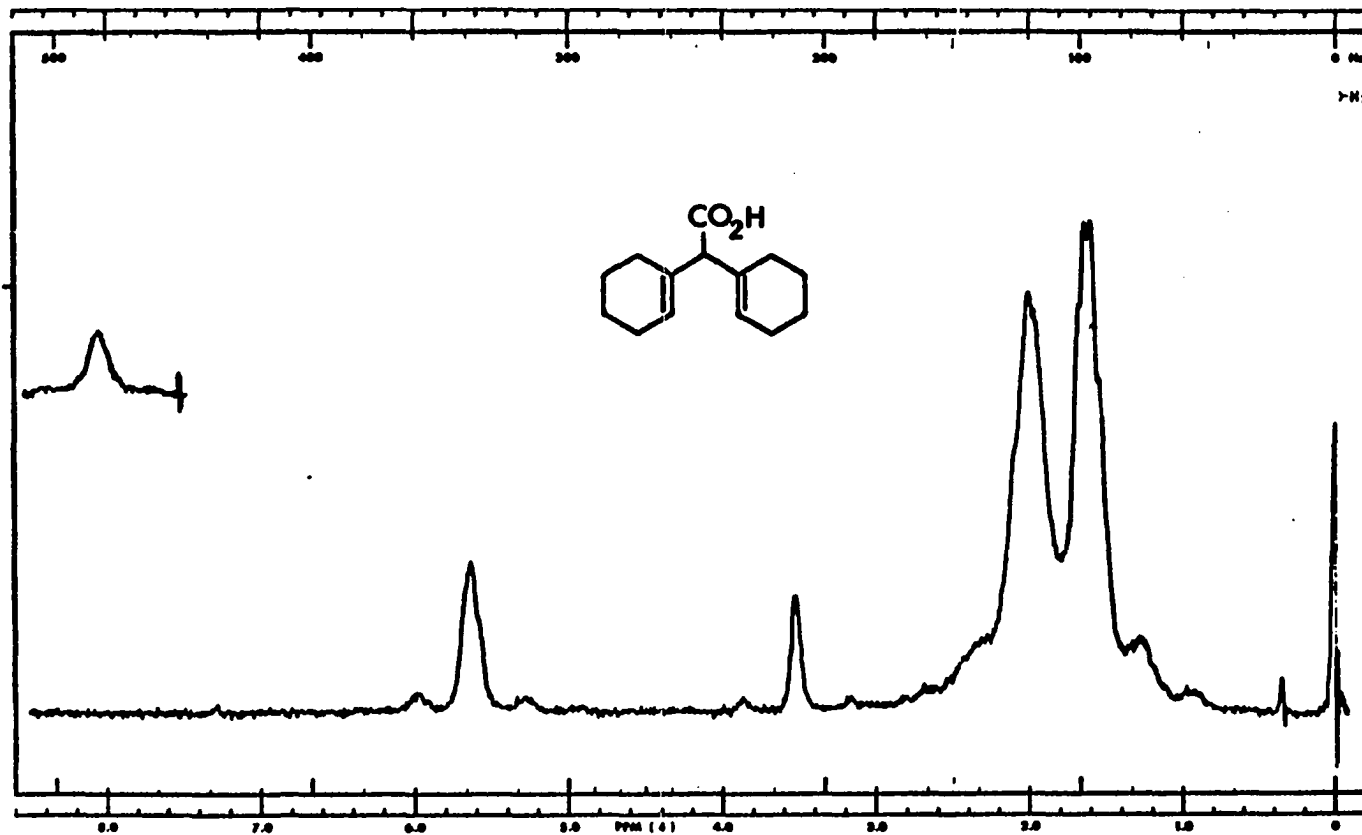


Figure 7 60 MHz PMR Spectrum (CDCl₃) of XXXVIII, Upper Trace Offset +2δ

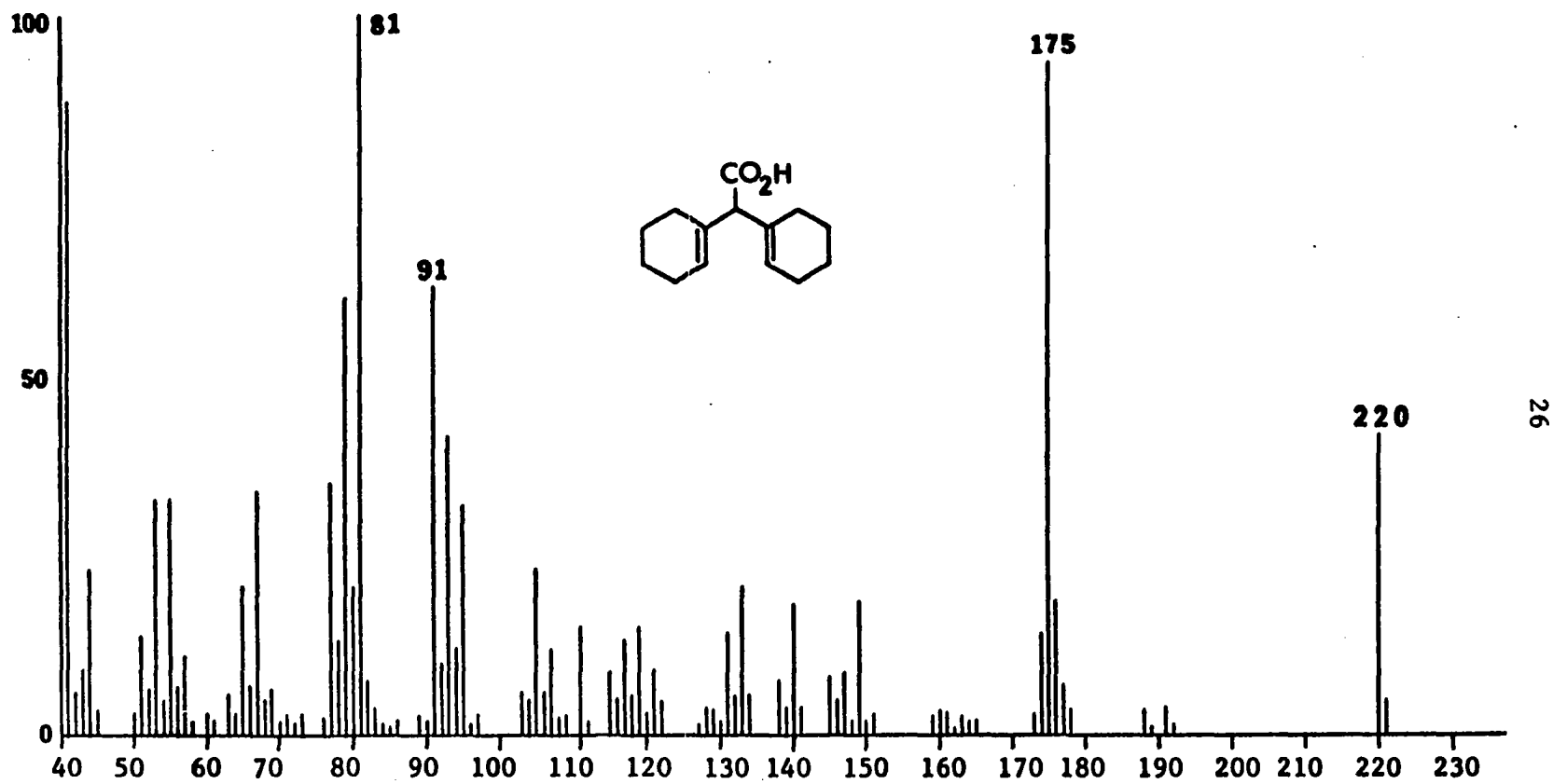


Figure 8 70 eV Mass Spectrum of XXXVIII

mixture (elution with 20% EtOAc/hexane) followed by iodine staining allowed visualization of the acid (XXXVIII) and the ester (XL). Since the ester was derived only from the acid chloride present, this procedure served to monitor the progress of formation of XXXIX. The ester (XL) formed from XXXIX was identical by TLC and gas liquid chromatography (GLC) to that produced by treatment of XXXVIII with diazomethane in ether, as shown in Scheme 6. When formation of the acid chloride (XXXIX) was judged to be completed, the mixture was concentrated to yield XXXIX as a viscous slightly yellowed oil. The IR spectrum (film) showed: cm^{-1} 1790 (C=O). The acid chloride (XXXIX) was used without further purification or characterization.

Treatment of XXXIX in ice cold, dry, olefin-free hexane with an excess of sodium t-butyl peroxide³¹ gave the peroxyacetate (XXXIV) in excellent yields. When adequate care was taken to shield reaction and work-up vessels from sunlight and to maintain them at ice bath temperatures, whenever possible, the peroxyacetate (XXXIV) was obtained as a white solid from work-up. Yields were ca. 80% overall from the acid (XXXVIII). Recrystallization from degassed hexane (-76°) gave XXXIV as pure white crystals which melted sharply at $34-35^\circ$. Solid XXXIV could be stored in the freezer (-20°) under oxygen-free nitrogen for months without appreciable decomposition. The 100 MHz PMR spectrum of XXXIV (Figure 9) in degassed benzene- d_6 at 5° showed: δ 5.82 (2H multiplet, olefinic protons), 3.62 (1H broad singlet, proton α to C=O), 1.7-2.3 (8H multiplet, allylic ring protons), 1.3-1.7 (8H multiplet, ring protons), 1.19 (9H singlet, t-butyl protons). The IR spectrum (Figure 10) in degassed carbon tetrachloride showed: cm^{-1} 1770 (peroxyester C=O), 1380 and 1365 ($-\text{C}(\text{CH}_3)_3$), 1075 and 1060 (C-O). The carbonyl stretching frequency at 1770 cm^{-1} is

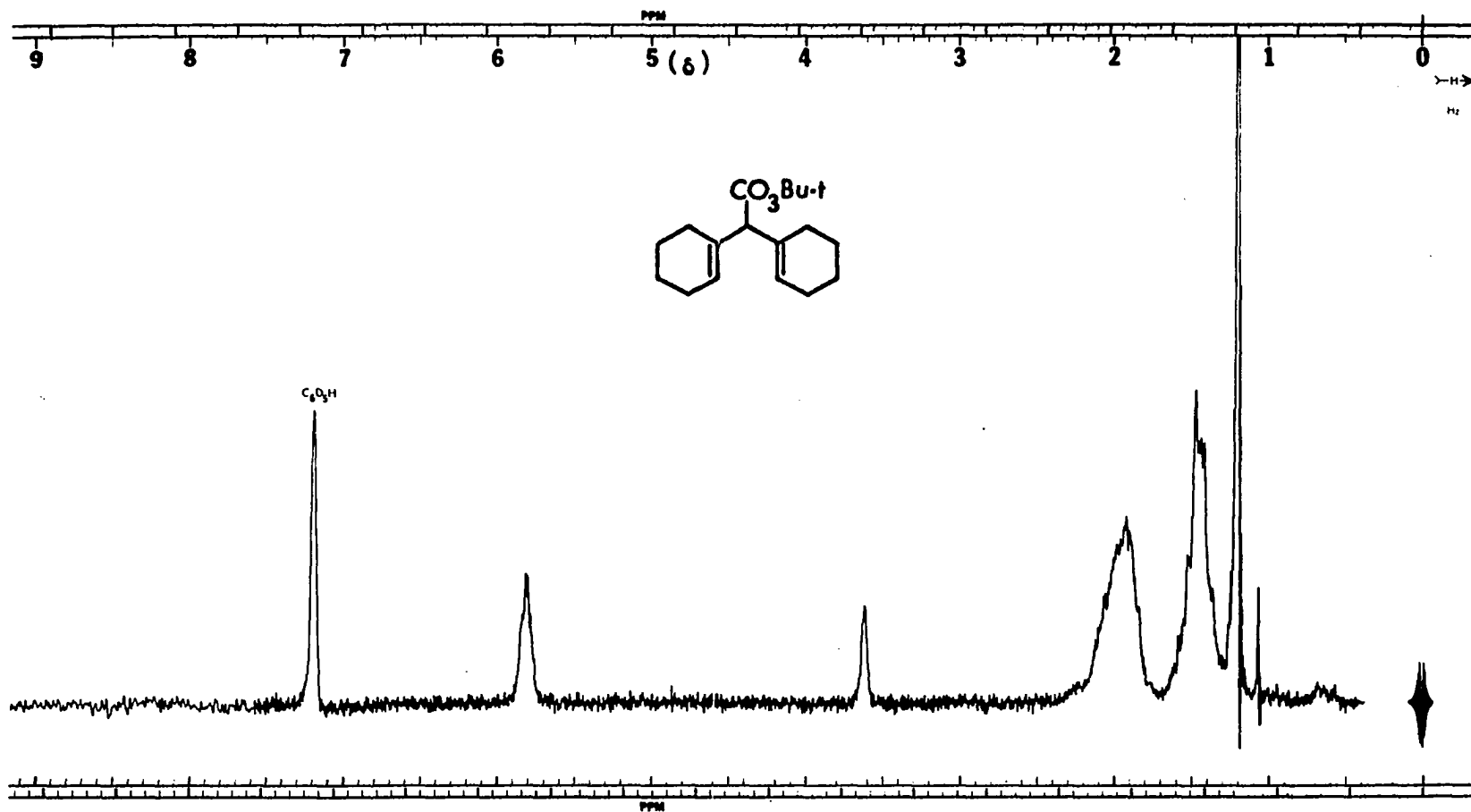


Figure 9 100 MHz PMR Spectrum (C₆D₆, 5°C) of XXXIV

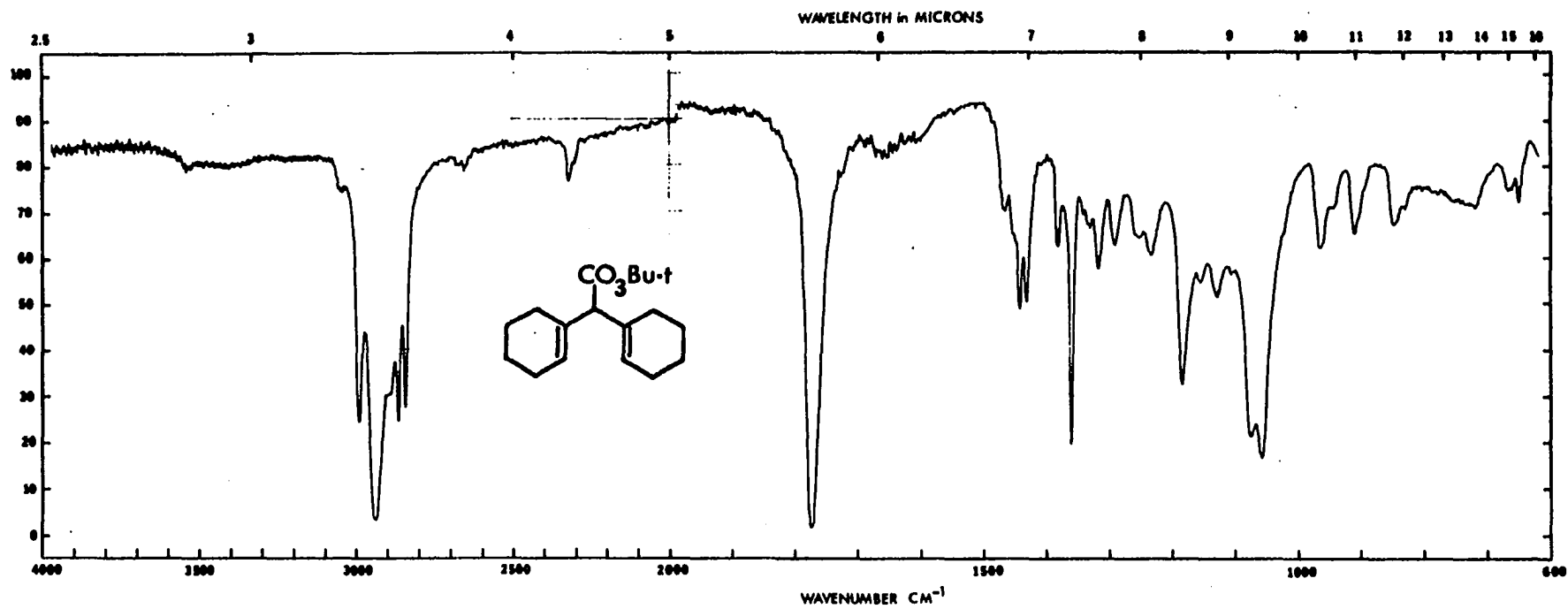


Figure 10 IR Spectrum (CCl_4) of XXXIV

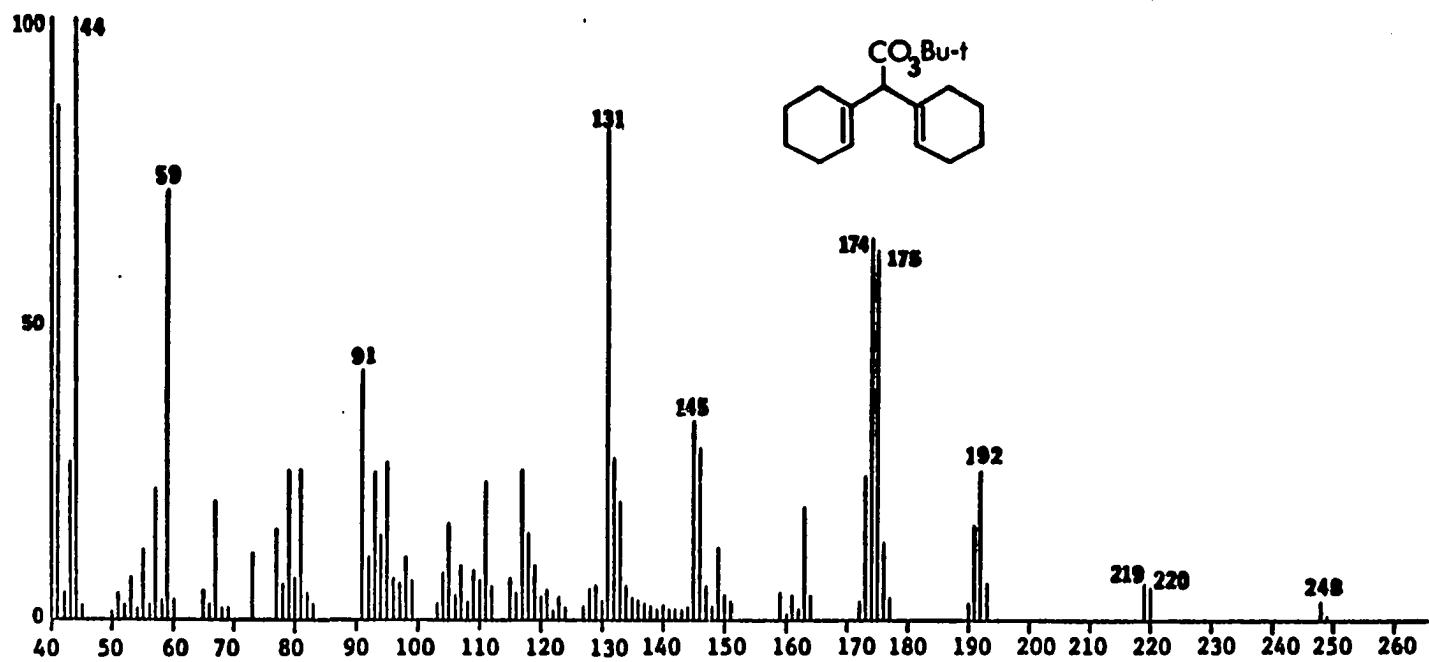
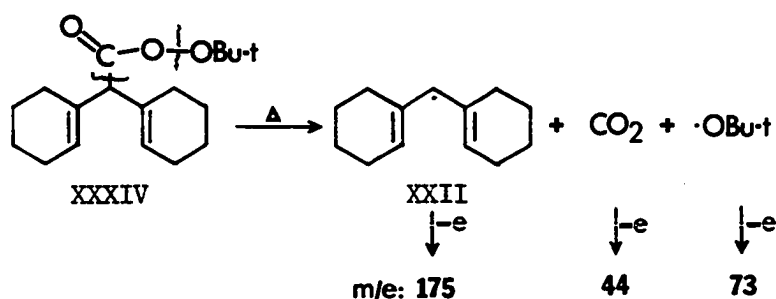


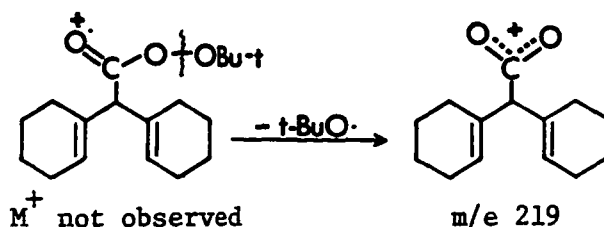
Figure 11 70 eV Mass Spectrum of XXXIV

typical for peroxyesters.²⁷

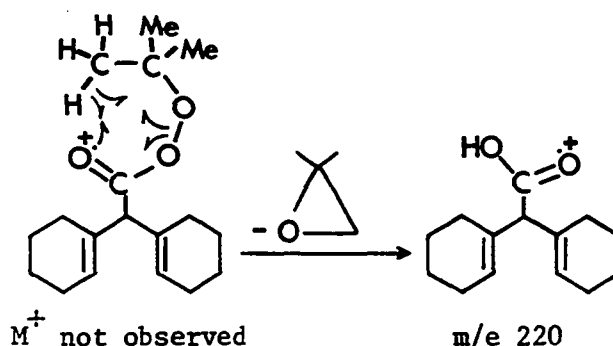
The 70 eV mass spectrum of XXXIV is shown in Figure 11. The parent ion (mol. wt. of XXXIV is 292) was not observed. This was not an unexpected result since XXXIX decomposes at ambient room temperature. The base peak appeared at m/e 44. This was attributed to the formation of CO₂ and was the expected result of thermal peroxyester decomposition (see Scheme 4). Sizeable ions appeared at m/e 175 (62% of base peak) and m/e 73 (11%). These ions may be attributed to the fragmentation of XXXIV upon ionization or prior to ionization as depicted below. It was not possible,



however, to distinguish between contributions to the m/e 175 and 73 ions as depicted above and contributions to those ions which were due to neutral compounds formed from XXII and the t-butoxy radical (\cdot OBu-t). This is due to the fact that the mass spectrometer does not possess any intrinsic ability to distinguish between ions formed from neutral molecules and those formed from free radicals. The ions at m/e 248 and 174 are very probably due to products formed by thermal decomposition of XXXIV prior to ionization. These products will be the subject of a later discussion. The ion appearing at m/e 219 (6% of base peak) corresponds to a loss of t-BuO \cdot from the parent ion. This is depicted below.



The ion at m/e 220 (5.5% of base peak) corresponds to the parent ion for the acid XXXVIII. This ion may arise via a rearrangement-fragmentation process such as is shown below.



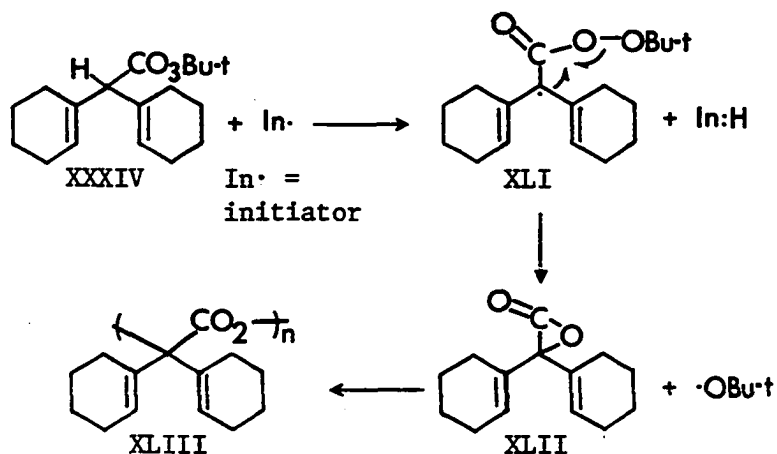
Here again, it was not possible to distinguish whether the ions at m/e 219 and 220 arose from processes occurring before or after ionization.

Stability of the Peroxyacetate (XXXIV)

The peroxyacetate (XXXIV) was found to be unstable at ambient room temperature. Crystalline XXXIV would soften and melt into a clear viscous mass after exposure to ambient room temperature for several hours. This process was accelerated by the presence of air or exposure to sunlight. Bubbles of a gas (presumably CO_2) formed slowly in the melt. Solutions of XXXIV in hexane, which had not been degassed, evolved CO_2 (presumed) slowly over ca. 30-40 minutes at room temperature. The course of such

decomposition could be followed via IR spectroscopy by observing the disappearance of the carbonyl absorption at 1770 cm^{-1} and the appearance of the CO_2 absorption at 2320 cm^{-1} .

During such decompositions, a clear viscous film was formed on the vessel walls and was largely hexane insoluble. This substance exhibited a broad carbonyl absorption in the IR centered at 1745 cm^{-1} . This is attributed to a polyester of the general formula (XLIII) which is shown as arising from the radical-induced decomposition pathway in Scheme 7.



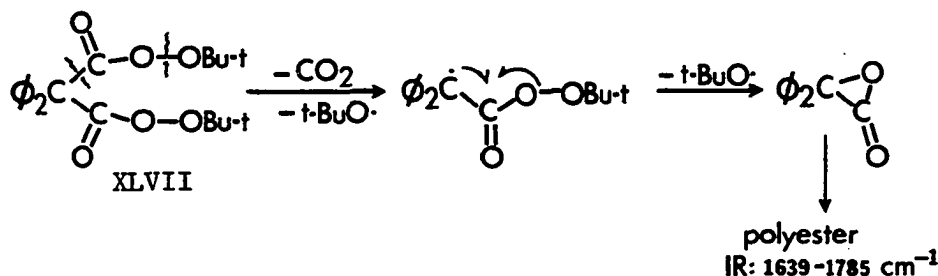
Scheme 7

The induced decomposition is initiated by radical abstraction of the hydrogen α to the carbonyl group of XXXIV, giving rise to an intermediate radical (XLI). Fragmentation and cyclization of XLI leads to the formation of an unstable α -lactone (XLII) which then polymerizes to XLIII. The *t*-butoxy radical serves as a further chain carrier. Our observation of air sensitivity implies that the induced decomposition may be initiated by O_2 . Singer²⁷ suggests that such induced decomposition is usually significant in *t*-butyl peroxyesters containing α -hydrogens,

particularly in solvents of poor hydrogen atom transferring ability (i.e., hexane). This process assumes varying degrees of importance for the t-butyl peroxyesters of isobutyric (XLIV),³² diphenylacetic (XLV)³³ and exo- and endo-norbornane carboxylic acids (XLVI).³⁴



Bartlett and Gortler³³ were able to show that the polyester (principal IR absorption $1639\text{--}1785\text{ cm}^{-1}$) derived via the induced decomposition of t-butyl diphenylperoxyacetate (XLV) was the same as that which arose via the homolytic decomposition of di-t-butyl diphenylperoxymalonate (XLVII) shown below.



Solutions of XXXIV in hexane which had been degassed (by the freeze-pump-thaw method) showed more stability. This was evidenced by scanning the IR spectrum periodically. After about 1 hour at ambient room temperature, the carbonyl absorption at 1770 cm^{-1} showed a small decrease and the CO_2 absorption at 2320 cm^{-1} was barely perceptible. When crystalline XXXIV was maintained under a vacuum of ca. 0.01 torr (in the dark) with dry ice

isopropanol bath trapping, the white crystalline form persisted as a loose white powder for ca. 6 days. The products of decomposition were collected in the cold trap. After 6 days only a small amount of residue remained (presumably the polyester (XLIII)). The products which were produced in this manner will be discussed presently. The peroxyacetate (XXXIV) could be examined by TLC. Care was taken to shield the chromatography plate (silica gel PF, UV indicating) from sunlight and to complete the process as rapidly as possible. After elution with 15% EtOAc/hexane, XXXIV appeared on the plate at R_f 0.66, as a slightly UV active spot which stained heavily with iodine. Although a certain amount of decomposition inevitably occurred on the plate, the TLC provided a useful means of diagnosing the presence of XXXIV and was used throughout this work.

Ambient Temperature Decompositions of XXXIV

When crystalline XXXIV was maintained under a vacuum of ca. 0.01 torr (in the dark) at ambient room temperature in the apparatus shown schematically in Figure 12, the peroxyacetate underwent slow decomposition. The products of decomposition collected in the dry ice-isopropanol cooled

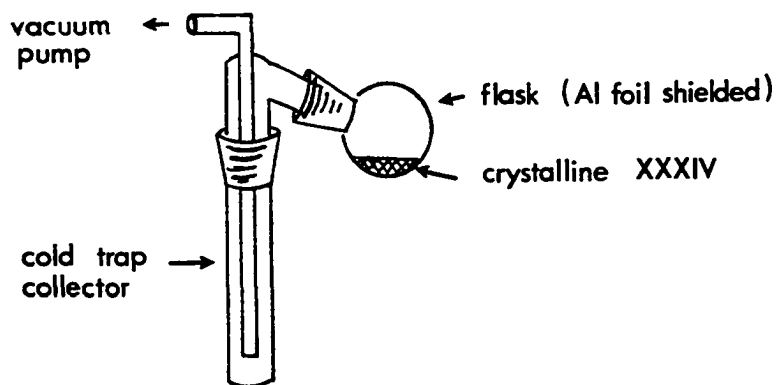


Figure 12 Schematic of Vacuum Decomposition Apparatus

collector. Examination of the product mixture by TLC showed that no peroxyacetate (XXXIV) survived under these conditions. Examination of the mixture by GLC revealed five major components. The GLC trace shown in Figure 13 is typical for this method of decomposition. The trace was run on a 100 ft. FFAP support coated open tubular (S.C.O.T.) column. By a combination of PLC (silica gel) and preparative GLC (FFAP), the components of the mixture were separated and identified as shown below.

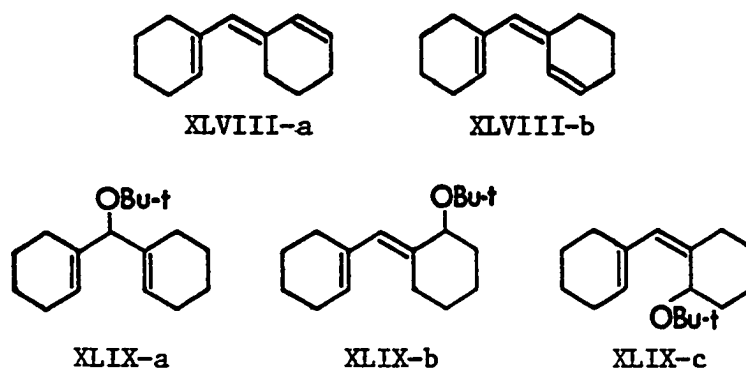


Table 1

Product Distribution; Ambient Temperature Vacuum
Decomposition of XXXIV

Compound:	XLVIII-a	XLVIII-b	XLIX-a	XLIX-b	XLIX-c
% Yield:	8.08	12.11	28.71	9.49	21.54

The percent composition figures shown in Table 1 represent percent of the theoretical yield. They were determined by quantitative GLC. The method employed for quantitation will be discussed in a later section. The products identified account for 79.93% of theory. Structural assignments are based on the spectral data presented in the following discussion.

The trienes (XLVIII-a) and (XLVIII-b) were isolated together from the reaction mixture by PLC (silica gel). They were separated from each

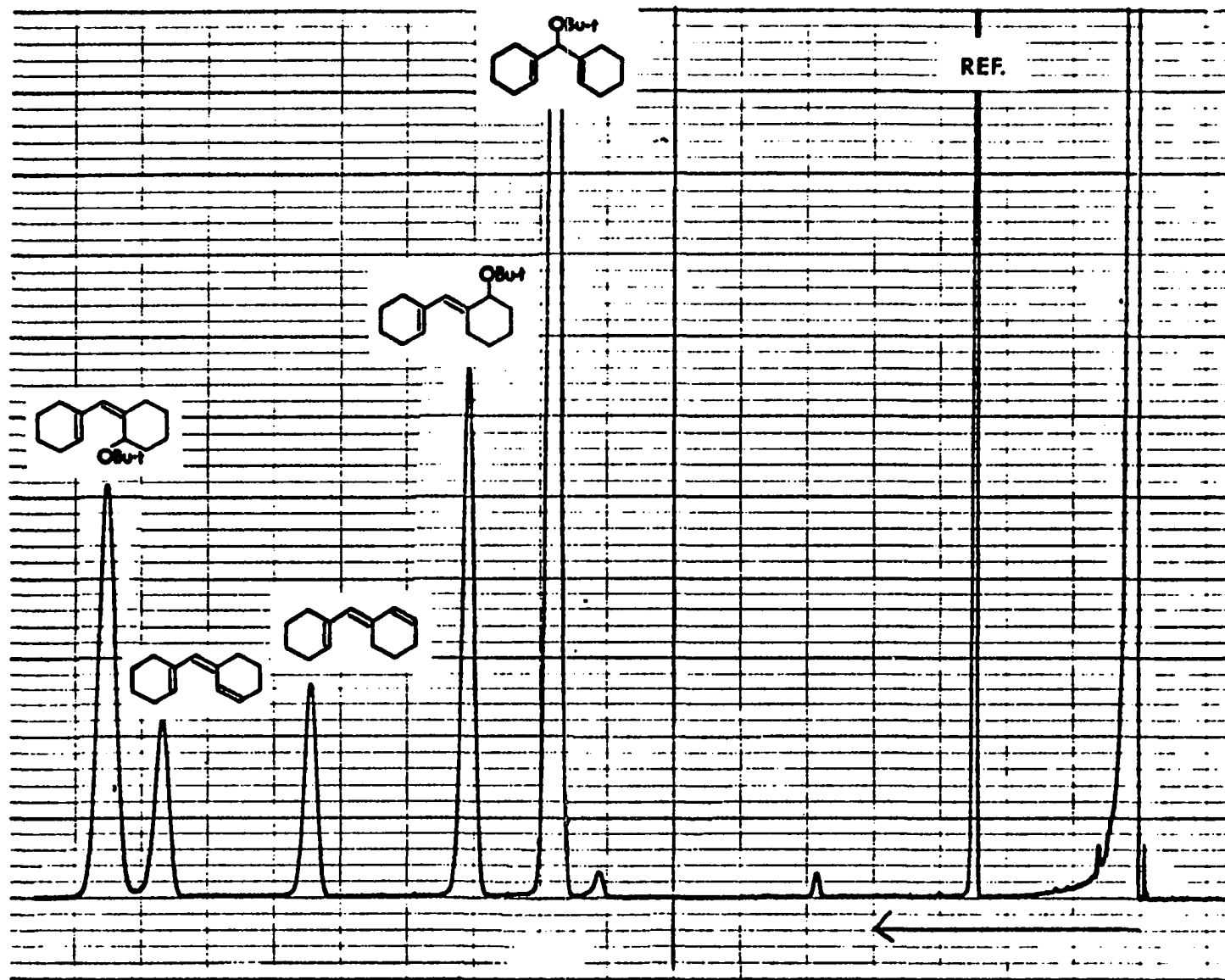


Figure 13 GLC Trace of Products Produced by Ambient Temperature Vacuum Decomposition of XXXIV

other by preparative GLC (FFAP). The 60 MHz PMR spectrum of XLVIII-a (Figure 14) in CDCl_3 showed: δ 6.4-6.8 (1H broadened doublet, $J = 10\text{Hz}$, olefinic proton H_b), 5.4-6.0 (3H multiplet, the remaining olefinic protons H_a), 1.2-2.4 (14H multiplet, ring protons). The 70 eV mass spectrum (Figure 15) showed: m/e 174 (M^+ , parent ion), 145 ($\text{M}^+ - \text{C}_2\text{H}_5$), 131 (base peak, $\text{M}^+ - \text{C}_3\text{H}_7$). The IR spectrum (Figure 16) showed: cm^{-1} 3030 (olefinic C-H), 1640 and 1615 (C=C), 915 and 870 (C=CH). The UV spectrum (hexane) gave λ_{max} 273 nm, ϵ_{max} 17,781; λ 265 nm, ϵ 17,380.

The 60 MHz PMR spectrum of XLVIII-b (Figure 17) in CDCl_3 showed: δ 5.9-6.2 (1H broadened doublet, $J = 10\text{Hz}$, olefinic proton H_b), 5.4-5.9 (3H multiplet, the remaining olefinic protons H_a), 2.35-2.65 (2H broadened triplet, $J = 6\text{Hz}$, allylic protons), 1.2-2.3 (12H multiplet, remaining ring protons). The 70 eV mass spectrum (Figure 18) showed: m/e 174 (M^+ , parent ion), 145 ($\text{M}^+ - \text{C}_2\text{H}_5$), 131 (base peak, $\text{M}^+ - \text{C}_3\text{H}_7$). The IR spectrum (Figure 19) showed: cm^{-1} 3030 (olefinic C-H), 1635 and 1605 (C=C), 915 and 875 (C=CH). The UV spectrum (hexane) gave λ_{max} 273 nm, ϵ_{max} 23,934; λ 265, ϵ 22,421.

The three isomeric *t*-butyl ethers (XLIX-a), (XLIX-b), and (XLIX-c) were isolated by PLC (silica gel). The unconjugated isomer (XLIX-a) did not exhibit UV activity on indicating silica gel. This distinguished XLIX-a from the two conjugated isomers, both of which showed bright blue on indicating silica gel under the short wavelength (254 nm) UV lamp.

The 100 MHz PMR Fourier-transform spectrum of XLIX-a (Figure 20) in CDCl_3 showed: δ 5.61 (2H multiplet, olefinic protons), 4.04 (1H broad singlet, proton on carbon bearing oxygen), 1.3-2.1 (16H multiplet, ring protons), 1.13 (9H singlet, *t*-butyl protons). The 70 eV mass spectrum (Figure 21) showed: m/e 248 (M^+ , parent ion), 192 ($\text{M}^+ - \text{Me}_2\text{C}=\text{CH}_2$), 191

($M^+ - Me_3C \cdot$), 174 ($M^+ - Me_3C - OH$), 59 (base peak, $Me_2C = OH^+$). The IR spectrum (Figure 22) showed: cm^{-1} 1660 (C=C), 1380 and 1360 ($-CMe_3$), 1190 and 1050 (C-O).

The 100 MHz PMR Fourier-transform spectrum of XLIX-b (Figure 23) in $CDCl_3$ showed: δ 5.42 (2H multiplet, olefinic protons), 4.72 (1H broad singlet, proton on carbon bearing oxygen), 2.58 (1H multiplet; allylic proton), 1.3-2.2 (15H multiplet, ring protons), 1.08 (9H singlet, t-butyl protons). The 70 eV mass spectrum (Figure 24) showed: m/e 248 (M^+ , parent ion), 192 ($M^+ - Me_2C = CH_2$), 174 ($M^+ - Me_3C - OH$), 59 (base peak, $Me_2C = OH^+$). The IR spectrum (Figure 25) showed: cm^{-1} 1640 (C=C), 1380 and 1355 ($-CMe_3$), 1190 and 1060 (C-O). The UV spectrum (hexane) gave λ_{max} 232.5 nm, ϵ_{max} 9,039.

The 100 MHz PMR Fourier-transform spectrum of XLIX-c (Figure 26) in $CDCl_3$ showed: δ 5.81 (1H broad singlet, olefinic proton), 5.45 (1H multiplet, olefinic proton), 3.79 (1H multiplet, proton on carbon bearing oxygen), 2.7 (1H multiplet, allylic proton), 1.3-2.2 (15H multiplet, ring protons), 1.16 (9H, singlet, t-butyl protons). The 70 eV mass spectrum (Figure 27) showed: m/e 248 (M^+ , parent ion), 192 ($M^+ - Me_2C = CH_2$), 174 ($M^+ - Me_3C - OH$), 59 (base peak, $Me_2C = OH^+$). The IR spectrum (Figure 28) showed: cm^{-1} 1640 (C=C), 1380 and 1355 ($-CMe_3$), 1190 and 1085 (C-O). The UV spectrum (hexane) gave λ_{max} 234 nm, ϵ_{max} 11,217.

The above spectral data are consistent with the structural assignments made for XLVIII-a, XLVIII-b, XLIX-a, XLIX-b, and XLIX-c, but do not clearly distinguish between the isomeric trienes (XLVIII-a) and (XLVIII-b) and between the isomeric ethers (XLIX-b) and (XLIX-c). At a later point in this dissertation, arguments based on subtle differences in their PMR spectra will be made which support these structural assignments.

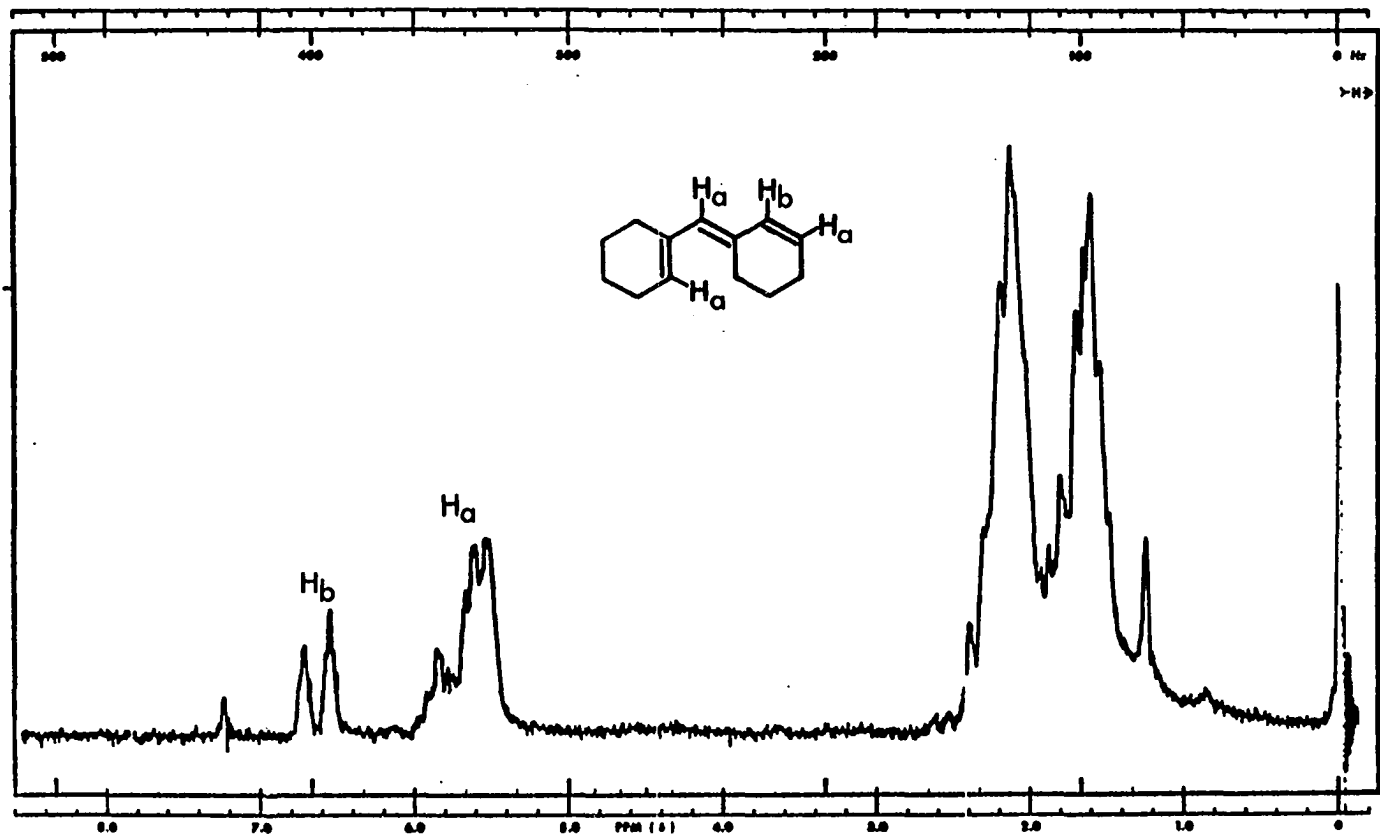


Figure 14 60 MHz PMR Spectrum (CDCl₃) of XLVIII-a

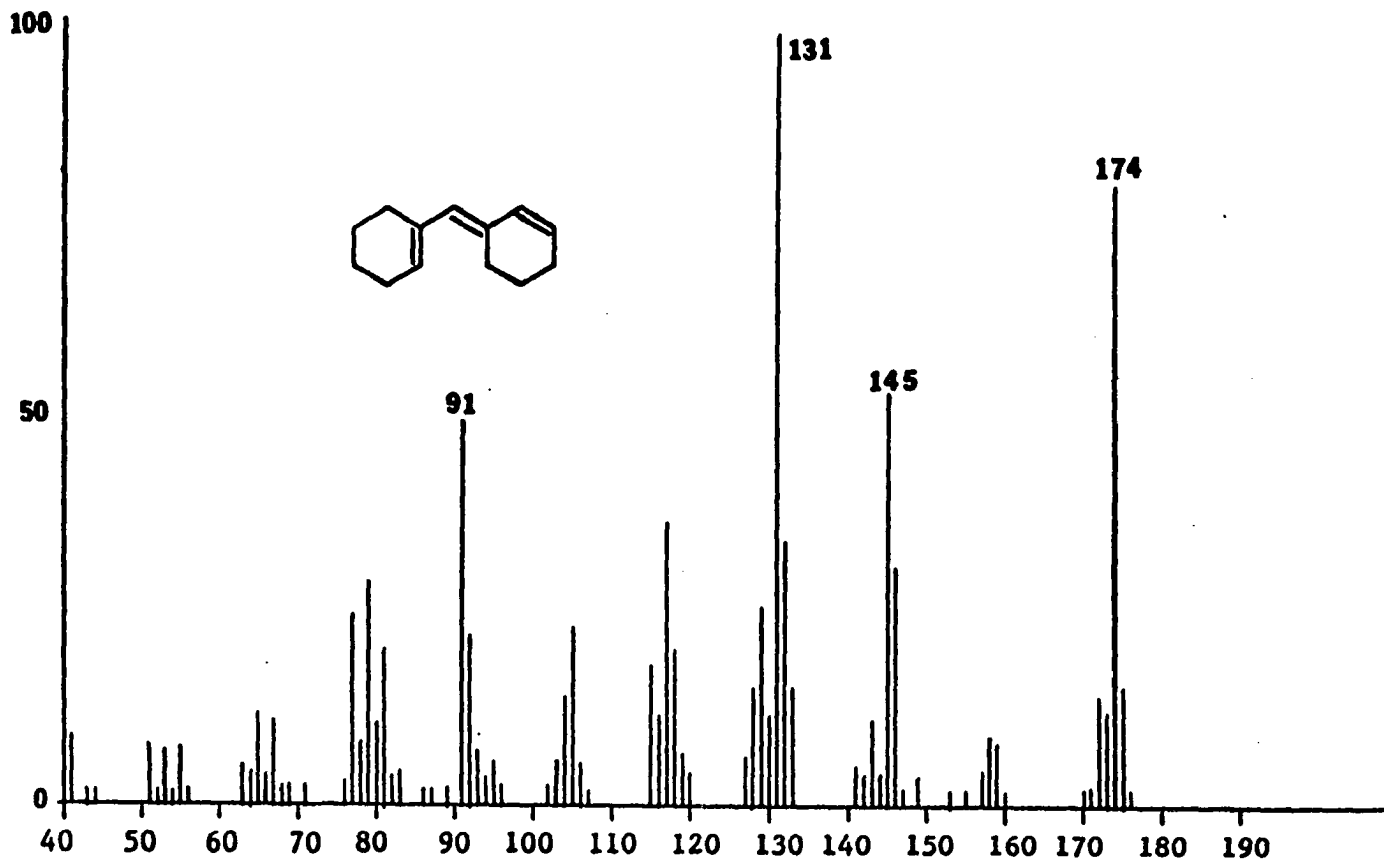


Figure 15 70 eV Mass Spectrum of XLVIII-a

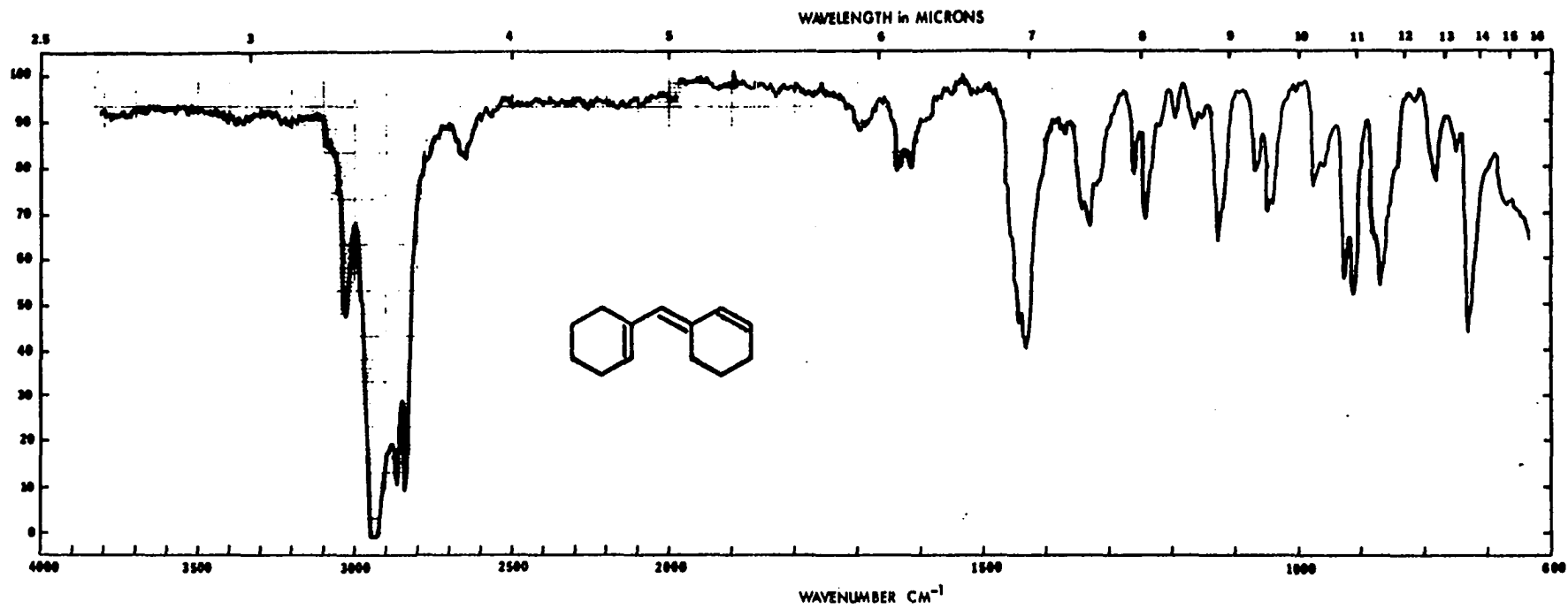


Figure 16 IR Spectrum (film) of XLVIII-a

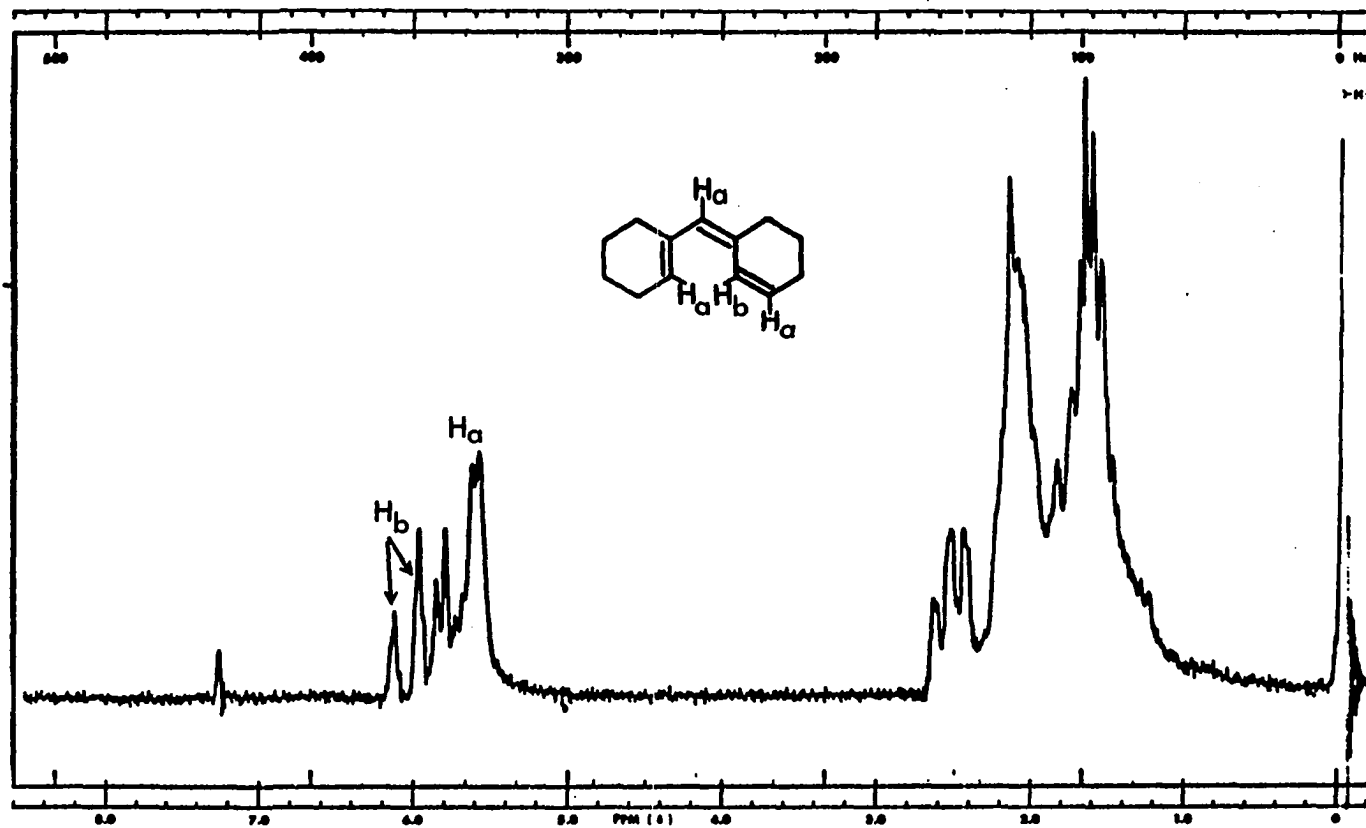


Figure 17 60 MHz PMR Spectrum (CDCl₃) of XLVIII-b

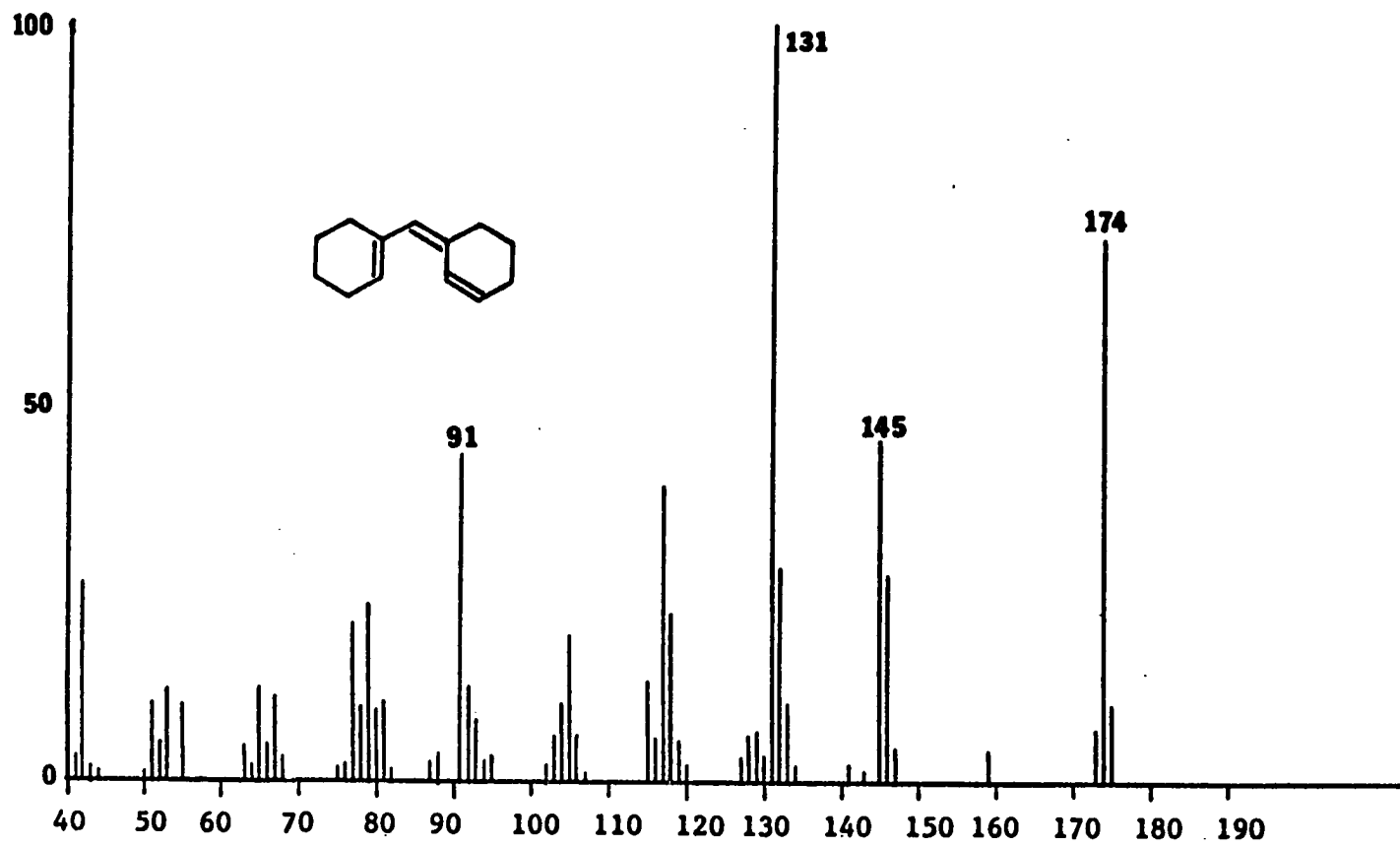


Figure 18 70 eV Mass Spectrum of XLVIII-b

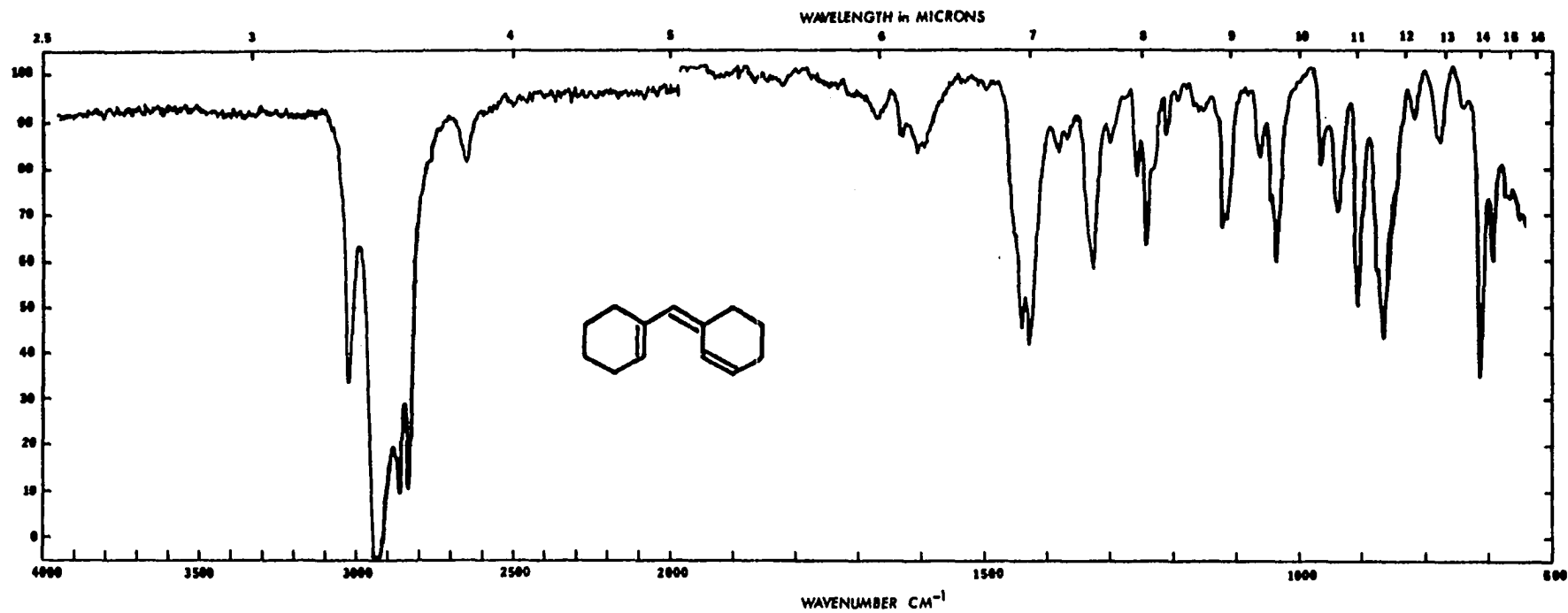


Figure 19 IR Spectrum (film) of XLVIII-b

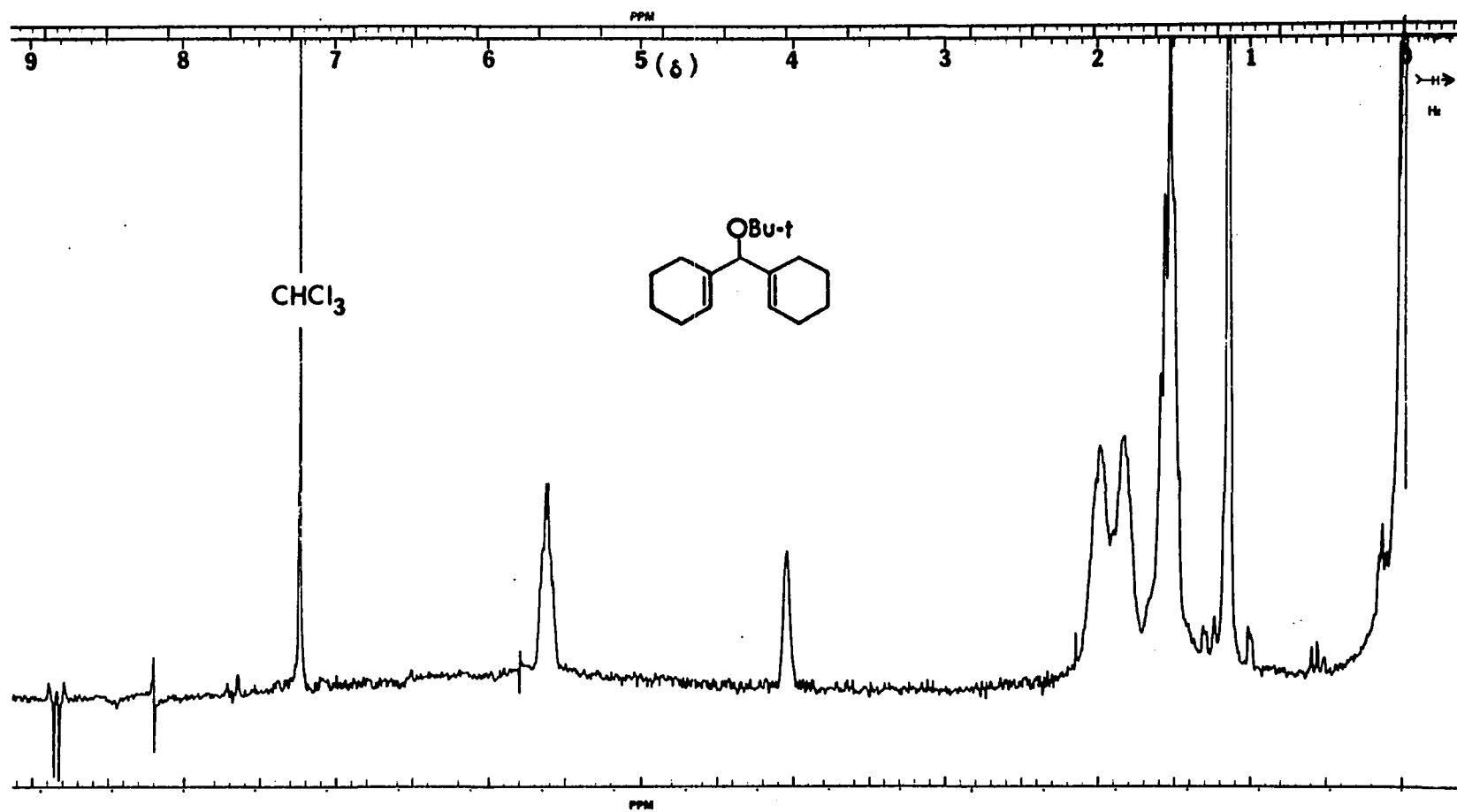


Figure 20 100 MHz PMR Fourier-Transform Spectrum (CDCl_3) of XLIX-a

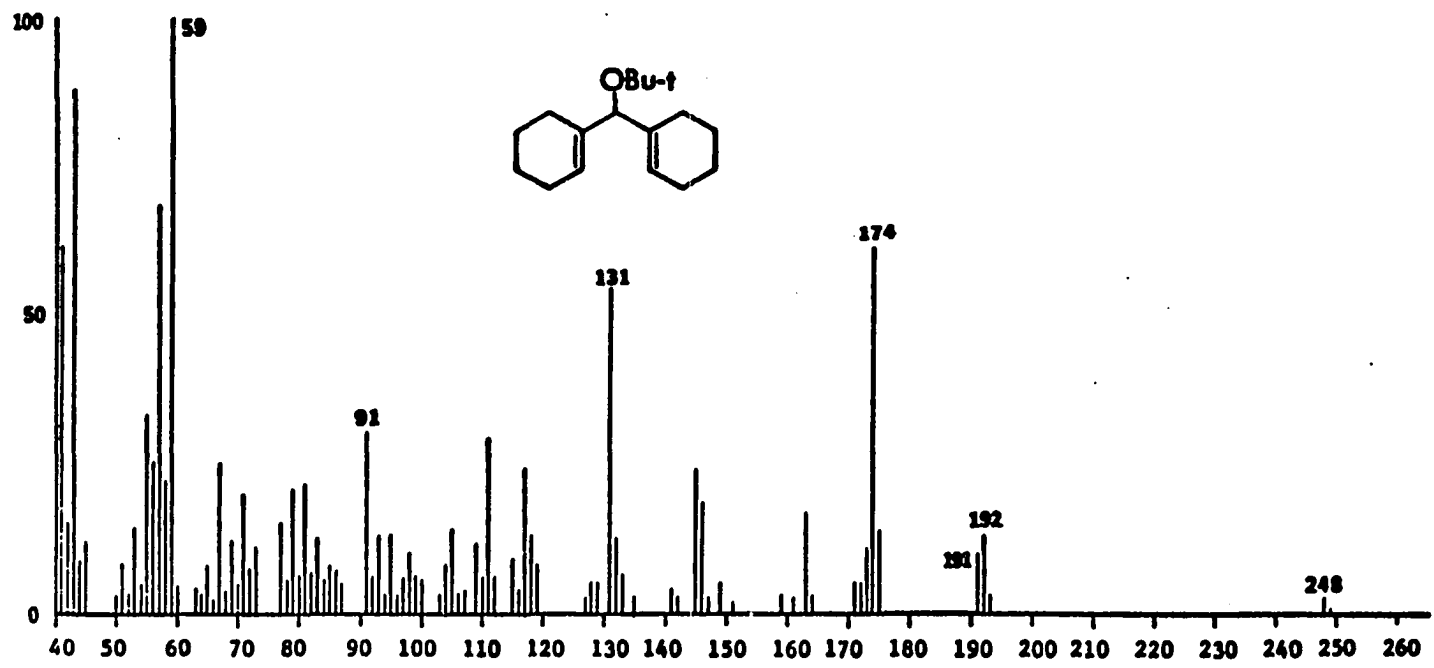


Figure 21 70 eV Mass Spectrum of XLIX-a

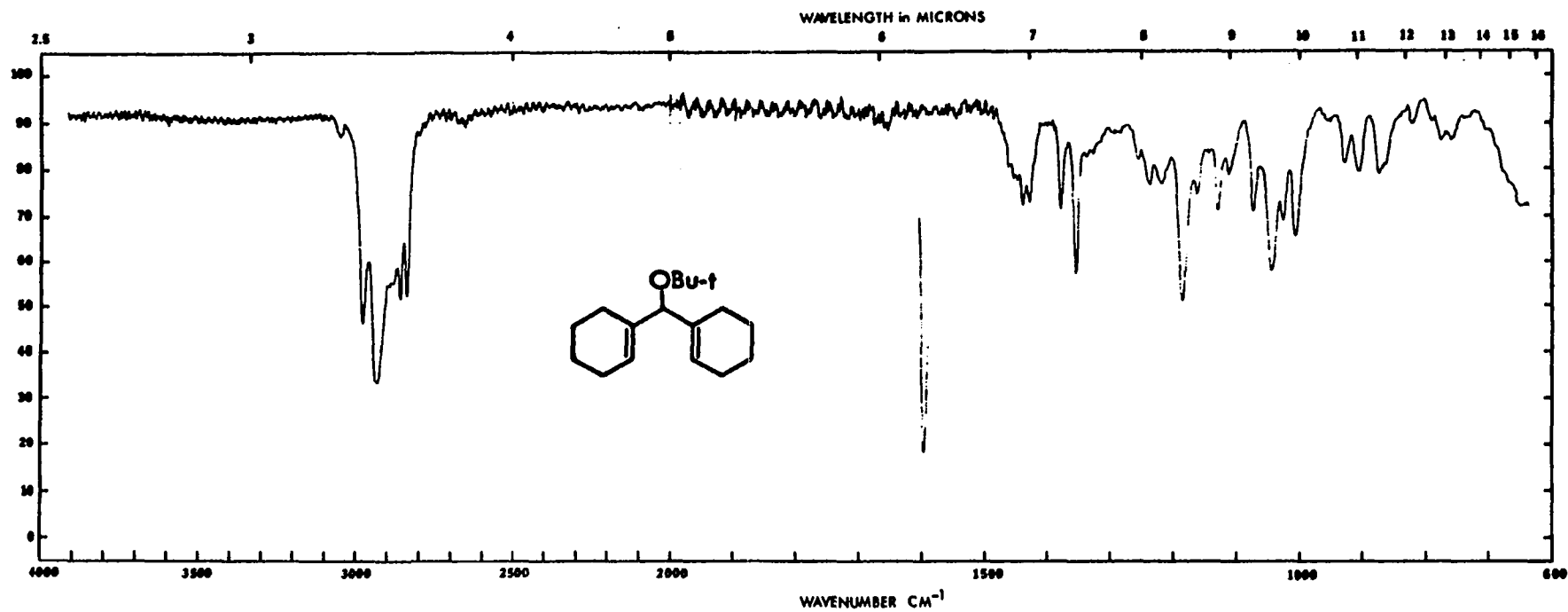


Figure 22 IR Spectrum (film) of XLIX-a

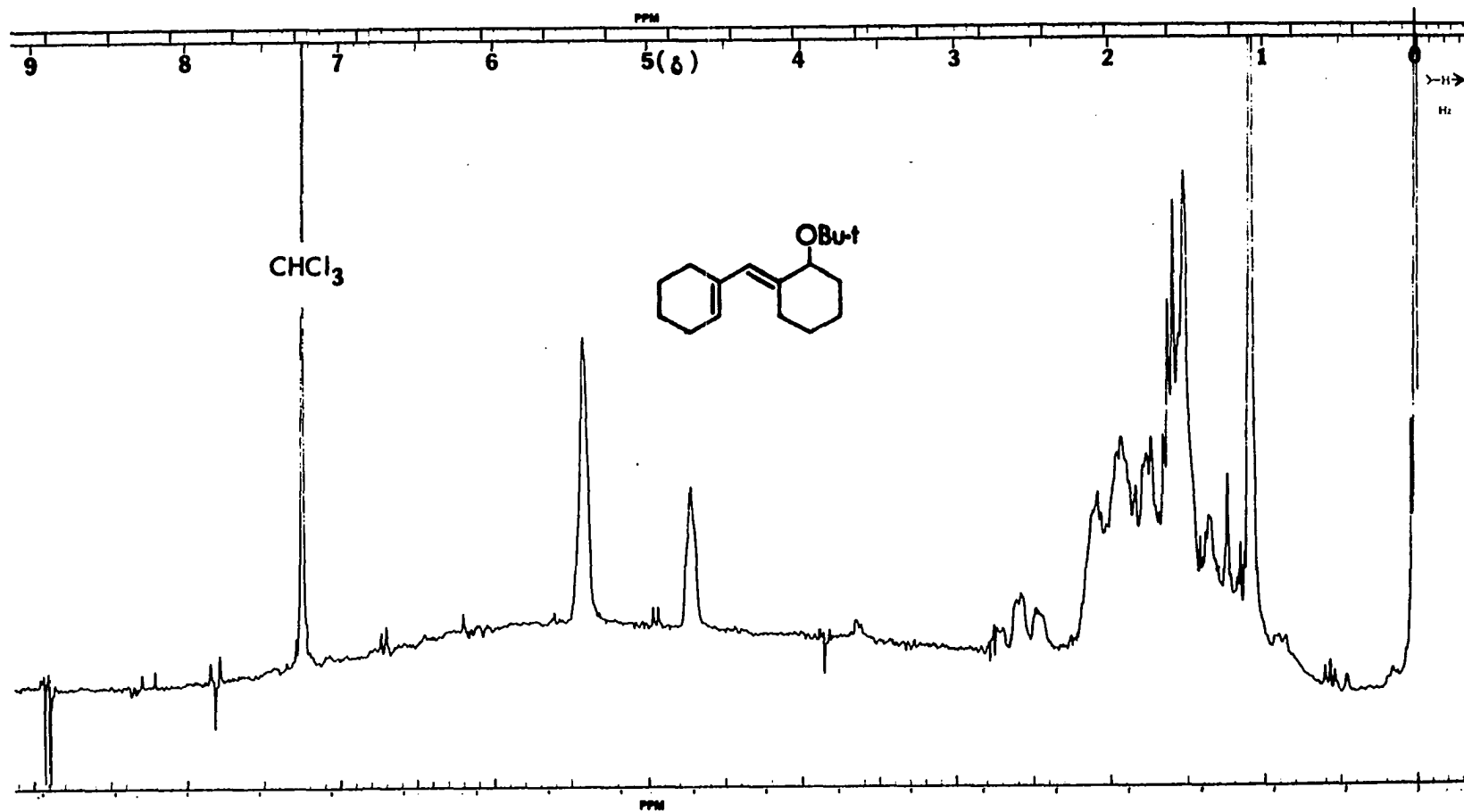


Figure 23 100 MHz PMR Fourier-Transform Spectrum (CDCl₃) of XLIX-b

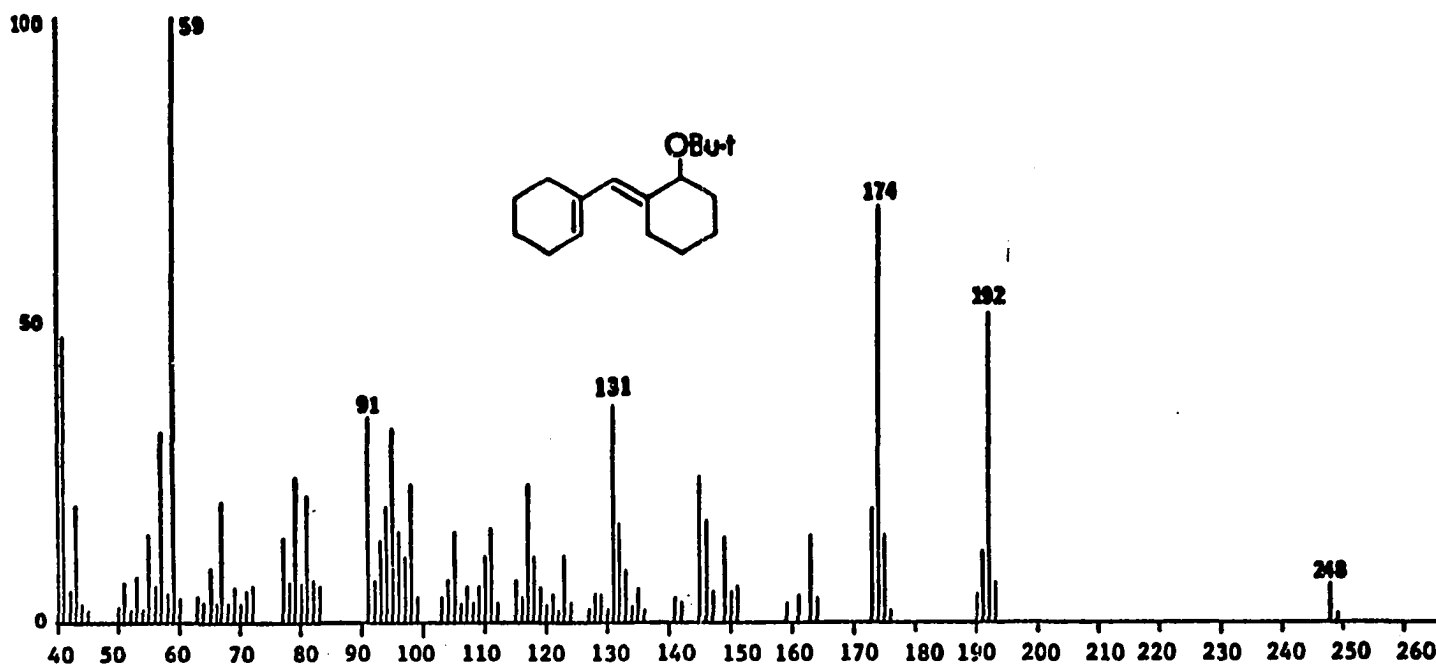


Figure 24 70 eV Mass Spectrum of XLIX-b

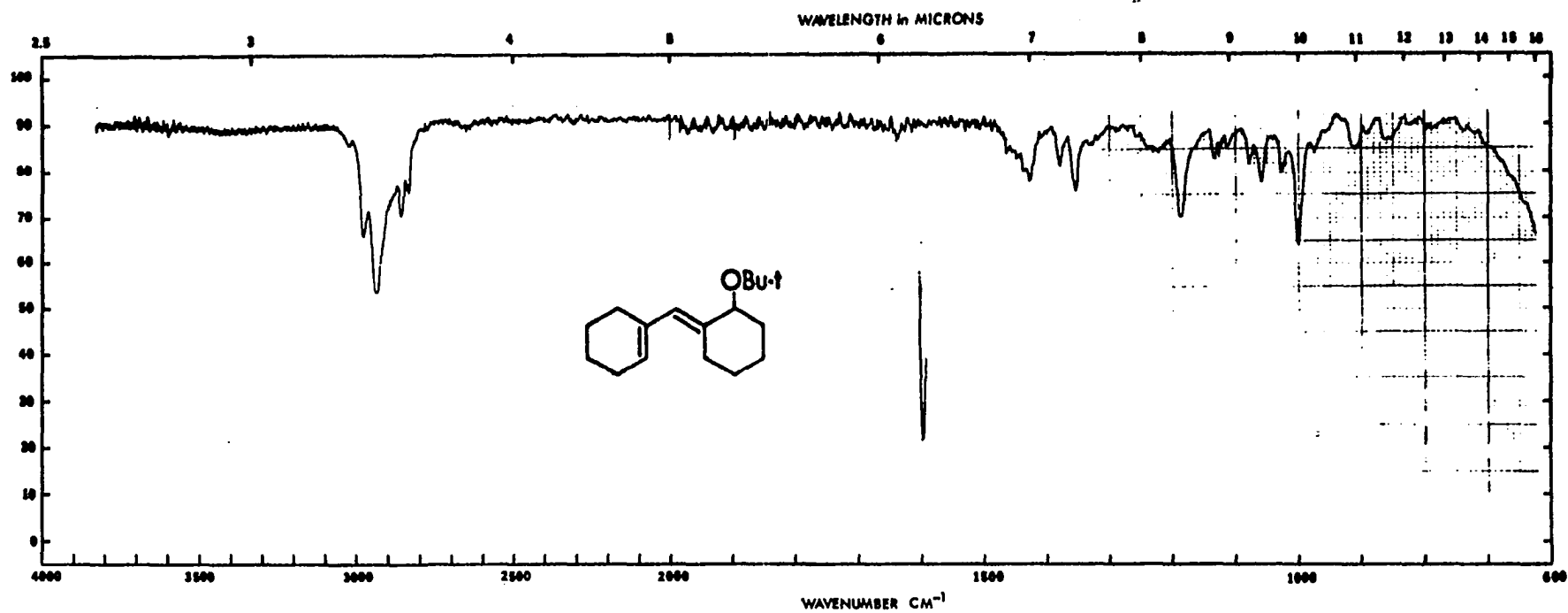


Figure 25 IR Spectrum (film) of XLIX-b

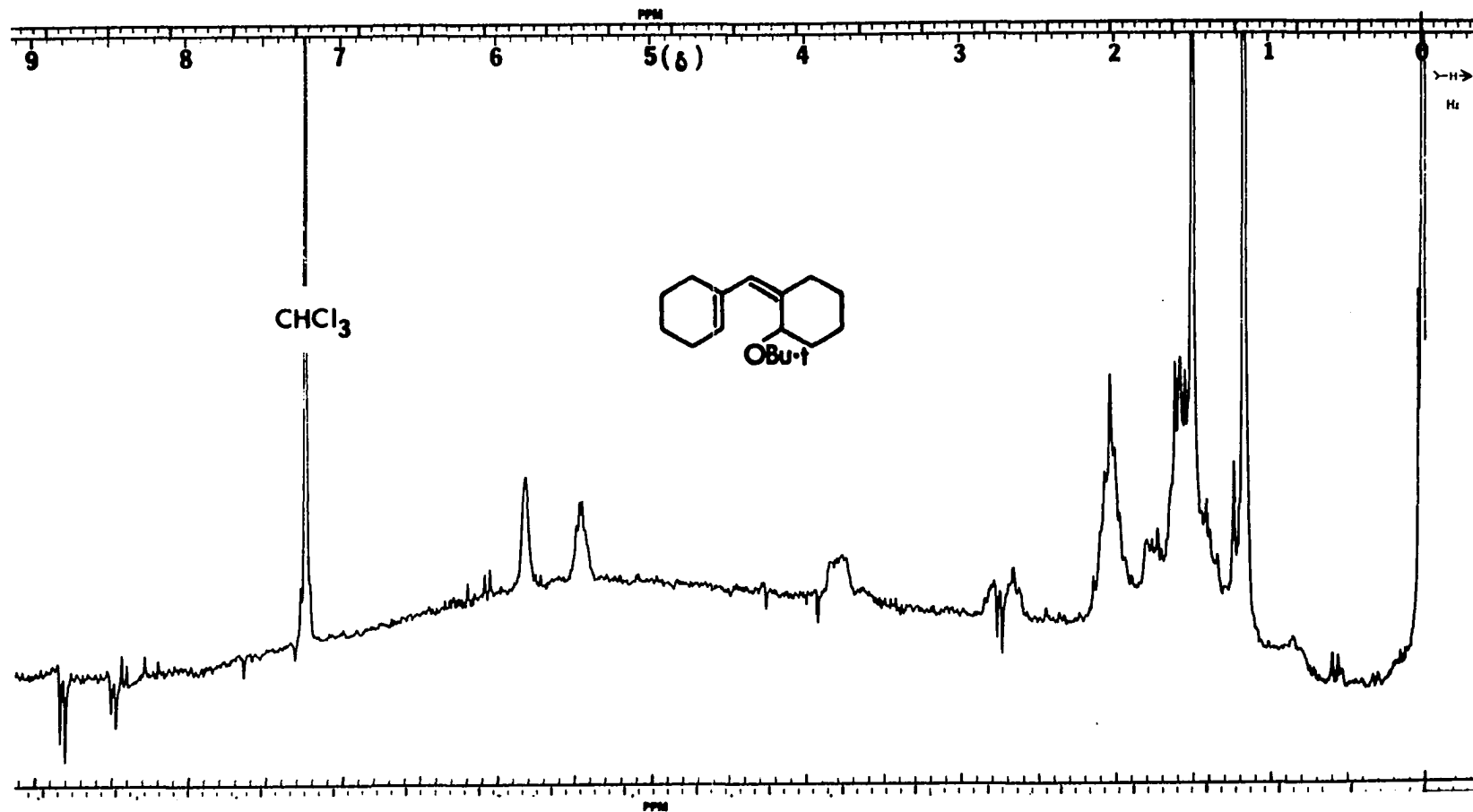


Figure 26 100 MHz PMR Fourier-Transform Spectrum (CDCl₃) of XLIX-c

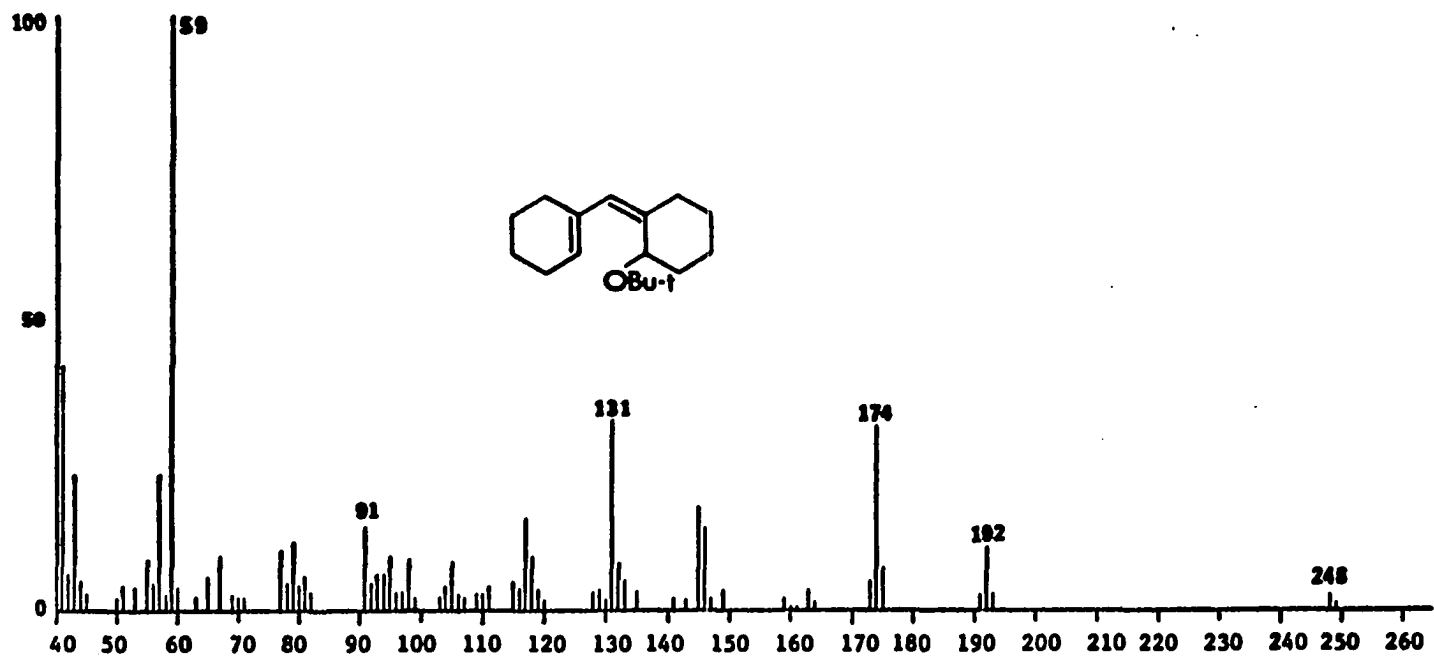


Figure 27 70 eV Mass Spectrum of XLIX-c

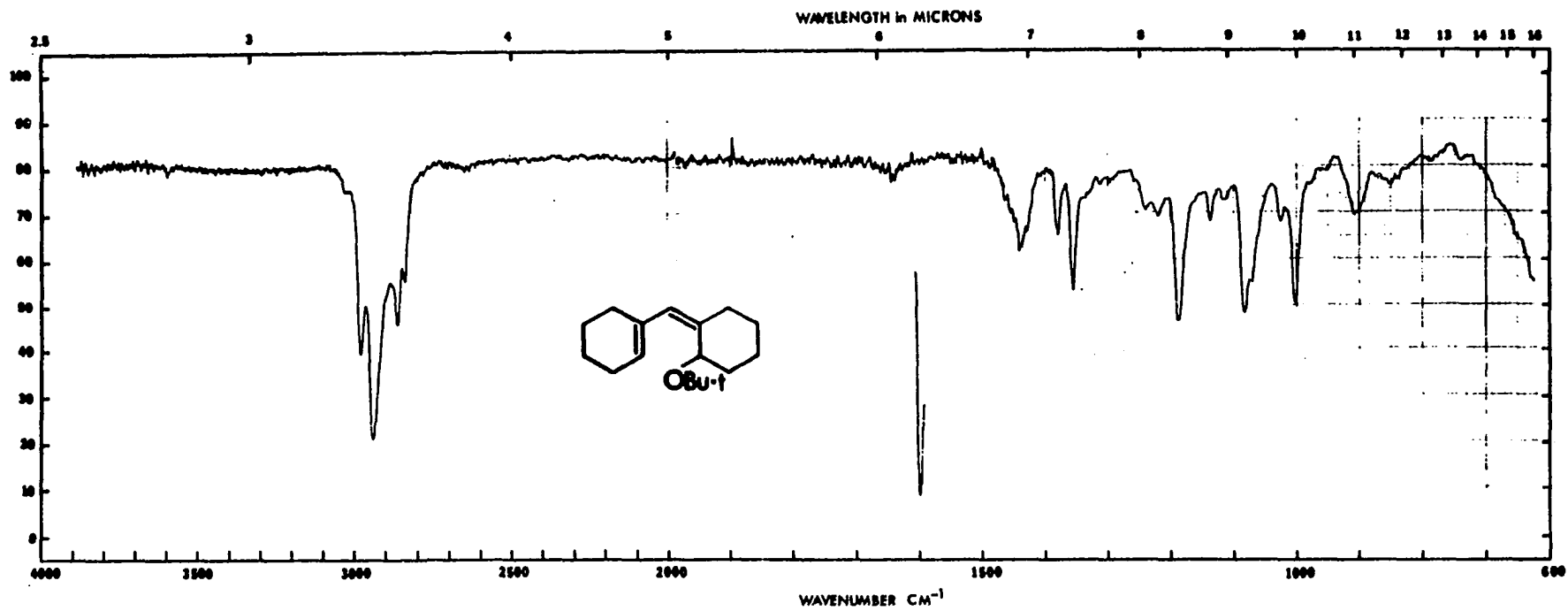


Figure 28 IR Spectrum (film) of XLIX-c

Ambient Temperature Decomposition of XXXIV in Hexane Solution

Hexane solutions of the peroxyacetate (XXXIV) which were allowed to decompose in the dark at ambient room temperature gave rise to mixtures of the trienes (XLVIII-a) and (XLVIII-b) and the ethers (XLIX-a), (XLIX-b), and (XLIX-c). The overall yield of products was much lower than that obtained by decomposition of XXXIV under vacuum. The lower product yield is presumably due to the greater amount of induced decomposition (Scheme 7) which occurs in solution leading to the polyester (XLIII). In a typical experiment, a 0.0185 M solution of XXXIV in olefin-free degassed hexane was allowed to decompose in the dark at ambient temperature (ca. 23°). Examination of the product distribution was accomplished by GLC. The results shown in Table 2 represent decomposition times of 45, 95 and 120 hour; the yields given are percent of theory.

Table 2

Product Distribution versus Time; Decomposition
of Hexane Solution of XXXIV

	XLVIII-a	XLVIII-b	XLIX-a	XLIX-b	XLIX-c	Total
45 hr	2.5%	4.0%	11.8%	8.1%	9.9%	36.3%
95 hr	trace	trace	12.9%	7.7%	6.5%	27.1%
120 hr	-	-	9.0%	5.2%	4.3%	18.5%

The presence of undecomposed peroxyacetate (XXXIV) could not be detected by TLC after about 72 hour. It is apparent from the data in Table 2 that the products were not stable under the conditions of reaction. The solution decomposition of XXXIV offered no new information over that previously gained by vacuum decomposition. The latter method was used

for isolation and identification of the trienes (XLVIII-a) and (XLVIII-b) and the ethers (XLIX-a), (XLIX-b), and (XLIX-c).

Elevated Temperature Decompositions of XXXIV

Decomposition of the peroxyacetate (XXXIV) by direct injection of a hexane solution into the gas chromatograph gave rise to mixtures of the trienes (XLVIII-a) and (XLVIII-b) and the ethers (XLIX-a), (XLIX-b), and (XLIX-c). The GLC trace shown in Figure 29 is a typical example of this decomposition method. The trace in Figure 29 was obtained by injection of XXXIV onto a 100 ft. S.C.O.T. FFAP column. The glass-lined injection port was held at 230°; the column oven was at 125°. The product distribution shown in Table 3 was obtained by quantitative GLC under slightly different conditions. The 100 ft. S.C.O.T. FFAP column was held at 115° and the glass-lined injection port was at 220°. The data in Table 3 are

Table 3

Product Distribution; Decomposition of XXXIV in GLC Injection Port

XLVIII-a	XLVIII-b	XLIX-a	XLIX-b	XLIX-c	Total
11.2%	22.4%	10.6%	7.4%	9.8%	61.4%

percent of theoretical yield based on the injection of 5.55×10^{-9} moles of XXXIV. The product distribution was variable depending upon the exact GLC conditions employed and the amount of XXXIV injected. No new products were identified by this decomposition method.

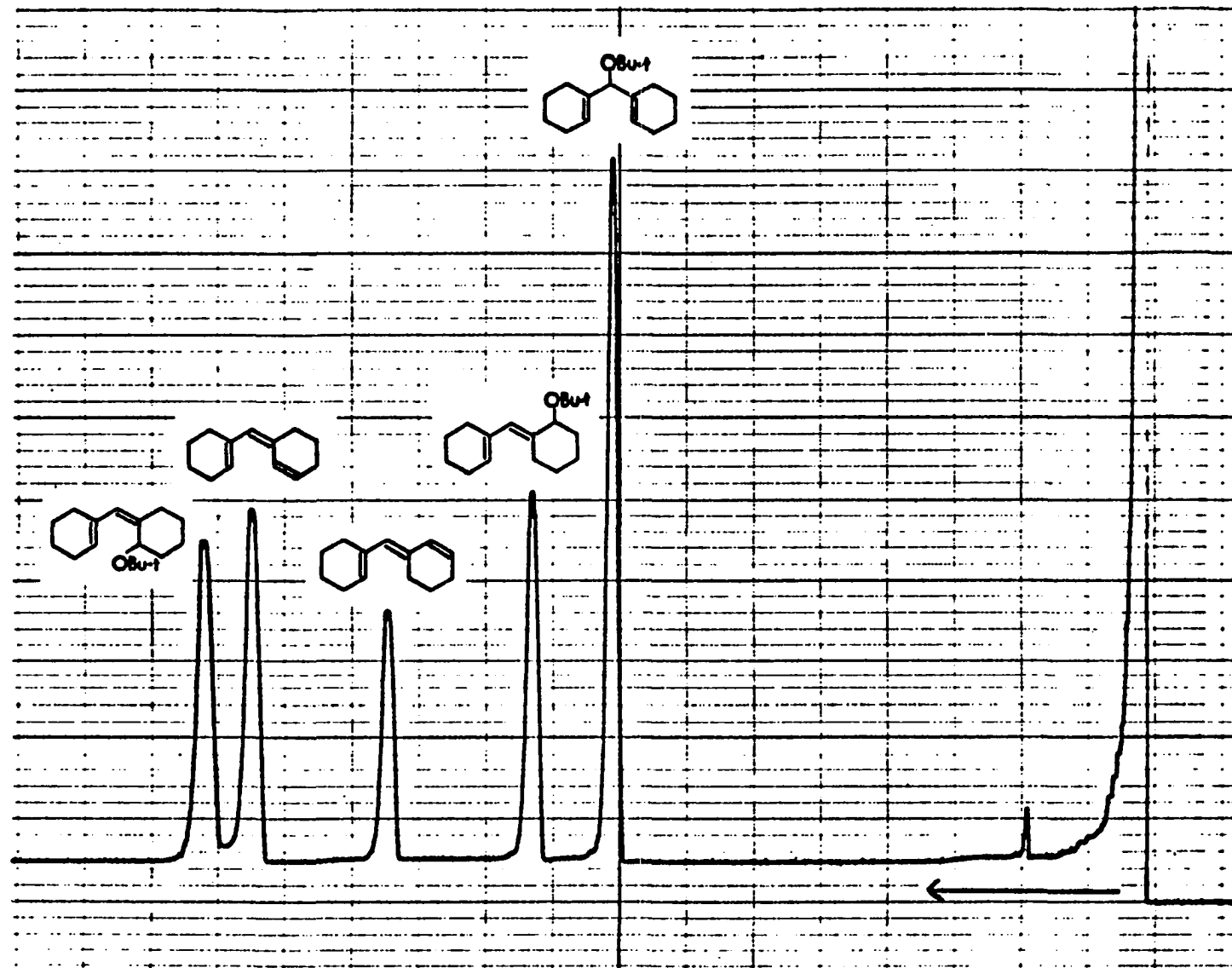


Figure 29 GLC Trace of Products Produced by Decomposition of XXXIV in GLC Injection Port

From considerations of the three previous methods of decomposition, it became apparent that to effect the desired electrocyclization (XXII→XXIII), another method of decomposition was required. Ideally, vapor-phase decomposition seemed desirable. However, from the results of ambient temperature vacuum decomposition, it was unlikely that a method of elevated temperature vapor-phase decomposition would be possible to achieve. Thus, we sought a method of flash thermolysis under conditions as close to vapor-phase as possible. These considerations were embodied in the design of the vacuum hot tube shown schematically in Figure 30.

The vacuum hot tube consisted of a quartz tube 50 cm long by 15 mm (O.D.). The tube was heated electrically by resistance wire wound around the outer skin of the tube. The device was equipped with a silicon rubber injector septum and a cold-trap collector. The tube was filled with 3 mm glass beads which had been previously treated with hexamethyldisilazane. The system was maintained under vacuum at the cold-trap collector. The temperature of the tube was measured by a thermocouple placed on the outer skin at the middle of the tube. The heated parts of the tube, including the thermocouple, were insulated with generous layers of asbestos. The cold trap collector was cooled by a slurry of dry ice in isopropanol. Through the use of a variable auto-transformer to control the voltage to the heating wire, the temperature of the tube could be easily varied to 1000°. In practice, the tube was operated below the softening point of the pyrex glass beads (ca. 550°).

Samples to be thermolyzed were introduced into the vacuum hot tube as hexane solutions by injections via syringe. Injection into the vacuum served to strip the solvent away and introduce samples onto the heated glass beads as a fine mist. This method was employed to study the

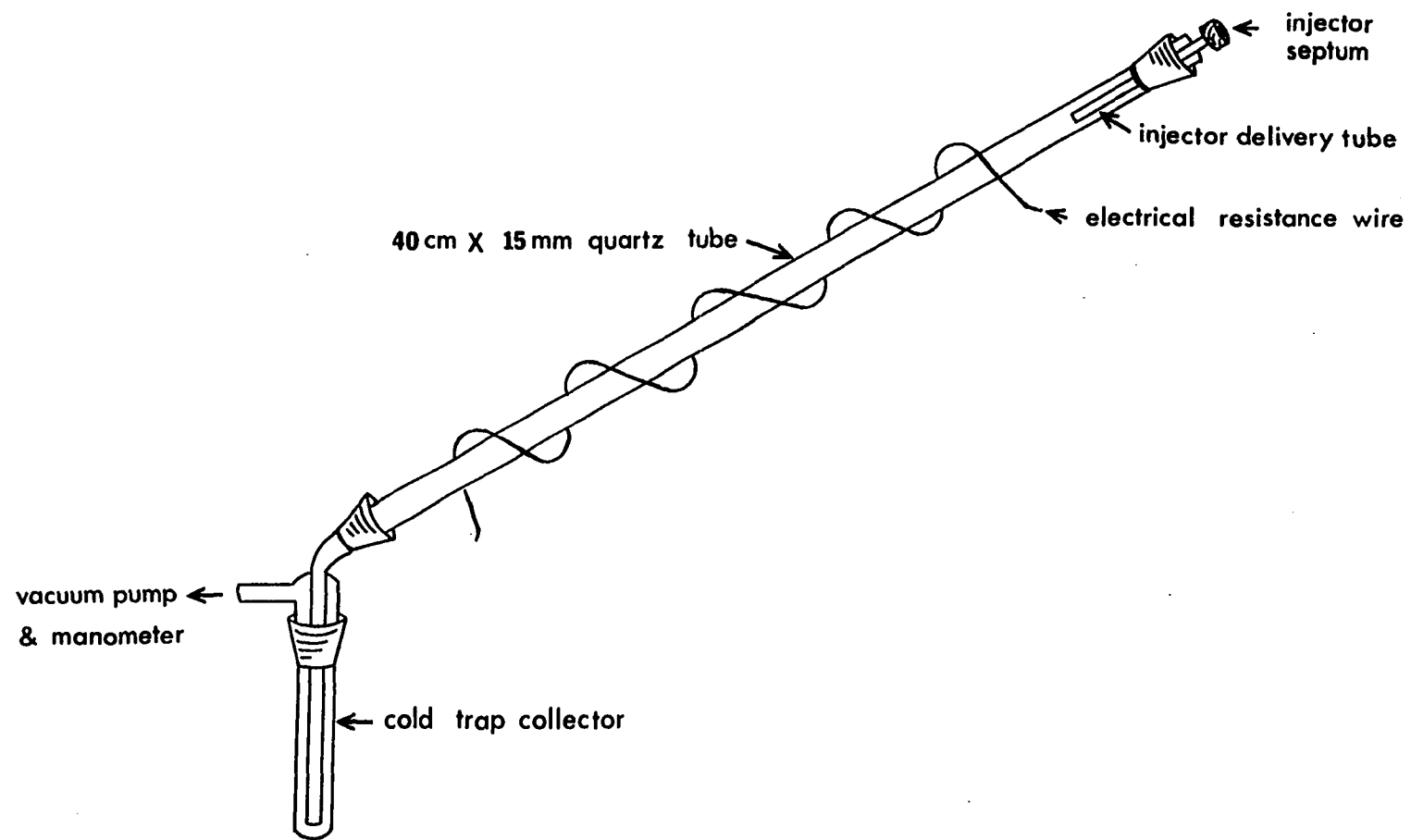
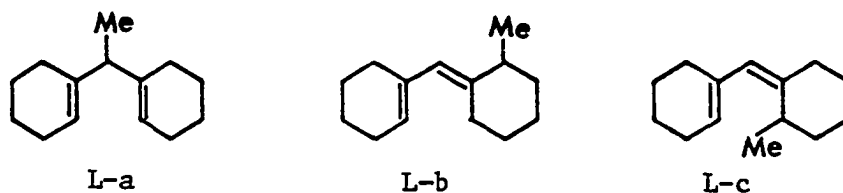


Figure 30 Schematic of Vacuum Hot Tube

thermal decomposition of the peroxyacetate (XXXIV) referred to in the following discussions.

Under a vacuum of 0.05–0.01 torr, a temperature greater than ca. 210° was required to cause complete decomposition of the peroxyacetate (XXXIV) in the vacuum hot tube. Typically, in preparative scale runs, no more than 50×10^{-6} moles of XXXIV were injected at once. Between injections, the vacuum was allowed to recover to 0.05–0.01 torr.

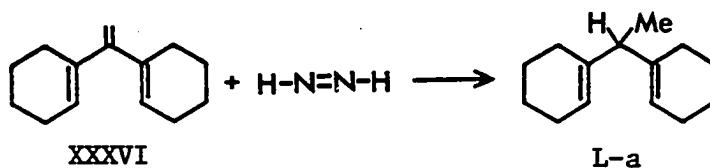
The trienes (XLVIII-a) and (XLVIII-b) and the ethers (XLIX-a), (XLIX-b), and (XLIX-c) were produced in the vacuum hot tube at all tube temperatures investigated in the range 210–400°. In addition to these, three new major compounds were also produced at these tube temperatures. These were isolated and identified as the isomeric methylated dienes (L-a), (L-b), and (L-c). Their structural identities were established on the basis of the spectral data in the following discussion.



The three isomeric dienes (L-a), (L-b), and (L-c) were obtained as a mixture by PLC (silica gel). They were further separated and purified by preparative GLC (FFAP). The unconjugated isomer (L-a) did not show UV activity on indicating silica gel, whereas the two conjugated isomers (L-b) and (L-c) appeared as bright blue under the short wavelength (254 nm) UV lamp.

The 100 MHz PMR Fourier-transform spectrum of L-a (Figure 31) in CDCl_3 showed: δ 5.43 (2H multiplet, olefinic protons), 2.52 (1H broad

quartet, $J = 7\text{Hz}$, diallylic proton adjacent to methyl), 1.44-2.14 (16H multiplet, ring protons), 1.05 (3H doublet, $J = 7\text{Hz}$, secondary methyl protons). The 70 eV mass spectrum (Figure 32) showed: m/e 190 (M^+ , parent ion), 175 ($M^+ - \text{CH}_3$), 161 ($M^+ - \text{C}_2\text{H}_5$), 147 (base peak, $M^+ - \text{C}_3\text{H}_7$). The IR spectrum (Figure 33) showed: cm^{-1} 3040 (olefinic C-H), 1645 (C=C). Authentic L-a was prepared by diimide reduction of XXXVI in ca. 80% yield (see Scheme 8). Authentic L-a and that obtained by vacuum hot tube decomposition of XXXIV were identical in all characteristics.



Scheme 8

The 100 MHz PMR Fourier-transform spectrum of L-b (Figure 34) in CDCl_3 showed: δ 5.46 (2H multiplet, olefinic protons), 3.09 (1H multiplet, allylic proton adjacent to methyl), 1.43-2.20 (16H multiplet, ring protons), 1.09 (3H doublet, $J = 8\text{Hz}$, secondary methyl protons). The 70 eV mass spectrum (Figure 35) showed: m/e 190 (M^+ , parent ion), 175 ($M^+ - \text{CH}_3$), 161 ($M^+ - \text{C}_2\text{H}_5$), 147 ($M^+ - \text{C}_3\text{H}_7$), 79 (base peak). The IR spectrum (Figure 36) showed: cm^{-1} 3020 (olefinic C-H), 1640 (C=C). The UV spectrum (hexane) gave λ_{max} 233 nm, ϵ_{max} 8,323.

The 100 MHz PMR Fourier-transform spectrum of L-c (Figure 37) in CDCl_3 showed: δ 5.47 (2H multiplet, olefinic protons), 2.67 (1H multiplet, allylic proton adjacent to methyl), 1.38-2.20 (16H multiplet, ring protons), 1.01 (3H doublet, $J = 7\text{Hz}$, secondary methyl protons). The 70 eV mass spectrum (Figure 38) showed: m/e 190 (M^+ , parent ion), 175 ($M^+ - \text{CH}_3$), 161 ($M^+ - \text{C}_2\text{H}_5$), 147 ($M^+ - \text{C}_3\text{H}_7$), 79 (base peak). The IR spectrum (Figure 39) showed: cm^{-1} 3020 (olefinic C-H), 1640 (C=C). The UV spectrum (hexane)

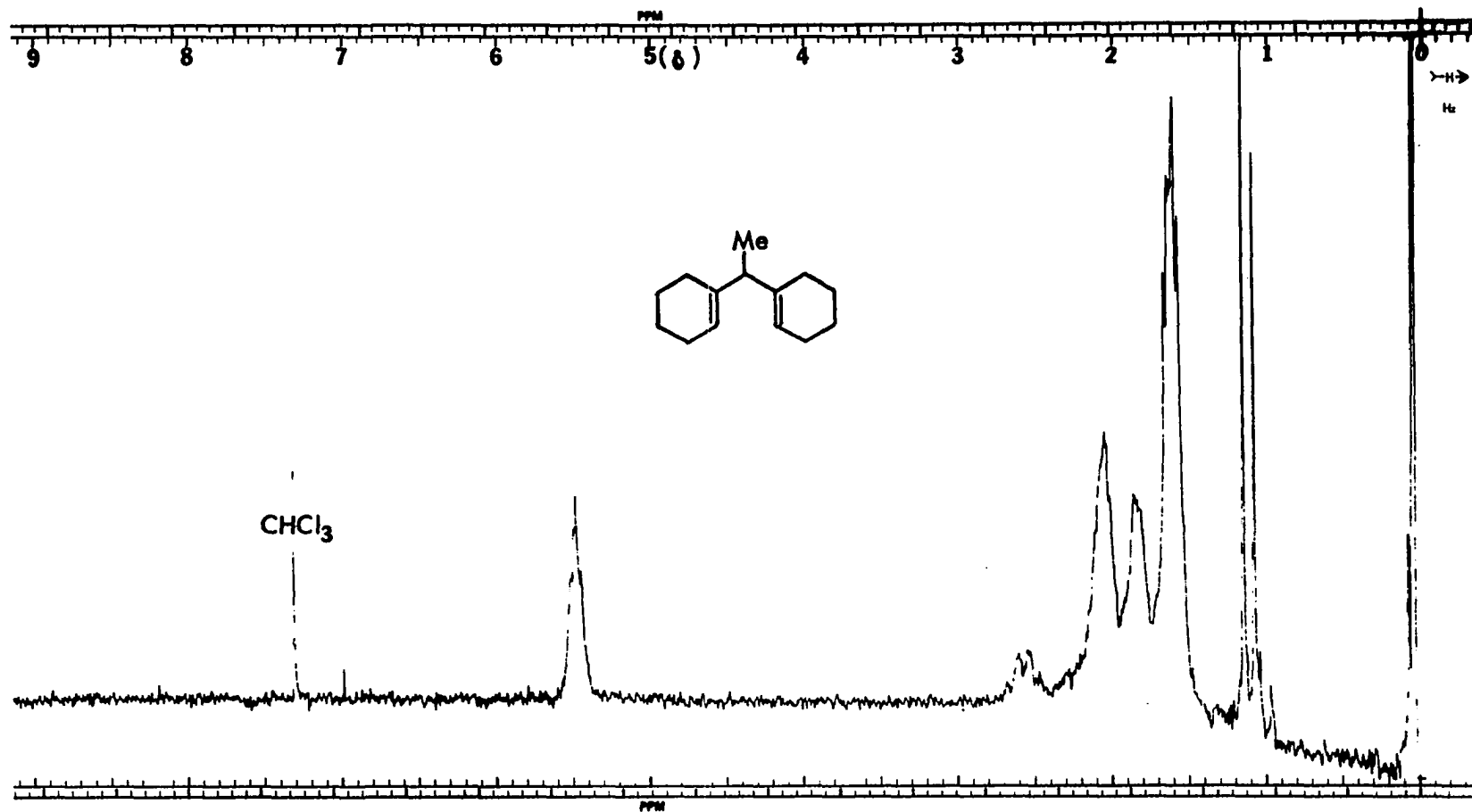


Figure 31 100 MHz PMR Fourier-Transform Spectrum (CDCl_3) of L-a

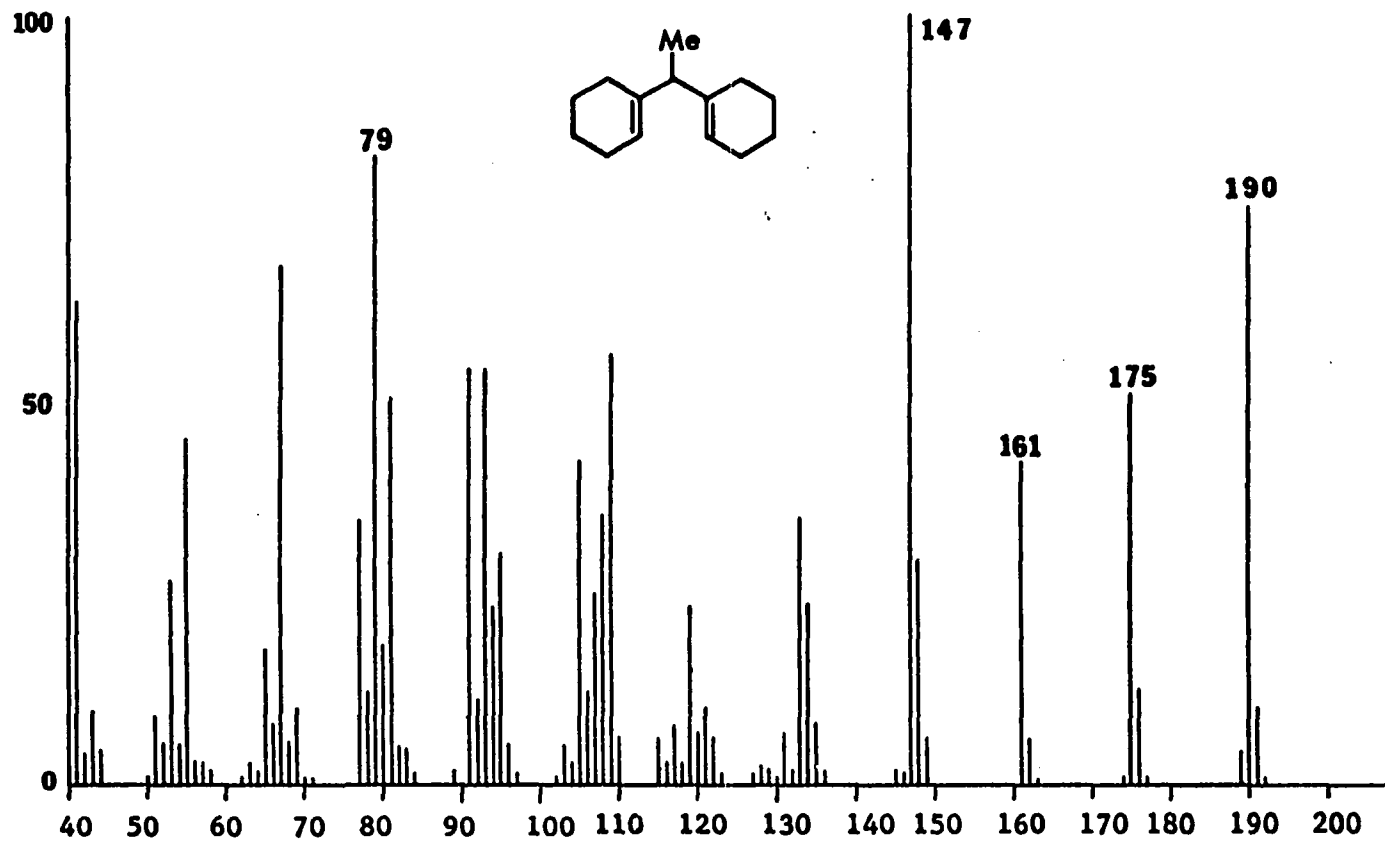


Figure 32 70 eV Mass Spectrum of L-a

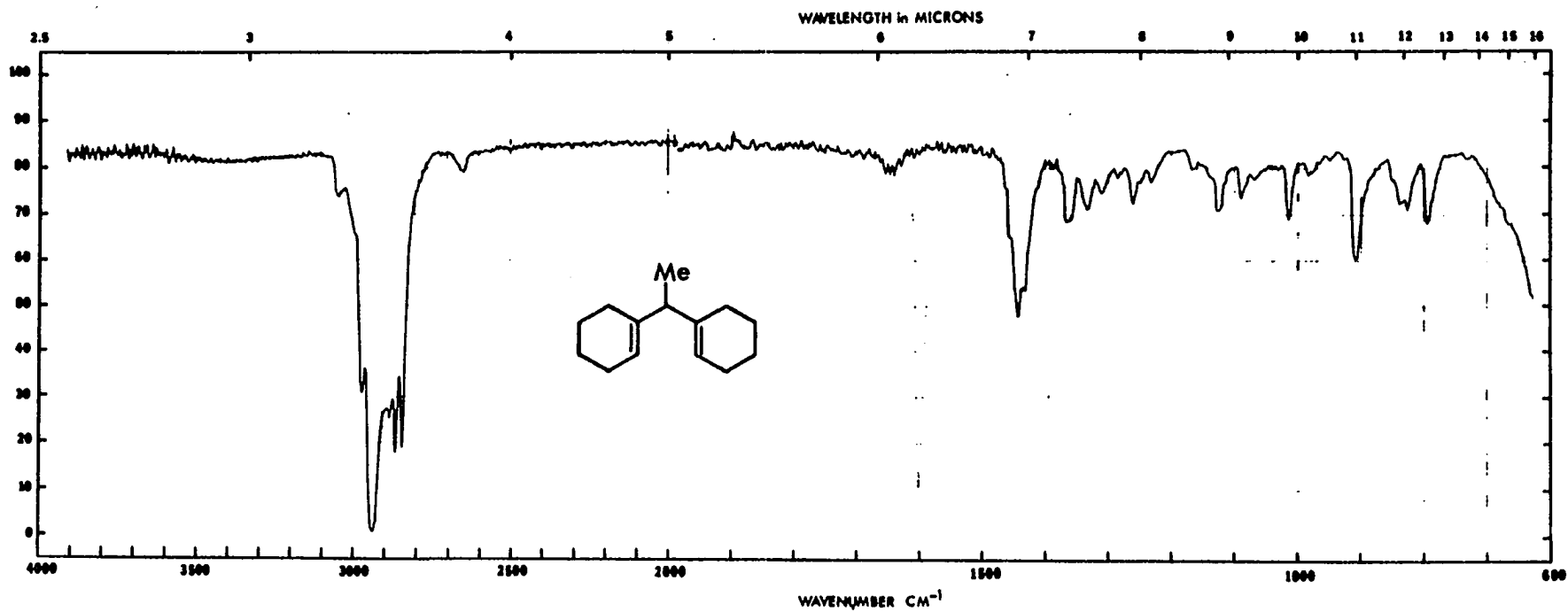


Figure 33 IR Spectrum (film) of L-a

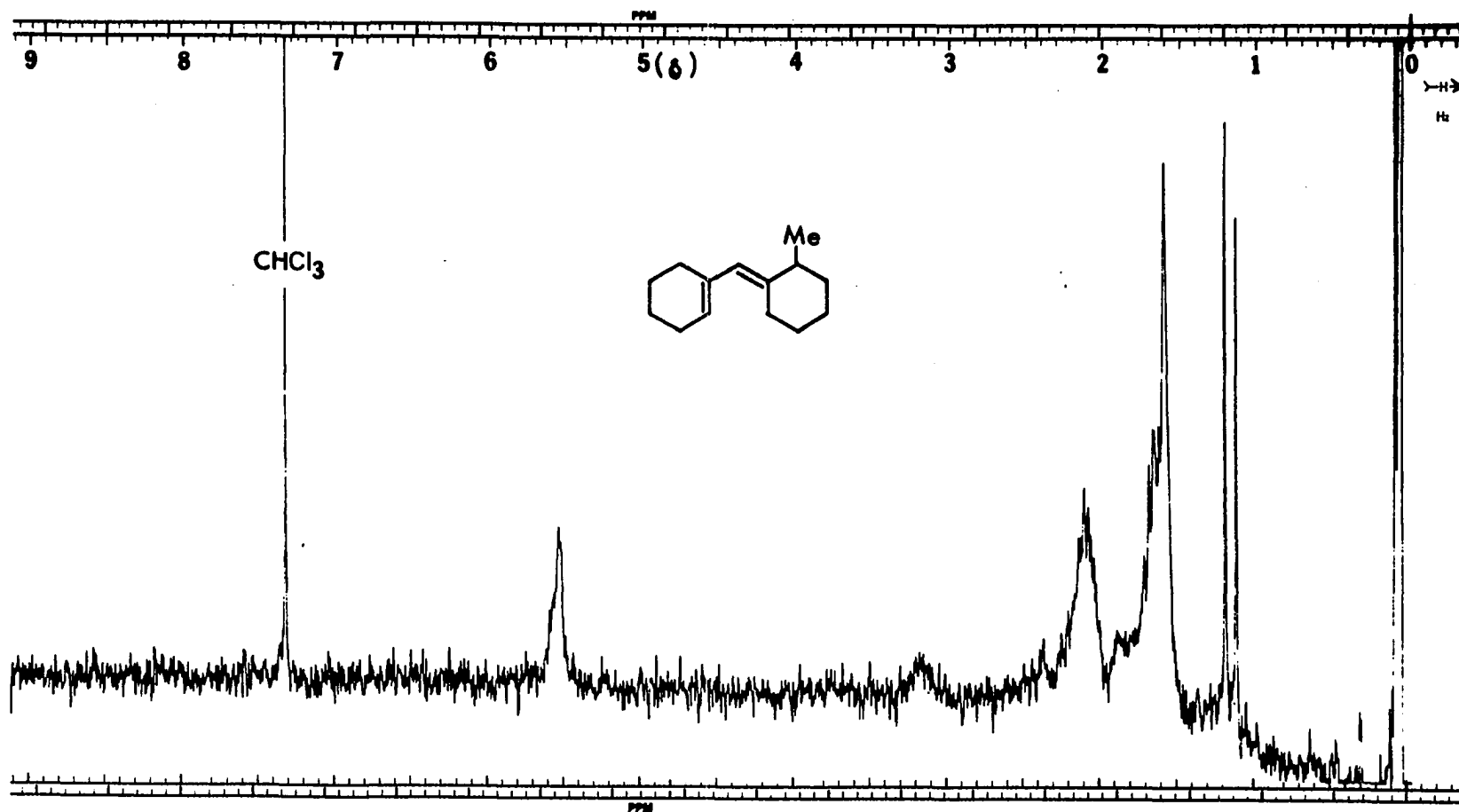


Figure 34 100 MHz PMR Fourier-Transform Spectrum (CDCl₃) of L-b

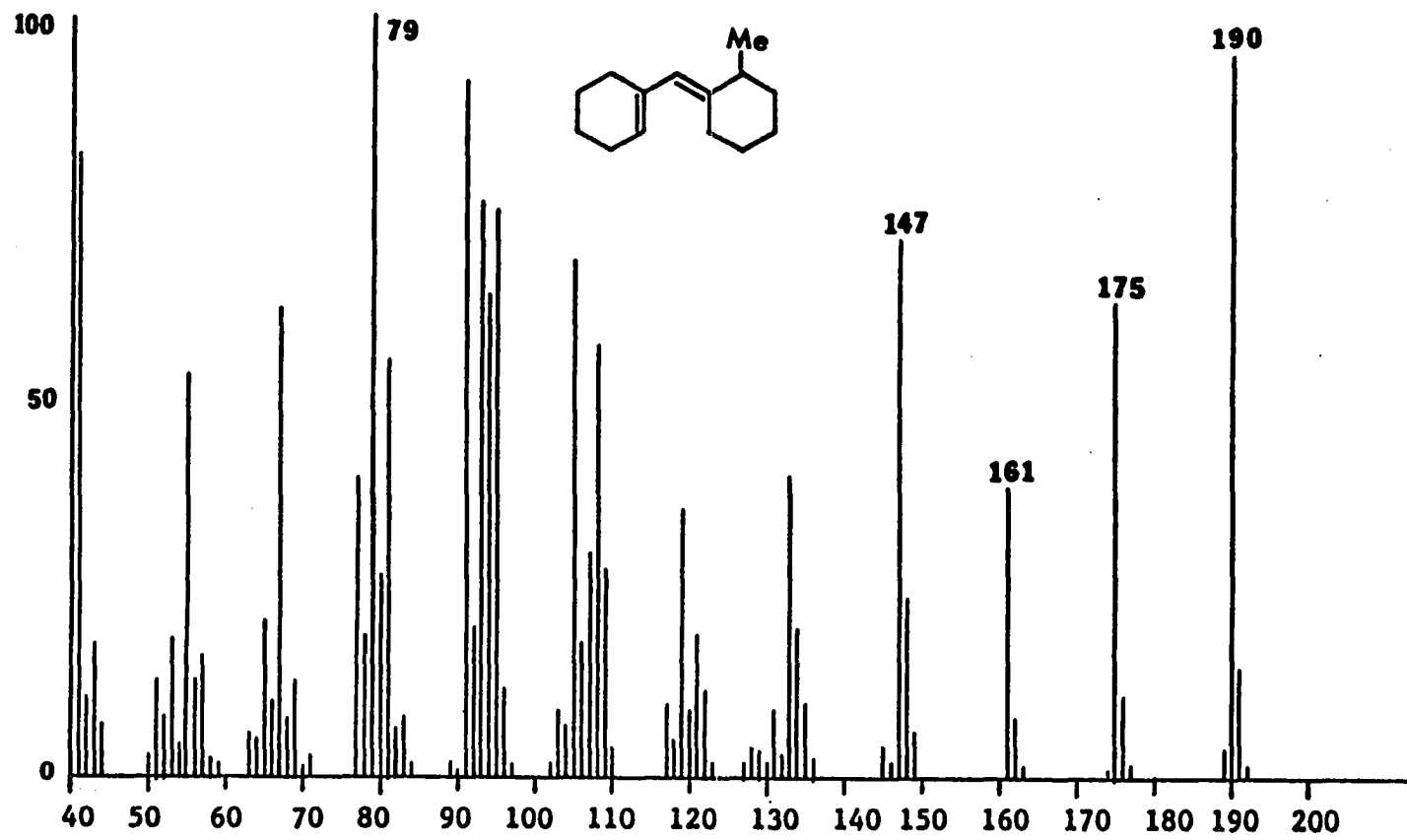


Figure 35 70 eV Mass Spectrum of L-b

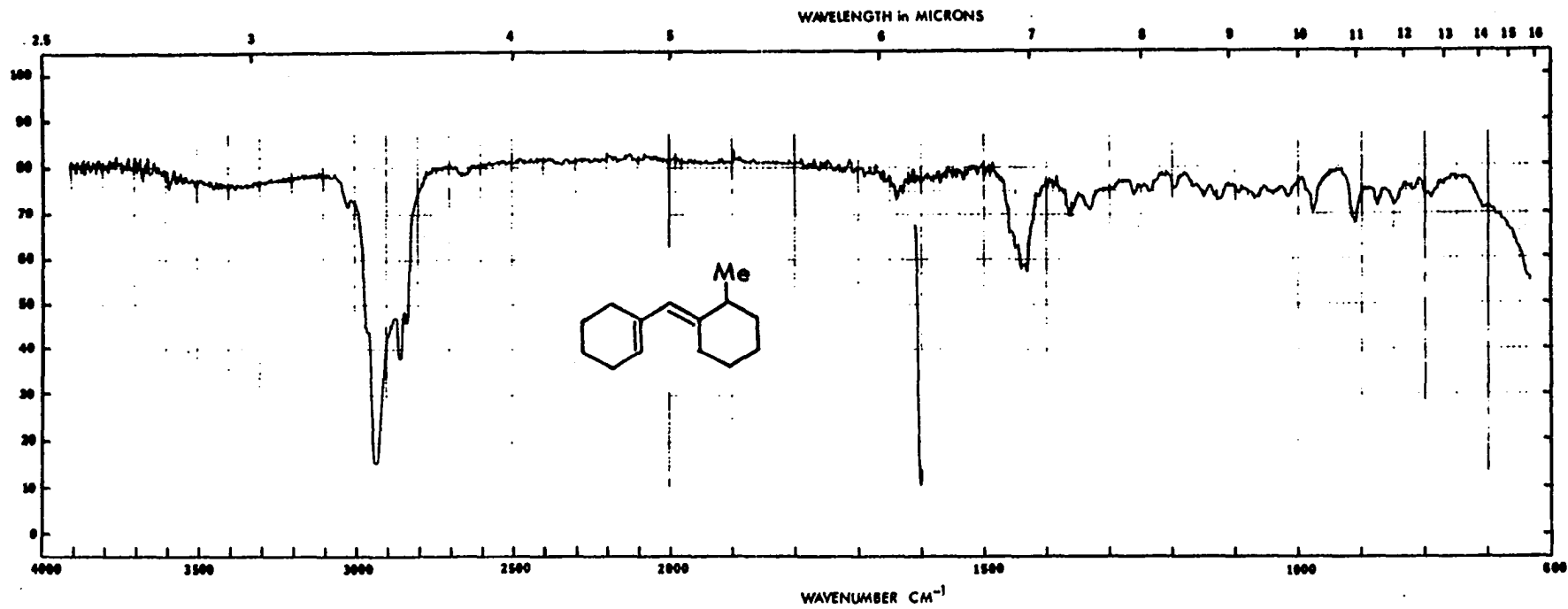


Figure 36 IR Spectrum (film) of L-b

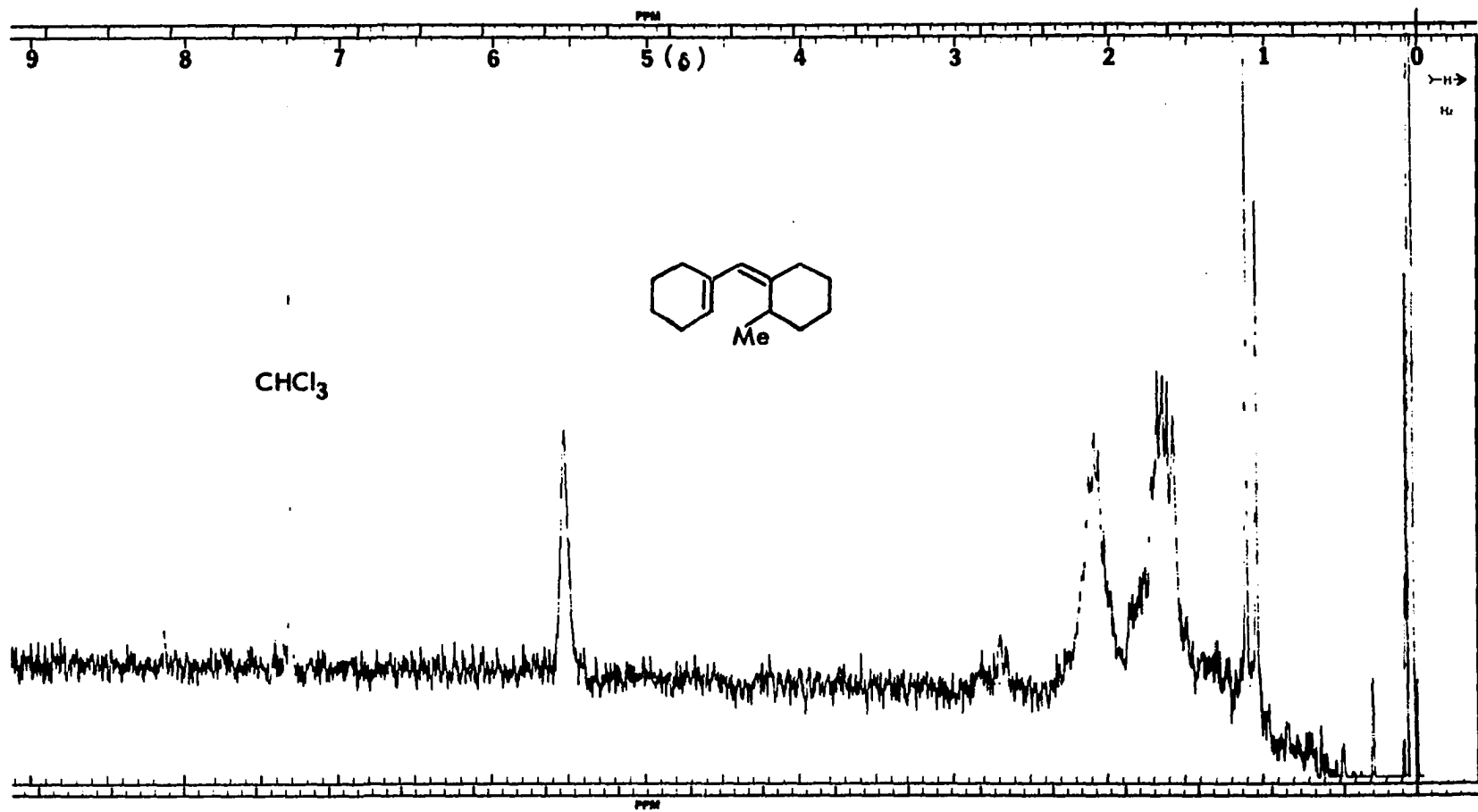


Figure 37 100 MHz PMR Fourier-Transform Spectrum (CDCl₃) of L-c

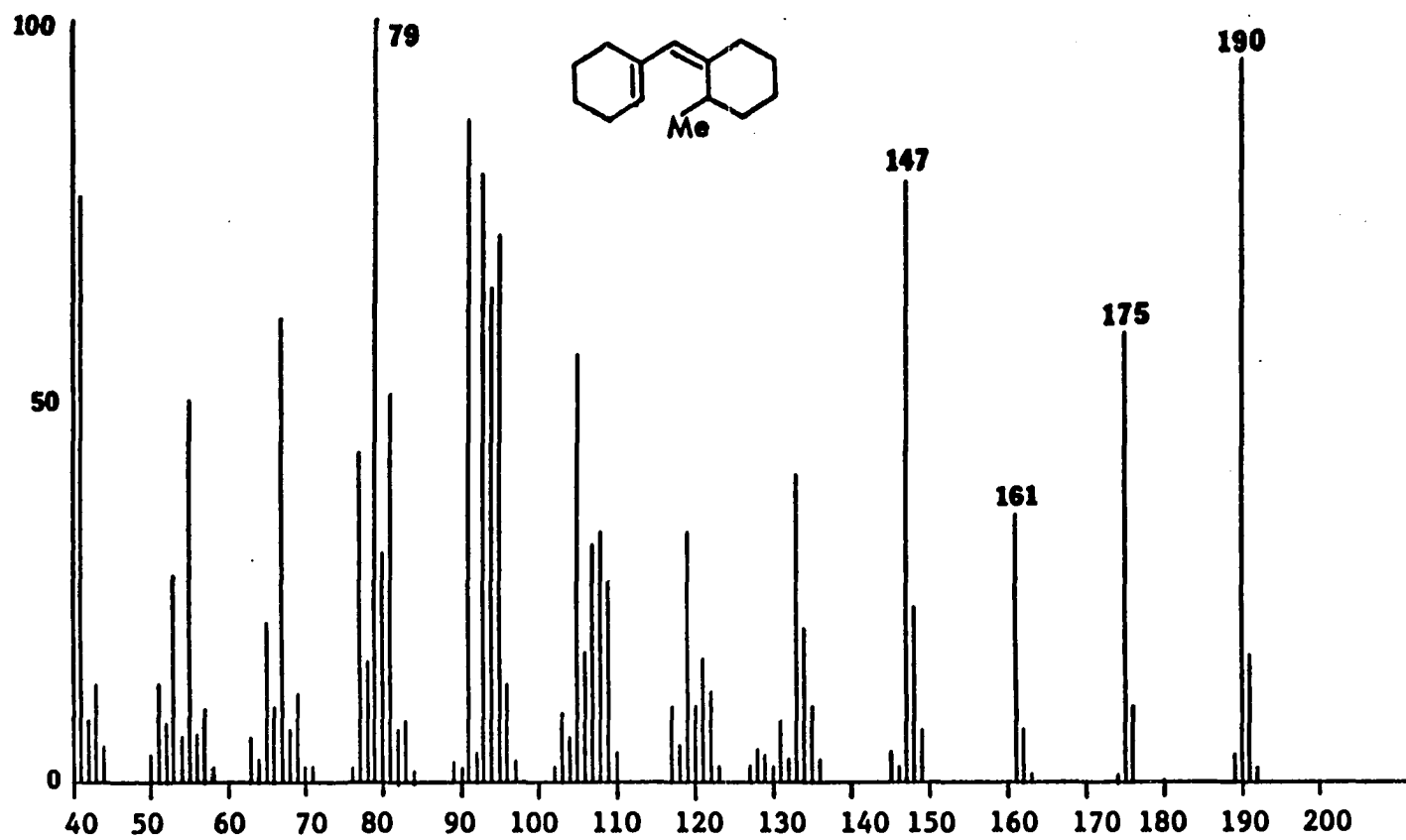


Figure 38 70 eV Mass Spectrum of L-c

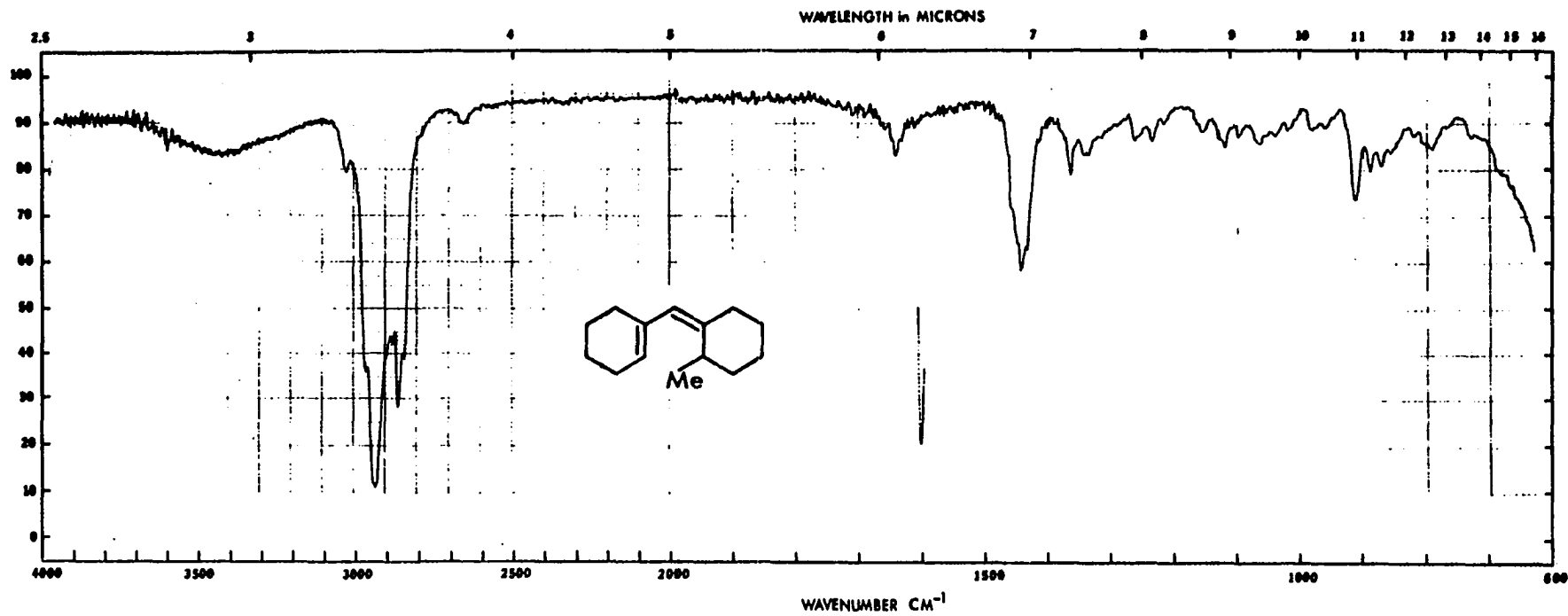
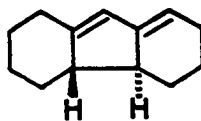


Figure 39 IR Spectrum (film) of L-c

gave λ_{\max} 233 nm, ϵ_{\max} 8,517.

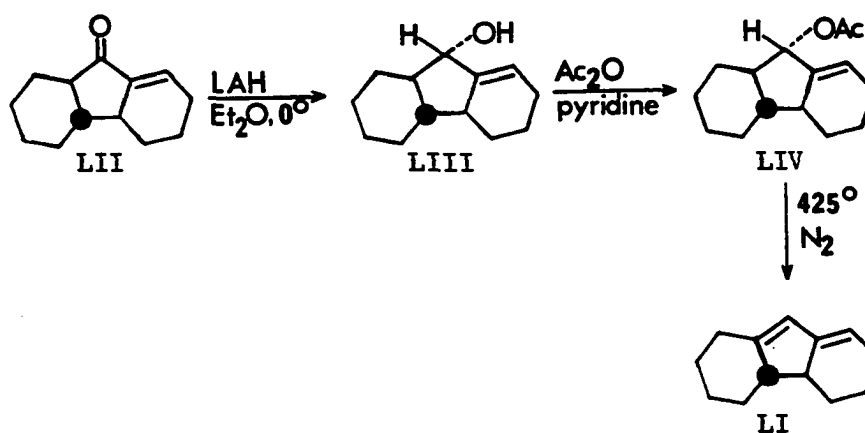
The spectral characteristics which distinguish L-b and L-c will be discussed at a later point in this dissertation.

Decomposition of XXXIV in the vacuum hot tube at temperatures around 350° produced another compound in sufficient amount to allow its isolation and identification. It was isolated by PLC together with the trienes (XLVIII-a) and (XLVIII-b) and was further purified by preparative GLC (FFAP). We have established its structure as that of the anti-diene (LI), by comparison of all spectral and physical data with authentic LI.



LI

Authentic anti-diene (LI) was prepared by the route shown in Scheme 9 starting with the ketone (LII), whose skeletal backbone has been firmly established as anti by X-ray crystallography.³⁵



Scheme 9

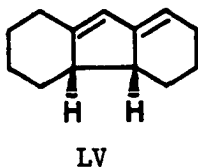
The ketone (LII) was cleanly reduced to the unsaturated alcohol (LIII) by lithium aluminum hydride in ether at ice bath temperatures (0-5°). The alcohol (LIII) was obtained from reaction work-up as a white solid in 93% of theory. After recrystallization from hexane, LIII melted at 87-89°. In assigning the structure for LIII, we assumed a least-hindered side approach of the reducing agent. Examination of molecular models of LII indicates that the structure given for LIII is reasonable, based on this assumption. The 60 MHz PMR spectrum of LIII (Figure 40) in CDCl_3 showed: δ 5.75 (1H multiplet, olefinic proton), 4.0 (1H multiplet, proton on carbon bearing oxygen), 0.8-2.3 (18H multiplet, ring protons and hydroxyl proton). The 70 eV mass spectrum (Figure 41) showed: m/e 192 (M^+ , parent ion and base peak), 175 ($\text{M}^+ - \text{OH}$), 174 ($\text{M}^+ - \text{H}_2\text{O}$), 163 ($\text{M}^+ - \text{C}_2\text{H}_5$). The IR spectrum (KBr) showed: cm^{-1} 3260 (-OH), 1670 (C=C), 1095 (C-O).

Treatment of LIII with acetic anhydride in pyridine under reflux gave the acetate (LIV). The acetate was isolated in 91% yield by PLC as a clear oil which solidified on standing. Recrystallization from hexane gave LIV which melted at 57-58.5°C. The 60 MHz PMR spectrum of LIV (Figure 42) in CCl_4 showed: δ 5.75 (1H multiplet, olefinic proton), 5.15 (1H broad doublet, $J = 7\text{Hz}$, proton on carbon bearing oxygen), 1.95 (3H singlet, acetate methyl protons), 0.8-2.2 (17H multiplet, ring protons). The 70 eV mass spectrum (Figure 43) showed: m/e 234 (M^+ , parent ion), 192 ($\text{M}^+ - \text{H}_2\text{C}=\text{C}=\text{O}$), 174 (base peak, $\text{M}^+ - \text{CH}_3\text{CO}_2\text{H}$), 43 ($\text{CH}_3\text{C}=\text{O}^+$). The IR spectrum (film) showed: cm^{-1} 1735 (acetate C=O), 1240 (C-O).

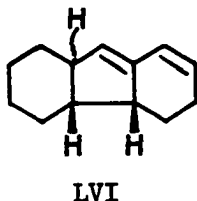
The acetate (LIV) was thermolyzed at 425° in a heated tube filled with glass beads under a nitrogen flow of ca. 45 ml/min. The diene (LI) was collected in a dry ice-isopropanol cooled, U-shaped collector. Purification of LI was achieved by preparative GLC (Carbowax 20M) followed by

bulb to bulb distillation at 70°/0.5 torr. The diene (LI) was obtained in 45% yield as a clear oil which quickly yellowed upon exposure to atmosphere. The 60 MHz PMR spectrum of LI (Figure 44) in CCl₄ showed: δ 5.65 (1H broad singlet, olefinic proton H_b), 5.15 (1H multiplet, olefinic proton H_a), 0.75-2.70 (16H multiplet, ring protons). The 70 eV mass spectrum (Figure 45) showed: m/e 174 (M⁺, parent ion and base peak), 145 (M⁺-C₂H₅), 131 (M⁺-C₃H₇). The IR spectrum (Figure 46) showed: cm⁻¹ 3040 (olefinic C-H), 1660 and 1615 (C=C), 890 and 860 (C=CH). The UV spectrum (hexane) gave λ_{max} 248 nm, ε_{max} 16,344.

In order to test the possibility that the syn-diene (LV) was formed in the vacuum hot tube decomposition of XXXIV, we sought to prepare an authentic sample of LV. Starting with the known³⁵ ketone (LVII), we



pursued a reaction sequence analogous to that used in the preparation of the anti-diene (LI). This course of action, however, led mainly to the formation of the diene (LVI) as shown in Scheme 10. The preparation of the syn-diene (LV) was accomplished by direct dehydration of the alcohol (LVIII).



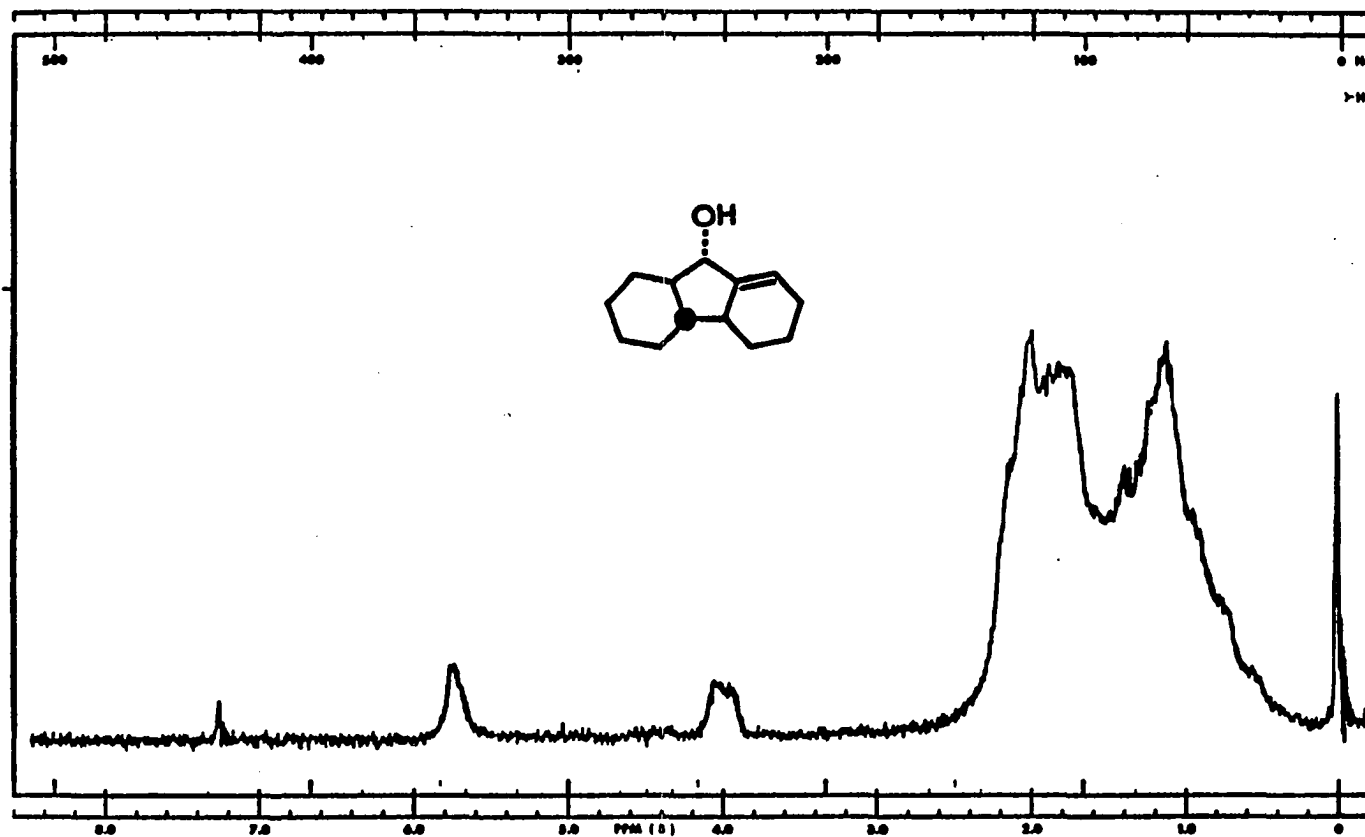


Figure 40 60 MHz PMR Spectrum (CDCl_3) of LIII

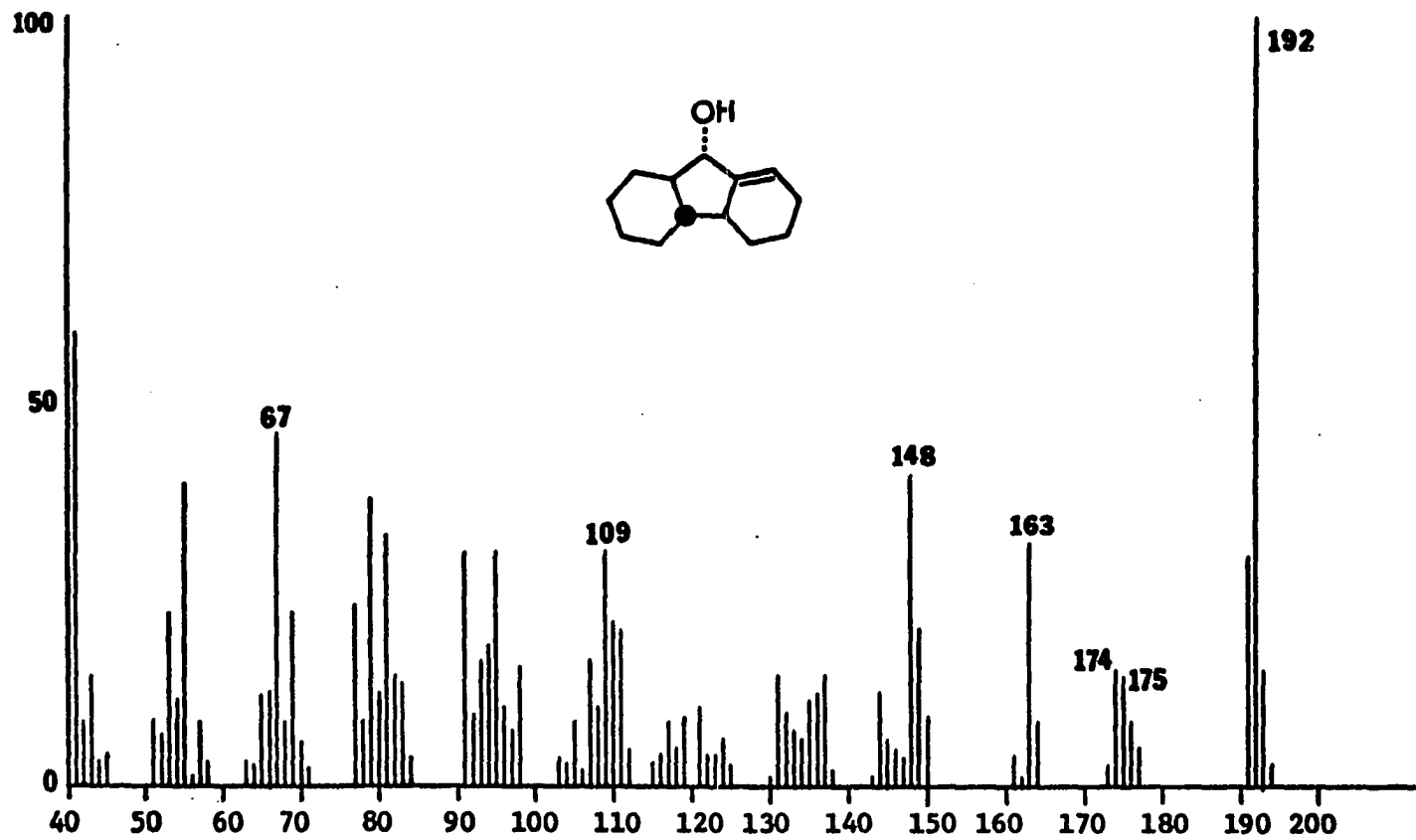


Figure 41 70 eV Mass Spectrum of LIII

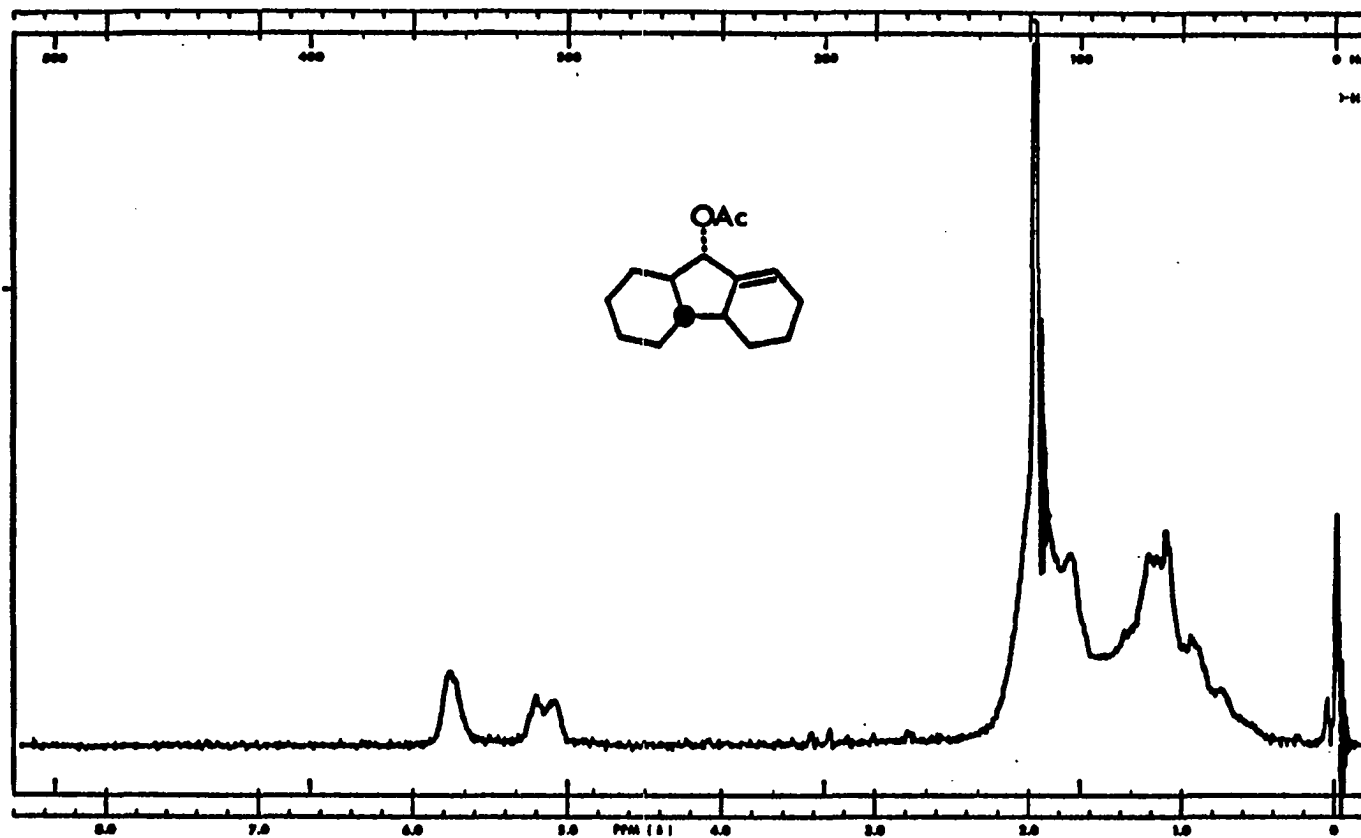


Figure 42 60 MHz PMR Spectrum (CCl₄) of LIV

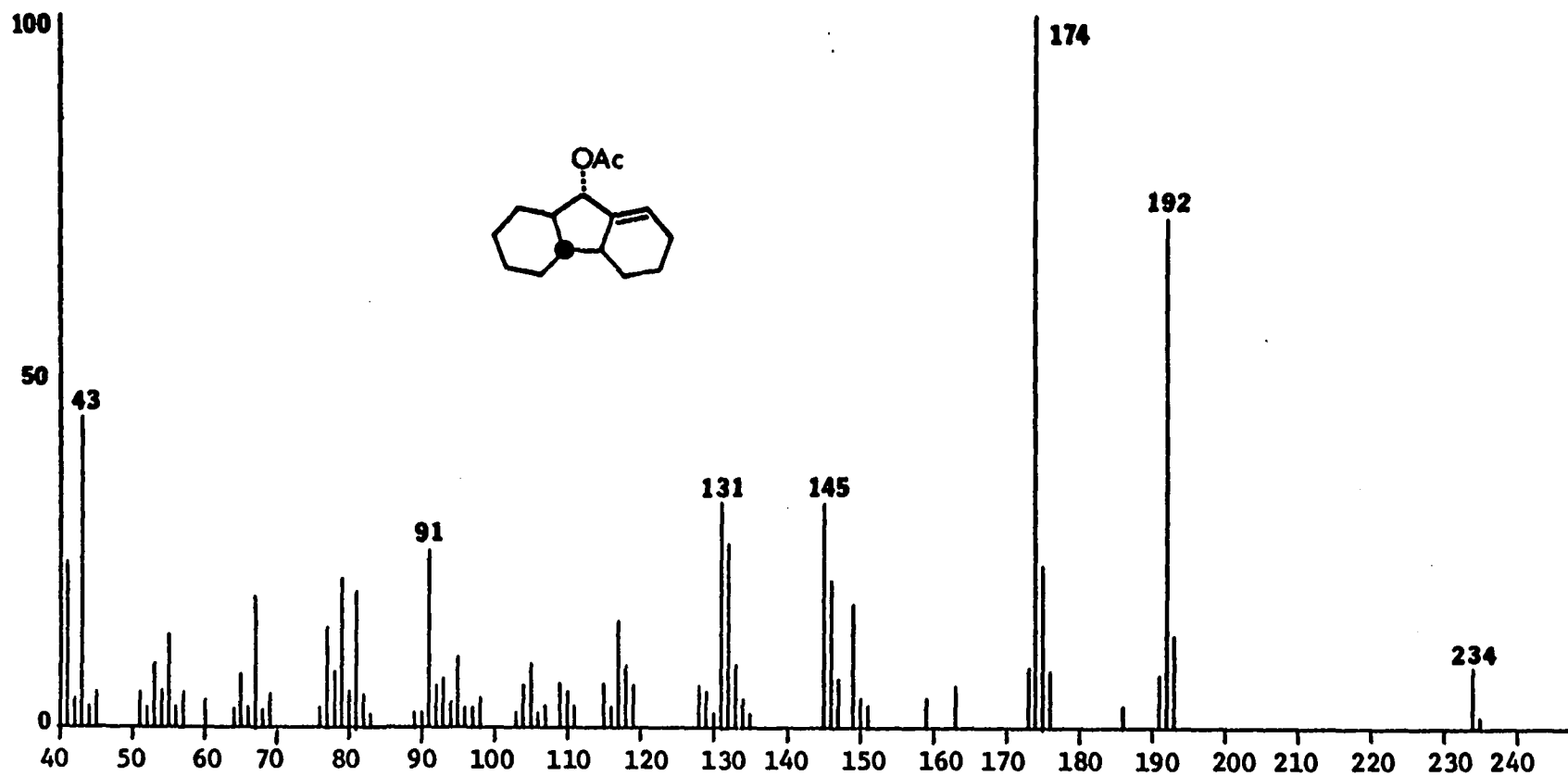


Figure 43 70 eV Mass Spectrum of LIV

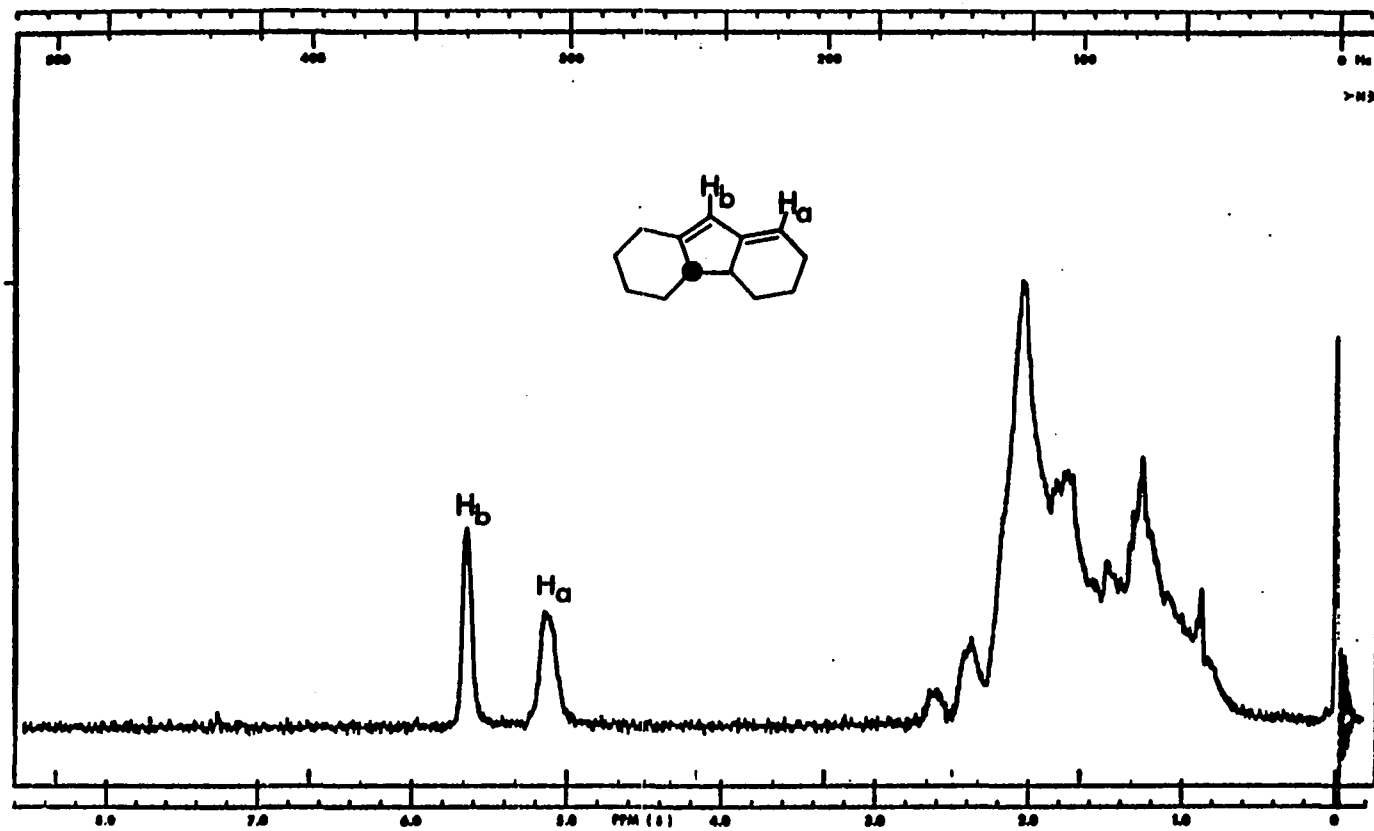


Figure 44 60 MHz PMR Spectrum (CCl₄) of LI

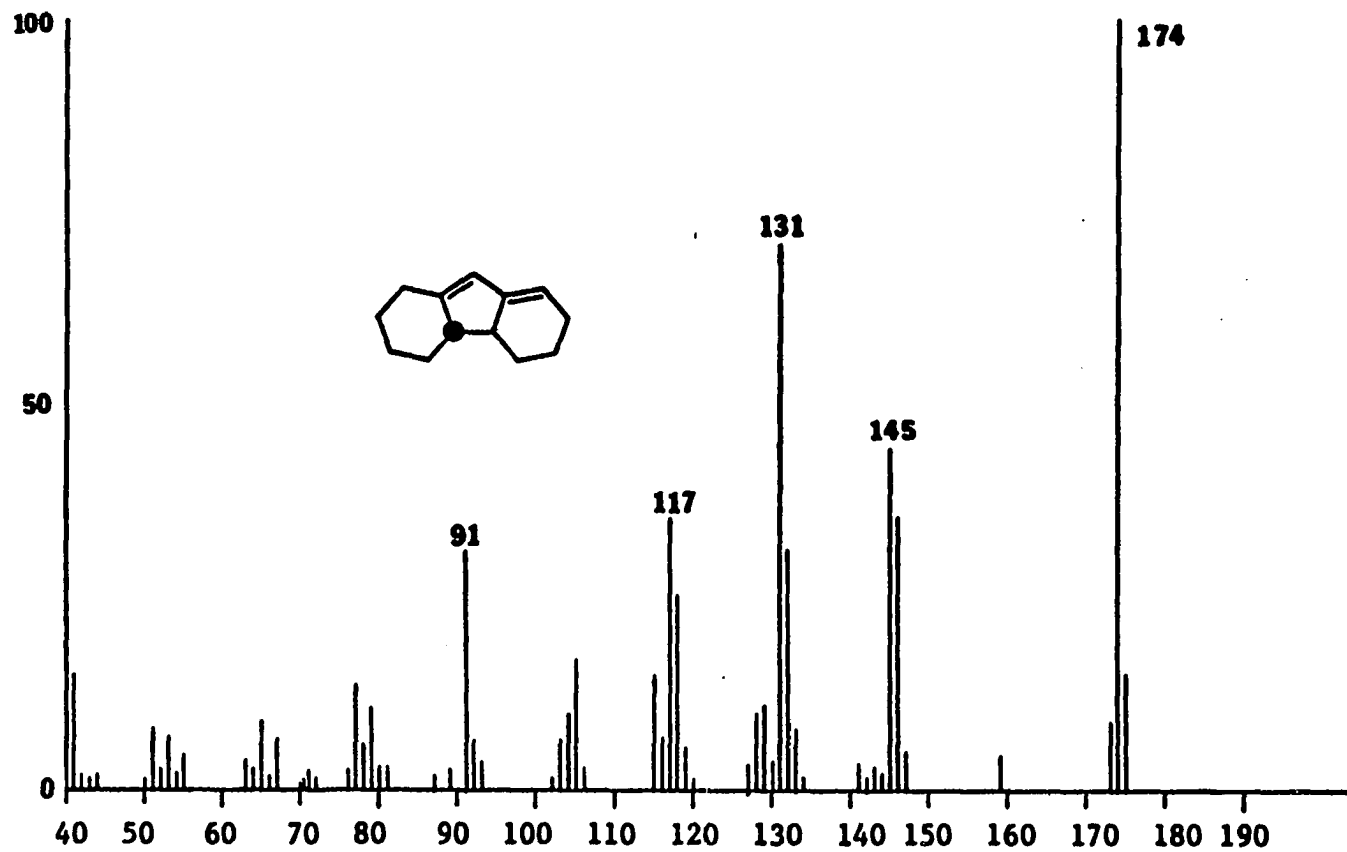


Figure 45 70 eV Mass Spectrum of LI

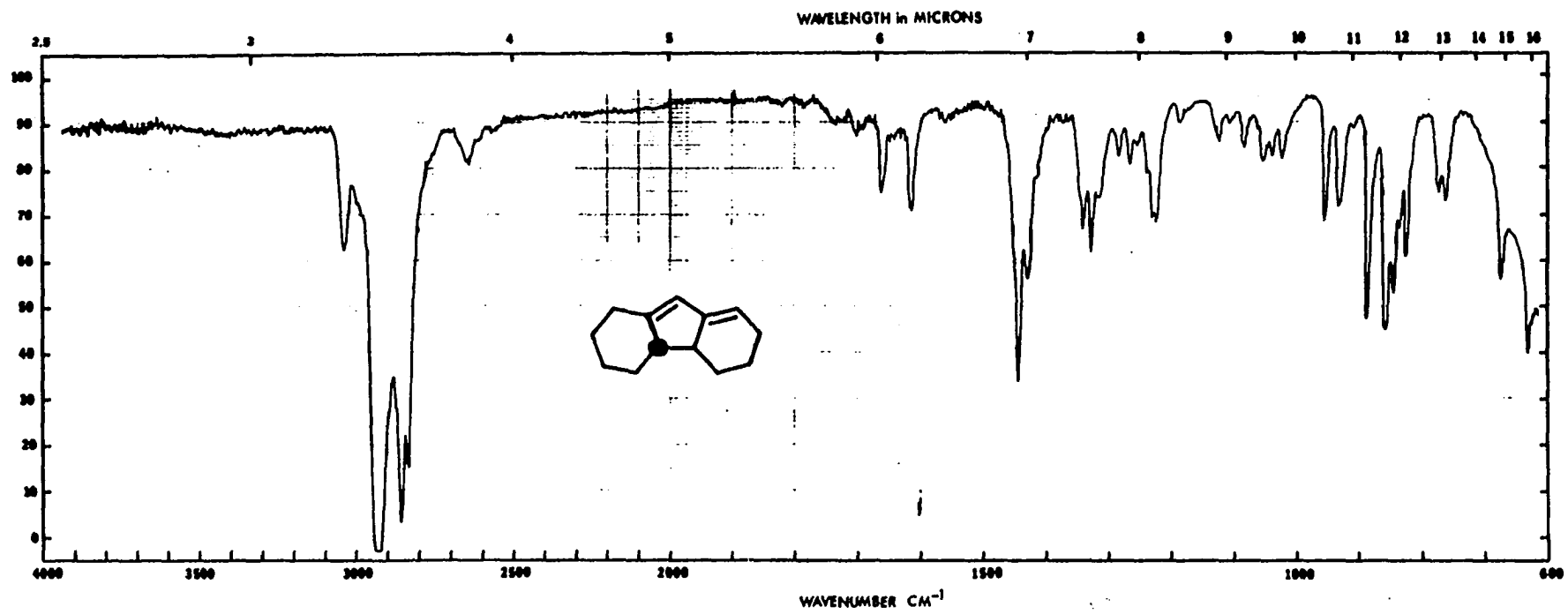
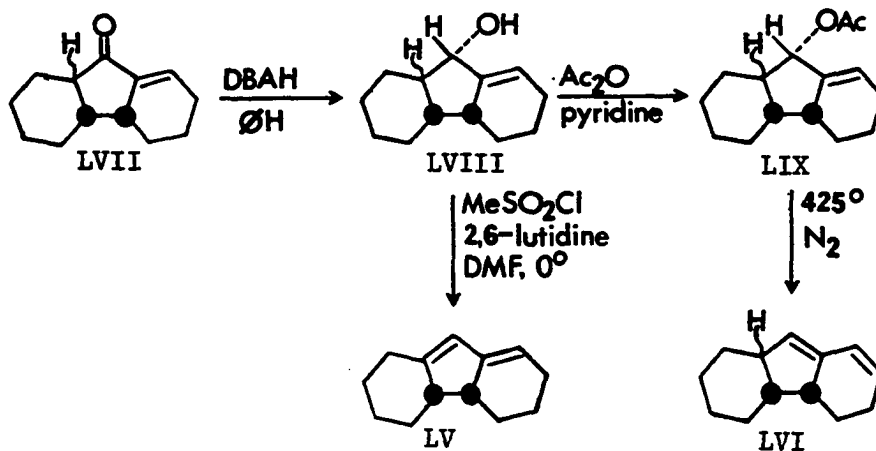


Figure 46 IR Spectrum (film) of LI



Scheme 10

The ketone (LVII) was reduced to the unsaturated alcohol (LVIII) by diisobutyl aluminum hydride (DBAH)³⁶ in benzene with ice bath cooling under an atmosphere of dry nitrogen. The reduction did not proceed cleanly to the unsaturated alcohol (LVIII), but rather always led to mixtures containing products in which the double bond in LVII had been reduced. This latter was ascertained mainly by PMR and mass spectral examination of the by-products. Other reducing agents including: NaBH_4 , LiAlH_4 , $\text{LiAlH}(\text{OEt})_3$, $\text{LiAlH}(\text{OBu-t})_3$, and $\text{NaAlH}_2(\text{OCH}_2\text{CH}_2\text{OCH}_3)_2$ gave lower yields of the desired alcohol (LVIII). The alcohol (LVIII) was isolated from the DBAH reduction by chromatography in 69% yield as a clear slightly yellowed oil which crystallized on standing. Recrystallization from hexane gave LVIII which melted at $48\text{--}50^\circ$. In assigning the structure for LVIII, we assumed a least-hindered side approach of the reducing agent to the ketone (LVII). Examination of molecular models of LVII support the structure given for LVIII. The 60 MHz PMR spectrum of LVIII (Figure 47) in CCl_4 showed: δ 5.75 (1H multiplet, olefinic proton), 4.35 (1H multiplet, proton on carbon bearing oxygen), 0.8–2.2 (18H multiplet, ring protons and hydroxyl proton). The 70 eV mass spectrum (Figure 48)

showed: m/e 192 (M^+ , parent ion), 174 ($M^+ - H_2O$), 163 ($M^+ - C_2H_5$), 67 (base peak). The IR spectrum (CCl_4) showed: cm^{-1} 3620 (-OH), 1670 (C=C), 1110 (C-O).

The acetate (LIX) was prepared by the treatment of LVIII with acetic anhydride in pyridine under reflux. Isolation by PLC gave LIX in 94% yield as a slightly yellowed oil which solidified on standing. Recrystallation from hexane gave pure white LIX which melted at 36-37.5°. The 60 MHz PMR spectrum of LIX (Figure 49) in CCl_4 showed: δ 5.6 (2H multiplet, olefinic proton and proton on carbon bearing oxygen), 2.05 (3H singlet, acetate methyl protons), 0.8-2.2 (17H multiplet, ring protons). The 70 eV mass spectrum (Figure 50) showed: m/e 234 (M^+ , parent ion), 192 ($M^+ - H_2C=C=O$), 174 ($M^+ - CH_3CO_2H$), 43 (base peak, $CH_3C=O^+$). The IR spectrum (CCl_4) showed: cm^{-1} 1735 (acetate C=O), 1240 (C-O).

Thermolysis of the acetate (LIX) at 425° in a glass bead filled heated tube under a nitrogen flow of ca. 45 ml/min produced the diene (LVI) as the major product in 28% yield. The diene (LVI) was isolated by preparative GLC (Carbowax 20M) and further purified by bulb to bulb distillation at 85°/0.1 torr to give LVI as a clear colorless oil which very quickly yellowed on exposure to atmosphere. A smaller amount (ca. 9%) of the syn-diene (LV) was also obtained by this procedure. The 60 MHz PMR spectrum of LVI (Figure 51) in CCl_4 showed: δ 6.2 (1H broad doublet, $J_{bc} = 10Hz$, olefinic proton H_c), 5.7 (1H multiplet, approximately six broad lines, $J_{bc} = 10 Hz$, $J = 4 Hz$, olefinic proton H_b), 5.25 (1H broad singlet, olefinic proton H_a). The 70 eV mass spectrum (Figure 52) showed: m/e 174 (M^+ , parent ion and base peak), 145 ($M^+ - C_2H_5$), 131 ($M^+ - C_3H_7$). The IR spectrum (Figure 53) showed: cm^{-1} 3030 (olefinic C-H), 1625 (C=C), 860 and 815 (C=CH). The UV spectrum (hexane) gave λ_{max} 243 nm, ϵ_{max} 17,423.

Treatment of the alcohol (LVIII) with methanesulfonylchloride and dry 2,6-lutidine in dry DMF³⁷ at 0-5° gave the syn-diene (LV) as the major product (ca. 22%) along with smaller amounts of the diene (LVI) (ca. 7%). Dehydration of LVIII was also attempted using hot polyphosphoric acid, phosphorous oxychloride in pyridine, toluenesulfonylchloride in pyridine, and KHSO₄. These other reagents produced complex mixtures of hydrocarbons and were therefore unsatisfactory for our purposes. The dienes (LV) and (LVI) were isolated by chromatography on a short column of florisil and further separated and purified by preparative GLC (FFAP) and bulb to bulb distillation at 40°/0.01 torr. The syn-diene (LV) was obtained as a clear colorless oil which yellowed on exposure to atmosphere. The 60 MHz PMR spectrum of LV (Figure 54) in benzene-d₆ showed: δ 5.8 (1H broad singlet, olefinic proton H_b), 5.2 (1H multiplet, olefinic proton H_a), 0.8-2.8 (16H multiplet, ring protons). The 70 eV mass spectrum (Figure 55) showed: m/e 174 (M⁺, parent ion and base peak), 145 (M⁺-C₂H₅), 131 (M⁺-C₃H₇). The IR spectrum (Figure 56) showed: cm⁻¹ 3040 (olefinic C-H), 1660 and 1615 (C=C), 880 and 850 (C=CH). The UV spectrum (hexane) gave λ_{\max} 245 nm, ϵ_{\max} 15,624.

GLC Enhancement of Minor Products

The minor products produced in the vacuum hot tube decomposition of XXXIV were investigated by the co-injection of authentic potential products with the hot tube mixtures onto the gas chromatograph. These investigations were conducted using three different S.C.O.T. columns: 100 ft. FFAP, 50 ft. SE-30, and 50 ft. OS-138.

The potential products investigated by this method include

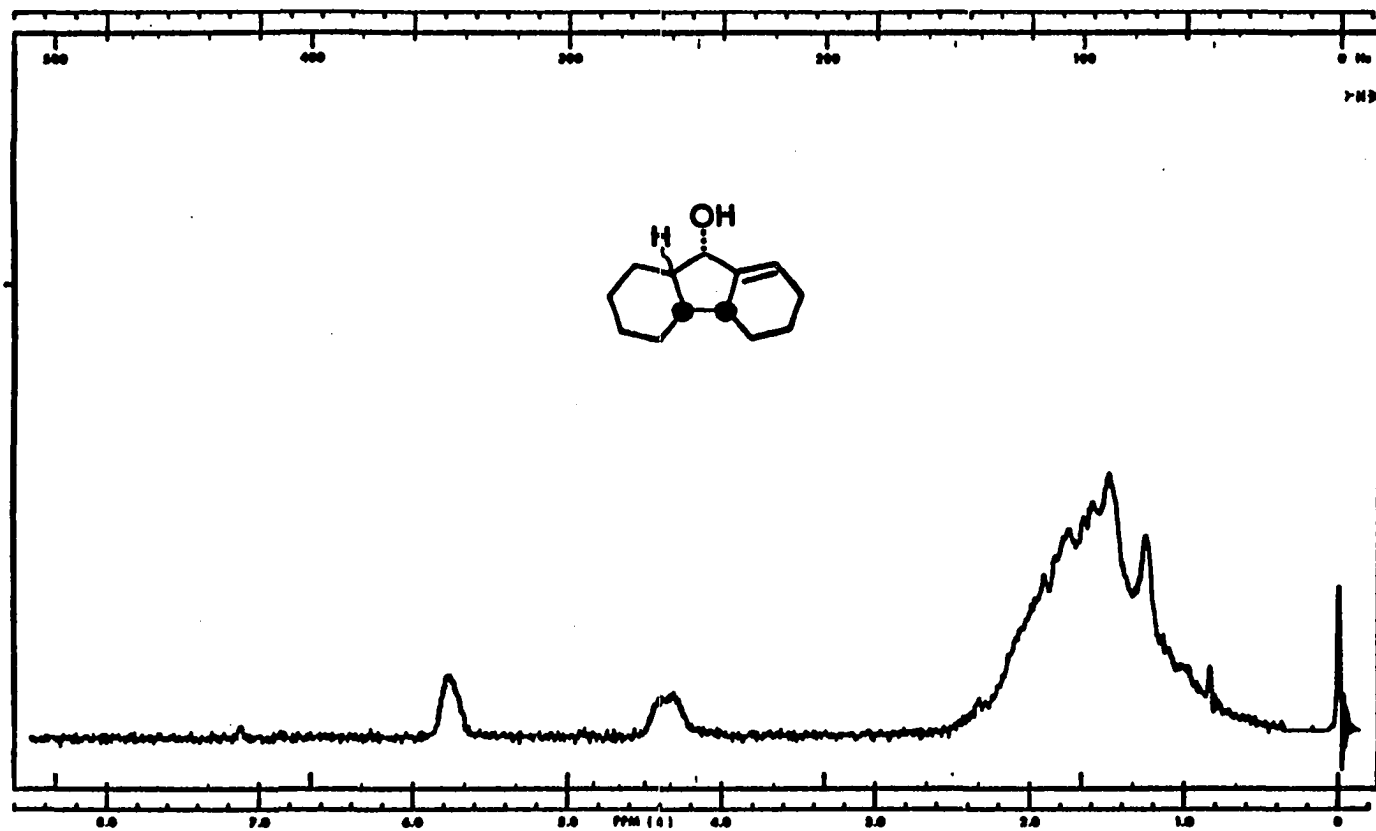


Figure 47 60 MHz PMR Spectrum (CCl₄) of LVIII

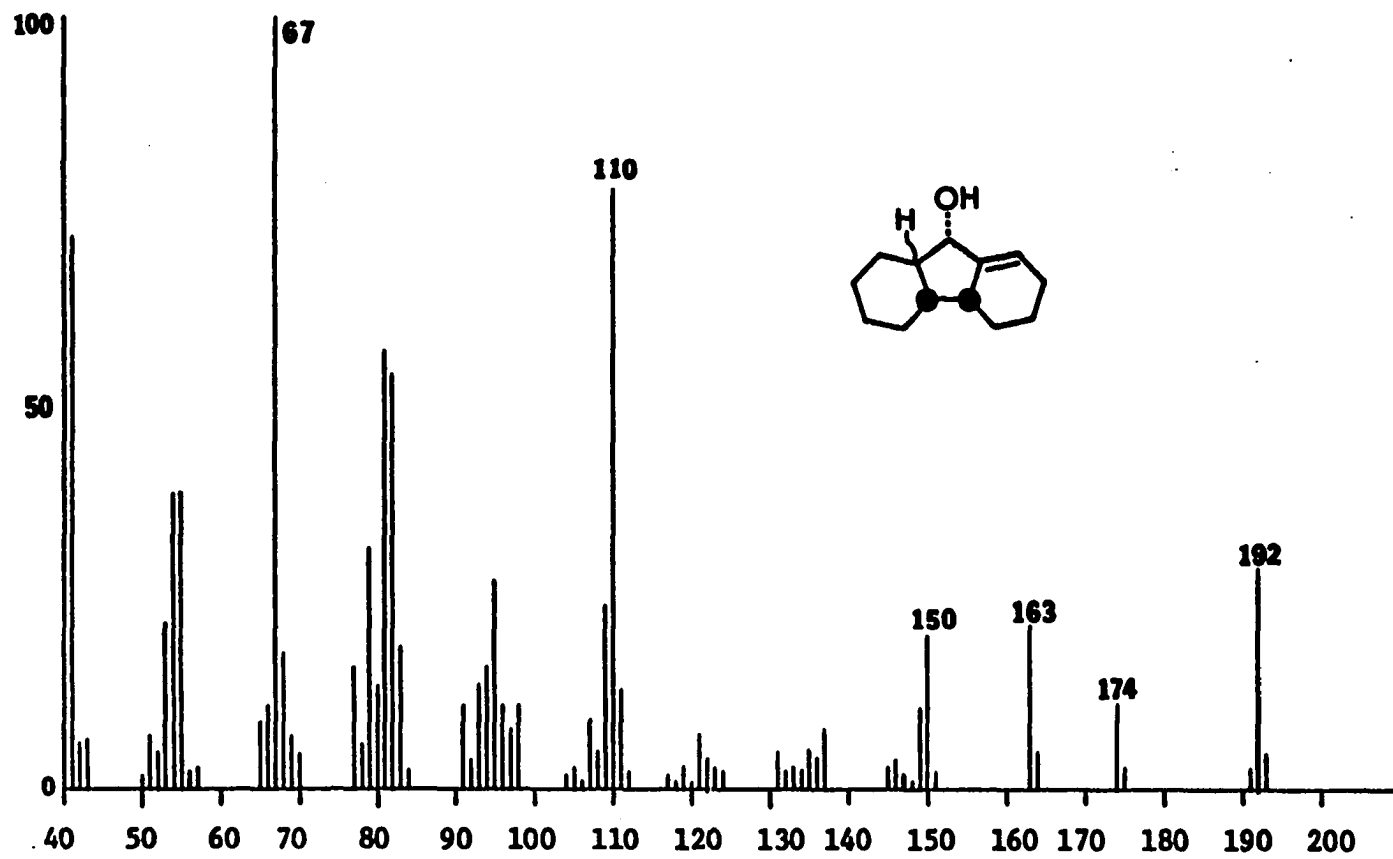


Figure 48 70 eV Mass Spectrum of LVIII

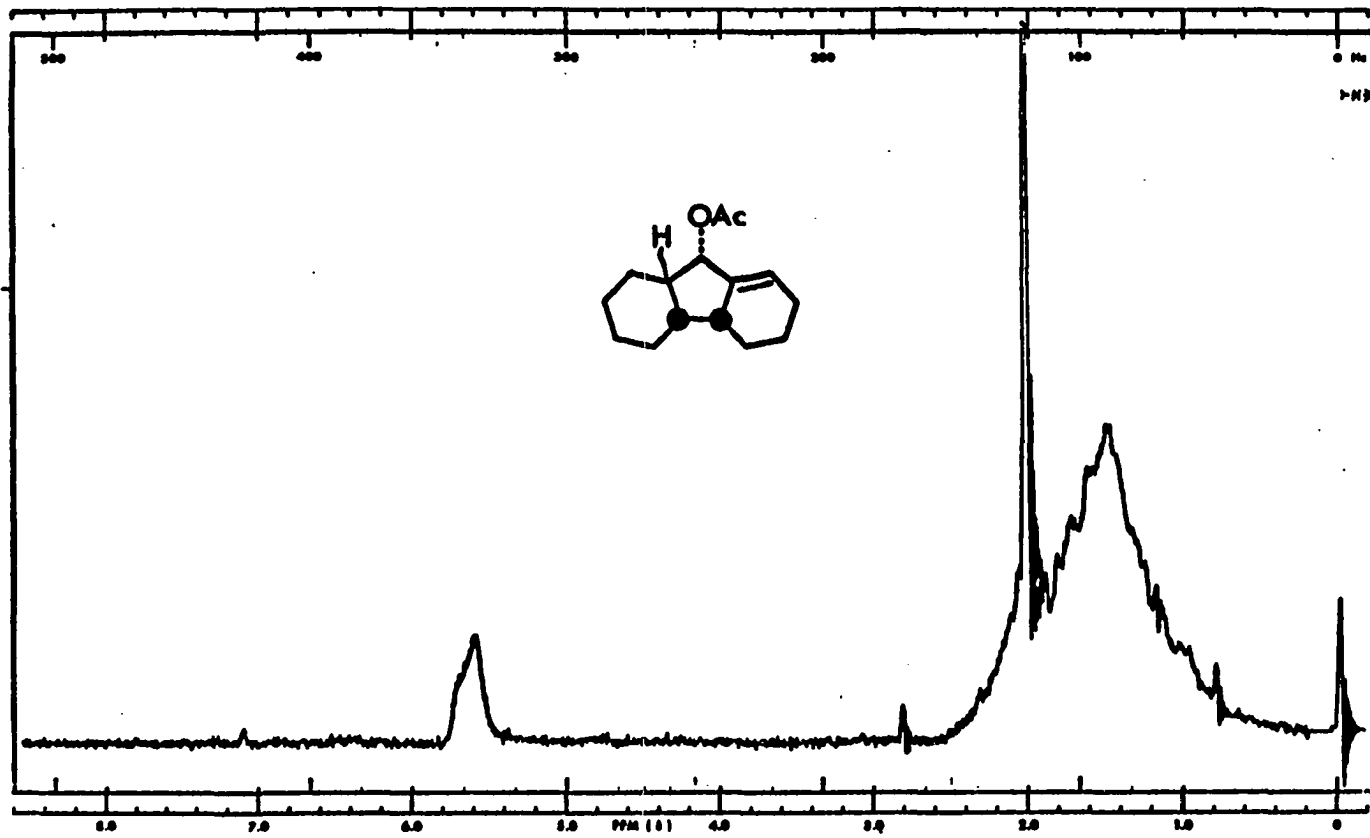


Figure 49 60 MHz PMR Spectrum (CCl_4) of LIX

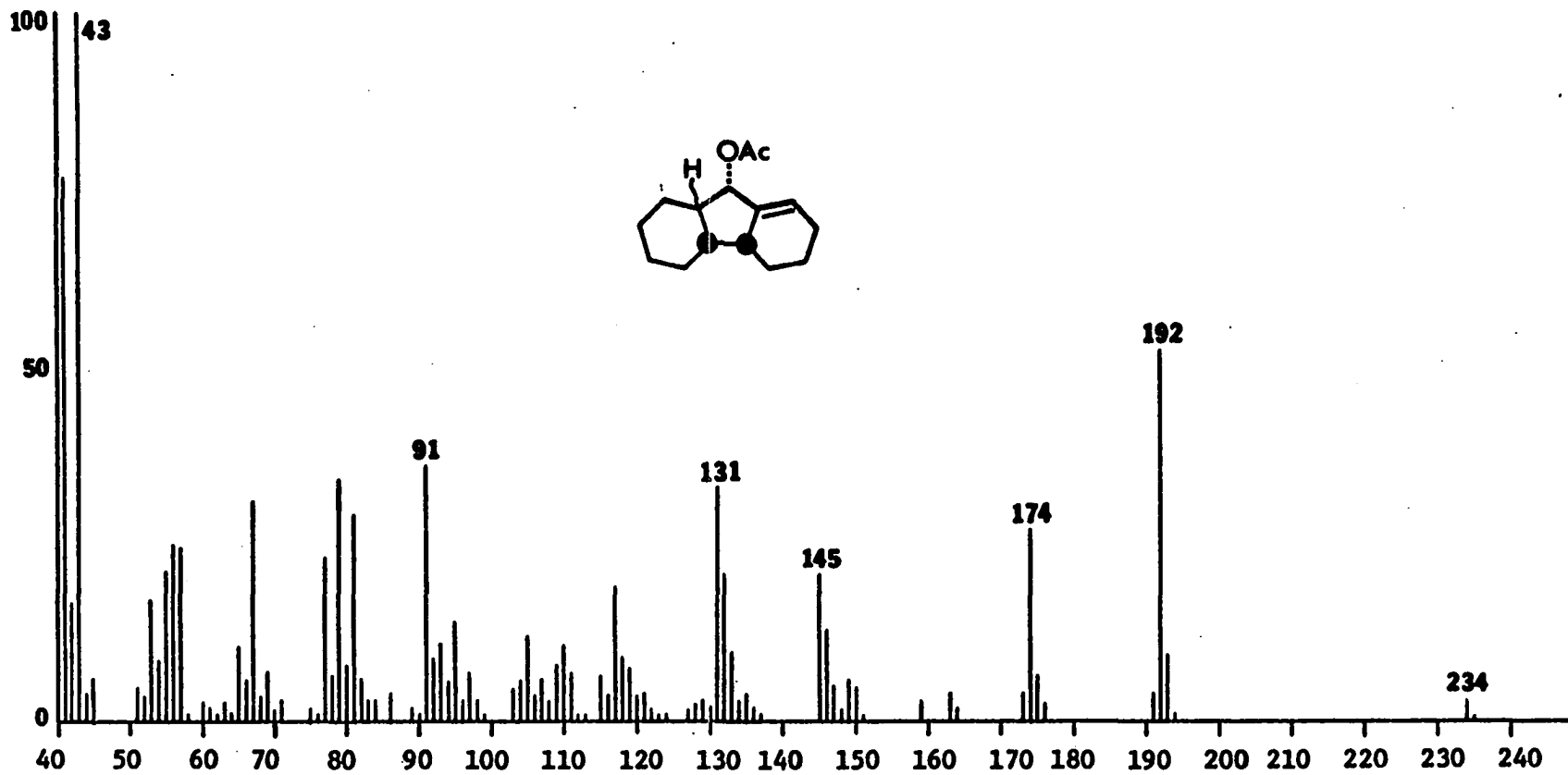


Figure 50 70 eV Mass Spectrum of LIX

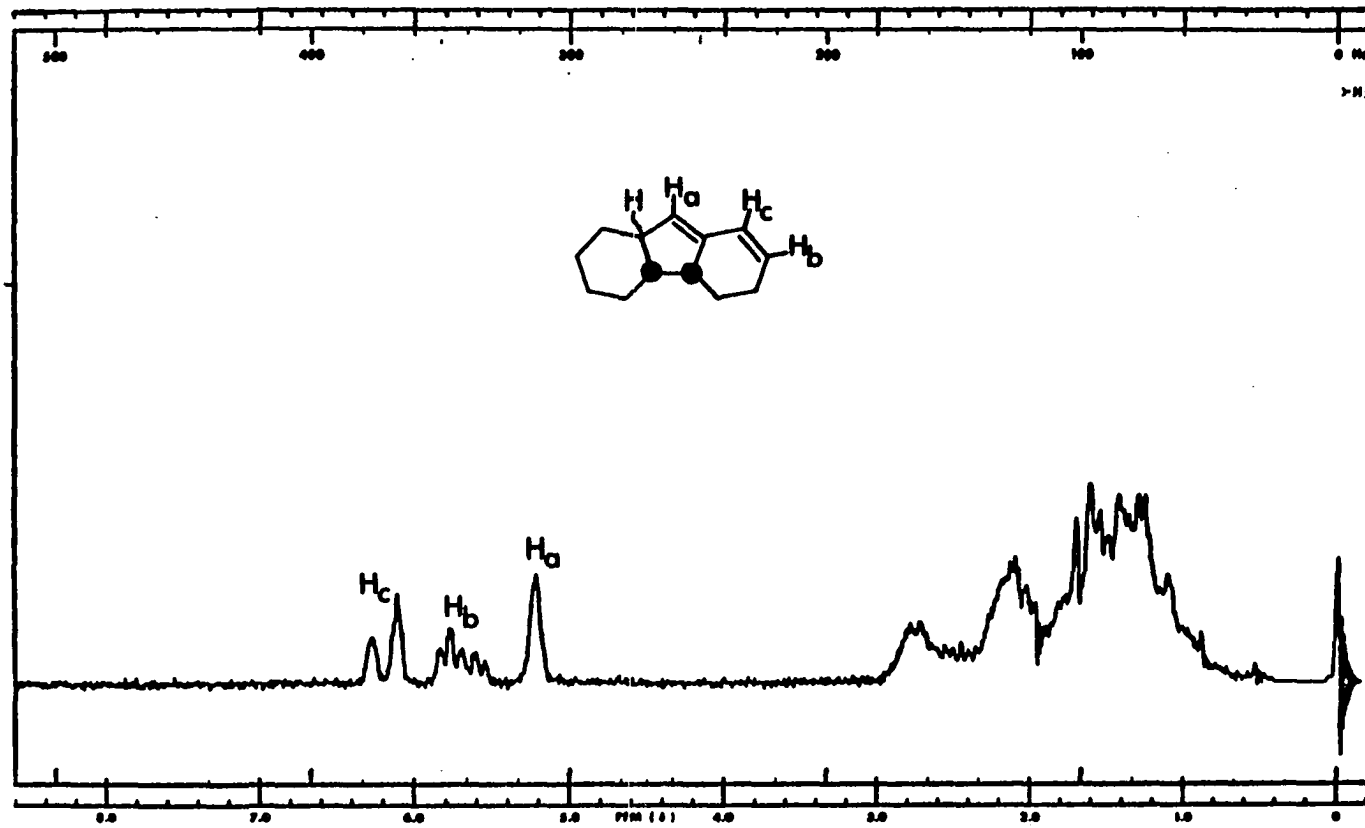


Figure 51 60 MHz PMR Spectrum (CCl_4) of LVI

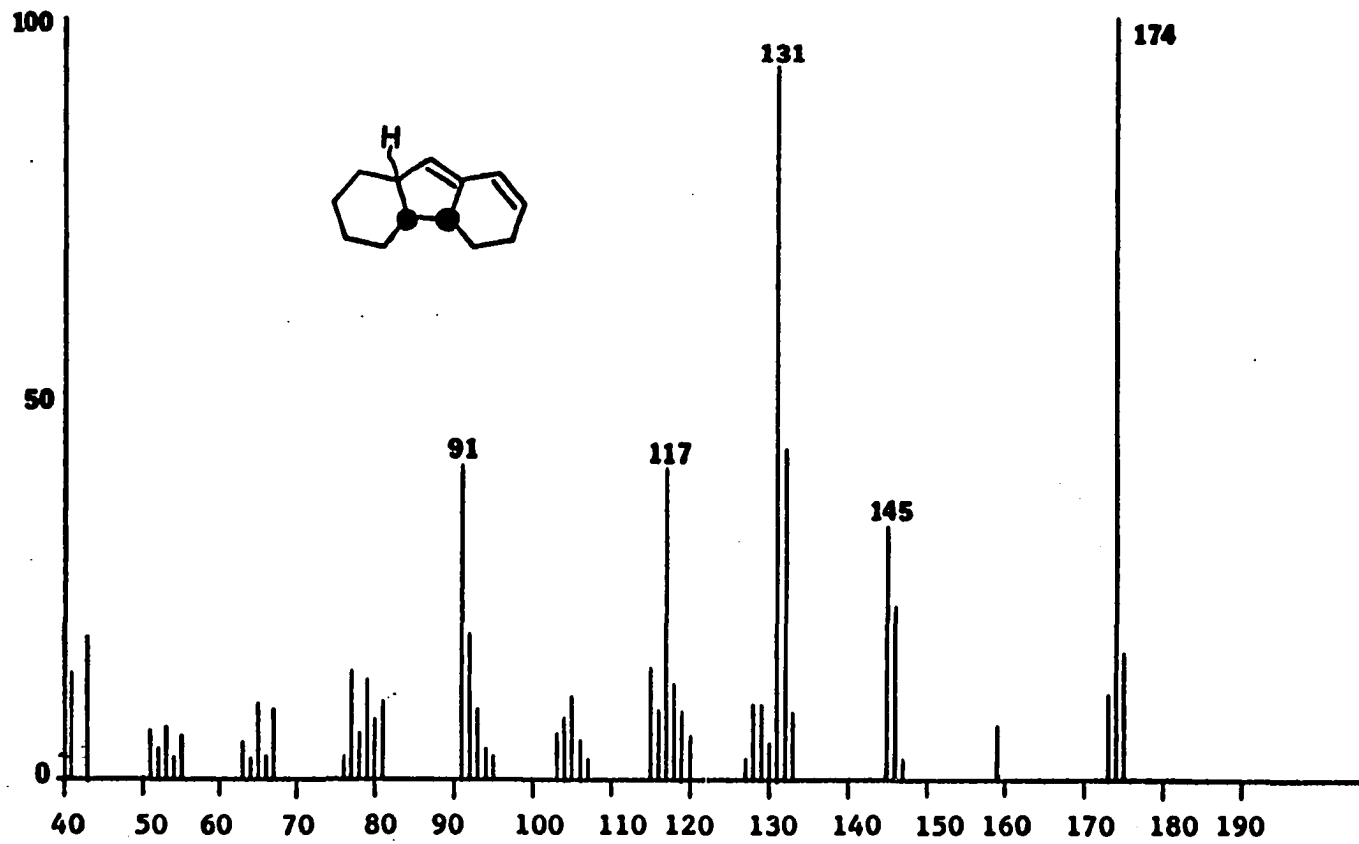


Figure 52 70 eV Mass Spectrum of LVI

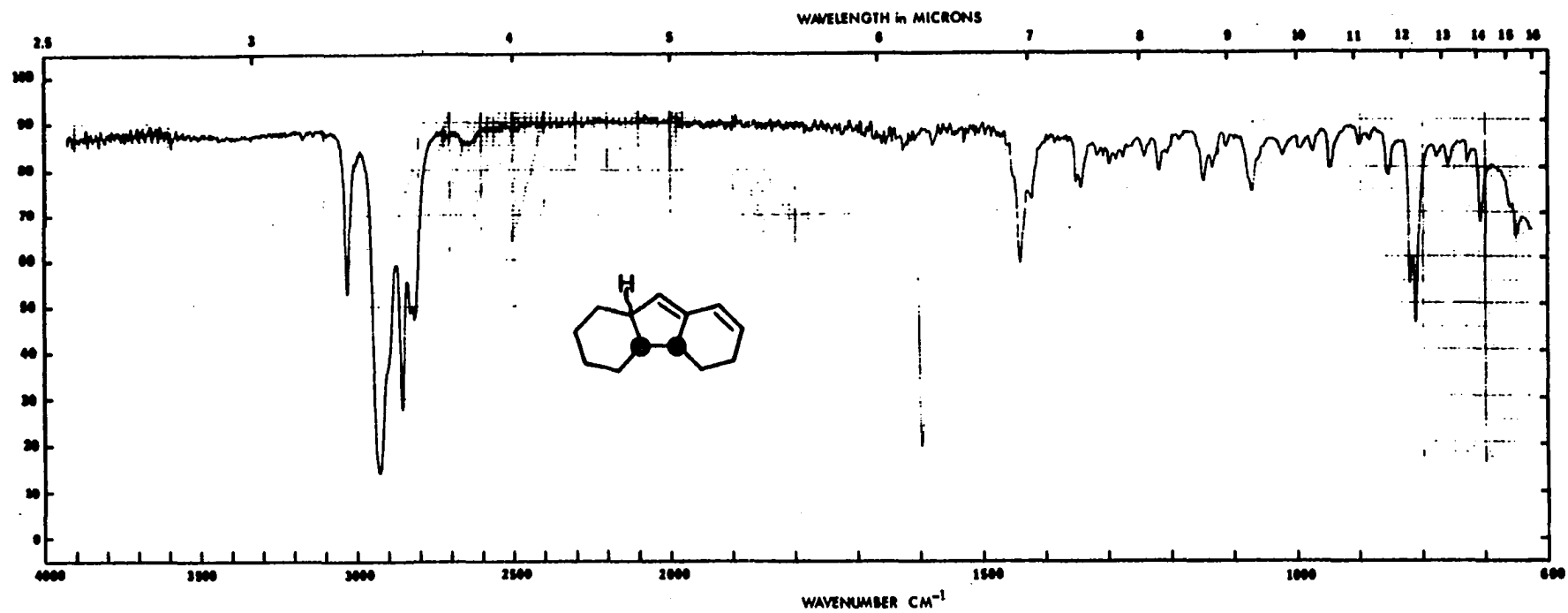


Figure 53 IR Spectrum (film) of LVI

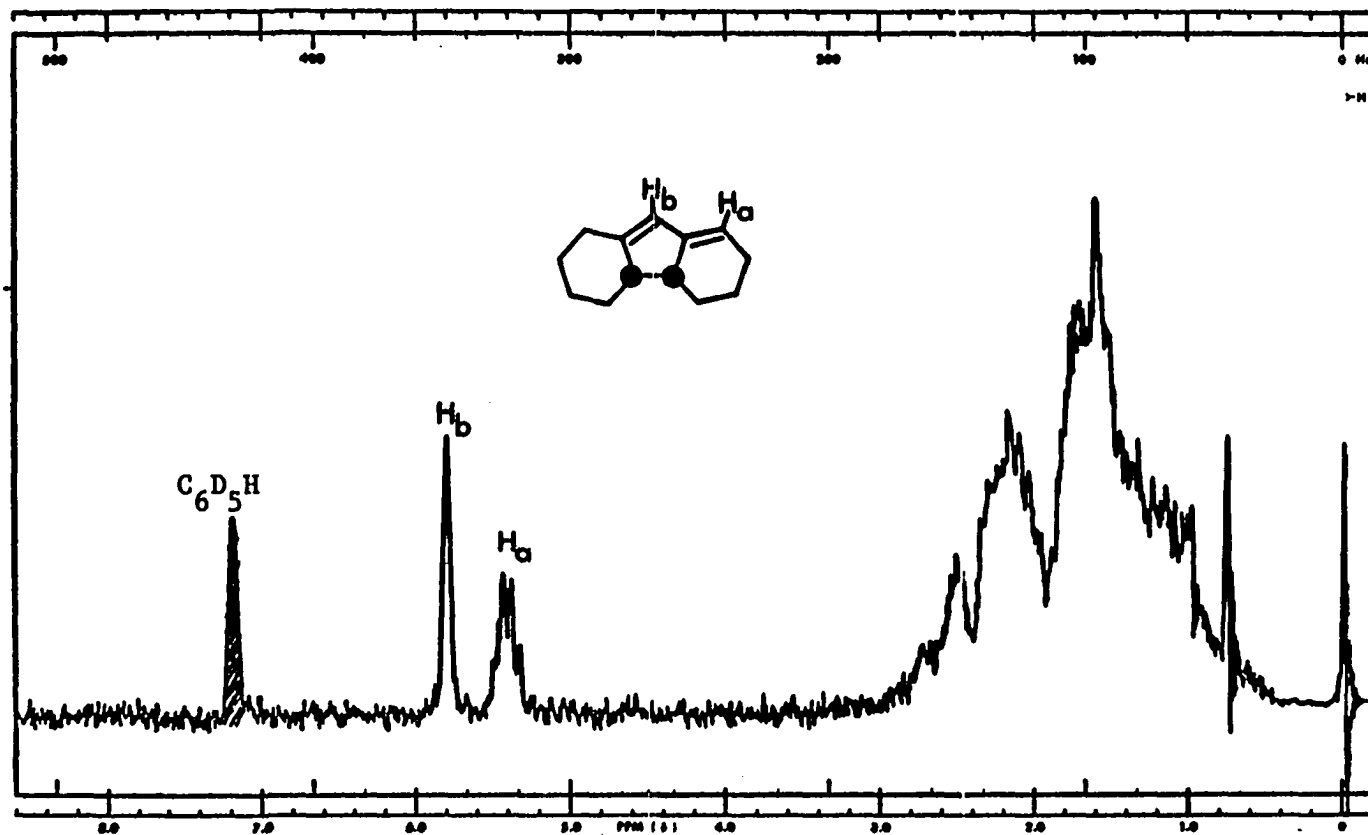


Figure 54 60 MHz PMR Spectrum (C_6D_6) of LV

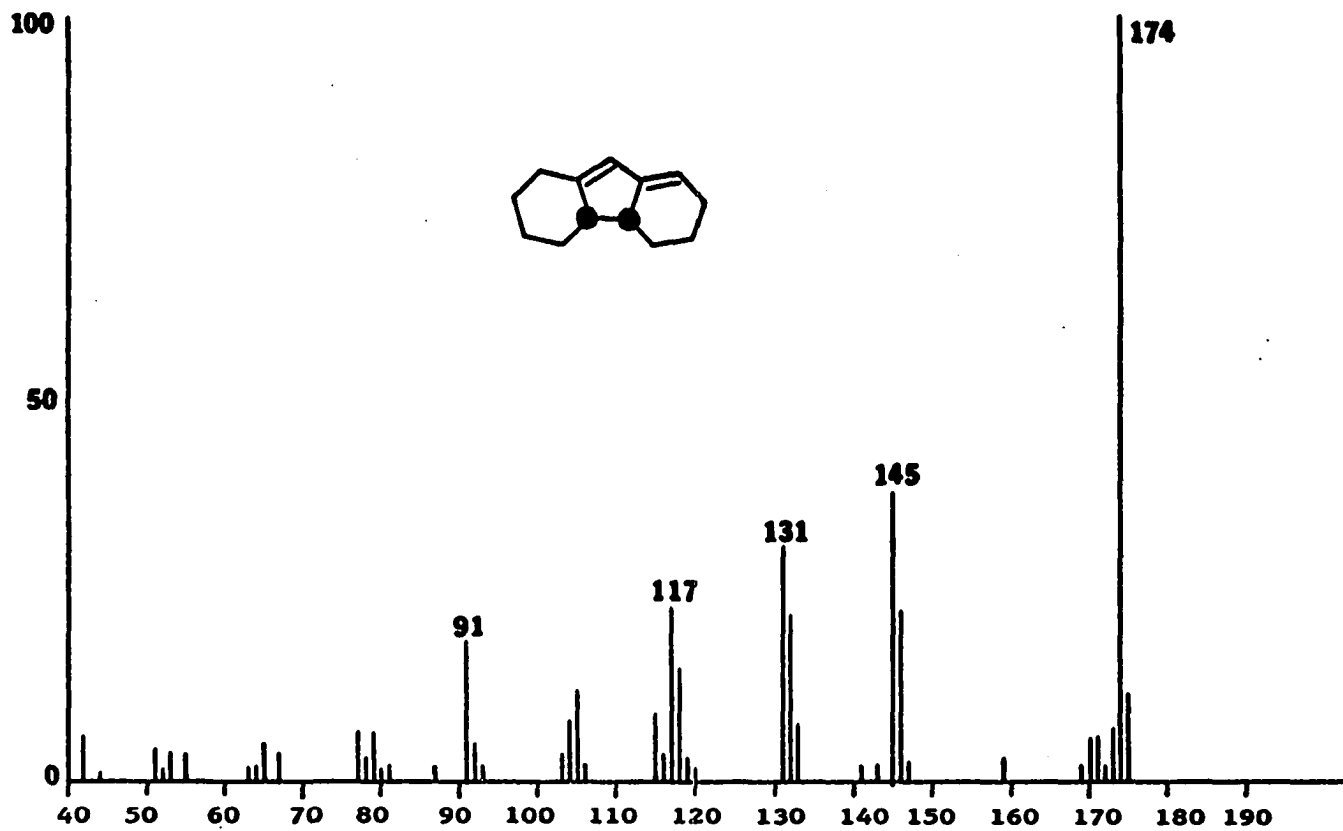


Figure 55 70 eV Mass Spectrum of LV

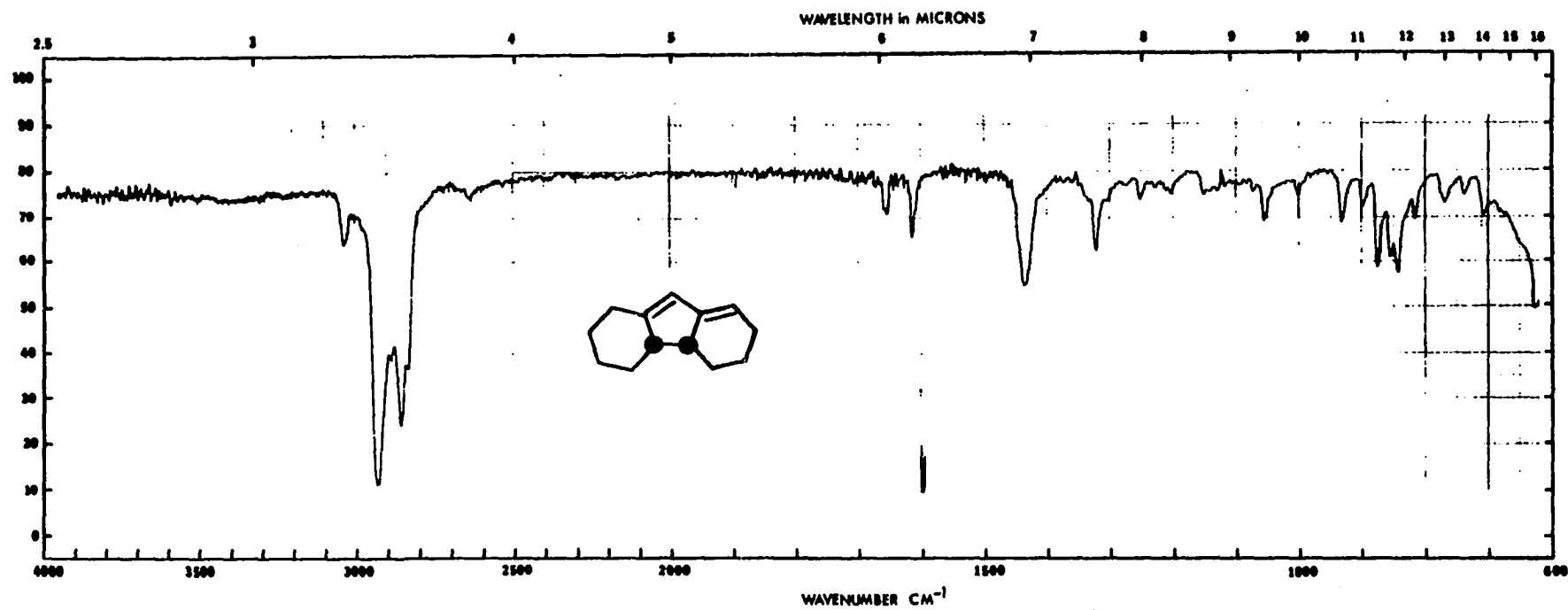
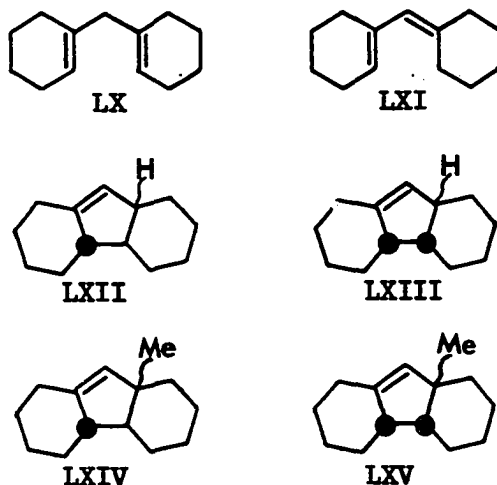


Figure 56 IR Spectrum (film) of LV

the previously discussed syn-diene (LV), the acyclic dienes (LX) and (LXI),³⁸ the cyclic monoalkenes (LXII) and (LXIII),³⁹ and the cyclic methylated monoalkenes (LXIV) and (LXV).⁴⁰



Peak enhancement of a minor component was observed when the syn-diene (LV) was co-injected with mixtures produced by vacuum hot tube decomposition of XXXIV at temperatures greater than ca. 300°. The peak enhancement was observed on all three GLC columns mentioned and under a variety of GLC conditions. The acyclic dienes (LX) and (LXI) enhanced peaks in the mixtures produced by vacuum hot tube decomposition of XXXIV at all the hot tube temperatures investigated in this study. Peak enhancement of minor components was also observed for both isomers of the cyclic anti-monoalkene (LXII) and both isomers of the cyclic methylated anti-monoalkene (LXIV). No peak enhancement was observed for any of the isomers of the corresponding syn-compounds (LXIII) and (LXV).

While peak enhancement by no means establishes the structures

of these minor components, it does provide at least a tentative basis for structural assignments. Lacking any other evidence, then, we assume the presence of the compounds (LV), (LX), (LXI), (LXII), and (LXIV) in these mixtures. On the other hand, the failure to observe peak enhancement for the syn-compounds (LXIII) and (LXV) more firmly establishes the absence of any significant amounts of these compounds.

Figure 57 shows three GLC traces of mixtures produced by vacuum hot tube decomposition of XXXIV at temperatures of a) 250°, b) 300°, and c) 350°. The structural assignments of the peaks in these traces include those components whose identities were firmly established and those whose identities were based only on GLC peak enhancement. All three traces were obtained on a 100 ft. S.C.O.T. FFAP column with the column oven held at 115°.

Control Experiments

In order to test against the possibility that the minor products identified in the vacuum hot tube decomposition of XXXIV might be derived by the thermolysis of other products under the reaction conditions, a short series of control experiments were conducted. In particular, we sought to eliminate the possibility that the cyclized components of the mixtures were being formed from the more major components. These control experiments were conducted by injecting hexane solutions of various product mixtures into the vacuum hot tube under the same conditions employed for the decomposition of XXXIV.

A mixture of the trienes (XLVIII-a) and (XLVIII-b) and the ethers (XLIX-a), (XLIX-b), and (XLIX-c) in hexane solution was thermo-

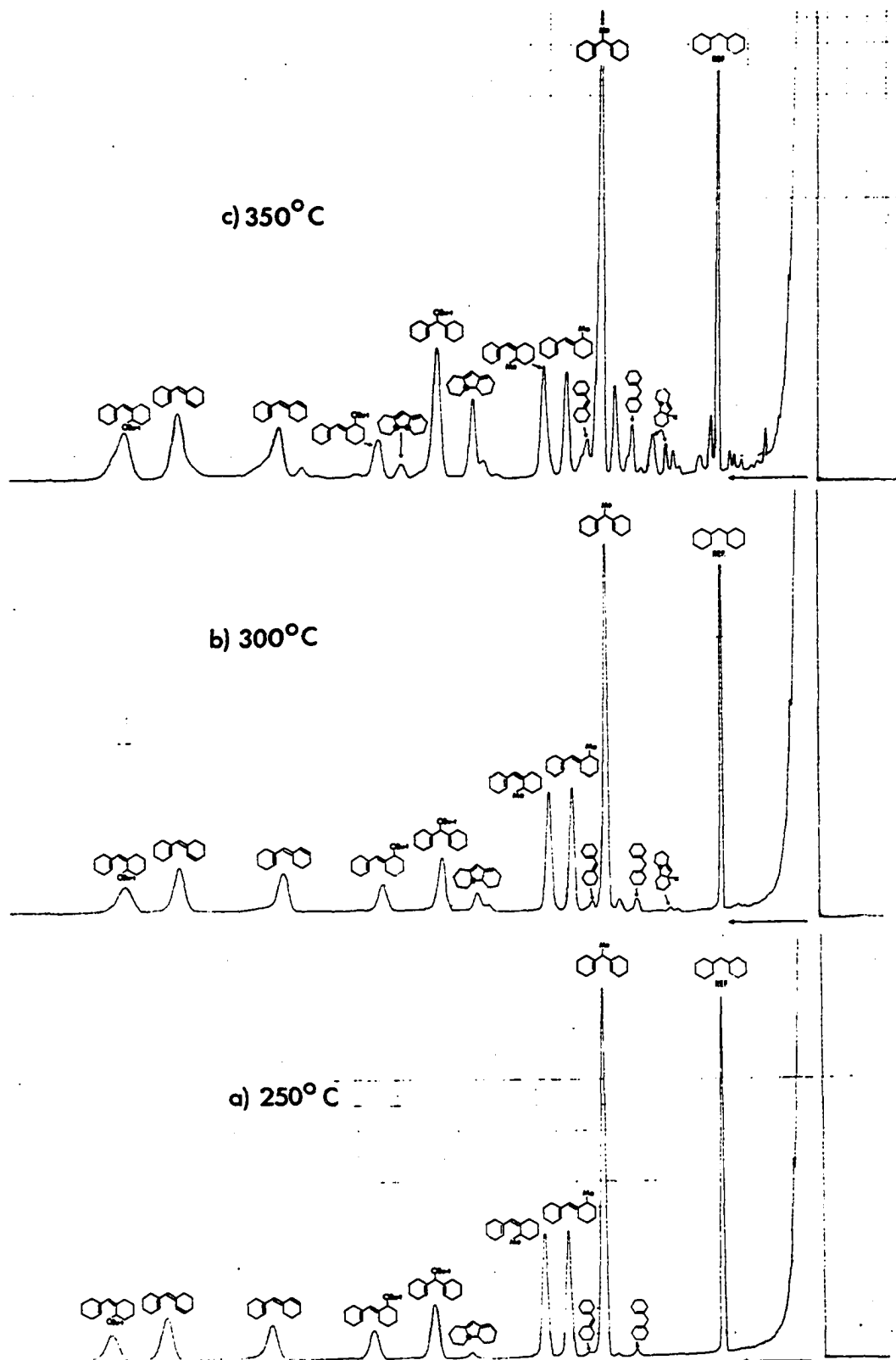


Figure 57 GLC Traces of Products Produced by Vacuum Hot Tube Decomposition of XXXIV at a) 250°, b) 300°, and c) 350°

lyzed in the vacuum hot tube at 400° and 0.05 torr. Examination of the resulting mixture by GLC showed that no other identifiable products were formed from these compounds. At this extreme temperature (400°) some decomposition of these compounds did occur, but none of the compounds we have identified were formed in this experiment.

We have also thermolyzed mixtures which were originally obtained by the vacuum hot tube decomposition of XXXIV. One of these, obtained by the decomposition of XXXIV at 250°, contained mainly the methylated dienes (L-a), (L-b), and (L-c); the trienes (XLVIII-a) and (XLVIII-b); and the ethers (XLIX-a), (XLIX-a), (XLIX-b), and (XLIX-c). This mixture was subjected to thermolysis in the vacuum hot tube at 350° and 0.01 torr. Examination of the GLC trace before and after thermolysis revealed no essential changes in the mixture composition. Another mixture, obtained by the decomposition of XXXIV at 325°, contained the dienes (LI) and (LV) and other minor components in addition to the components mentioned above. This mixture was subjected to thermolysis in the vacuum hot tube at 325° and 0.01 torr. GLC examination again revealed no essential changes in the mixture composition.

We have also tested the possibility that the syn-diene (LV) might be significantly destroyed under the reaction conditions employed for the decomposition of XXXIV. Thus, a solution of LV (1.11×10^{-3} M) and the GLC reference compound, dicyclohexylmethane*, (1.04×10^{-3} M)

*The dicyclohexylmethane used in this study was prepared by catalytic hydrogenation of a mixture of the trienes (XLVIII-a) and (XLVIII-b). All spectral properties were consistent with the structure of dicyclohexylmethane and the available physical data compared favorably with that given in the literature (Ref. 41).

in hexane was thermolyzed in the vacuum hot tube at 325° and 0.01 torr. Examination of the relative peak areas by GLC before and after thermolysis indicated that 25% of the diene (LV) had been destroyed relative to the dicyclohexylmethane reference. Under the same conditions, a hexane solution of the peroxyacetate (XXXIV) (36×10^{-3} M), the diene (LV) (0.74×10^{-3} M), and dicyclohexylmethane (0.70×10^{-3} M) was thermolyzed. GLC examination of the resulting mixture indicated that an additional 15% (total 40%) of the diene (LV) was destroyed under these conditions. We assumed no loss of the dicyclohexylmethane reference under these reaction conditions.

These control experiments have established that the compounds identified from the decompositions of XXXIV were derived from XXXIV and not via thermal conversion of one product to another. The experiments with the syn-diene (LV) indicate that LV was not destroyed to a significant extent under the reaction conditions and that LV survived to the extent of 60% under these conditions. We did not conduct similar experiments with the anti-diene (LI) and therefore do not have a basis for comparison of the relative stabilities of the dienes (LI) and (LV) under the reaction conditions.

GLC Quantitation of Product Mixtures

The distribution of the products produced by the various decompositions of the peroxyacetate (XXXIV) in this study were determined by GLC analysis. All analyses were done using a 100 ft. S.C.O.T. FFAP column with the column oven held at 115°. The gas chromatograph was equipped with a flame-ionization detector.

The detector response to each compound we analyzed was standardized by relating the relative response of each compound to the reference compound, dicyclohexylmethane. Standard solutions of each compound (freshly purified) in hexane were prepared. A measured amount of each solution was independently co-injected with a measured amount of the dicyclohexylmethane standard into the gas chromatograph. The resulting peak areas for each compound and the reference compound were integrated by hand using the formula,

$$\text{Peak Area} = (\text{Height})(\text{Width at Half-Height}).$$

By this procedure, we determined a unitless normalization value (N) for each compound under consideration. The value (N) was calculated by the formula,

$$N = \frac{\text{Moles Sample}}{\text{Area Sample}} \times \frac{\text{Area Reference}}{\text{Moles Reference}} .$$

Table 4 shows the "N" value determined for each compound analyzed. These values are averages of two or three runs for each case.

The product yields for the vacuum hot tube decomposition of XXXIV at seven temperatures have been determined using the "N" values given in Table 4. In each of these runs, a total of 21.6×10^{-6} moles of the peroxyacetate (XXXIV) was injected into the vacuum hot tube. To each resulting mixture, 1.04×10^{-6} moles of dicyclohexylmethane was added. The mixtures were then diluted with hexane to a volume of 1 ml. After integration of the resulting GLC traces, the yield of each component we analyzed was calculated by the formula,

$$\text{Moles Compound} = \frac{(\text{N}) (\text{Area Compound}) (\text{Moles Reference})}{\text{Area Reference}}$$

Moles compound refers to total moles of compound produced in the hot tube decomposition of XXXIV when total moles of reference was used

Table 4

"N" Values for Compounds Analyzed by GLC

<u>Compound</u>	<u>"N"</u>	<u>Compound</u>	<u>"N"</u>
XLVIII-a	1.24	L-c	1.02
XLVIII-b	1.19	LI	1.18
XLIX-a	0.83	LV	1.36
XLIX-b	0.82	LX	1.00
XLIX-c	0.83	LXI	1.06
L-a	1.00	LXII	0.85
L-b	1.10		

for the calculation. The results of these analyzes are given in Table 5. The yields given are in percent of theory. The product distributions given in Tables 1, 2, and 3 were also determined by the procedure discussed above.

Distinguishing the Isomers (XLVIII-a) and (XLVIII-b), (XLIX-b) and (XLIX-c), and (L-b) and (L-c)

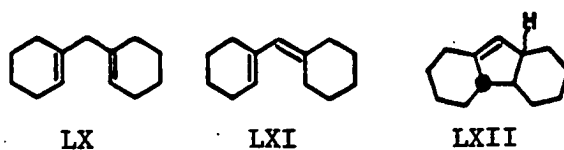
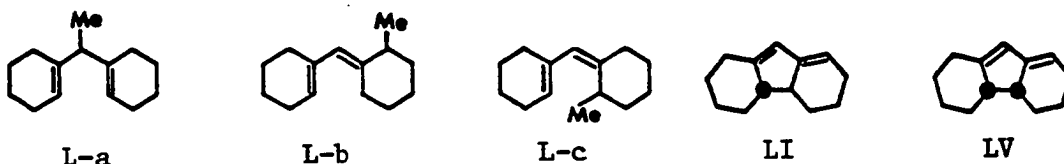
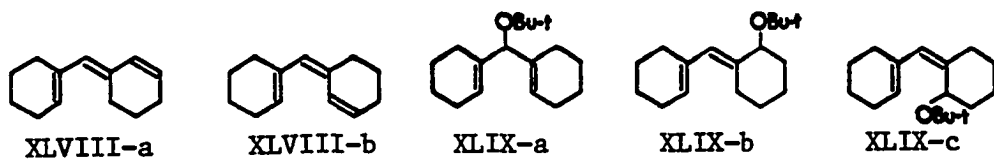
The previous discussions of spectral data for the trienes (XLVIII-a) and (XLVIII-b), and the ethers (XLIX-b) and (XLIX-c), and

Table 5

Product Distribution; Vacuum Hot Tube Decompositions of XXXIV

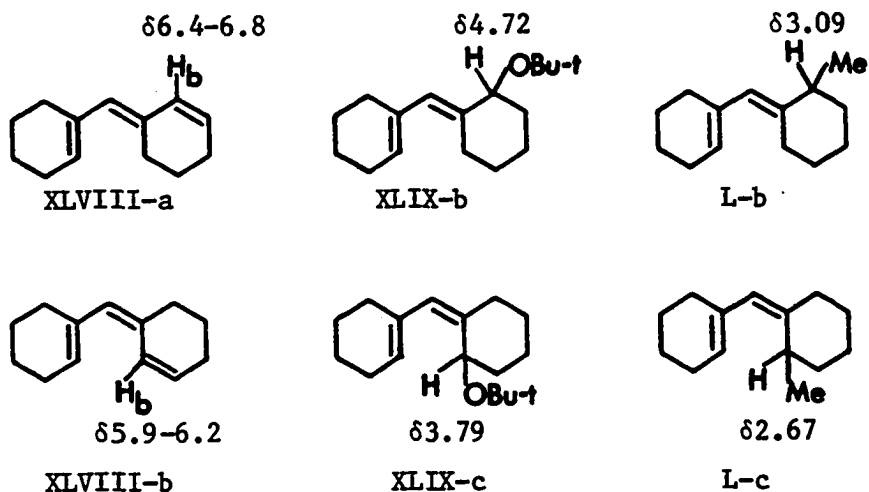
<u>Run#</u>	<u>T°C</u>	<u>P(torr)</u>	<u>XLVIII-a</u>	<u>XLVIII-b</u>	<u>XLIX-a</u>	<u>XLIX-b</u>	<u>XLIX-c</u>
1	210	0.05	1.59	2.82	1.22	0.76	0.79
2	250	0.03	2.34	4.39	1.81	1.17	1.60
3	275	0.03	1.52	1.94	1.36	0.82	1.14
4	300	0.01	2.97	3.84	2.37	1.29	1.96
5	325	0.01	2.46	3.05	2.72	1.11	1.35
6	350	0.01	3.29	4.35	4.27	1.30	2.46
7	375	0.03	1.80	2.60	3.84	1.16	2.28

<u>Run#</u>	<u>L-a</u>	<u>L-b</u>	<u>L-c</u>	<u>LI</u>	<u>LV</u>	<u>LX</u>	<u>LXI</u>	<u>LXII</u>	<u>Total</u>
1	5.77	2.55	2.31	0.20	--	tr	tr	--	18.01
2	8.31	3.78	3.45	0.19	--	0.09	0.04	--	27.17
3	5.97	2.70	2.44	0.32	--	0.11	0.07	--	18.37
4	10.30	4.62	4.44	0.96	0.08	0.31	0.25	0.08	33.47
5	8.01	3.09	2.96	2.76	0.25	0.74	0.66	1.30	30.46
6	9.17	2.74	3.15	2.70	0.39	1.02	1.09	1.22	37.15
7	11.78	2.02	2.87	3.11	0.49	1.26	1.11	1.87	36.19



and the methylated dienes (L-b) and (L-c) have served to establish the gross structural features in each case, but have not clearly distinguished between isomers in each pair. The structural assignments previously given were based on subtle differences occurring in the PMR spectra of the isomers. These differences are the topic of the present discussion.

In the PMR spectra of the trienes (XLVIII-a) and (XLVIII-b) (Figures 14 and 17, respectively), the signal for the olefinic proton H_b is easily distinguished. The assignment for proton H_b in each case was made primarily due to the fact that the signal is coupled with the adjacent cis-olefinic proton with $J = 10$ Hz. In the PMR spectra of the ethers (XLIX-b) and (XLIX-c) (Figures 23 and 26, respectively) and the dienes (L-b) and (L-c) (Figures 34 and 37, respectively), the protons which hold the same relative position of molecular attachment as protons H_b in the trienes are also easily distinguished. For the ethers, the protons which correspond to H_b in the trienes are the protons on carbon bearing oxygen. For the methylated dienes, the corresponding protons are on carbon bearing methyl. The structural relationships which exist between XLVIII-a, XLIX-b, and L-b and between XLVIII-b, XLIX-c, and L-c can be seen below. The chemical shifts given below are for the protons indicated. These chemical shifts reflect the structural relationships. For the related compounds (XLVIII-a, XLIX-b, and L-b), the PMR signals for the labelled protons appear at a lower field position than that given for the corresponding isomer in the related compounds (XLVIII-b, XLIX-c, and L-c).



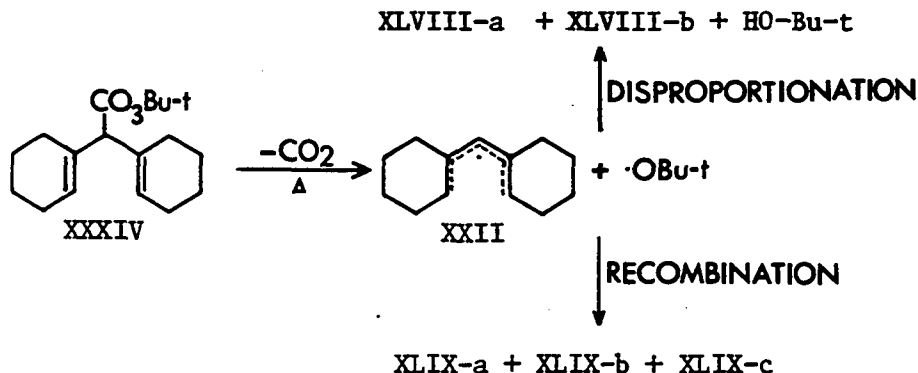
Molecular models of each of these compounds were examined. For the related compounds (XLVIII-b, XLIX-c, and L-c), the models revealed that the protons under consideration are expected to lie above or below the plane of the double bond of the adjacent Δ^1 -cyclohexenyl ring and are subject to shielding by the double bond anisotropy. The models also showed steric crowding in conformations of the molecules in which the protons under consideration were placed in the plane of the Δ^1 -cyclohexenyl double bond (deshielding area). Thus, the structures (XLVIII-b, XLIX-c, and L-c) were assigned to those compounds whose PMR signals for the labelled protons appeared at higher fields relative to the corresponding isomer in each case. The models of the related compounds (XLVIII-a, XLIX-b, and L-b) showed that the protons under consideration occupied spatial positions which were relatively unaffected by the anisotropy of the Δ^1 -cyclohexenyl double bond. Thus, the structures (XLVIII-a, XLIX-b, and L-b) were assigned to those compounds whose PMR signals for the labelled protons appeared at lower fields

relative to those of the corresponding isomer in each case.

In our best judgement, the above structural assignments are correct. However, they were made on the basis of a priori arguments and must necessarily be regarded as tentative.

Discussion of Products Formed from XXXIV

The products formed in the decompositions of the peroxyacetate (XXXIV) are logically derived from the $\Delta^{1,1'}$ -dicyclohexenylmethyl radical (XXII) and the t-butoxy radical ($\cdot\text{OBu-t}$) which are the expected result of thermal peroxyester decomposition (see Scheme 4). The trienes may be seen to arise by a disproportionation process (see below) occurring between XXII and $\cdot\text{OBu-t}$. We assume the formation of t-butyl alcohol here. The ethers (XLIX-a), (XLIX-b), and (XLIX-c)



are the result of recombination occurring between XXII and $\cdot\text{OBu-t}$. Disproportionation and recombination are well documented processes which occur competitively^{22,27,42} between radicals formed by decompositions of peroxyesters, as well as other radical sources. Kochi et al.²² has shown that disproportionation and recombination between alkylalkoxy radical pairs occurs almost exclusively from geminate pairs

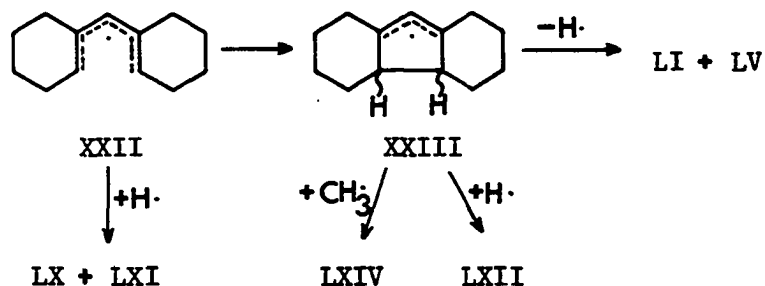
(originating from the same precursor molecule) in the so-called "cage effect".

The methylated dienes (L-a), (L-b), and (L-c) arise via combination of XXII with methyl radical ($\cdot\text{CH}_3$) which is the result of fragmentation of $\cdot\text{OBu-t}$ to acetone and methyl. The fragmentation of alkoxy radicals (especially $\cdot\text{OBu-t}$) is known to occur^{22,43} under conditions of high energy (i.e., the conditions employed in the vacuum hot tube decompositions of XXXIV). The formation of acetone is assumed here.



The cyclized products are the result of the electrocyclization (XXII \rightarrow XXIII) followed by further reaction. Thus, the loss of a hydrogen atom from XXIII (see below) leads to the formation of the dienes (LI) and (LV). The combination of XXIII with a hydrogen atom or methyl radical leads to the formation of the alkenes (LXII) and (LXIV), respectively. The minor amounts of LX and LXI are formed by the combination of XXII with hydrogen atoms. Despite our efforts to do so, we were not able to identify any products resulting from the combination of the cyclized radical (XXIII) and the t-butoxy radical.

The higher yields of the trienes (XLVIII-a) and (XLVIII-b) and the ethers (XLIX-a), (XLIX-b), and (XLIX-c) which were formed in the ambient temperature decompositions of XXIV are attributed to the "cage effect" in which the geminate pairs of XXII - $\cdot\text{OBu-t}$ react primarily by recombination and disproportionation processes. The



formation of the methylated products and those derived from the cyclized radical (XXIII) which occurred in the vacuum hot tube decompositions of XXXIV are regarded as being formed from radicals which escaped the geminate pair reactions. The increased amount of diffusion in a vacuum and the higher temperatures employed in the vacuum hot tube experiments are considered responsible for this.

Conclusions

The identification of the cyclic products (LI, LV, LXII, and LXIV) formed in the vacuum hot tube decompositions of XXXIV establish that the electrocyclization (XXII→XXIII) was effected under these reaction conditions. The greater occurrence of products possessing the anti-backbone structure (LI, LXII, and LXIV) over those possessing the syn-backbone structure (LV only) indicates that the preferred stereochemical mode for the cyclization was conrotatory.

These results have shown that the electrocyclization (XXII→XXIII) is at least a stereoselective conrotatory process. This contradicts the prediction of Woodward and Hoffmann^{4a} which was based on the symmetry of the singly occupied HOMO as the controlling factor

in the electrocyclization of conjugated radicals. This is, perhaps, not too surprising if one considers the orbital correlation diagrams shown in Figure 2 for the electrocyclization of pentadienyl radical. While neither the disrotatory nor the conrotatory mode of cyclization is "ideally allowed", the disrotatory mode leads to a doubly excited cyclopentenyl radical, whereas, the conrotatory mode leads to a singly excited cyclopentenyl radical and, therefore, may be the energetically favored mode. This provides a basis for the rationalization of the preferred conrotatory electrocyclization (XXII→anti-XXIII) which our results have indicated.

These stereochemical results parallel those observed by Bauld et al.¹⁴ with the ring-opening of the anion radicals of cis- and trans-3,4-diphenylcyclobutenes (XI) and (XII) and cis- and trans-1,2-diphenylphenanthro[1]cyclobutenes (XV) and (XVI) and by Rüchart et al.¹³ with the ring opening in the cyclopropyl radicals (III) and (IV). The studies of Winstein et al.¹⁶ are alone among the reports of electrocyclic reactions of open shell systems proceeding by HOMO symmetry control. These observations clearly indicate that more sophisticated considerations may be required to successfully rationalize and predict the stereochemical outcome of electrocyclic reactions of open shell systems.

Summary

In this chapter, the preparation of t-butyl $\Delta^{1,1'}$ -dicyclohexenylperoxyacetate (XXXIV) and its thermal decomposition as a means of generating and studying the reactions of $\Delta^{1,1'}$ -dicyclohexenylmethyl radical (XXII) have been described. A variety of products formed by the decomposition of XXXIV and originating from the radical (XXII) were identified. The results of product analysis have also shown that the radical (XXII) underwent electrocyclization to a cyclopentenyl radical (XXIII) via a stereoselective conrotatory process.

CHAPTER 3

EXPERIMENTAL

All melting points were obtained on a Gallenkampf MF 370 capillary melting point apparatus and are uncorrected. Infrared spectra were obtained on a Beckmann IR-8 spectrophotometer. Mass spectra were obtained on a Hitachi-Perkin Elmer RMU-7E mass spectrometer operated at 70 eV. Ultraviolet spectra were obtained on a Varian Techtron 635 spectrophotometer. The 60 and 100 MHz PMR spectra were obtained on Varian T-60 and XL-100 spectrometers, respectively. Preparative gas chromatography work was done on a Varian 90-P gas chromatograph. Analytical gas chromatography work was done on a Hewlett Packard 5760 gas chromatograph equipped with a flame-ionization detector. The support coated open tubular (S.C.O.T.) columns used were Perkin Elmer brand. Preparative and thin layer chromatography (PLC and TLC) was done using silica gel PF (254 + 366) UV indicating gel. Olefin-free, dry hexane refers to hexane which had been treated with concentrated sulfuric acid prior to distillation from calcium hydride. Degassed solvents refer to solvents which had been frozen and thawed several times under a vacuum. Microanalyses were performed by Galbraith Laboratories, Inc., Knoxville, Tennessee.

1,1-Bis(Δ^1 -cyclohexenyl)ethylene (XXXVI)

Finely powdered triphenylmethyl phosphonium iodide (16.36 g, 40.5 mmol) and 450 ml dry ether were placed in a one liter flask. The system was equipped with a magnetic stirrer and was stoppered with a rubber septum. The system was stirred and flushed with dry nitrogen which was introduced and exhausted via syringe needles. A slight nitrogen pressure was maintained on the system by a balloon of nitrogen attached to a syringe needle. Normal butyllithium (41.7 mmol in hexane) was added via syringe and the mixture was stirred for 1 hour. The $\Delta^{1,1'}$ -dicyclohexenyl ketone (XXV)²⁸ (5.16 g, 27.2 mmol) in dry hexane (15 ml) was added via syringe and the mixture was stirred for 1 hour. The mixture was then filtered through supercel (filter-aid), concentrated, and chromatographed on a short column of silica gel with hexane to give XXXVI as a clear slightly yellowed oil, yield: 4.29 g = 84%. The microanalytical sample was prepared by bulb to bulb distillation at 50°/0.05 torr which gave XXXVI as a colorless oil.

PMR Spectrum: Figure 3, Mass Spectrum: Figure 4, IR Spectrum: discussed in text. Analysis for $C_{14}H_{20}$: calculated, C 89.29, H 10.71; found, C 89.19, H 10.69.

2,2-Bis(Δ^1 -cyclohexenyl)ethanol (XXXVII)

The procedure here for hydroboration oxidation using 9-bora-bicyclo-(3.3.1.)nonane (9-BBN) is essentially that given by Knights and Brown.²⁹

The triene (XXXVI) (1.1 g, 5.8 mmol) was dissolved in dry

tetrahydrofuran (freshly distilled from LAH, 50 ml) in a 100 ml flask which was stoppered with a rubber septum and flushed with dry nitrogen (introduced and exhausted via syringe needles). A slight positive nitrogen pressure was maintained during the hydroboration procedure by a balloon of nitrogen attached to a syringe needle. The solution was stirred magnetically and cooled in an ice bath for 5-10 minutes. A solution of 9-BBN (5.92 mmol) in dry tetrahydrofuran was added via syringe over 10 minutes with vigorous stirring. The reaction mixture was allowed to stir in the cold for 30 min. and then at ambient room temperature for 2.5 hours. The mixture was again cooled with an ice bath and the septum stopper was removed. To the cooled and stirred solution was added 6 N NaOH (2.5 ml) followed by the slow addition of 30% H₂O₂ (2 ml). A reflux condenser was attached and the mixture was heated under reflux for 5 hours. The mixture was concentrated on the rotary evaporator to near dryness, diluted with water (50 ml), and extracted with three portions of ether (200 ml total). The combined extracts were washed with two 25 ml portions of water and were dried over MgSO₄. After filtration, the solution was concentrated and then chromatographed by preparative layer on silica gel with 20% EtOAc/hexane to give XXXVII as a slightly yellowed oil which crystallized on standing, yield: 0.94 g = 77.9%. Recrystallization from hexane (dry ice-isopropanol bath cooling) gave XXXVII as a pure white solid which melted at 38-39.5°. The microanalytical sample was prepared by sublimation at 35°/0.05 torr.

PMR Spectrum: Figure 5, Mass Spectrum: Figure 6, IR Spectrum: discussed in text. Analysis for C₁₄H₂₂O: calculated,

C 81.50, H 10.75, O 7.75; found, C 81.76, H 10.90.

$\Delta^{1,1'}$ -Dicyclohexenylacetic Acid (XXXVIII)

The alcohol (XXXVII) (1 g, 4.85 mmol) was dissolved in reagent grade acetone (100 ml) in a 250 ml flask equipped with an addition funnel and magnetic stirrer. With vigorous stirring, the Jones reagent³⁰ (5 ml containing 13.35 mmol of CrO_3) was added as rapidly as possible (5-10 sec) and the mixture was stirred under ambient conditions for 5 minutes. The reaction was then quenched by the addition of enough isopropyl alcohol to discharge the orange color of the oxidizing agent. The mixture was concentrated on the rotary evaporator to near dryness. To this was added hexane (100 ml) with stirring followed by water (50 ml). The phases were separated and the aqueous phase was further extracted with hexane (50 ml). The combined hexane extracts were washed with three 50 ml portions of water. The almost colorless hexane solution was then extracted with three portions of a 10% NaOH aqueous solution (200 ml total). The basic extracts were washed with one 50 ml portion of hexane. The basic solution was cooled with an ice bath and then carefully acidified with cold 20% sulfuric acid to pH 1. The acidified solution was extracted with three portions of hexane (200 ml total). The hexane extracts were washed with water (50 ml) and dried over MgSO_4 . After filtration, concentration gave XXXVIII as a white solid which melted at 112-114°, yield: 0.52 g = 48.7%. Recrystallization from hexane (-20°) gave XXXVIII as pure white crystals which melted at 114-115.5°. The micro-analytical sample was prepared by sublimation at 60°/0.05 torr.

PMR Spectrum: Figure 7, Mass Spectrum: Figure 8, IR Spectrum: discussed in text. Analysis for $C_{14}H_{20}O_2$: calculated, C 76.33, H 9.15, O 14.52; found, C 76.60, H 9.21.

Methyl $\Delta^{1,1'}$ -Dicyclohexenylacetate (XL)

The acid (XXXVIII) (12 mg, 0.055 mmol) in a small volume of ether was treated with an ethereal solution of diazomethane until a slight yellow diazomethane color persisted. The mixture was concentrated on the rotary evaporator and further under a high vacuum to give ca. 13 mg of XL as a clear oil in essentially quantitative yield. The ester appeared to be pure by TLC and GLC and was not purified further. The 60 MHz PMR spectrum (CCl_4) showed: δ 5.5 (2H multiplet, olefinic protons), 3.6 (3H singlet, methoxyl protons), 3.35 (1H broad singlet, proton α to carbonyl), 1.3-2.2 (16H multiplet, ring protons). The IR spectrum (film) showed: cm^{-1} 1740 (C=O). The 70 eV mass spectrum showed: m/e 234 (M^+ , parent ion) and 175 (base peak, $M^+ - CO_2Me$). The ester (XL) was not further characterized and was used only as an authentic sample for monitoring the progress of formation of the acid chloride (XXXIX) as previously described in the text.

tert-Butyl $\Delta^{1,1'}$ -Dicyclohexenylperoxyacetate (XXXIV)

The acid (XXXVIII) (220 mg, 1 mmol) was dissolved in 5 ml dry benzene in a 50 ml flask which was stoppered with a rubber septum and flushed with dry nitrogen (via syringe needles). Oxalyl chloride (.213 ml, 2.5 mmol) was injected via syringe and the mixture was stirred magnetically (gas evolved) for 1.5 hr. The method used for

monitoring the progress of formation of the intermediate acid chloride (XXXIX) was previously described in the text. The mixture was concentrated on the rotary evaporator and further under high vacuum to give XXXIX as a thick viscous slightly yellowed oil. In the same reaction vessel, the acid chloride (XXXIX) was dissolved in dry, olefin-free hexane (20 ml). The vessel was shielded from light with aluminum foil, stoppered, and stirred for a few minutes with ice bath cooling. Finely powdered sodium t-butylperoxide³¹ (280 mg, 2.5 mmol) was added, the flask was again stoppered, and stirred magnetically in the cold for 3.5 hours. During the remainder of this procedure, special care was taken to shield reaction and work-up vessels from light and to maintain them at as cold a temperature as possible. The reaction mixture was filtered with suction through a precooled supercel filter into a dry ice cooled flask (Al foil shielding). The filtrate was washed with ice cold hexane (50 ml). The colorless hexane solution was concentrated on the rotary evaporator without heat. Further concentration and drying was accomplished under high vacuum and ice bath cooling. Thus, the peroxyacetate (XXXIV) was obtained as a white solid which melted at 33-34°, yield: 245 mg = 84%. Further purification was accomplished by dissolving the solid in ice cold, dry, olefin-free degassed hexane and recrystallizing at dry ice-isopropanol bath temperature. In this manner, XXXIV was obtained as pure white crystals which melted sharply at 34-35°. Solid XXXIV could be stored in the freezer (-20°) under dry nitrogen for months without appreciable decomposition. Microanalysis was not obtained for this compound.

PMR Spectrum: Figure 9, IR Spectrum: Figure 10, Mass

Spectrum: Figure 11.

Authentic 1,1-Bis(Δ^1 -cyclohexenyl)ethane (L-a)

The triene (XXXVI) (408 mg, 2.17 mmol) and potassium azodicarboxylate (825 mg, 4.26 mmol) were dissolved in methanol (20 ml) in a 50 ml flask equipped with a magnetic stirrer. To the stirred solution was added glacial acetic acid (0.25 ml, 4.26 mmol). The evolution of a gas began immediately and continued for ca. 1 hour, at which time the yellow color of potassium azodicarboxylate disappeared. Examination of the reaction mixture by GLC (FFAP) showed the reduction of XXXVI to be ca. 50% completed. Thus, additional acetic acid (1 ml, 17.04 mmol) was added and potassium azodicarboxylate (3.3 g, 17.04 mmol) was added in small portions (10-20 mg) over 3-4 hours, at which time the GLC trace showed complete reduction of XXXVI. The mixture was concentrated to near dryness, diluted with hexane (150 ml), washed with three 50 ml portions of water, and dried over $MgSO_4$. Filtration and concentration gave L-a as a clear oil which was essentially pure by GLC and TLC examination, yield: 334 mg = 81%. Further purification was achieved by bulb to bulb distillation at 40°/0.05 torr. The authentic L-a was identical in all characteristics with that produced by the vacuum hot tube decomposition of XXXIV.

Authentic Dicyclohexylmethane

A mixture of the trienes (XLVIII-a) and (XLVIII-b) (190 mg, 1.092 mmol) was hydrogenated in hexane (20 ml) over 5% Pd/C (20 mg) overnight under hydrogen at atmospheric pressure. Filtration and

concentration of the mixture gave dicyclohexylmethane (slightly impure) as a clear colorless oil, yield: 187 mg = 95.5%. Further purification was achieved by preparative gas chromatography (JXR) followed by bulb to bulb distillation at 70°/0.1 torr which gave pure dicyclohexylmethane. The purified sample had n_D^{25} 1.4770; the literature value⁴¹ was n_D^{20} 1.4752. The PMR and mass spectra were consistent with the structure for dicyclohexylmethane. The authentic dicyclohexylmethane sample prepared in this manner was used as the reference compound for the quantitative GLC procedure which was discussed in the text.

2,3,4,4 α ,4 β ,5,6,7,8,8 α -Decahydro-9H-fluoren-9 α -ol (LIII)

The ketone (LII)³⁵ (1.57 g, 8.26 mmol) was dissolved in dry ether (100 ml) in a 250 ml flask equipped with a magnetic stirrer and an addition funnel. The solution was stirred while being cooled with an ice bath. An ethereal solution of lithium aluminum hydride (2.45 mmol in 1 ml ether) was added slowly dropwise. After stirring for a few minutes (in the cold), the reaction was quenched by the slow addition of 30 ml of 20% acetic acid. The phases were separated and the ether phase was washed with water (25 ml), 10% NaHCO₃ (25 ml), and water (25 ml) and then dried over Na₂SO₄. Filtration and concentration gave LIII as a white solid which melted at 85-88°, yield: 1.48 g = 93.4%. The microanalytical sample was prepared by recrystallization from hexane (ice salt bath cooling) which gave LIII as pure white crystals that melted at 87-89°.

PMR Spectrum: Figure 40, Mass Spectrum: Figure 41, IR

Spectrum: discussed in text. Analysis for $C_{13}H_{20}O$: calculated, C 81.20, H 10.48, O 8.32; found, C 81.09, H 10.62.

2,3,4,4a α ,4b β ,5,6,7,8,8a α -Decahydro-9H-fluoren-9 α -yl Acetate (LIV)

The alcohol (LIII) (1.48 g, 7.7 mmol), pyridine (20 ml), and acetic anhydride (15 ml) were heated under reflux for 3 hours. The mixture was diluted with ether (100 ml), washed with four 100 ml portions of water, and dried over Na_2SO_4 . The mixture was filtered, concentrated, and chromatographed by preparative layer with 10% EtOAc/hexane to give the acetate (LIV) as a clear oil which solidified on standing in the cold (-20°), yield: 1.65 g = 91.5%. The micro-analytical sample was prepared by recrystallization from hexane (dry ice-isopropanol bath cooling) which gave pure white LIV that melted at $57-58.5^\circ$.

PMR Spectrum: Figure 42, Mass Spectrum: Figure 43, IR Spectrum: discussed in text. Analysis for $C_{15}H_{22}O_2$: calculated, C 76.88, H 9.46, O 13.65; found, C 77.13, H 9.58.

2,3,4,4a β ,4b β ,5,6,7,8,8a-Decahydro-9H-fluoren-9 α -ol (LVIII)

The ketone (LVII)³⁵ (2 g, 10.5 mmol) was dissolved in dry benzene (75 ml) in a 250 ml flask equipped with a magnetic stirrer, addition funnel, and a nitrogen gas inlet. The system was flushed with dry nitrogen, stirred, and cooled with an ice bath. Diisobutyl aluminum hydride³⁶ (4 g, 28.2 mmol) in dry benzene (30 ml) was added, under dry nitrogen, dropwise over 15-20 minutes. The reaction mixture was stirred in the cold for 1 hour. Methanol (40 ml) was added slowly

and the mixture was then concentrated on the rotary evaporator to near-dryness. Ether (100 ml) was added and the mixture was filtered. The aluminum precipitates were washed with ether (200 ml). The ether washings were combined and concentrated to give a viscous oil. This was chromatographed by preparative layer with 20% EtOAc/hexane to give LVIII as a slightly yellowed oil which crystallized on standing, yield: 1.4 g = 69.4%. The microanalytical sample was prepared by recrystallization from hexane (ether trace) (dry ice-isopropanol bath cooling) which gave LVIII as pure white crystals that melted at 36-37.5°.

PMR Spectrum: Figure 47, Mass Spectrum: Figure 48, IR Spectrum: discussed in text. Analysis for $C_{13}H_{20}O$: calculated, C 81.20, H 10.48, O 8.32; found, C 81.01, H 10.56.

2,3,4,4a β ,4b β ,5,6,7,8,8a-Decahydro-9H-fluoren-9 α -yl Acetate (LIX)

The alcohol (LVIII) (1 g, 5.21 mmol), pyridine (15 ml), and acetic anhydride (10 ml) were heated under reflux for 2.25 hours. The mixture was diluted with ether (100 ml), washed with four 100 ml portions of water, and dried over Na_2SO_4 . The mixture was filtered, concentrated, and chromatographed by preparative layer with 10% EtOAc/hexane to give the acetate (LIX) as a slightly yellowed oil which solidified into a tacky solid on standing, yield; 1.15 g = 94%. The microanalytical sample was prepared by multiple recrystallizations from hexane (dry ice-isopropanol bath cooling) which gave pure white LIX that melted at 36-37.5°.

PMR Spectrum: Figure 49, Mass Spectrum: Figure 50, IR

Spectrum: discussed in text. Analysis for $C_{15}H_{22}O_2$: calculated, C 76.88, H 9.46, O 13.65; found, C 77.13, H 9.67.

Thermolysis of the Acetates (LIV) and (LIX)

For the thermolysis of the acetates (LIV) and (LIX), a special adaptation of the hot tube was employed which allowed the introduction of solids into the quartz hot tube under a nitrogen gas flow. This device is shown schematically in Figure 58. The solids to be thermolyzed were introduced into the glass bead filled hot tube

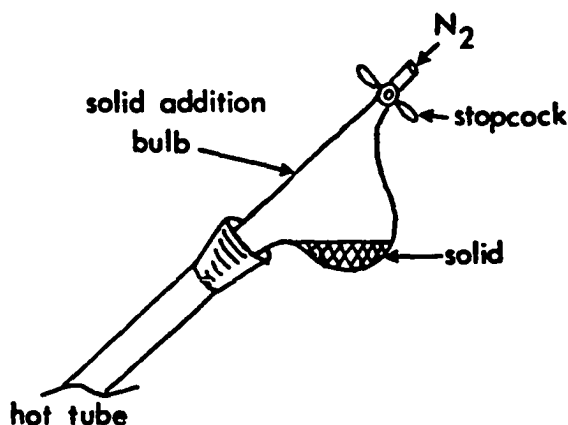


Figure 58 Solid Addition Bulb for Hot Tube Thermolyses

by rotating the solid addition bulb 180° from the position shown in Figure 58. The acetates (LIV) and (LIX) were deposited on Chromsorb W (45/60 mesh) by preparing a slurry of the acetate and Chromsorb W with hexane and evaporating to dryness under a vacuum. This was then introduced into the hot tube via the solid addition bulb. The use of Chromsorb W aided in preventing melting of the acetates at the mouth of the hot tube. A glass bead filled U-shaped collector was employed for the collection of the products formed by thermolysis.

The collector was cooled with a slurry of dry ice-isopropanol.

1,2,4,4a α ,4b β ,5,6,7-Octahydro-3H-fluorene (LI)

The acetate (LIV) (317 mg, 1.29 mmol) was deposited on Chromsorb W (45/60 mesh, 1.2 g). This was introduced slowly into the hot tube over 5-10 minutes. The tube temperature was 425° and a nitrogen flow of ca. 45 ml/min was used. The crude product was washed from the collector with ether. The solution was concentrated and the crude diene (LI) was purified by preparative gas chromatography (Carbowax 20M). This gave LI as a slightly yellowed oil, yield: 102 mg = 45%. The microanalytical sample was prepared by bulb to bulb distillation at 70°/0.05 torr which gave LI as a clear colorless oil. The diene (LI) yellowed on exposure to atmosphere.

PMR Spectrum: Figure 44, Mass Spectrum: Figure 45, IR Spectrum: Figure 46. The UV spectrum (hexane) gave λ_{\max} 248 nm, ϵ_{\max} 16,344. Analysis for C₁₃H₁₈: calculated, C 89.59, H 10.41; found, C 89.30, H 10.61.

4,4a β ,4b β ,5,6,7,8,8a-Octahydro-3H-fluorene (LVI)

The acetate (LIX) (1 g, 4.28 mmol) was deposited on Chromsorb W (45/60 mesh, 4 g). This was introduced slowly into the hot tube over 15-20 minutes. The tube temperature was 425° and a nitrogen flow of ca. 45 ml/min was used. The crude product was washed from the collector with hexane. The yellow hexane solution was concentrated and distilled bulb to bulb at 85°/0.1 torr to give a slightly yellowed oil. This was chromatographed by preparative gas chromatography (Carbowax 20M)

to give LVI as a yellow oil, yield: 212 mg = 28%. The microanalytical sample was prepared by bulb to bulb distillation at 55°/0.01 torr which gave LVI as a clear colorless oil. The diene (LVI) yellowed very quickly on exposure to atmosphere. A smaller amount of the diene (LV) (ca. 9%, impure) was also obtained by this procedure.

PMR Spectrum (of LVI): Figure 51, Mass Spectrum: Figure 52, IR Spectrum: Figure 53. The UV spectrum (hexane) gave λ_{\max} 243 nm, ϵ_{\max} 17,423. Analysis for $C_{13}H_{18}$: calculated, C 89.59, H 10.41; found, C 89.42, H 10.53.

1,2,4,4 α ,4 β ,5,6,7-Octahydro-3H-fluorene (LV)

The alcohol (LVIII) (103 mg, 0.54 mmol) was dissolved in dry dimethylformamide (3 ml) and dry 2,6-lutidine (0.4 ml) in a 25 ml flask which was stoppered with a rubber septum. The system was flushed with dry nitrogen (introduced and exhausted via syringe needles), stirred magnetically, and cooled with an ice-salt bath for a few minutes. Methanesulfonylchloride (0.125 ml), which had been enriched with SO_2 by distillation at atmospheric pressure,³⁷ was added via syringe. The reaction mixture was stirred in the cold for 2.5 hours. The mixture was allowed to warm to room temperature, 1 ml of water was added, and the mixture was poured into hexane (75 ml) and shaken. The hexane phase was separated and washed with water (50 ml), two 50 ml portions of cold 5% H_2SO_4 , saturated $NaHCO_3$ (50 ml), and dried over Na_2SO_4 . Filtration and concentration of the hexane solution gave a yellow oil which was quickly chromatographed on a short column of florisil with hexane. Only the column effluent which contained UV active

components was collected. This was determined by periodically spotting the effluent on TLC plates (UV indicating gel) and examining under the 254 nm UV lamp. This chromatography fraction was concentrated to give 28 mg of a clear, slightly yellowed oil. Examination of the oil by GLC (FFAP) showed it to contain the diene (LV) in ca. 22% of theory and the diene (LVI) in ca. 7% of theory. The dienes were separated and purified by preparative gas chromatography (FFAP). The microanalytical sample of the diene (LV) was prepared by bulb to bulb distillation at 40°/0.01 torr which gave LV as a clear colorless oil that yellowed on exposure to atmosphere.

PMR Spectrum (of LV): Figure 54, Mass Spectrum: Figure 55, IR Spectrum: Figure 56. The UV spectrum (hexane) gave λ_{\max} 245 nm, ϵ_{\max} 15,624. Analysis for $C_{13}H_{18}$: calculated, C 89.59, H 10.41; found, C 89.49, H 10.53.

Decomposition of tert-Butyl $\Delta^{1,1'}$ -Dicyclohexenylperoxyacetate (XXXIV)

Freshly recrystallized peroxyacetate (XXXIV) was used for all the decomposition studies in this work.

The ambient temperature vacuum decomposition of XXXIV was done under a pressure of 0.01 torr using the apparatus shown in Figure 12. The product distribution arising from this method of decomposition was determined by the quantitative GLC procedure discussed in the text and the results are reported in Table 1. The data in Table 1 are based on the decomposition of 25 mg (0.086 mmol) of XXXIV, which required ca. 6 days for complete decomposition.

The ambient temperature solution decomposition of XXXIV was

done using a 0.0185 M solution of XXXIV in dry, olefin-free, degassed hexane. The solution (2 ml) was prepared in a small test tube which was stoppered with a rubber septum and flushed with dry nitrogen. The vessel was shielded from light with aluminum foil and allowed to stand at ambient room temperature. The samples for GLC analysis were removed through the septum via syringe. The product distribution was determined by the quantitative GLC procedure and the results are reported in Table 2.

For the vacuum hot tube decompositions of XXXIV, a 0.108 M solution of XXXIV in dry, olefin-free, degassed hexane was used. The resulting product distributions for seven decomposition temperatures and pressures were determined by quantitative GLC and are reported in Table 5. For each of the runs reported in Table 5, two 50 microliter injections (21.6×10^{-6} mol total of XXXIV) were made using a gas tight syringe. Between injections, the vacuum was allowed to recover to 0.05-0.01 torr before proceeding. Between runs, the vacuum hot tube (see Figure 30) was allowed to "cure" at ca. 450°/0.05 torr for several hours. After each run, the GLC standard, dicyclohexylmethane, (1.042×10^{-6} mol) was added to the decomposition mixture which was then diluted to a volume of 1 ml with hexane for GLC analysis.

Isolation of Δ^1 -Cyclohexenyl-(E)-cyclohex-2-enylidenemethane (XLVIII-a), Δ^1 -Cyclohexenyl-(Z)-cyclohex-2-enylidenemethane (XLVIII-b), Bis(Δ^1 -cyclohexenyl)-1,1-dimethylethoxymethane (XLIX-a), Δ^1 -Cyclohexenyl-(E)-2-(1,1-dimethylethoxy)cyclohexylidenemethane (XLIX-b), and Δ^1 -Cyclohexenyl-(Z)-2-(1,1-dimethylethoxy)cyclohexylidenemethane (XLIX-c)

The trienes (XLVIII-a) and (XLVIII-b) and the ethers (XLIX-a), (XLIX-b), and (XLIX-c) were most easily isolated and purified from mixtures produced by the ambient temperature vacuum decomposition of XXXIV. The procedure below describes the methods used for the separation and purification of these compounds produced by this method of decomposition.

The reaction mixture was chromatographed by preparative layer with 2% EtOAc/hexane. This produced two major zones on the PLC plate which were visualized under the 254 nm UV lamp. The first and foremost zone contained the trienes (XLVIII-a) and (XLVIII-b). The second zone contained the ethers (XLIX-a), (XLIX-b), and (XLIX-c).

The trienes were leached from the silica gel with hexane. Concentration gave a yellowed oil which contained mainly XLVIII-a and XLVIII-b. The trienes were further separated and purified by preparative gas chromatography on FFAP or Carbowax 20M. The micro-analytical samples of XLVIII-a and XLVIII-b were prepared by bulb to bulb distillation at 90°/0.1 torr which gave both isomers as clear colorless oils which yellowed on exposure to atmosphere.

PMR Spectrum (of XLVIII-a): Figure 14, Mass Spectrum: Figure 15, IR Spectrum: Figure 16. The UV spectrum (hexane) gave λ_{\max} 273 nm, ϵ_{\max} 17,781; λ 265 nm, ϵ 17,380. Analysis for $C_{13}H_{18}$:

calculated, C 89.59, H 10.41; found, C 89.68, H 10.29.

PMR Spectrum (of XLVIII-b): Figure 17, Mass Spectrum: Figure 18, IR Spectrum: Figure 19. The UV spectrum (hexane) gave λ_{\max} 273 nm, ϵ_{\max} 23,934; λ 265, ϵ 22,421. Analysis for $C_{13}H_{18}$: calculated, C 89.59, H 10.41; found, C 89.30, H 10.44.

The ethers were leached from the silica gel with dichloromethane. This solution was concentrated and then chromatographed by preparative layer with 2% EtOAc/hexane. Usually, the preparative layer plates were developed two or three times to separate the three isomeric ethers. This produced three zones on the plates. The first and foremost zone contained XLIX-b and was visualized under the 254 nm UV lamp. The third zone contained XLIX-c and was also visualized under the UV lamp. The second zone which contained the unconjugated ether (XLIX-a) could not be visualized under the UV lamp but was ascertained as the area between the first and third zones. The ethers were leached from the silica gel with dichloromethane. Concentration gave clear oils in each case which were pure by GLC and TLC examination. The microanalytical samples of XLIX-a, XLIX-b, and XLIX-c were prepared by bulb to bulb distillation at 110°/0.01 torr which gave all three isomers as colorless oils.

PMR Spectrum (of XLIX-a): Figure 20, Mass Spectrum: Figure 21, IR Spectrum: Figure 22. Analysis for $C_{17}H_{28}O$: calculated, C 82.20, H 11.36, O 6.44; found, C 81.94, H 11.20.

PMR Spectrum (of XLIX-b): Figure 23, Mass Spectrum: Figure 24, IR Spectrum: Figure 25. The UV spectrum (hexane) gave λ_{\max} 232.5 nm, ϵ_{\max} 9,039. Analysis for $C_{17}H_{28}O$: calculated, C 82.20, H 11.36,

O 6.44; found, C 82.07, H 11.18.

PMR Spectrum (of XLIX-c): Figure 26, Mass Spectrum: Figure 27, IR Spectrum: Figure 28. The UV spectrum (hexane) gave λ_{\max} 234 nm, ϵ_{\max} 11,217. Analysis for $C_{17}H_{28}O$: calculated, C 82.20, H 11.26, O 6.44; found, C 82.33, H 11.49.

Isolation of 1,1-Bis(Δ^1 -cyclohexenyl)ethane (L-a), Δ^1 -Cyclohexenyl-(E)-2-methylcyclohexylidenemethane (L-b), Δ^1 -Cyclohexenyl-(Z)-2-methylcyclohexylidenemethane (L-c), and 1,2,4,4 α ,4 β ,5,6,7-Octahydro-3H-fluorene (LI)

The methylated dienes (L-a), (L-b), and (L-c) and the anti-diene (LI) were isolated from mixtures produced by the vacuum hot tube decomposition of XXXIV. The product mixtures from several experiments were combined and used for the isolation of these compounds. A general procedure for this is described below.

The reaction mixture was chromatographed by preparative layer with 2-3% EtOAc/hexane. This produced two major zones on the PLC plates which were visualized under the 254 nm UV lamp. The foremost zone contained hydrocarbons including L-a, L-b, L-c, LI, XLVIII-a, XLVIII-b and other minor hydrocarbon components. Alternately, such mixtures could be chromatographed on columns of florisil or silica gel with hexane, collecting only the fractions containing these hydrocarbons. The purpose here was to separate the hydrocarbons from the t-butyl ethers (second zone). The zone containing the hydrocarbons was leached with hexane and concentrated to give an oil. This was chromatographed by preparative layer with dry hexane. This produced

two zones of hydrocarbons which were visualized under the 254 nm UV lamp. The first and foremost zone contained the methylated dienes (L-a), (L-b), and (L-c) along with smaller amounts of other minor components (i.e., LX, LXI, LXII, and LXIV). The second zone contained mainly the anti-diene (LI) and the trienes (XLVIII-a) and (XLVIII-b). The zone containing the methylated dienes was leached with hexane and concentrated. From this mixture, L-a, L-b, and L-c were separated and purified by preparative gas chromatography (FFAP). The microanalytical samples of these compounds were prepared by bulb to bulb distillation at 35-40°/0.05 torr which gave all three isomers as clear, colorless oils.

PMR Spectrum (of L-a): Figure 31, Mass Spectrum: Figure 32, IR Spectrum: Figure 33. Analysis for $C_{14}H_{22}$: calculated, C 88.35, H 11.65; found, C 88.40, H 11.71.

PMR Spectrum (of L-b): Figure 34, Mass Spectrum: Figure 35, IR Spectrum: Figure 36. The UV spectrum (hexane) gave λ_{max} 233 nm, ϵ_{max} 8,323. Analysis for $C_{14}H_{22}$: calculated, C 88.35, H 11.65; found, C 88.50, H 11.60.

PMR Spectrum (of L-c): Figure 37, Mass Spectrum: Figure 38, IR Spectrum: Figure 39. The UV spectrum (hexane) gave λ_{max} 233 nm, ϵ_{max} 8,517. Analysis for $C_{14}H_{22}$; calculated, C 88.35, H 11.65; found, C 88.22, H 11.58.

The zone containing LI was leached with hexane and concentrated. From this mixture, the anti-diene (LI) was separated and purified by preparative gas chromatography (FFAP). Further purification was achieved by bulb to bulb distillation at 40°/0.05 torr. The

anti-diene (LI) obtained in this manner was identical in all characteristics (PMR, Mass, IR, and UV spectra and GLC retention time) with the authentic sample.

Bibliography

1. A. Streitwieser, Jr., "Molecular Orbital Theory," J. Wiley and Sons, Inc., New York, N. Y., 1961.
2. L. Salem, "The Molecular Orbital Theory of Conjugated Systems," W. A. Benjamin, Inc., New York, N. Y., 1966.
3. M. J. S. Dewar, "The Molecular Orbital Theory of Organic Chemistry," McGraw-Hill, Inc., New York, N. Y., 1969.
4. a) R. B. Woodward and R. Hoffmann, J. Amer. Chem. Soc., 87, 395 (1965).
b) ibid., 87, 2046 (1965).
c) ibid., 87, 2511 (1965).
5. R. B. Woodward and R. Hoffmann, "The Conservation of Orbital Symmetry," Academic Press, Inc., New York, N. Y., 1970.
6. a) H. C. Longuet-Higgins and E. W. Abrahamson, J. Amer. Chem. Soc., 87, 2045 (1965).
b) K. Fukui, Accounts Chem. Res., 4, 57 (1971).
c) R. G. Pearson, ibid., 4, 152 (1971).
d) H. E. Zimmermann, ibid., 4, 272 (1971).
e) M. J. S. Dewar, Tetrahedron Suppl. 8, 75 (1966).
7. R. E. Lehr and A. P. Marchand, "Orbital Symmetry: A Problem-Solving Approach," Academic Press, Inc., New York, N. Y., 1972.

8. R. Hoffmann, J. Chem. Phys., 39, 1397 (1963); ibid., 40, 2480 (1964).
9. M. J. S. Dewar, Angew. Chem. Internat. Edit., 10, 761 (1971).
10. a) M. J. S. Dewar and S. Kirschner, J. Amer. Chem. Soc., 93, 93, 4290 (1971).
b) ibid., 93, 4291 (1971).
11. a) M. J. S. Dewar and E. Haselbach, J. Amer. Chem. Soc., 92, 590 (1970).
b) N. Bodor, M. J. S. Dewar, A. Harget, and E. Haselbach, ibid., 92, 3854 (1970).
12. G. Greig and J. C. J. Thynne, Trans. Faraday Soc., 62, 3338 (1966); ibid., 63, 1369 (1967).
13. a) S. Sustmann, C. Rüchart, A. Bierbach, and G. Boche, Tetrahedron Lett., 4759 (1972).
b) S. Sustmann and C. Rüchart, ibid., 4765 (1972).
c) A. Barmetler, C. Rüchart, R. Sustmann, S. Sustmann, and R. Verhülsonk, ibid., 4389 (1974).
d) G. Boche and G. Szeimies, Angew. Chem. Internat. Edit., 10, 911, 912 (1971).
14. a) N. L. Bauld, C. S. Chang, and F. R. Farr, J. Amer. Chem. Soc., 94, 7164 (1972).
b) N. L. Bauld and J. Cessac, ibid., 97, 2284 (1975).
15. a) R. Huisgen and H. Siegel, Tetrahedron Lett., 3381 (1964).
b) H. H. Freedman, G. A. Doorakian, and V. R. Sandel, J. Amer. Chem. Soc., 87, 3019 (1965).

- c) H. Schechter, W. J. Link, and G. V. D. Tiers, ibid., 85, 1601 (1963).
16. a) R. Rieke, M. Ogliaruso, R. McClung, and S. Winstein, ibid., 88, 4729 (1966).
b) G. Moshuk, G. Petrowski, and S. Winstein, ibid., 90, 2179 (1968).
c) S. Winstein, G. Moshuk, R. Rieke, and M. Ogliaruso, ibid., 95, 2624 (1973).
d) T. J. Katz and C. Talcott, ibid., 88, 4733 (1966).
17. T. J. Katz, ibid., 82, 3784, 3785 (1960).
18. G. R. Stevenson and J. G. Concepción, ibid., 95, 5692 (1973).
19. L. A. Paquette, S. V. Ley, R. H. Meisinger, R. K. Russel, and M. Oku, ibid., 96, 5806 (1974).
20. K. W. Egger and S. W. Benson, ibid., 88, 241 (1966).
21. P. D. Bartlett and R. R. Hiatt, ibid., 80, 1398 (1958).
22. R. A. Sheldon and J. K. Kochi, ibid., 92, 5175 (1970).
23. P. E. Eaton and T. W. Cole, ibid., 86, 3157 (1964).
24. K. B. Wiberg, B. R. Lowry and T. H. Colby, ibid., 83, 3998 (1961).
25. P. D. Bartlett, R. E. Pincock, J. H. Rolston, W. G. Schindel, and L. A. Singer, ibid., 87, 2590 (1965).
26. L. H. Slaugh, ibid., 87, 1522 (1965).
27. L. A. Singer, "Peroxyesters," Chapter V of "Organic Peroxides," Vol. I, D. Swern, Ed., Wiley-Interscience, New York, N. Y., 1970, pp. 265-312.
28. E. A. Braude and J. A. Coles, J. Chem. Soc., 2014 (1952).

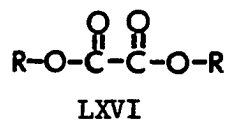
29. E. F. Knights and H. C. Brown, J. Amer. Chem. Soc., 90, 5280 (1968).
30. C. D. Djerassi, R. R. Engle, and A. Bowers, J. Org. Chem., 21, 1547 (1956).
31. J. P. Lorand and P. D. Bartlett, J. Amer. Chem. Soc., 88, 3294 (1966).
32. N. A. Milas and A. Golubovic, ibid., 80, 5994 (1958).
33. P. D. Bartlett and L. B. Gortler, ibid., 85, 1864 (1963).
34. P. D. Bartlett and J. M. McBride, ibid., 87, 1727 (1965).
35. R. E. Lehr, Ph.D. Dissertation, Harvard University (1969).
36. K. E. Wilson, R. T. Seidner, and S. Masamune, J. Chem. Soc. D., 213 (1970).
37. G. G. Harzen and D. W. Rosenburg, J. Org. Chem., 29, 1930 (1964).
38. B. R. Hayes, B. S. Thesis, University of Oklahoma (1970).
39. J. W. Harder, B. S. Thesis, University of Oklahoma (1974).
40. R. E. Lehr, University of Oklahoma, private communication.
41. R. Adams and J. R. Marshall, J. Amer. Chem. Soc., 50, 1970 (1928).
42. M. J. Gibian and R. C. Corley, Chemical Reviews, 73, 441 (1973).
43. D. C. Nonhebel and J. C. Walton, "Free-Radical Chemistry," Cambridge University Press, England (1974).

II. THERMOLYSIS OF BIS($\Delta^{1,1'}$ -DICYCLOHEXYLMETHYL) OXALATE

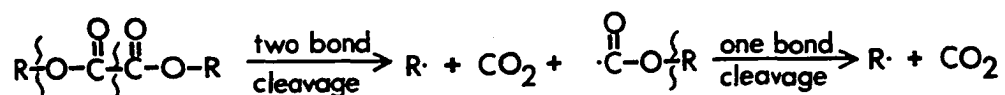
CHAPTER 1

INTRODUCTION

In recent years, a variety of free radicals which lack hydrogen atoms β to the radical site have been generated and studied by the thermal decomposition of organic oxalates (LXVI). Thus, the

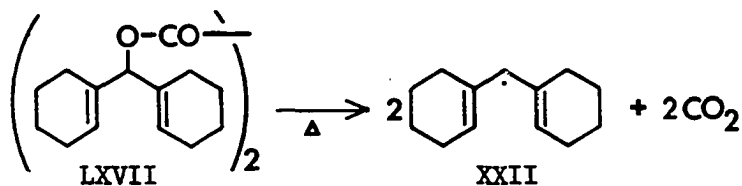


vapor phase thermolysis of diallyl¹ and dibenzyl² oxalates has led to the formation of products which were indicative of free radical processes. The results of thermolysis of bis(benzhydryl) oxalates³ neat and in diphenyl solution have also implicated a radical decomposition mechanism. Trahanovsky *et al*^{2,3} has shown that the thermal decomposition of oxalates to radicals occurs mainly by the sequence shown in Scheme 1.



Scheme 1

As an alternate method generating $\Delta^{1,1'}$ -dicyclohexenylmethyl radical (XXII), we chose to prepare and study the thermolysis of bis ($\Delta^{1,1'}$ -dicyclohexenylmethyl) oxalate (LXVII). The following section



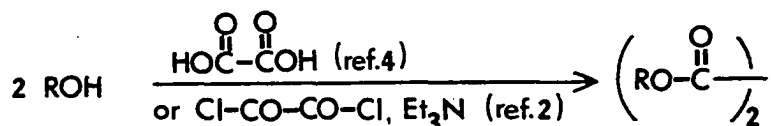
reports our preparation of LXVII and the results of its thermal decomposition.

CHAPTER 2

RESULTS AND DISCUSSION

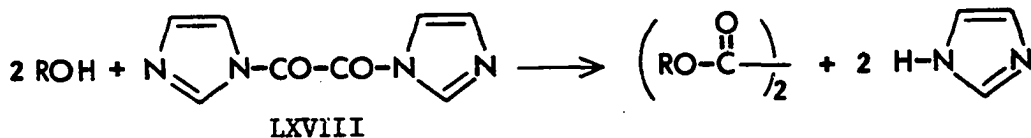
Preparation of Bis($\Delta^{1,1'}$ -dicyclohexenylmethyl) Oxalate (LXVII)

One of the attractive features of using organic oxalates as radical precursors is their convenient preparation from the corresponding alcohols. The usual methods for oxalate preparation (shown below) involve reaction conditions whereby an acid is used directly in the reaction⁴ or is generated during the reaction as a by-product.²



The application of the usual methods of oxalate synthesis toward the preparation of LXVII resulted in low or zero yields. Since we have found the oxalate (LXVII) to be sensitive to even trace amounts of acids, we sought to develop an alternate approach to oxalate synthesis that would avoid acids at all stages.

This method involves the reaction of N,N'-oxalyl-di-imidazolide (LXVIII) with the appropriate alcohol as shown in Scheme 2. This approach was suggested by analogy with the reaction of N,N'-carbonyl-di-imidazolide with alcohols, which leads to the formation of carbonate



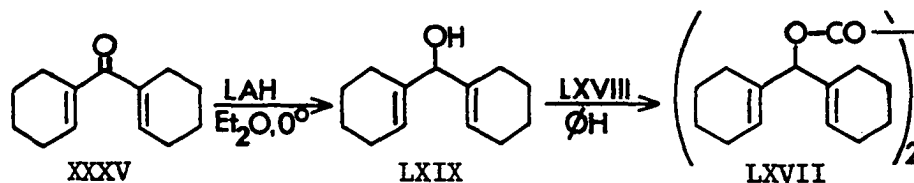
Scheme 2

esters.⁵ The virtue of this method is seen in Scheme 2. By using LXVIII, acids are avoided; the only by-product in the reaction is imidazole. The use of the reagent (LXVIII) for the preparation of the acid-sensitive oxalate (LXVII) and the oxalate esters of several common benzylic alcohols has been described in the literature.⁶ This method should be especially valuable for the preparation of other acid-sensitive oxalates.

The required reagent, N,N'-oxalyl-di-imidazolidine (LXVIII)⁷ was prepared by the addition of oxalyl chloride to a solution of imidazole (4 moles) in dry tetrahydrofuran under ice bath cooling. Filtration of the precipitated imidazolium chloride and concentration of the solution gave LXVIII in 72% yield as a yellow amorphous solid which darkened at 105° and melted with decomposition at 110-112°. The reagent (LXVIII) produced in this manner was sufficiently pure to be used for the oxalate preparations⁶ and was used without further purification. The PMR, mass, and IR spectra of LXVIII are shown in Figures 1, 2, and 3, respectively, and are consistent with the structure for LXVIII.

The preparation of bis($\Delta^{1,1'}$ -dicyclohexenylmethyl) oxalate

(LXVII) was accomplished according to the route shown in Scheme 3 starting with the known $\Delta^{1,1'}$ -dicyclohexenyl ketone (XXXV).⁸



Scheme 3

The ketone (XXXV)⁸ was smoothly reduced by ethereal lithium aluminum hydride (LAH) at ice bath temperature to the alcohol (LXIX). The reaction was quenched with ethyl acetate and worked up with 20% acetic acid which gave LXIX as a white solid in essentially pure form in 72% yield. Recrystallization from hexane gave LXIX which melted at 44-45°. The PMR, mass, and IR spectra are shown in Figures 4, 5, and 6, respectively, and are consistent with the structure for LXIX.

The treatment of the alcohol (LXIX) in dry benzene with *N,N'*-oxalyl-di-imidazolide (LXVIII) gave the oxalate (LXVII) reproducibly in yields of 50-60%. Recrystallization from benzene-hexane gave pure crystalline LXVII which melted at 83.5-84.5°. The oxalate (LXVII) was found to be unstable in the presence of even trace amounts of acids. For example, the PMR spectrum could not be obtained using CDCl_3 . Presumably, the traces of acid present in that solvent catalyzed the rapid decomposition of the oxalate. The PMR spectrum was obtained in acid-free benzene- d_6 and is shown in Figure 7. The IR spectrum is shown in Figure 8. The mass spectrum (shown in Figure 9) does not show the parent ion for LXVII (mol. wt. is 438). The ion with the largest m/e value was observed at m/e 348 and was not identified. The

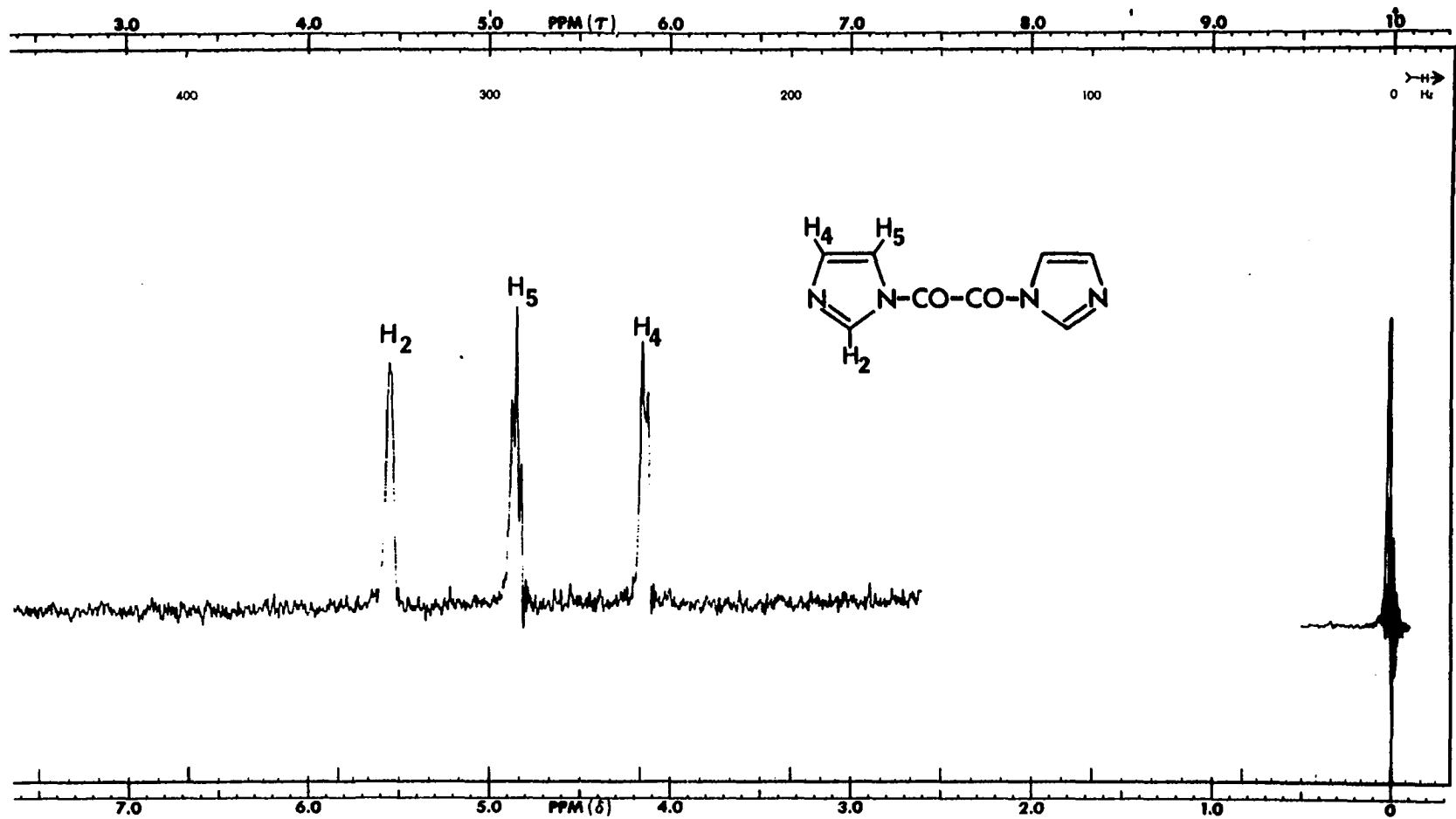


Figure 1 60 MHz PMR Spectrum (THF) of LXVIII; Offset +3δ

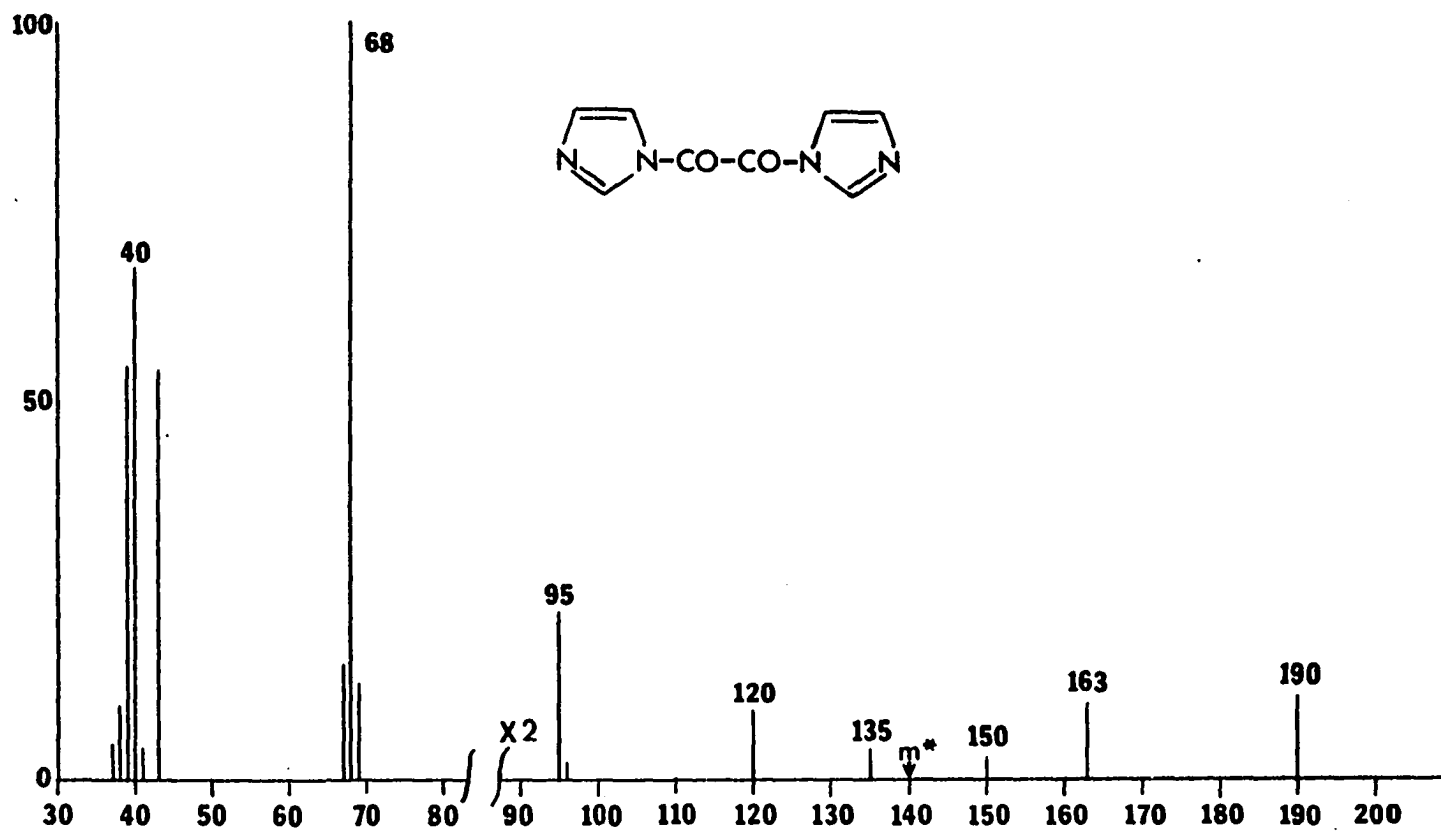


Figure 2 70 eV Mass Spectrum of LXVIII

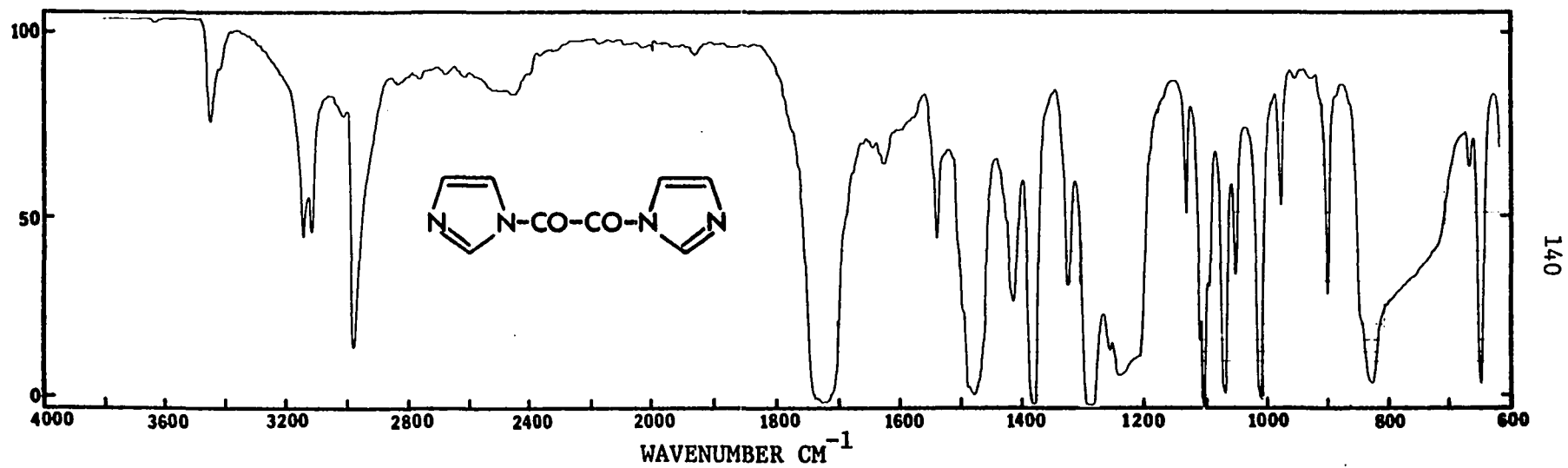


Figure 3 IR Spectrum (CHCl_3) of LXVIII

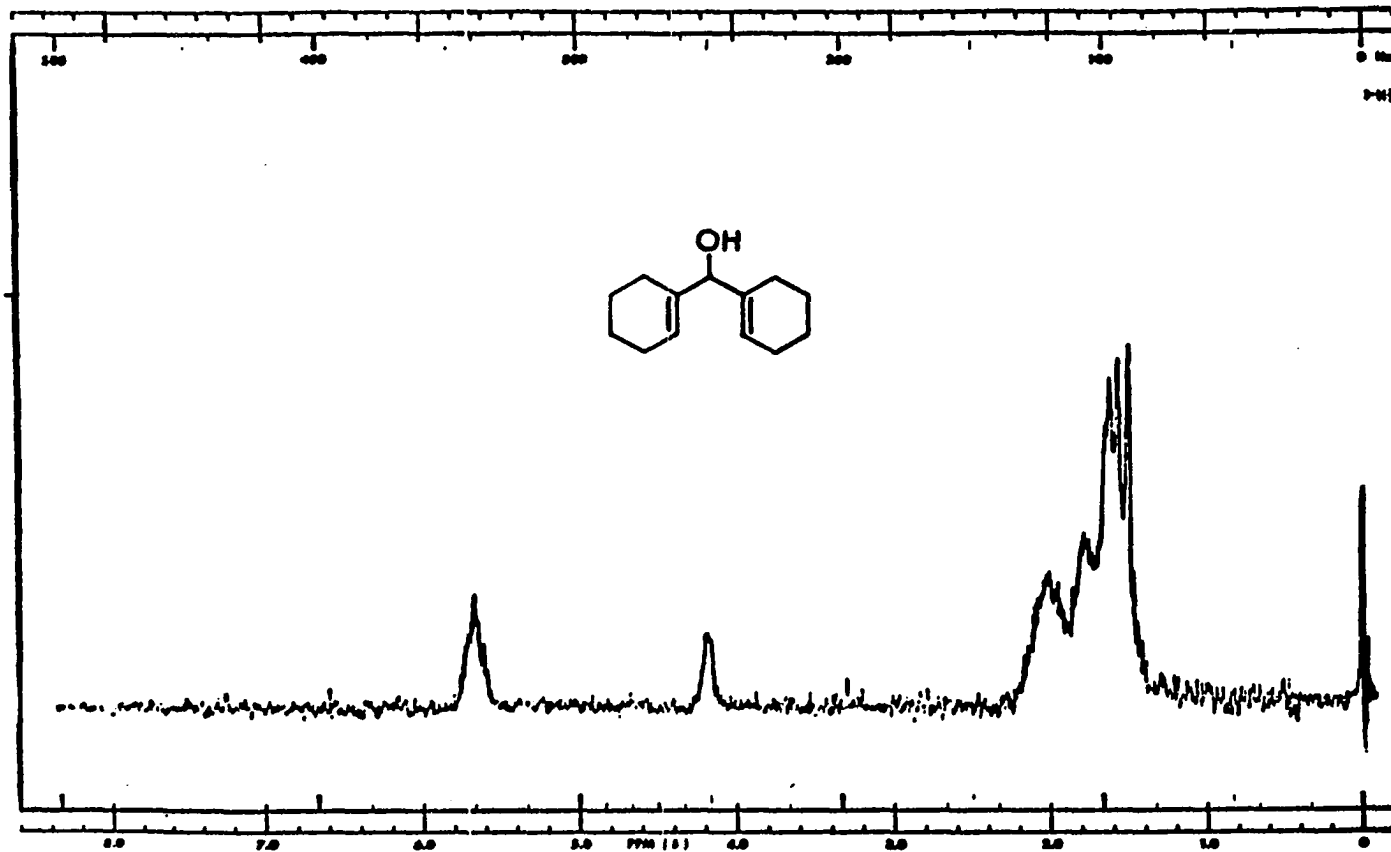


Figure 4 60 MHz PMR Spectrum (CCl_4) of LXIX

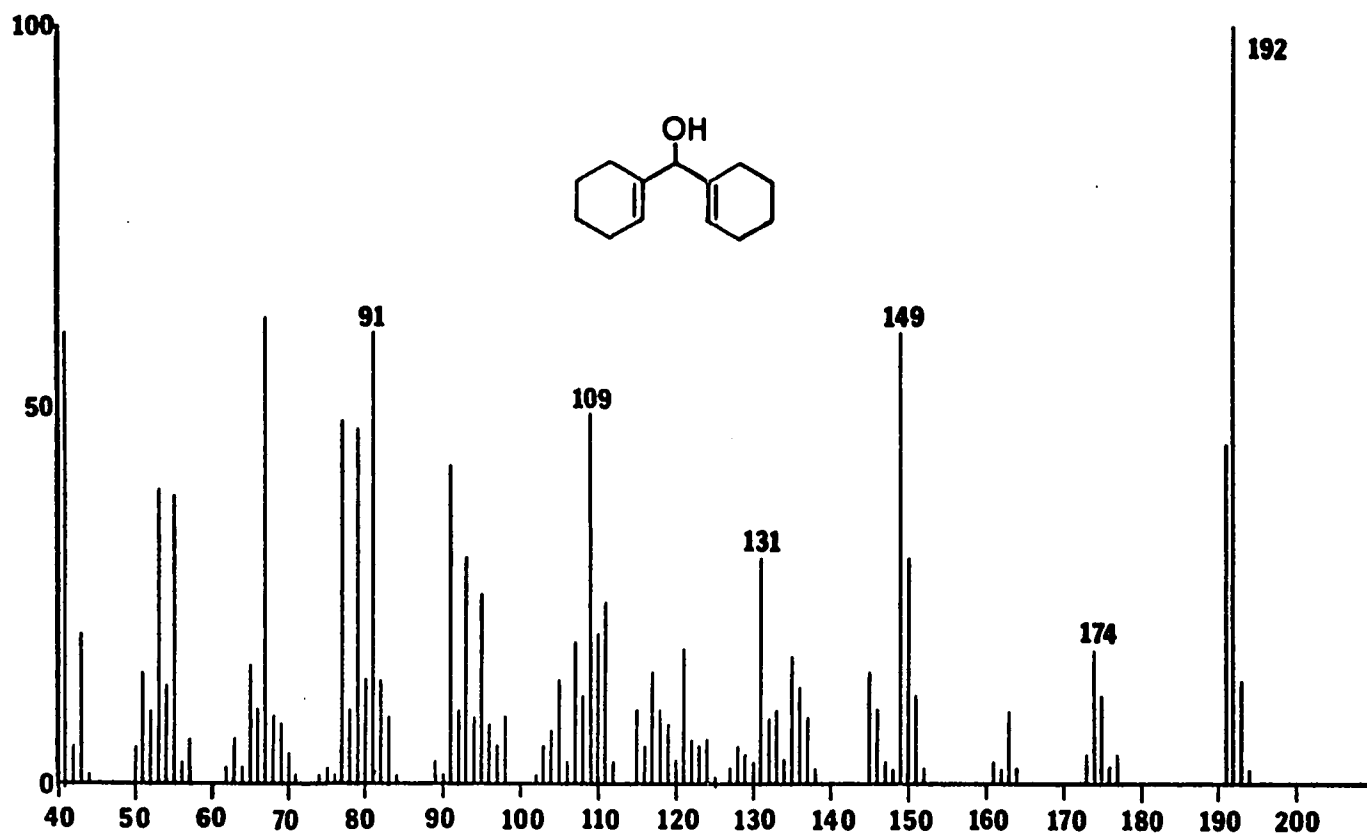
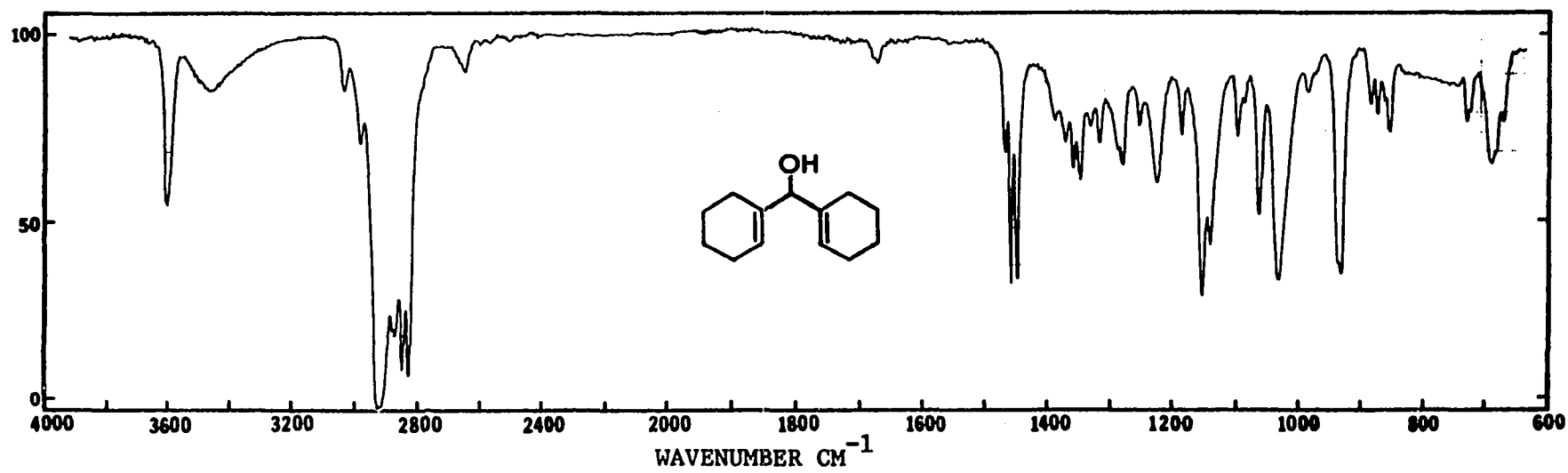


Figure 5 70 eV Mass Spectrum of LXIX



143

Figure 6 IR Spectrum (CCl_4) of LXIX

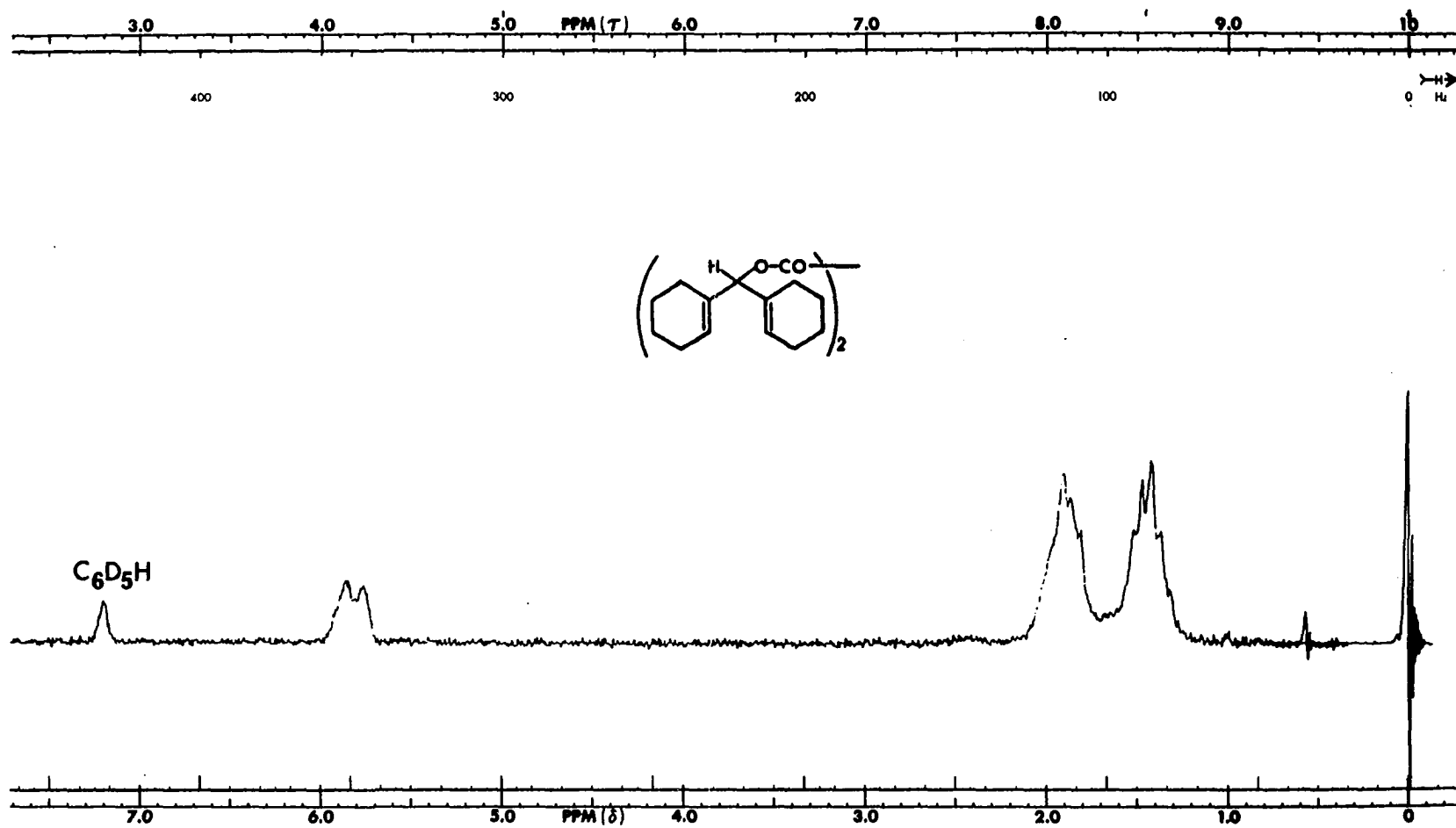
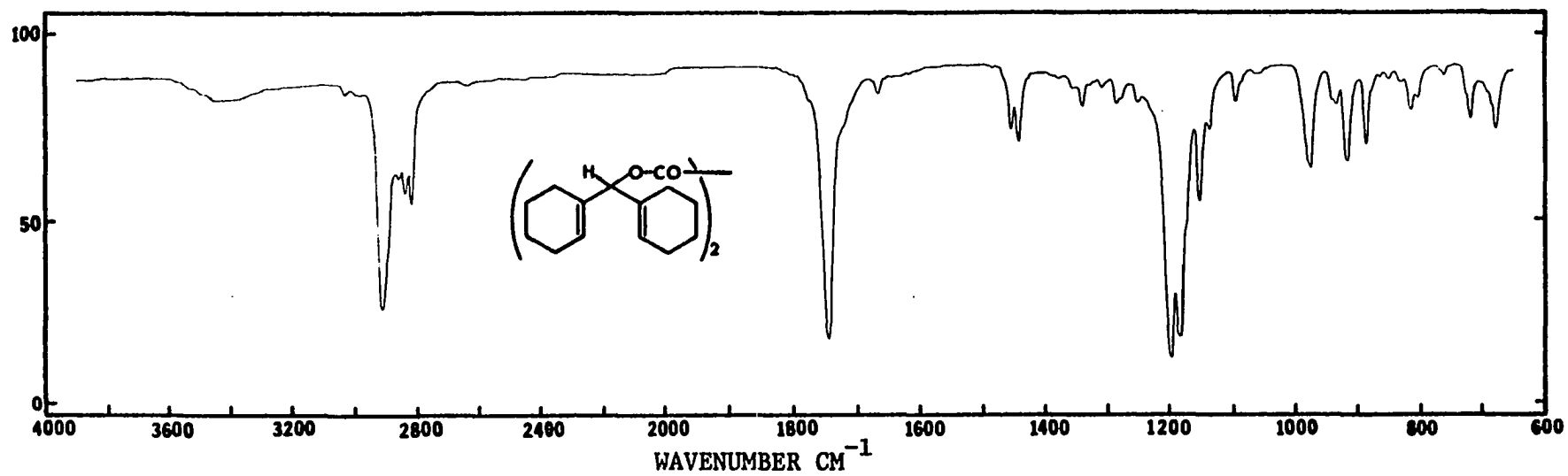


Figure 7 60 MHz PMR Spectrum (C_6D_6) of LXVII



145

Figure 8 IR Spectrum (KBr) of LXVII

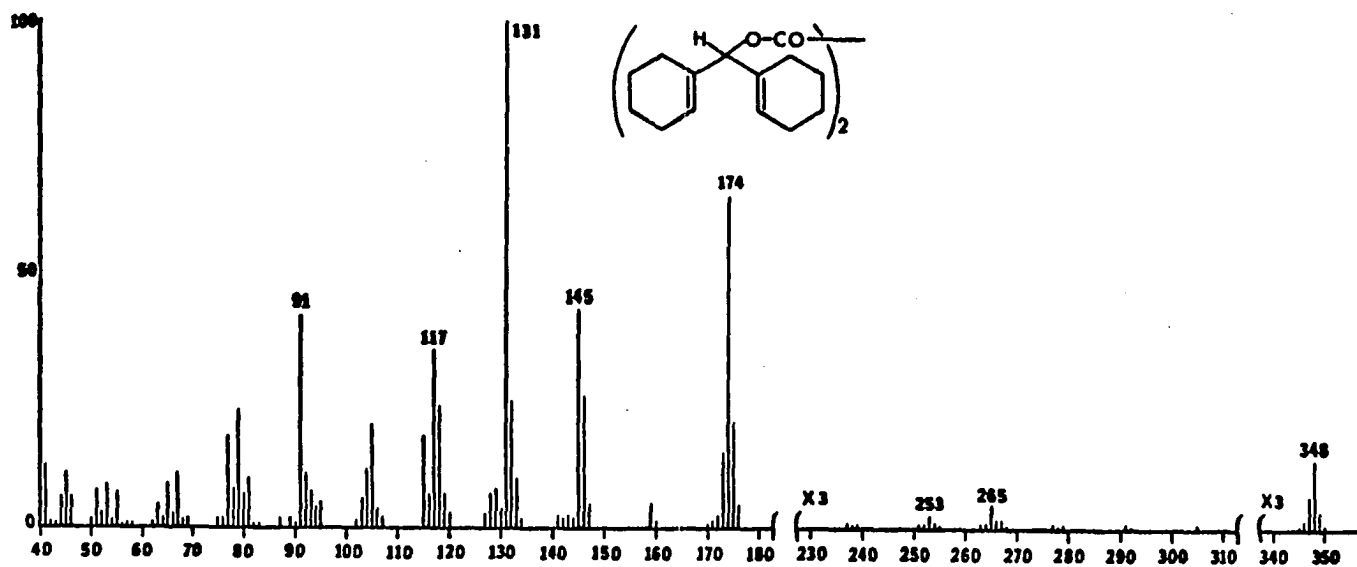


Figure 9 70 eV Mass Spectrum of LXVII

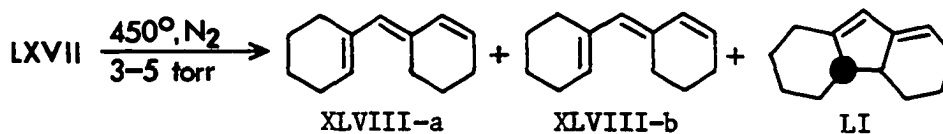
prominant ion at m/e 174 is attributed to the formation of hydrocarbons (unidentified) of molecular weight 174 which were produced by the thermal (or possibly acid-catalyzed) decomposition of LXVII in the mass spectrometer probe. The PMR and IR spectra are consistent with the structure for LXVII and provide the major proof of its structure.

The failure to obtain a suitable mass spectrum was not entirely an unexpected result since the attempted sublimation of LXVII at 75°/0.05 torr resulted in the formation of a clear oil (a mixture by GLC examination on FFAP) on the cold finger plus a water soluble white solid. The solid was presumed to be oxalic acid. The mass spectrum of the clear oil gave m/e 174 as the largest observed ion. This mixture was similar by GLC inspection to those obtained when LXVII was dissolved in CDCl_3 (PMR solvent) or in CHCl_3 which contained HCl. Such acid-catalyzed decompositions of LXVII gave mixtures of hydrocarbons from which the trienes (XLVIII-a) and (XLVIII-b) were isolated in yields of 21% and 34%, respectively. Other minor products formed were not identified.

Hot Tube Decomposition of LXVII

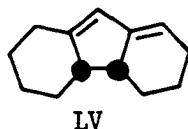
The oxalate (LXVII) was thermolyzed using the quartz hot tube which was packed with NH_4OH -washed quartz chips at a temperature of 450°. The thermolysis was accomplished by depositing the oxalate (LXVII) as 20% by weight on NH_4OH -washed Chromsorb W (45/60 mesh) and introducing this slowly into the hot tube under a nitrogen flow of ca. 40 ml/min and a pressure of 3-5 torr. The products of decomposition

were collected in a dry ice isopropanol cooled, U-shaped collector.



By a combination of preparative layer chromatography and preparative gas chromatography, three major products were isolated and identified as the trienes (XLVIII-a) and (XLVIII-b) and the anti-diene (LI). Analysis of the mixture by GLC gave estimated yields for XLVIII-a, XLVIII-b, and LI as 12.6%, 13.3%, and 8.1% of theory, respectively. Other major products were formed, but we were unable to successfully isolate (by GLC) these for identification. This was largely due to their instability to the GLC conditions employed for separation of the mixture components. The mixtures produced in the hot tube decomposition of LXVII were rather unstable and showed an apparent tendency to polymerize even in hexane solution. This tendency interfered with our attempted separations of the mixture components.

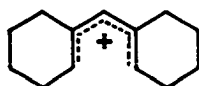
Using authentic syn-diene (LV), for GLC enhancement experiments on a S.C.O.T. FFAP column, we were unable to detect any significant amounts of LV in these mixtures.



Conclusions

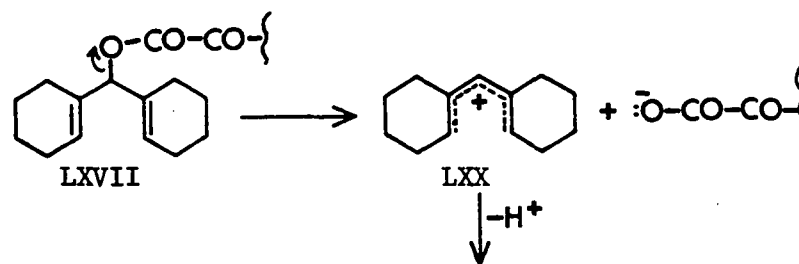
The results of analysis of the products produced in the thermal decomposition of the oxalate (LXVII) are at best incomplete. The identification of XLVIII-a, XLVIII-b, and LI and the lack of significant amounts of LV in the mixtures formed from LXVII are in tentative agreement with the results obtained from the thermal decomposition of the peroxyester (XXXIV) in Part I of this dissertation.

However, certain aspects of the behavior of the oxalate (LXVII) raise serious questions regarding the nature of the reactive species being produced from LXVII. For example, the tendency for the oxalate (LXVII) to decompose in the presence of trace amounts of acids (forming mainly XLVIII-a and XLVIII-b) clearly indicates an ionic decomposition pathway which probably proceeds via the carbonium ion (LXX).



LXX

Also, the tendency for the oxalate (LXVII) to decompose at temperatures lower than its melting point (i.e., 70°/0.05 torr) is inconsistent with the behavior of other oxalates¹⁻³ which have successfully been used to generate and study radicals. Possibly, the oxalate (LXVII) decomposes thermally by an ionic mechanism, such as is shown below, leading to the carbonium ion (LXX) rather than by the usual mechanism (see Scheme 1) which would lead to the radical (XXII).



Products of mol. wt. 174

These observations have prompted us to conclude that the oxalate (LXVII) was not a suitable precursor for the generation of $\Delta^{1,1'}$ -dicyclohexenylmethyl radical (XXII). For the generation of XXII and the study of the electrocyclization (XXII \rightarrow XXIII), we have relied on the results of the thermal decomposition of the peroxyester (XXXIV).

CHAPTER 3

EXPERIMENTAL

All melting points were obtained on a Gallenkampf MF 370 capillary melting point apparatus and are uncorrected. Infrared spectra were obtained on a Beckman IR-18 spectrophotometer. Mass spectra were obtained on a Hitachi-Perkin Elmer RMU-7E mass spectrometer operated at 70 eV. The 60 MHz PMR spectra were obtained on a Varian A-60 spectrometer. Preparative gas chromatography was done on a Varian 90-P gas chromatograph. Analytical gas chromatography work was done on a Hewlett Packard 5760 gas chromatograph equipped with a flame-ionization detector. Preparative and thin layer chromatography was done using silica gel PF (254 + 366) UV indicating gel. Microanalyses were performed by Galbraith Laboratories, Inc., Knoxville, Tennessee or by Chemlytics, Inc., Tempe, Arizona.

N,N'-Oxalyl-di-imidazolide (LXVIII)⁷

Imidazole (24 g, 352.8 mmol) was dissolved in dry tetrahydrofuran (600 ml) in a 1 liter flask equipped with a magnetic stirrer. The solution was stirred and cooled in an ice bath. Oxalyl chloride (11.4 g, 88.8 mmol) in dry tetrahydrofuran (80 ml) was added via dropping funnel over 20-30 minutes with stirring and cooling. The

mixture was then stirred for 45 minutes at ambient room temperature. The mixture was filtered with suction and concentrated on the rotary evaporator which had been purged with dry nitrogen. This gave LXVIII as a yellow amorphous solid, yield: 12 g = 72%. The LXVIII produced in this manner darkened at 105° and melted with decomposition at 110-112° and was sufficiently pure for use in the oxalate synthesis. We were unable to obtain a suitable microanalysis for LXVIII, due to its hygroscopic nature. Although this reagent is moisture-sensitive, it may be stored for long periods in a vacuum desiccator over phosphorous pentoxide and may be quickly weighed in air without appreciable loss of activity.

The 60 MHz PMR spectrum (Figure 1) in tetrahydrofuran showed: δ 8.56 (1H multiplet, Proton H₂), 7.87 (1H unsymmetrical triplet, proton H₅), 7.15 (1H multiplet, proton H₄). The 70 eV mass spectrum (Figure 2) showed: m/e 190 (M⁺, parent ion), 163 (M⁺ - HCN), 95 (C₄H₃N₂O⁺), and 68 (base peak, C₃H₄N₂⁺). The IR spectrum (Figure 3) in CHCl₃ showed: cm⁻¹ 1720 (C=O).

$\Delta^{1,1'}$ -dicyclohexenylmethanol (LXIX)

The ketone (XXXV)⁸ (15 g, 79.4 mmol) was dissolved in absolute ether (250 ml) in a flask equipped with a magnetic stirrer and an addition funnel. The solution was stirred and cooled in an ice bath. Lithium aluminum hydride (22.05 mmol) in ether (30 ml) was added slowly over 20 minutes. The mixture was stirred in the cold for an additional 30 minutes. Ethyl acetate (10 ml) was added; the mixture was poured into cold water (200 ml) and acidified with 20% acetic acid

to pH 6. The phases were separated and the aqueous phase was extracted with ether (150 ml). The combined ether phases were washed with saturated NaHCO_3 (150 ml) and then water (150 ml) and dried over MgSO_4 . Filtration and concentration gave a clear oil which was crystallized from hexane (-20°) to give LXIX as white crystals, yield: 10.9 g = 72%. Recrystallization from hexane (-20°) gave LXIX which melted at $44-45^\circ$. The microanalytical sample was prepared by sublimation at $45^\circ/0.5$ torr.

The 60 MHz PMR spectrum (Figure 4) in CCl_4 showed: δ 5.65 (2H multiplet, olefinic protons), 4.20 (1H broad singlet, proton on carbon bearing oxygen), 1.2-2.2 (17H multiplet, ring protons and hydroxyl proton). The 70 eV Mass spectrum (Figure 5) showed: m/e 192 (M^+ , parent ion and base peak), 174 ($\text{M}^+ - \text{H}_2\text{O}$). The IR spectrum (Figure 6) in CHCl_3 showed: cm^{-1} 3530 (OH), 1670 (C=C), 1025 (C-O). Analysis for $\text{C}_{13}\text{H}_{20}\text{O}$: calculated, C 81.19, H 10.48, O 8.32; found, C 81.14, H 10.27.

Bis($\Delta^{1,1'}$ -dicyclohexenylmethyl) Oxalate (LXVII)

The alcohol (LXIX) (2 g, 10.4 mmol) and the imidazolidine (LXVIII) (0.99 g, 5.2 mmol) were dissolved in dry benzene (60 ml) in a 100 ml flask equipped with a magnetic stirrer. The flask was stoppered and the mixture was stirred for 1.5 hours. The mixture was washed with two 50 ml portions of water. The aqueous washings were combined and extracted with ether (50 ml). The ethereal phase was back-washed with water (50 ml). The organic phases were combined and dried over Na_2SO_4 . Filtration and concentration of the organic phase gave

LXVII as a white solid. Recrystallization from benzene-hexane (ice bath cooling) gave LXVII which melted at 80-81°, yield: 1.45 g = 63.5%. The microanalytical sample was prepared by recrystallization from benzene-hexane which gave LXVII that melted at 83.5-84.5°.

The 60 MHz PMR spectrum (Figure 7) in C_6D_6 showed: δ 5.7-6.0 (3H multiplet, olefinic protons and proton on carbon bearing oxygen), 1.2-2.1 (16H multiplet, ring protons). The IR spectrum (Figure 8) showed: cm^{-1} 1745 (C=O), 1190 and 1175 (C-O). The 70 eV mass spectrum is shown in Figure 9 and was discussed in the text. Analysis for $C_{28}H_{38}O_4$: calculated, C 76.67, H 8.73, O 14.59; found, C 76.86, H 8.69.

Acid Catalyzed Decomposition of LXVII

The Oxalate (LXVII) (600 mg, 1.37 mmol) was dissolved in chloroform (25 ml). One drop of concentrated HCl was added (the mixture turned blue immediately) and the mixture was stirred magnetically for 1.5 hours. The mixture was diluted with chloroform (25 ml) and stirred into an aqueous saturated $NaHCO_3$ solution (75 ml). The chloroform layer (yellow) was separated, washed with water (75 ml), and dried over Na_2SO_4 . After filtration and concentration, a greenish oil was obtained which was distilled bulb to bulb at 95°/0.1 torr to give 377 mg of a slightly yellowed oil. The oil was subjected to preparative gas chromatography on Carbowax 20M. Thus, the triene (XLVIII-a) was isolated (100 mg) in 21% yield and the triene (XLVIII-b) was isolated (162 mg) in 34% yield. The trienes (XLVIII-a) and (XLVIII-b) were characterized completely (PMR, mass, IR, and UV spectra) and were identical in all characteristics with those discussed in Part I of this dissertation.

Thermal Decomposition of LXVII

The oxalate (LXVII) was thermolyzed in the quartz hot tube using the solid addition bulb which was described in Part I (see Figures 30 and 58 of Part I). The hot tube was packed with NH_4OH -washed quartz chips. During the thermolysis a dry nitrogen flow of 40-45 ml/min was maintained through the system under a pressure of 3-5 torr. The vacuum was applied at the glass bead filled, U-shaped collector. The collector was cooled with a slurry of dry ice-isopropanol. The oxalate was deposited on NH_4OH -washed Chromsorb W (45/60 mesh) as 20% by weight by preparing a slurry of LXVII and Chromsorb W in benzene and then drying under vacuum. This was slowly introduced into the hot tube via the solid addition bulb. In a typical experiment, the hot tube was heated to 450° . The product mixture was washed from the collector with hexane. The mixture was subjected to preparative layer chromatography with hexane. The major product zone was visualized under the 254 nm UV lamp. This zone contained the trienes (XLVIII-a) and (XLVIII-b) and the anti-diene (LI) as major components. These compounds were isolated by preparative gas chromatography on Carbowax 20M and were identified by comparison of spectral data and GLC retention times with those of authentic samples. At least two other major components were present in amounts comparable to that for LI (ca. 5-8%), but we were unable to successfully isolate these by gas chromatography for identification. The yields of XLVIII-a, XLVIII-b, and LI were estimated by GLC on TCEP and FFAP columns. For these estimations, a known amount of the partially chromatographed hot tube mixture was injected into the gas chromatograph and the resulting GLC trace was totally integrated.

It was assumed that no other components than those appearing in the trace were present in the mixture and that each component in the trace had the same relative sensitivity to the flame-ionization detector. The yields of 12.6%, 13.3%, and 8.1% for the compounds (XLVIII-a), (XLVIII-b), and (LI), respectively, were estimated by dividing the relative peak areas for each of these components by the area of the total GLC trace. These yields were based on the decomposition of 100 mg (0.228 mmol) of the oxalate (LXVII) at 450°.

The presence of the syn-diene (LV) could not be detected by GLC on a S.C.O.T. FFAP column, using authentic LV for peak enhancement. For this purpose, the total thermolysis mixture was used rather than one which had been subjected to preparative layer chromatography, since we have found the diene (LV) to be unstable to preparative layer chromatography.

Bibliography

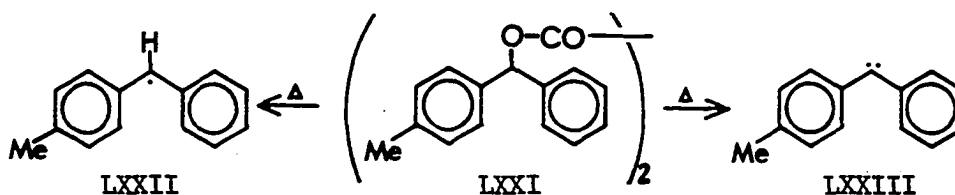
- a) D. M. Golden, N. A. Gac, and S. W. Benson, J. Amer. Chem. Soc., 91, 2136 (1969).
 - b) W. S. Trahanvosky, J. A. Lawson, and C. C. Ong, ibid., 92, 7174 (1970).
 - c) D. G. L. James and S. M. Kambanis, Trans. Faraday Soc., 65, 1350 (1969).
- W. S. Trahanovsky, C. C. Ong, and J. A. Lawson, J. Amer. Chem. Soc., 90, 2839 (1968).
- W. S. Trahanovsky, J. A. Lawson, and D. E. Zabel, J. Org. Chem., 32, 2287 (1967).
- C. Lespagnol, Bull. Soc. Chim. Fr., 110 (1960).
- H. A. Staab, Angew. Chem. Int. Edit., 1, 355 (1962).
- J. M. Wilson and R. E. Lehr, Synthetic Communications, 1, 253 (1971).
- American Cyanamid Co., Neth. Appl. 6,612,650 (Cl. co9c), March, 1967; U. S. Appl. 8,23,30 Sept., 1965, Jan., 1966, and May, 1966; Chem. Abstr., 68, 21847a (1968). No experimental details or physical properties were given for the imidazolide (LXVIII).
- E. A. Braude and J. A. Coles, J. Chem. Soc., 1014 (1952).

III. THERMOLYSIS OF BIS(4-METHYLBENZHYDRYL) OXALATE:
COMPETING FRAGMENTATION TO RADICALS AND CARBENES

CHAPTER 1

INTRODUCTION

During the course of our studies involving oxalates as precursors for the generation and study of radicals, we have investigated the thermolysis of bis(4-methylbenzhydryl) oxalate (LXXI). Our results have indicated a competing fragmentation of LXXI to the radical (LXXII) and to the carbene (LXXIII).¹ Previous studies of oxalate thermolyses²

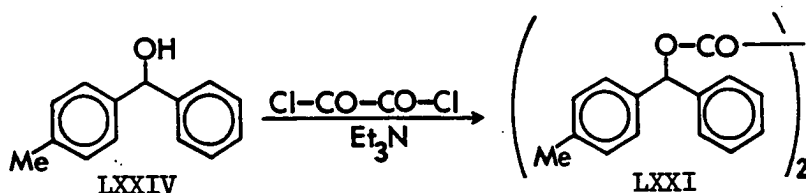


have not acknowledged the possible occurrence of such carbene intermediates. The following section reports the results of our studies with LXXI.

CHAPTER 2

RESULTS AND DISCUSSION

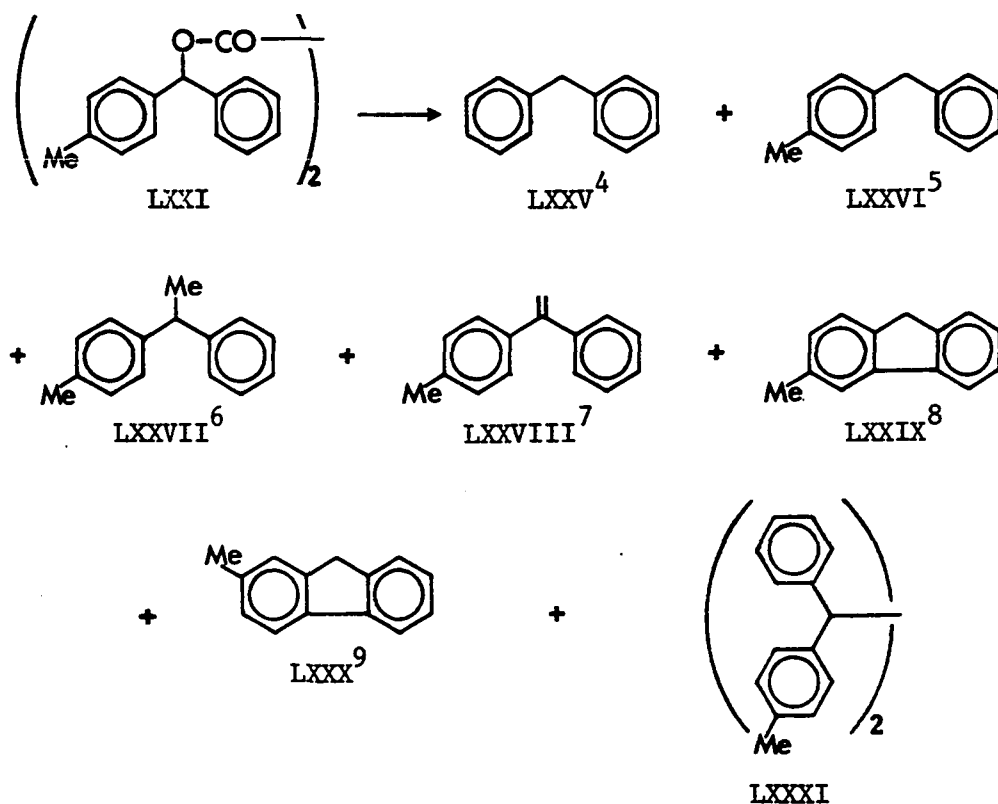
Bis(4-methylbenzhydryl) oxalate (LXXI) was prepared from 4-methylbenzhydrol (LXXIV)³ by its reaction with oxalyl chloride in the presence of triethylamine. Recrystallization from hexane-ether gave LXXI which melted at 83.5–85° in 77% yield. The PMR, mass, and IR spectra of LXXI are shown in Figures 1, 2, and 3, respectively, and are consistent with the structure for LXXI.



The oxalate (LXXI) was thermolyzed at various temperatures by two methods. In method A, the oxalate (LXXI) was adsorbed on Chromsorb W and was introduced into the quartz hot tube at 5 torr using a nitrogen flow of 10 ml/min. In method B, the oxalate (LXXI) was introduced into the quartz hot tube as a benzene solution at 95 torr using a nitrogen flow of 85 ml/min. Either method produced

similar mixtures of products.

Seven products were produced in the thermolysis of LXXI and are shown in Scheme 1. Compounds (LXXV-LXXX) are known⁴⁻⁹ and were identified by isolation (GLC) and comparison of spectral data and GLC retention times with authentic samples. The dimer (LXXXI) was isolated by preparative layer chromatography and was further purified by sublimation at 125°/0.25 torr which gave LXXXI as a white solid that melted at 145-150°. Identification of LXXXI was made on the basis of its PMR, mass, and IR spectra which are shown in Figures 4, 5, and 6, respectively.



Scheme 1

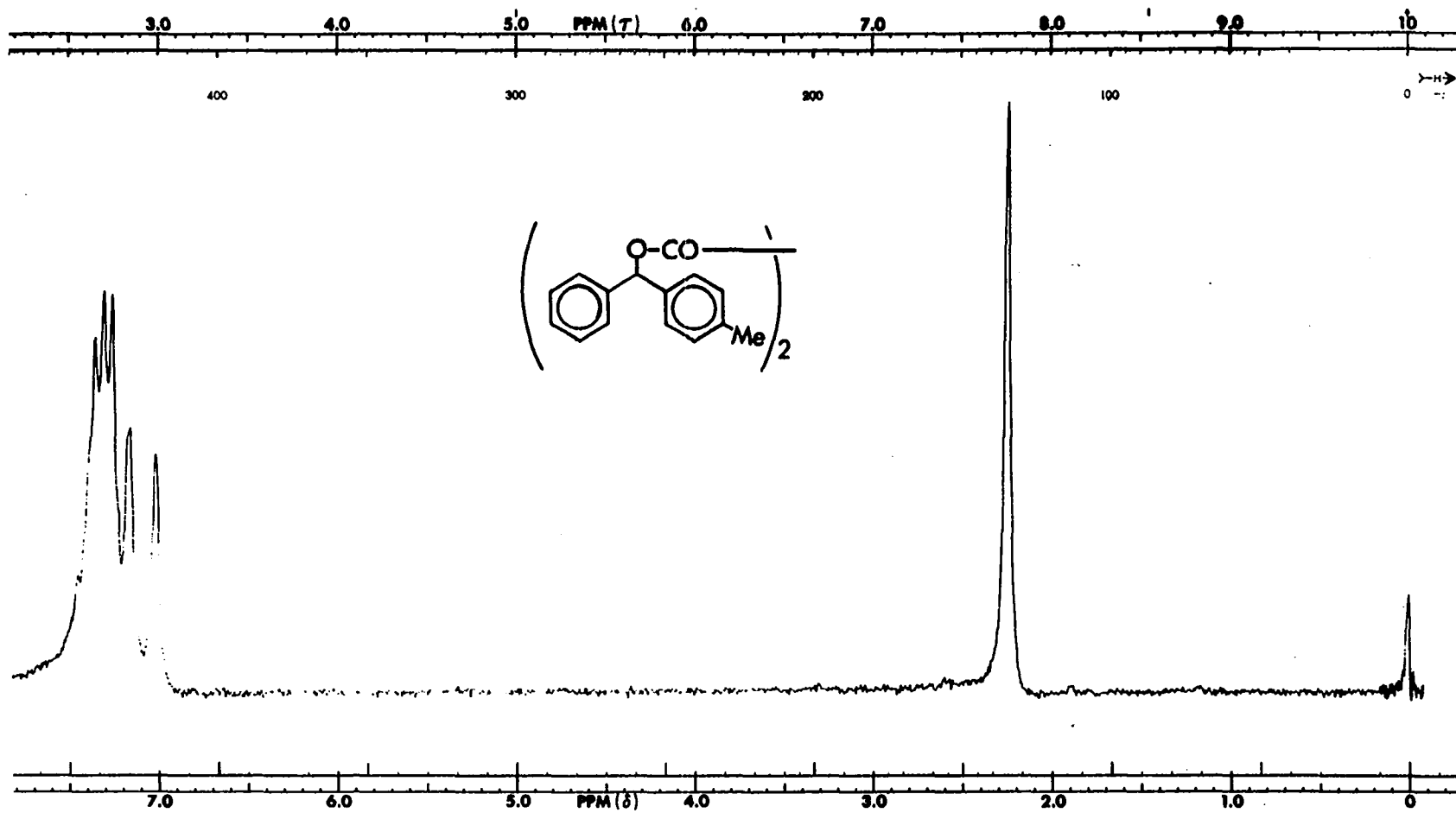


Figure 1 60 MHz PMR Spectrum (CDCl_3) of LXXI

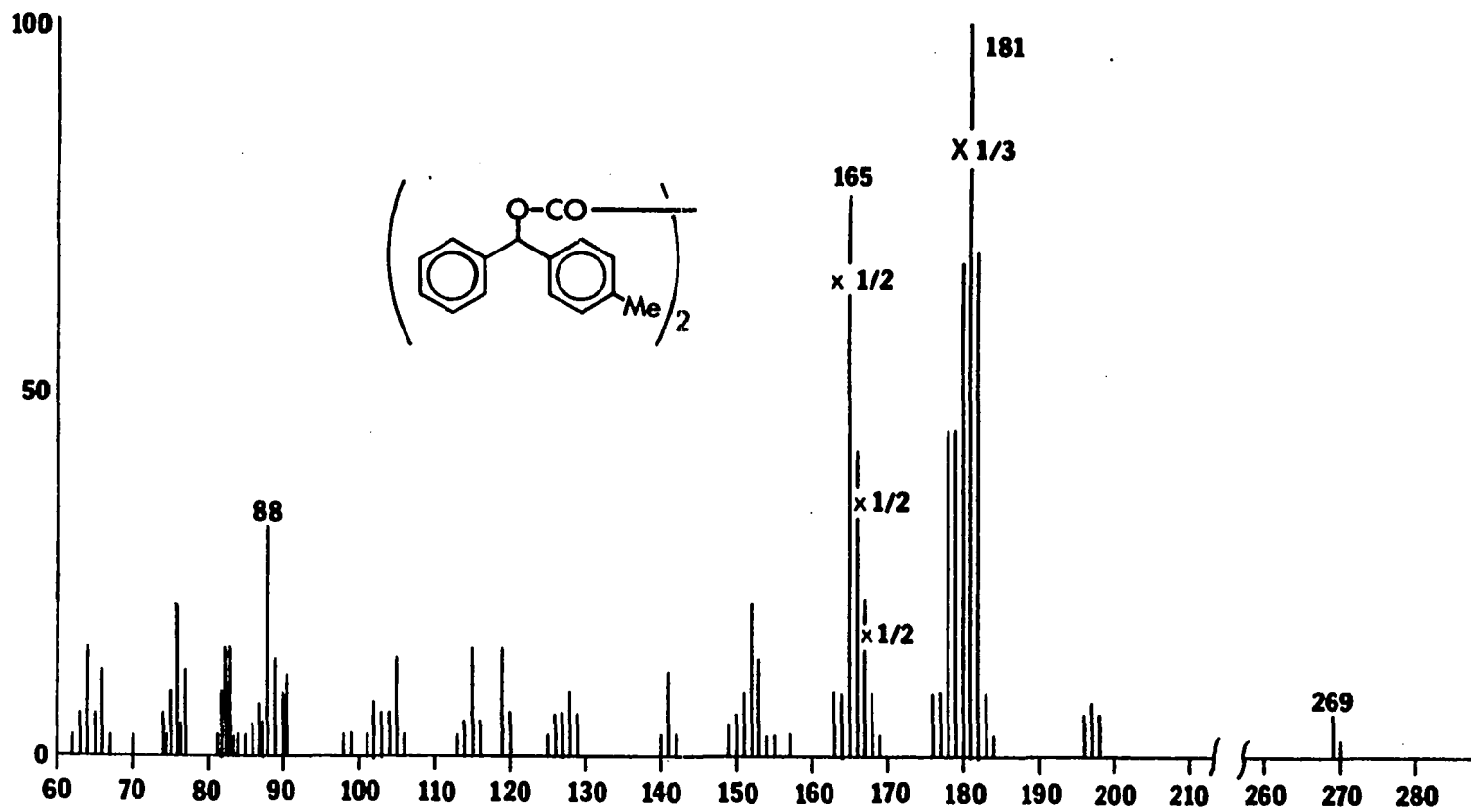


Figure 2 70 eV Mass Spectrum of LXXI

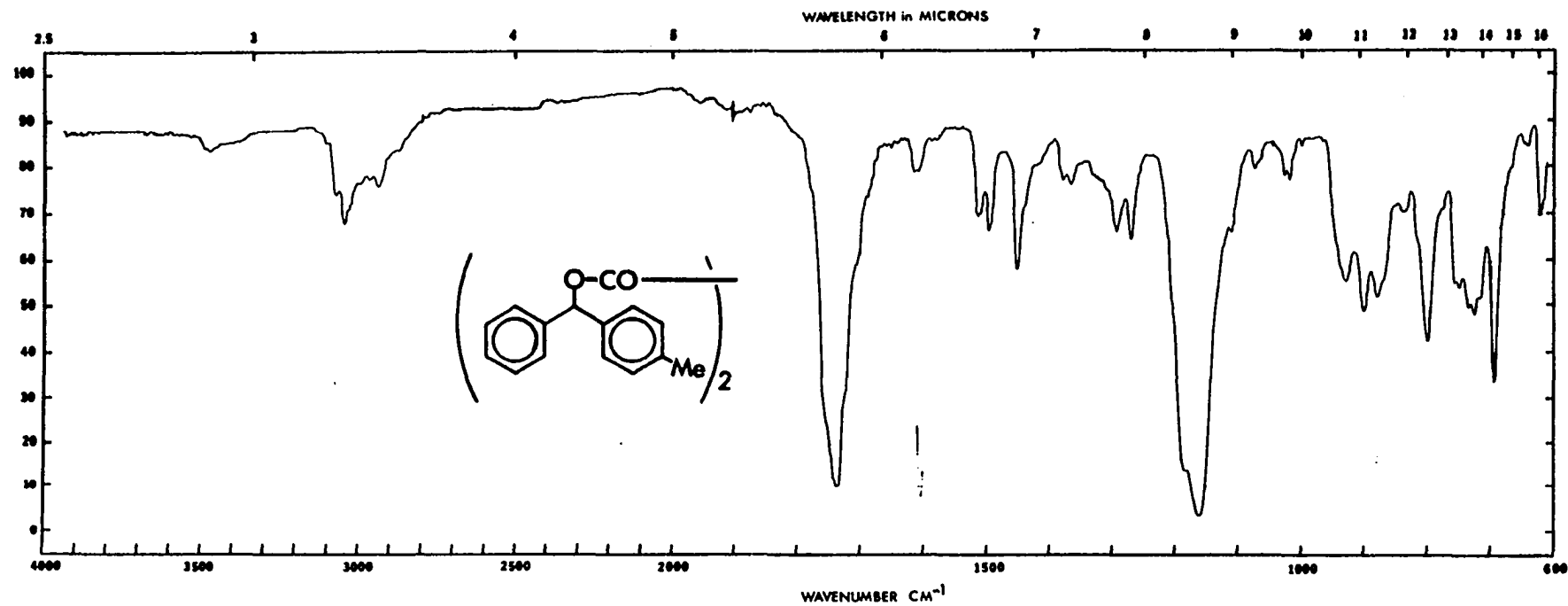


Figure 3 IR Spectrum (KBr) of LXXI

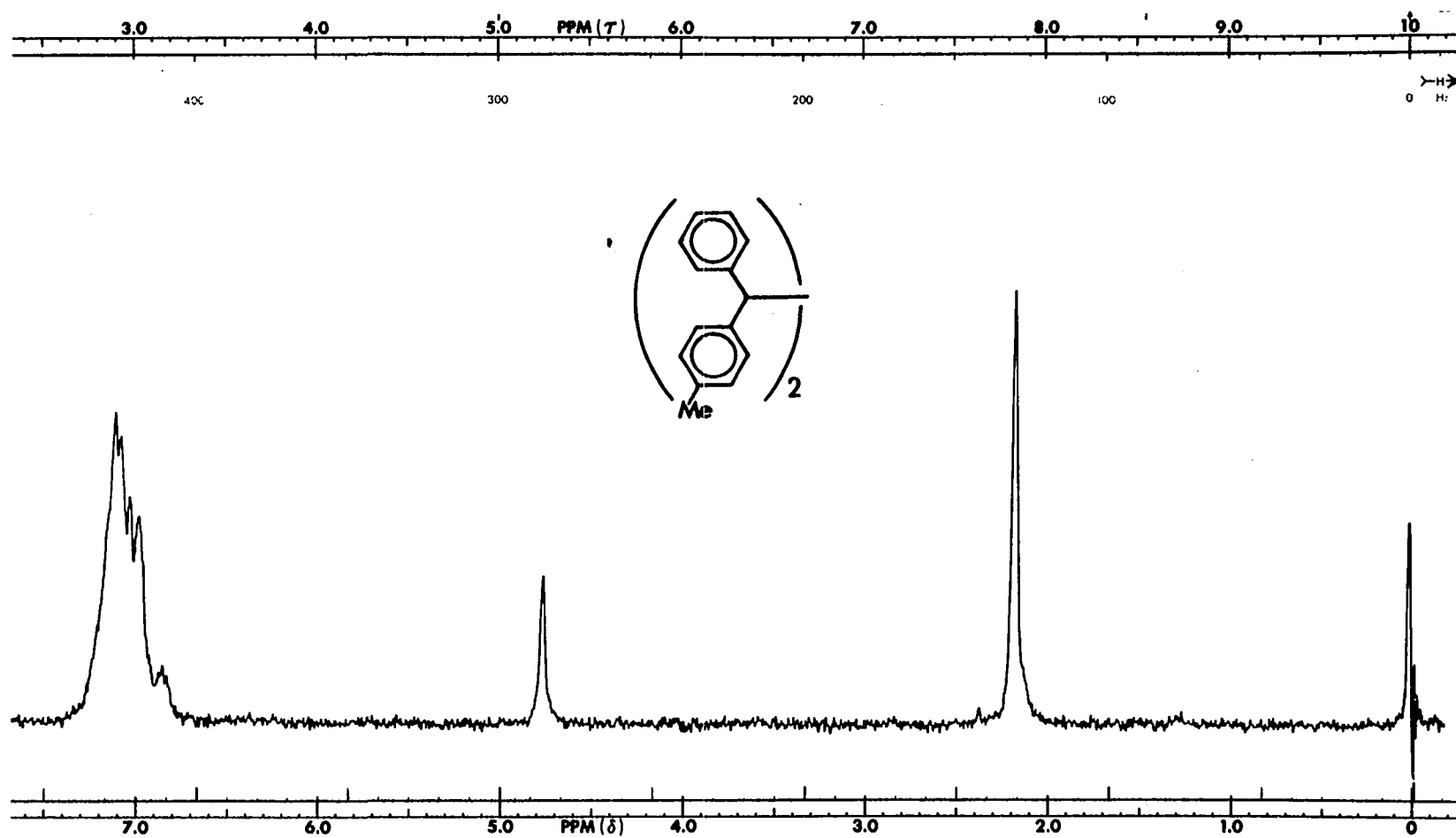


Figure 4 60 MHz PMR Spectrum (CDCl_3) of LXXXI

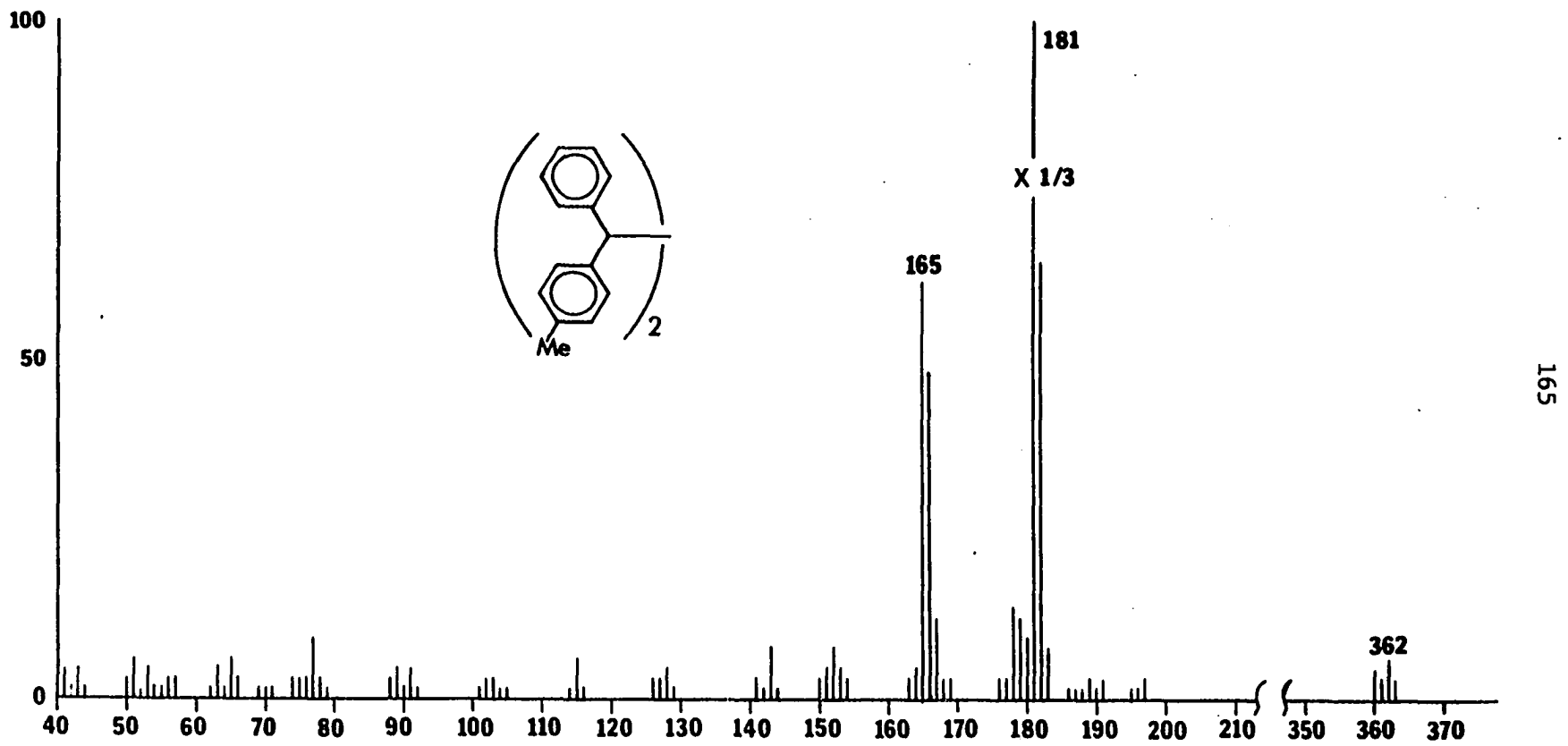


Figure 5 70 eV Mass Spectrum of LXXXI

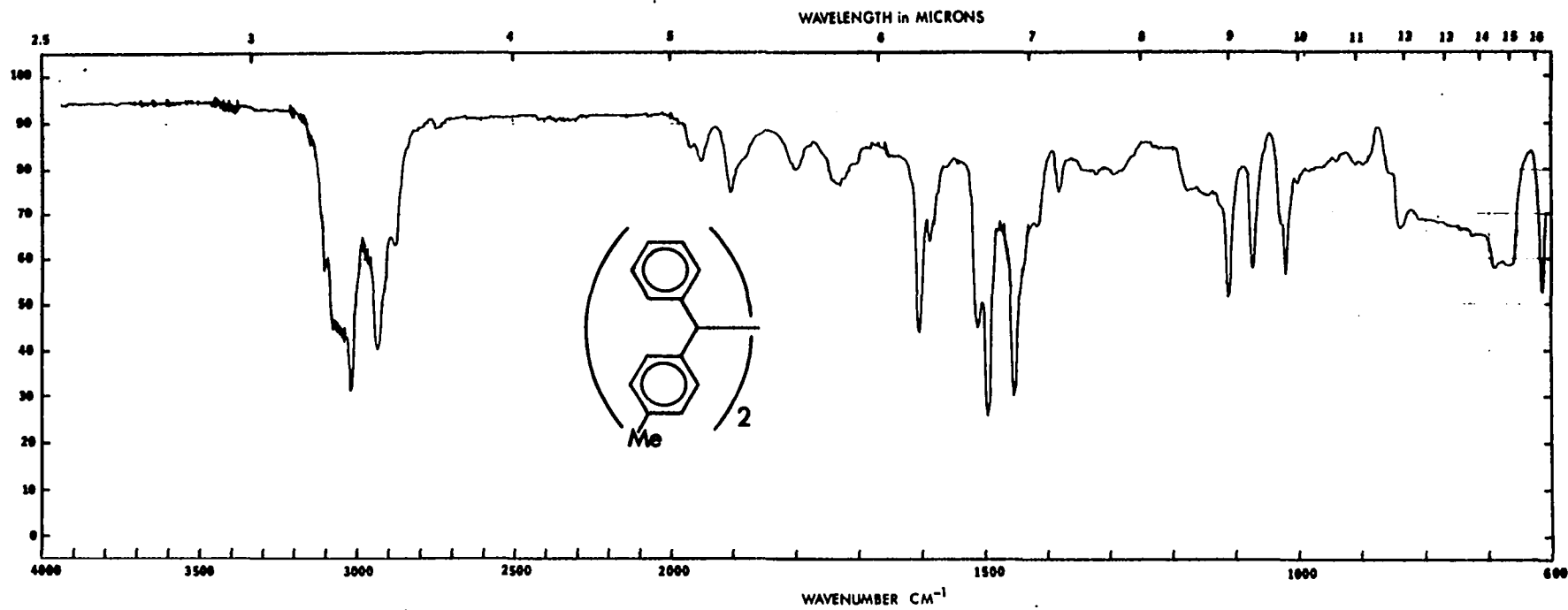


Figure 6 IR Spectrum (CHCl_3) of LXXXI

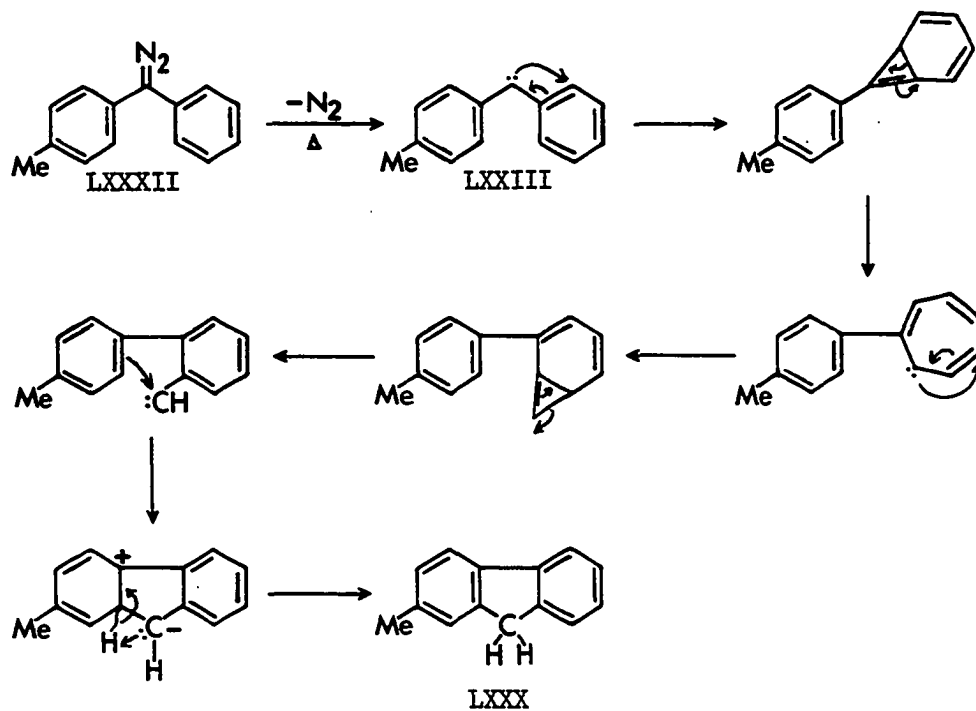
Table 1 gives the yields of compounds (LXXV-LXXXI) which were produced by the thermolysis of LXXI at various temperatures by the two methods discussed. The yields for compounds (LXXV-LXXX) were determined by GLC analysis on a S.C.O.T. Apiezon L column. The yields for the dimer (LXXXI) are isolated yields. All yields in Table 1 are reported as mole/mole oxalate.

Table 1

Product Distribution; Thermal Decomposition of LXXI

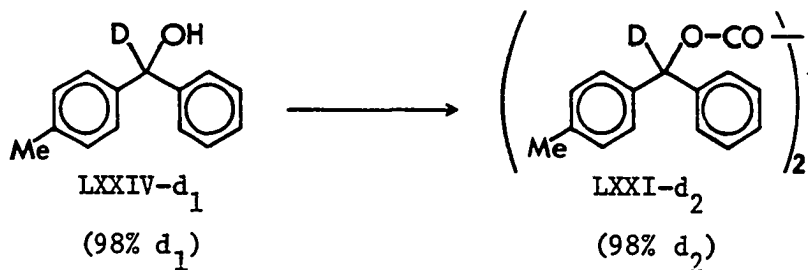
Method	Temp.	LXXV	LXXVI	LXXVII	LXXVIII	LXXIX	LXXX	LXXXI
A	750°	.04	.87	.02	.02	.02	.01	.05
A	650°	.03	1.15	.03	.01	.01	.02	.10
A	550°	.001	.24	.01	.001	.001	.004	.44
B	950°	.005	.17	.01	.004	.005	.01	.35
B	900°	.007	.20	.03	.002	.02	.06	.40

Products LXXV-LXXIX can reasonably be imagined to result from the 4-methylbenzhydryl radical (LXXII). However, the formation of 2-methylfluorene (LXXX) was more difficult to rationalize in terms of the radical (LXXII). The possibility that the 4-methyldiphenyl-carbene (LXXIII) was the precursor of the LXXX was suggested by the recent results of Jones and co-workers.¹⁰ They demonstrated the formation of 2-methylfluorene (LXXX) in the thermolysis of 4-methyldiphenyldiazomethane (LXXXII), a reaction that apparently proceeds by a multiple carbene rearrangement as shown in Scheme 2. No 3-methylfluorene (LXXIX) was found in that reaction.



Scheme 2

In order to test the possibility of a carbene origin for the 2-methylfluorene (LXXX) obtained by thermolysis of the oxalate (LXXI), we prepared bis(α - d_1 -methylbenzhydryl) oxalate (LXXI- d_2) from α - d_1 -4-methylbenzhydryl (LXXIV- d_1) which was 98% deuterated by mass spectral analysis.



The deuterated oxalate (LXXI-d₂) was thermolyzed at 650° using method A. The products were isolated and the deuterium content for each was determined by mass spectral analysis. These results are shown in Table 2. The data in Table 2 show that the majority of products had to a large extent retained the deuterium label; the notable exception to this was 2-methylfluorene (LXXX).

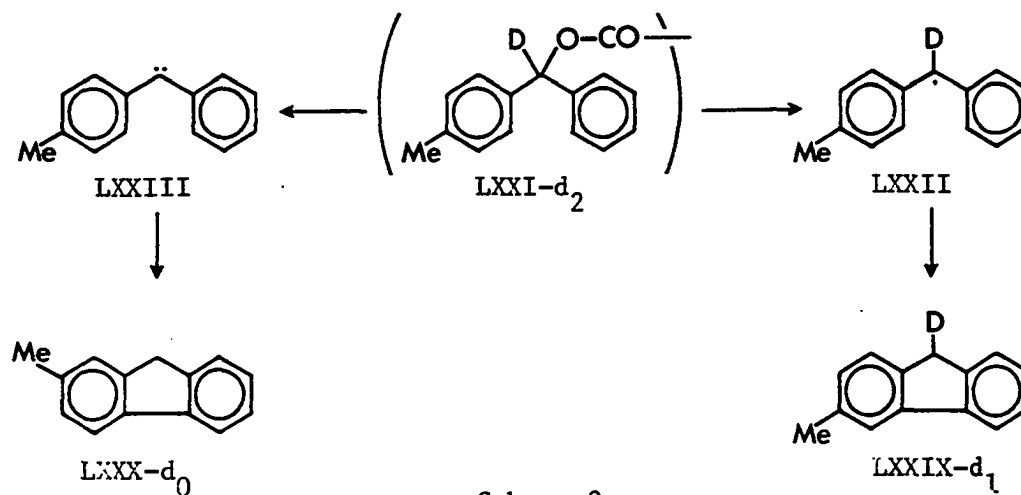
Table 2
Deuterium Content of Products Produced in the
Thermolysis of LXXI-d₂ at 650°

	<u>LXXV</u>	<u>LXXVI</u>	<u>LXXVII</u>	<u>LXXVIII</u>	<u>LXXIX</u>	<u>LXXX</u>	<u>LXXXI</u>
%d ₀	12.3	2.4	15.1	27.0	8.7	91.6	---
%d ₁	78.2	92.0	81.7	73.0	88.3	5.0	---
%d ₂	11.6	5.6	3.1	***	3.0	1.7	92.8

*** An accurate determination was not possible due to impurities present in the sample

The necessary consequence of an α -elimination process leading to 4-methyldiphenylcarbene (LXXVIII) followed by rearrangement to 2-methylfluorene (LXXX), is the loss of the deuterium label. The 2-methylfluorene recovered from the thermolysis of the deuterated oxalate (LXXI-d₂) had lost essentially all of the deuterium label (92% d₀). On the other hand, the 3-methylfluorene (LXXIX) had retained, to a large extent, its label (9% d₀, 88% d₁, 3% d₂). These results, combined with the work of Jones *et al.*,¹⁰ strongly implicate two competing pathways for the production of the methylfluorenes: a carbene route to 2-methyl-

fluorene (LXXX) and primarily a radical route to 3-methylfluorene (LXXIX) (see Scheme 3).

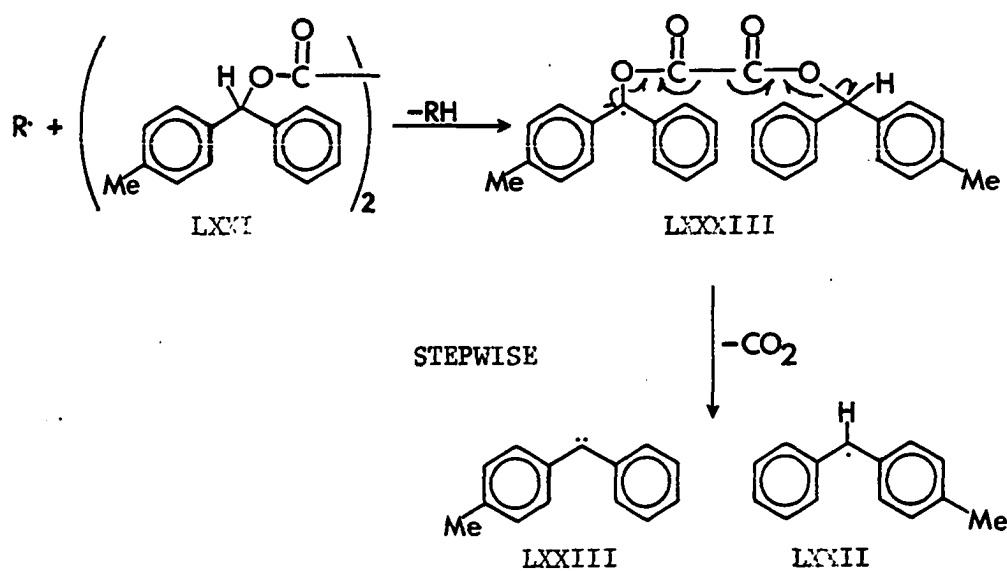
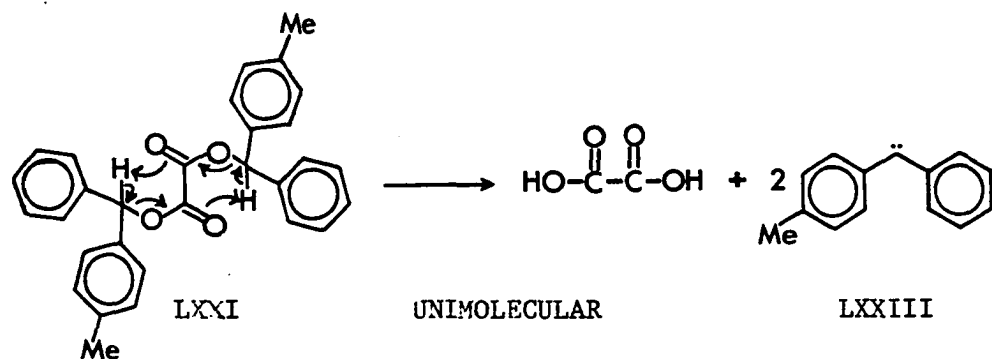


Scheme 3

In our considerations, there are two possible mechanistic routes which explain the formation of the carbene (LXXIII) from the oxalate (LXXI). One involves the unimolecular decomposition of LXXI via a transition state involving six-membered rings (see Scheme 4). The second, stepwise mechanism involves radical abstraction of an α -hydrogen atom leading to an intermediate radical (LXXXIII) which then fragments as shown in Scheme 4 to produce one carbene and one radical species.

Conclusions

The formation of LXXVI, LXXIX, and the dimer (LXXXI) from the oxalate (LXXI) can be easily rationalized as arising primarily by simple pathways involving the radical (LXXII). The large retention



Scheme 4

of the deuterium label (ca. 90% in Table 2) for these compounds supports this. For the 2-methylfluorene (LXXX), the results of deuterium labelling have clearly implicated its origin from the carbene (LXXIII). The lower

deuterium content (ca. 70-80%) shown in Table 2 for the compounds (LXXV), (LXXVII), and (LXXVIII) indicates more complex routes to these compounds and they may arise by both radical and carbene pathways.

The extent of carbene formation in this system is not very large, but it is mechanistically significant. Carbene intermediates in oxalate thermolyses should now be seriously considered as possible precursors to products that could be rationalized by either carbene or radical pathways. Several products previously reported in oxalate thermolyses^{2b} may, in fact, arise in part by carbene routes, rather than the suggested radical pathways.

CHAPTER 3

EXPERIMENTAL

All melting points were obtained on a Gallenkampf MF 370 capillary melting point apparatus and are uncorrected. Infrared spectra were obtained on a Beckmann IR-8 spectrophotometer. Mass spectra were obtained on a Hitachi-Perkin Elmer RMU-7E spectrometer operated at 70 eV. For the mass spectral deuterium analyses, the chamber voltage was lowered to 5-10 eV to minimize fragmentation of the ions. The 60 MHz PMR spectra were obtained on a Varian A-60 spectrometer. Preparative gas chromatography work was done on a Varian 90-P gas chromatograph. Analytical gas chromatography work was done on a Varian 1700 gas chromatograph equipped with a flame-ionization detector. Preparative layer chromatography was done using silica gel PF (254 + 366) UV indicating gel. Microanalyses were performed by Galbraith Laboratories, Inc., Knoxville, Tennessee.

Bis(4-methylbenzhydryl) Oxalate (LXXI)

A solution of 4-methylbenzhydrol (LXXIV)³ (4 g, 20.2 mmol) and triethylamine (2.42 g, 24 mmol) in dry ether (150 ml) was stirred magnetically and cooled with an ice bath. Oxalyl chloride (1.53 g, 12 mmol) in ether (50 ml) was added via an addition funnel over 15

minutes. The reaction was stirred in the cold for an additional 20 minutes. The mixture was poured into cold water (100 ml) and the phases were separated. The ethereal phase was washed with water (50 ml) and dried over Na_2SO_4 . Filtration and concentration gave LXXI as a crude solid. Recrystallization from hexane-ether (ice bath cooling) gave pure white LXXI that melted at $83.5\text{--}85^\circ$, yield: 3.5 g = 77%. The microanalytical sample was prepared by recrystallization from hexane-ether.

The 60 MHz PMR spectrum (Figure 1) in CDCl_3 showed: δ 6.9–7.6 (10H multiplet, aryl protons and proton on carbon bearing oxygen), 2.25 (3H singlet, aryl methyl protons). The 70 eV mass spectrum (Figure 2) did not show the parent ion (mol. wt. of LXXI is 450). The predominant ion (base peak) appeared at m/e 181. The m/e 181 ion ($\text{C}_{14}\text{H}_{13}^+$) was attributed to the fragmentation of the parent ion (LXXI^+) to 4-methylbenzhydryl carbonium ion. The IR spectrum (Figure 3) showed: cm^{-1} 1735 (C=O), 1165 (C-O). Analysis for $\text{C}_{30}\text{H}_{26}\text{O}$: calculated, C 79.97, H 5.81, O 14.20; found, C 79.78, H 5.84.

α - d_1 -4-methylbenzhydrol (LXXIV- d_1)

The title compound was prepared by the reduction of 4-methylbenzophenone³ with lithium aluminum deuteride (99% isotopic purity, SIC brand) in ether. Recrystallization from hexane-ether (ice bath cooling) gave white crystalline LXXIV- d_1 , in 45% yield, which melted at $55\text{--}56^\circ$. The literature³ melting point for the undeuterated LXXIV was $51\text{--}53^\circ$. Mass spectral deuterium analysis gave: 1.8% d_0 , 98.2% d_1 .

Bis(α -d₁-4-methylbenzhydryl) Oxalate (LXXI-d₂)

The title compound was prepared from α -d₁-4-methylbenzhydrol (LXXIV-d₁) (98% deuterated) using the same procedure described for the preparation of undeuterated LXXI. The deuterium content of 98% was assumed for LXXI-d₂.

Thermolysis of Bis(4-methylbenzhydryl) Oxalate (LXXI)

The thermolysis of the oxalate (LXXI) was done using the quartz hot tube which was previously described in Part I (see Figure 30 of Part I). The quartz hot tube was packed with quartz chips. A dry nitrogen flow was used in both methods (A and B below). In both methods, the vacuum was applied at the glass bead filled, U-shaped collector which was cooled with a slurry of dry ice-isopropanol.

Method A The oxalate (LXXI) was deposited on Chromsorb W (45/60 mesh) as 16.5% by weight by preparing a slurry of LXXI and Chromsorb W in acetone and evaporating to dryness under a vacuum. This was introduced slowly into the hot tube using the solid addition bulb (see Figure 58 of Part I), at 5 torr and a dry nitrogen flow of ca. 10 ml/min.

Method B The oxalate (LXXI) was introduced as a solution (45 mg/ml) in benzene into the hot tube by means of a pressure equalizing dropping funnel, at 95 torr and a dry nitrogen flow of ca 85 ml/min.

Separation and Identification of Mixture Components

The products obtained from thermolysis of LXXI by either

method A or B were washed from the collector with ether or dichloromethane and chromatographed by preparative layer with 10% EtOAc/hexane. This produced two major zones on the PLC plate which were visualized under the 254 nm UV lamp. The first and foremost zone contained the monomeric products (LXXV-LXXX) as a mixture. The second zone contained the dimer (LXXXI). The products were leached from the silica gel with ether or dichloromethane.

The mixture containing the compounds (LXXV-LXXX) was subjected to preparative gas chromatography on a 8' x 3/8", 1.5% JXR column which separated the compounds (LXXV), (LXXVI), (LXXVII), and (LXXVIII). The methylfluorenes (LXXIX) and (LXXX) were obtained as a mixture from the JXR column. They were further separated from each other by preparative gas chromatography on a 30" x 1/4", 13.5% azoxydiphenetole (a liquid crystal) column which was operated at 145° (in the nematic phase of azoxydiphenetole¹¹). Under these conditions, the methylfluorenes (LXXIX) and (LXXX) were completely separated. Due to excessive bleeding of the azoxydiphenetole column, it was necessary to further purify these samples by re-injection on either a JXR or SE-30 GLC column. The compounds (LXXV-LXXX) were all identified by comparison of their PMR and mass spectra with those of authentic samples⁴⁻⁹ and by comparison of GLC retention times on a S.C.O.T. Apiezon I. column.

The dimer (LXXXI) was essentially pure as obtained by preparative layer chromatography. Further purification was achieved by multiple sublimation at 125°/0.25 torr which gave LXXXI as a white solid that melted at 145-150°. The microanalytical sample was prepared in this manner.

The 60 MHz PMR spectrum (Figure 4) of LXXXI in CDCl_3 showed: δ 6.8-7.3 (9H multiplet, aryl protons), 4.75 (1H singlet, dibenzylic protons), 2.15 (3H singlet, aryl methyl protons). The 70 eV mass spectrum (Figure 5) showed: m/e 362 (M^+ , parent ion), 181 (base peak, attributed to a predominant fragmentation of M^+ to the 4-methylbenzhydryl ion). The IR spectrum (Figure 6) in CHCl_3 showed: cm^{-1} 3100-3000 (aromatic C-H), 1600 and 1500 (aromatic C=C). Analysis for $\text{C}_{28}\text{H}_{26}$: calculated, C 92.77, H 7.22; found, C 92.51, H 7.49.

Determination of Product Yields

The yields of the products produced in the thermolyses of the oxalate (LXXI) under a variety of conditions are shown in Table 1. In each case in Table 1, the product mixture was subjected to preparative layer chromatography to separate the monomeric products (LXXV-LXXX) from the dimer (LXXXI). The yields of the compounds (LXXV-LXXX) were determined by GLC analysis of the mixture obtained by PLC. For this purpose, a 50 ft S.C.O.T. Apiezon L column was employed which separated all components. The yields of the components were calibrated by co-injection of a single standard (LXXVIII) with each mixture. The assumption was made that each component had the same sensitivity to the flame-ionization detector. The yields in Table 1 are reported as mole per mole of oxalate. The yields of the dimer (LXXXI) represent actual yields as isolated by PLC.

Mass Spectral Deuterium Analyses

The components of the mixture obtained by the thermolysis

of LXXI-d₂ (98% deuterated) at 650° by method A were separated using the procedures described previously. Each component was independently subjected to low eV mass spectral deuterium analysis. The results are shown in Table 2. For each component, the conditions for analysis were established by introducing an undeuterated sample of the component into the mass spectrometer and reducing the chamber voltage until no (M⁺-1) ion was apparent (usually 5-10 eV). The deuterated sample was then introduced and the ratios of the M⁺ (d₀), M⁺+1 (d₁) and M⁺+2 (d₂) ions were determined. Compensation was made in each case for the natural occurrence of ¹³C. For compound LXXVIII an accurate determination could not be made due to the presence of an unknown impurity which interfered with the measurement of the M⁺+2 (d₂) ion. The %d₀ and %d₁ values for LXXVIII were estimated by assuming a zero value for the M⁺+2 ion. For the dimer (LXXXI), the parent ion could not be used due to the large M⁺-1 and M⁺-2 ions (see Figure 5). The %d₂ value given for LXXXI was estimated using the predominant ion appearing at m/e 181 (182 for the deuterated sample).

Bibliography

1. R. E. Lehr and J. M. Wilson, Chem. Commun., 666 (1971).
2. a) D. M. Golden, N. A. Gac, and S. W. Benson, J. Amer. Chem. Soc., 91, 2136 (1969).
b) W. S. Trahanovsky, J. A. Lawson, and C. C. Ong, ibid., 92, 7174 (1970).
c) D. G. L. James and S. M. Kambanis, Trans. Faraday Soc., 65, 1350 (1969).
d) W. S. Trahanovsky, C. C. Ong, and J. A. Lawson, J. Amer. Chem. Soc., 90, 2839 (1968).
3. A. G. Davies, J. Kenyon, B. J. Lyons, and T. A. Rohan, J. Chem. Soc., 3474 (1954).
4. W. W. Hartmar and R. Philips, Org. Syn., XIV, 34 (1934).
5. W. H. C. Rueggeberg, M. L. Cushing, and W. A. Cork, J. Amer. Chem. Soc., 68, 191 (1946).
6. K. v. Auwers, Chem. Ber., 49, 2401 (1916).
7. C. D. Hurd and C. N. Webb, J. Amer. Chem. Soc., 49, 549 (1927).
8. S. Sieglitz, Chem. Ber., 54, 2071 (1921).
9. O. Kruber, ibid., 65, 1395 (1932).
10. J. A. Myers, R. C. Joines, and W. M. Jones, J. Amer. Chem. Soc., 92, 4740 (1970).
11. H. Keller, Ber. Bunsenges, 67, 698 (1963).